Two new genera and species of sepioline squids (Cephalopoda: Sepiolidae) from Australia

(http://zoobank.org/urn:lsid:zoobank.org:pub:53DAFE4A-6C49-42A0-9D44-F37B03FBA7F0)

Chung Cheng Lu[1,2,*] and Takashi Okutani[3]

[1] Museum Victoria, Melbourne, Victoria 3000, Australia
[2] Department of Life Sciences, National Chung Hsing University, Taichung, Taiwan 402
[3] #714, Takaishi 4-17-1, Asao-ku, Kawasaki, Japan 215-0003
* To whom correspondence should be addressed. Email: cclu@nchu.edu.tw

Abstract

Lu, C.C., and Okutani, T. 2022. Two new genera and species of sepioline squids (Cephalopoda: Sepiolidae) from Australia. *Memoirs of Museum Victoria* 81: 1–23.

Two new genera and species of sepioline squid (Cephalopoda: Sepiolidae) are described from Australian waters. *Dextrasepiola taenia* is characterised by having copulatory organs (i.e. the hectocotylised arm in the males and the bursa copulatrix in the females) in the right side of the body. All other known sepiolinids have copulatory organs in the left side of the body. *Amutatiola macroventosa* is characterised by the absence of a hectocotylised arm in mature males; instead, it possesses many enormously enlarged suckers on some of the arms of the males. The bursa copulatrix is in the left side of the female body, as in other known sepioline squids. The discovery of these two new taxa indicates that the present definition of Sepiolinae needs to be broadened to accommodate these two new genera.

Keywords   Sepiolinae; *Dextrasepiola taenia*; *Amutatiola macroventosa*; Australia.

Introduction

Members of the family Sepiolidae are small to medium size benthic or pelagic cephalopods and are common in tropical, subtropical and temperate waters. Currently, 18 genera are recognised in the following three subfamilies: (i) Heteroteuthinae: *Heteroteuthis* Gray, 1849, *Stoloteuthis* Verrill, 1881, *Nectoteuthis* Verrill, 1883, *Iridoteuthis* Naef, 1912, and *Sepiolina* Naef, 1912; (ii) Sepiolinae: *Sepiola* Leach, 1817, *Inioteuthis* Verrill, 1881, *Euprymna* Steenstrup, 1887, *Rondeletiola* Naef, 1921, *Sepietta* Naef, 1912, *Adinaefiola* Bello, 2020, *Boletzkyola* Bello, 2020, *Lusepiola* Bello, 2020, and *Eumandya* Bello, 2020; and (iii) Rossiinae: *Rossia* Owen, 1834, *Semirossia* Steenstrup, 1881, *Austrorossia* Berry, 1918, and *Neorossia* Boletzky, 1971. For *Chonneteuthis* Lu and Boucher-Rodoni, 2006, the subfamilial placement is uncertain (Bello, 2020; Lu and Boucher-Rodoni, 2006; Nesis 1987). The three subfamilies are well defined. Table 1 shows the diagnostic characters of these subfamilies.

A member of Sepiolinae was first recorded from Australia by Lu and Phillips (1985) and assigned to the old genus *Sepiola* without specific identification. A dorsal view of a specimen was also presented in Lu and Dunning (1998). The record was accidentally omitted in Lu (2001). In this paper, we describe two new sepioline species and placed them in two new genera

in light of Bello's (2020) revision. These new genera and species appear to belong to Sepiolinae based on the main characters of this subfamily, apart from their peculiar male arm modifications that do not correspond to the normal sepioline hectocotylisation.

Material and methods

All materials examined are listed under each relevant taxon. All except one lot are in the collection of the Museum of Victoria. The materials were all formalin fixed and preserved in 70% ethyl alcohol. All measurements and indices are standard teuthological measurements and indices, following Roper and Voss (1983) and Lu and Boucher-Rodoni (2006), except for nuchal commissure index, which is the width of nuchal commissure expressed as a percentage of the width of mantle at the position of nuchal commissure. Nuchal commissure width is called occipital band width by some authors (e.g. Nesis, 1982). Roper and Voss (1983) used the mantle length as the standard reference size for free funnel index and nuchal commissure index. For arm lengths, arm sucker counts and sucker diameters, left arms were measured or counted. In males, the right arm I was also measured and suckers and sucker stalks counted to ascertain if any modification occurs in right arm I. The maturity stages used in the Tables are those used in Lu and Roper (1979).

Table 1. Comparison of distinguishing characters of subfamilies Heteroteuthinae, Rossiinae and Sepiolinae of the family Sepiolidae (after Nesis, 1982)

	Heteroteuthinae	Rossiinae	Sepiolinae
Anterior ventral mantle edge	extended into projecting ventral shield covering funnel from below and sometimes reaching level of eyes or farther forward; ventral shield with an incision in centre for funnel opening	not extended forward, not covering funnel	not extended forward, not covering funnel
Anterior dorsal mantle edge	fused with head, except in *Heteroteuthis*	not fused with head	fused with head
Nuchal cartilage	developed in *Heteroteuthis*; absent in other genera	developed	no nuchal cartilage
Arms connected by web	3 dorsal pairs of arms joined by deep web	2 dorsal pairs of arms not connected or connected only by shallow web	2 dorsal pairs of arms not connected or connected only by shallow web
Arm suckers	in 2 series; some suckers on lateral arms in males in some taxa greatly enlarged	in 2 or 4 series; no greatly enlarged suckers	in 2 or 4 series; some suckers in males maybe enlarged
Club	narrow or slightly widened, with very small suckers	narrow or widened, with very small, medium or large suckers	narrow or slightly widened, with small suckers
Fins	large, fin length 60–100% of mantle length	moderate size, much shorter than mantle	moderate size, much shorter than mantle
Photophores	on ventral side of ink sac	only one genus, *Semirossia*, is known to have a bilobed photophore on ink sac	saddle-shaped, two ear-shaped, lens-shaped or absent (*Inioteuthis*)
Hectocotylisation	usually both dorsal arms hectocotylised	left or both dorsal arms hectocotylised	left dorsal arm hectocotylised
Gladius	absent	present	rudimentary or absent
Habitat	benthic or pelagic	benthic, some species ascend to surface during reproduction	benthic, some species ascend to surface during reproduction

Abbreviations:

CSIRO: Commonwealth Scientific and Industry Research Organisation of Australia
IYGPT: International Young Gadoid Pelagic Trawl
MOV: Museum of Victoria, Melbourne, Victoria, Australia
Q: FRV *Courageous* of CSIRO
Q47/51: FRV *Courageous* of CSIRO cruise 47, station 51
SO: FRV *Soela* of CSIRO
FRV *Soela* SO1/85/124 (and similar): FRV *Soela* of CSIRO, 1985 cruise 1, station 124

Systematic description

Class Cephalopoda Cuvier, 1797

Subclass Coleoidea Bather, 1888

Order Sepiolida Fioroni, 1981

Family Sepiolidae Leach, 1817

Subfamily Sepiolinae Leach, 1817

Dextrasepiola **n. gen.**

Type Species: Dextrasepiola taenia n. gen., n. sp. by monotypy

Diagnosis: Sepiolinae with fins rounded with large anterior lobes, which do not reach the anterior mantle margin; fin length about 50–80% mantle length. Suckers biseriate on all arms. Tentacular club suckers in 4–8 longitudinal series. Nuchal commissure narrow, not reaching over the ocular globes. A pair of dumbbell-shaped photophores on ventral surface of ink sac. Gladius absent. Ventral mantle margin slightly sinuate, without any deep funnel indentation. Right arm I of male hectocotylised. Hectocotylus tripartite: basal part with five suckers in two series, two suckers in dorsal series and three in ventral series; copulatory apparatus long, fleshy, tape like, formed by fusion of two adjoining very elongate sucker stalks, no additional modified structure on the arm (i.e. hook-like stalks); distal to tape-like copulatory apparatus biserial suckers to arm tip (19 suckers in holotype, 23 suckers in paratype 2). Female bursa copulatrix on right side of mantle cavity, open type (cf. Bello, 2020), roughly ear shaped.

Etymology: Generic name *Dextrasepiola* is derived from Latin *dextra* meaning right or on the right side plus *sepiola* meaning a small cuttlefish. The name denotes the unique feature among the *Sepiola* and its kin having the right dorsal arm hectocotylised instead of the left dorsal one in mature males and the bursa copulatrix in females on the right side of the mantle cavity.

Remarks: The hectocotylisation in Sepiolinae has been thoroughly discussed and illustrated by Bello (2020), Naef (1912a, b; 1923) and Nesis (1982). All known species have the left dorsal arm hectocotylised and the sucker stalks of some

suckers are modified into a horn-like or hook-like copulatory organ. The present genus is unique in having the right dorsal arm hectocotylised and the copulatory organ as one thick tape-like structure. In addition, the hectocotylus has the regular tripartite structure typical of most sepioline genera except for *Euprymna* and *Eumandya* (cf. Bello, 2020). The females of all known species of Sepiolinae possess a bursa copulatrix on the left side of the mantle cavity. The present genus is unique in having the bursa copulatrix on the right side of the mantle cavity. This right-handedness of the copulatory organs of both sexes of this genus certainly facilitate copulation in a normal fashion as they are on the same side of the animal.

Dextrasepiola taenia n.gen., n.sp.

Figures 1–5, 13; Table 2

Material examined: Holotype: MOV F80458: Redland Bay, Queensland, 27° 36' S, 153° 19' E, 1.2 m, CSIRO Moreton Bay Survey, J43, Location 31, 10 Aug 1951, 1 male, mature, 8.2 mm mantle length (specimen #1).

Paratype 1: MOV F91359: Redland Bay, Queensland, 27° 36' S, 153° 19' E, 1.2 m, CSIRO Moreton Bay Survey, J43, Location 31, 10 Aug 1951, 1 female, mature, 7.8 mm mantle length (specimen #2).

Paratype 2: MOV F74469: Peel Island, Queensland, 27° 30' S, 153° 21' E, 1.2 m, CSIRO Moreton Bay Survey, J26, Location 41, 10 Aug 1951, 1 male, mature, 6.5 mm mantle length (specimen #3).

Paratype 3: MOV F91361: Peel Island, Queensland, 27° 30' S, 153° 21' E, 1.2 m, CSIRO Moreton Bay Survey, J26, Location 41, 10 Aug 1951, 1 female, mature, 8.7 mm mantle length (specimen #4).

Other material: MOV F91360: Peel Island, Queensland, 27° 30' S, 153° 21' E, 1.2 m, CSIRO Moreton Bay Survey, J26, Location 41, 10 Aug 1951, 2 specimens, poor condition, 1 female, juvenile, 5.4 mm mantle length, 1 specimen, sex indeterminate, 3.9 mm mantle length.

Diagnosis: Small sepioline with right arm I of mature male hectocotylised, copulatory apparatus in the form of a long tape-like process, no hook-like structure on the arm. Females with bursa copulatrix on right side of mantle cavity.

Description: Mantle (figs 1a–c) short dome-shaped, slightly longer than wide, fused with head dorsally for about 25% of width. Anterior ventral mantle margin shallowly concave with lateral projections at position of mantle-funnel connectives. Head wide, slightly narrower than mantle. Nuchal commissure narrow, not reaching beyond level of medial border of eyeball, approximately 25–40% of mantle width at level of nuchal commissure. Eyes large, elliptical, located dorso-laterally on head. Cornea membrane protecting eye attached to skin of head along dorsal margin. Olfactory papilla located behind posterior corner of eye orbit, ventral photosensitive vesicle not found. Funnel long and slender, reaching the level beyond anterior eye margin, free from head for 60–80% of funnel length. Funnel connects to head by an oblique muscle band extending from beneath anterior end of funnel locking cartilage to ventral side of head.

Funnel locking cartilage (fig. 1f) elongated oval with simple, slightly curved depression in the middle, mantle locking cartilage long, low ridge. Dorsal element of funnel organ (fig. 1g) Y-shaped pad with a small papilla at the apex. Behind each ramus is swelling that connects dorsal funnel organ with base of funnel retractor. Ventral elements of funnel organ (fig. 1g) a pronounced semi-spherical pad, becoming slightly narrower anteriorly, with a mamillar projection slightly posteriorly to centre. Funnel valve well developed on dorsal roof, tongue shaped, located well behind funnel aperture.

Fins (figs 1a–c) circular in outline, anterior border of fins projects forward prominently forming a deep cleft with mantle, anterior fin lobe reaching level halfway between fin insertion and mantle border or to mantle margin, posterior borders of fins convex, less pronounced. Length of fin base about 33% of mantle length.

Arms (figs 1a–c, 2a–c, 3) short, rounded aborally, flatten orally. All arms on both sexes with biserial suckers throughout. Because most suckers are lost, it was impossible to determine the sucker ring dentition and if the enlargement of suckers exists. In males, arm III is the longest and thickest, followed by arm II or arm IV. Right arm I of male (figs 1d–e, 3) with a flat, fleshy, tape-like long process, appeared to be modified sucker stalks of proximal third sucker of dorsal series and proximal fourth sucker of ventral series fused together throughout their length. Length of the process reaches to almost the level of arm tip, thickened along proximal portion ending in a blunt tip. No sucker on the tape-like process of holotype, but a remnant of a tiny sucker on the process of paratype 2 (fig. 3). Distal to the tape-like process, 19 suckers in two series to arm tip on holotype (23 suckers in paratype 2); no hook-like structures on the arm. Left arm I in males and both arms I in females with 28–30 suckers in two series, with no peculiar or unusual development or modification. Arm II with 27–35 suckers in both sexes with no noticeable special development in either sex. In males, arms III thickened proximally, slightly tapers distally to about half of arm length then abruptly tapers distally; swollen proximal part with no suckers except several remnants of suckers; distal part strongly curled towards mouth, with 17–19 suckers. In females, arm III similar to arm II with 21 suckers. Arm IV of both sexes with 26–31 suckers. In males, aboral keel and swimming membrane absent on arms I–III, well developed along whole length of arms IV. In females, aboral keel and swimming membrane present on distal half of arms I and II, and almost whole length of arms III and IV. Webs shallow between all arms except between arms III and IV (web D), which half encloses base of tentacles in both sexes, web E non-existent.

Tentacles weak, longer than arms. Club (fig. 4a) slightly expanded, minute carpal suckers in 4 series, minute manal suckers in 6 series, those on dorsal 2 series larger than the remaining suckers, numerous minute suckers in 8 series on dactylus. Sucker ring dentition of largest club sucker finely toothed around entire minute circle.

Gills with 15–20 lamellae per demibranch, plus a terminal lamella. A pair of dumbbell-shaped, yellowish photophores, opaque with both ends swollen on both sides of ink sac (figs 1g, 4b).

Upper beak (fig. 4d) rostrum slightly curved; jaw angle obtuse; wing long, shoulder (cutting edge) serrated; rostrum dark brown to black, hood, shoulder and dorsal part of lateral wall light brown, posterior part of hood, most of lateral wall unpigmented, transparent.

Table 2. *Dextrasepiola taenia* n.gen. & n.sp. measurement, counts and indices

Species	Dextrasepiola taenia			
Museum	MOV	MOV	MOV	MOV
Registration number	F80458	F74469	F91361	F91359
Specimen number	1	2	3	4
Type status	Holotype	Paratype 2	Paratype 3	Paratype 1
Cruise	Moreton Bay Survey	Moreton Bay Survey	Moreton Bay Survey	Moreton Bay Survey
Station number	J43, Loc.31	J26, Location 41	J26, Location 41	J43, Location 31
Sex	male	male	female	female
Maturity	5	5	5	5
DML (mm)	8.2	6.5	8.7	7.8
VMLI	93.9	113.8	103.4	102.6
HLI	29.3	36.9	51.7	43.6
HWI	75.6	95.4	74.7	88.5
NCI	26.4	22	40	36.1
MWI	87.8	90.8	86.2	92.3
FuLI	53.7	83.1	65.5	70.5
FuWI	46.3	43.1	47.1	51.3
FFuI	81.8	61.1	61.4	60
FLI	48.8	67.7	63.2	61.5
FBLI	35.4	35.4	31	32.1
FWI	43.9	64.6	44.8	56.4
A_1LI	54.9	84.6	51.7	57.7
A_2LI	67.1	84.6	69	64.1
A_3LI	85.4	107.7	63.2	64.1
A_4LI	54.9	92.3	57.5	51.3
Arm formula	3.2.1.=4.	3.4.1.=2.	2.3.4.1.	2.=3.1.4.
$A_{R1}LI$	67.1	92.3	–	–
TtLI	85.4	–	137.9	179.5
ClLI	30.5	–	23	38.5
ClRC	6	–	6	6
GLI	32.9	46.2	41.4	28.2
GWI	18.3	29.2	23	21.8
GiLC	18	20	–	15
A_1SC	28	30	29	30
A_2SC	27	31 right	30	30
A_3SC	–	–	–	27
A_4SC	26	31	29 right	27
$A_{R1}SC$	25	29	–	–
ClSI	2.2	–	–	–
A_1SI	–	4.6	–	–
A_2SI	–	–	–	–
A_3SI	–	–	–	–
A_4SI	–	–	–	–
SpLI	a:26; b:24.3; c:30.1; d:27.4; e:28.2	–	–	–
SpWI	a:3.9; b:4.2; c:3.4; d:3.7; e:4.8	–	–	–
SpRI	a:20.7; b:22.1; c:19; d:22.2; e:21.6	–	–	–
CBI	a:33.8; b:36.2; c:30.4; d:34.7; e:33.8	–	–	–
NidGI	–	–	54.4	36.6

Note: Maturity 4, subadult – sexual characters well distinguished but gonads and accessory organs not completely developed; Maturity 5, adult – sexually mature with spermatophores in Needham's sac in males; ovaries, nidamental and oviducal glands fully developed and ripe, eggs sometimes in oviducts, in females; DML, dorsal mantle length (mm) – measured from anterior-most point of mantle to posterior end of mantle; VMLI, ventral mantle length index – ventral mantle length, measured from anterior border of mantle at ventral midline, to apex of mantle, expressed as a percentage of DML; HLI, head length index – dorsal length of head measured from point of fusion of dorsal arms to anterior tip of dorsal mantle expressed as a percentage of DML; HWI, head width index – greatest width of head at level of eyes expressed as a percentage of DML; NCI, nuchal commissure width index – width of nuchal commissure expressed as a percentage of width of mantle at the position of nuchal commissure; MWI, mantle width index – mantle width at mantle opening expressed as a percentage of DML; FuLI, funnel length index – length of funnel from anterior funnel opening to posterior border of funnel measured along ventral midline expressed as a percentage of DML; FuWI, funnel width index – width of funnel at junction of funnel and head just anterior to funnel locking cartilages expressed as a percentage of DML; FFuI, free funnel index – length of funnel from the anterior opening to the point of dorsal attachment to head expressed as a percentage of funnel length; FLI, fin length index – greatest length of a single fin expressed as a percentage of DML; FBLI, fin base length index – length of fin attachment to mantle expressed as a percentage of DML; FWI, fin width index – greatest width of a single fin expressed as a percentage of DML; A_1LI, arm I length index – length of arm I expressed as a percentage of DML; A_2LI, arm II length index – length of arm II expressed as a percentage of DML; A_3LI, arm III length index – length of arm III expressed as a percentage of DML; A_4LI, arm IV length index – length of arm IV expressed as a percentage of DML; $A_{R1}LI$, right arm I length index – length of right arm I expressed as a percentage of DML (only in males); TtLI, tentacle length index – total length of tentacular stalk and club expressed as a percentage of DML; ClLI, club length index – length of club, measured from proximal-most basal sucker to distal tip of club expressed as a percentage of DML; ClRC, club row count – number of longitudinal rows of suckers across width of club; GLI, gill length index – length of gill expressed as a percentage of DML; GWI, gill width index – greatest width of gill expressed as a percentage of DML; GiLC, gill lamellae count – number of lamellae on outer demibranch, excluding terminal lamella; A_1SC, sucker counts of arm I – total number of suckers or sucker stalks on arm I; A_2SC, sucker counts of arm II – total number of suckers or sucker stalks on arm II; A_3SC, sucker counts of arm III – total number of suckers or sucker stalks on arm III; A_4SC, sucker counts of arm IV – total number of suckers or sucker stalks on arm IV; $A_{R1}SC$, sucker counts of right arm I – total number of suckers or sucker stalks on right arm I (only in males); ClSI, club sucker index – diameter of largest club sucker expressed as a percentage of DML; A_1SI, arm I sucker index – diameter of largest sucker on arm I expressed as a percentage of DML; A_2SI, arm II sucker index – diameter of largest sucker on arm II expressed as a percentage of DML; A_3SI, arm III sucker index – diameter of largest sucker on arm III expressed as a percentage of DML; A_4SI, arm IV sucker index – diameter of largest sucker on arm IV expressed as a percentage of DML; SpLI, spermatophore length index – length of spermatophore expressed as a percentage of DML; SpWI, spermatophore width index – greatest width of spermatophore expressed as a percentage of spermatophore length; SpRI, sperm reservoir index – length of sperm reservoir expressed as a percentage of spermatophore length; CBI, cement body index – length of cement body expressed as a percentage of spermatophore length; NidGI, nidamental gland index – length of nidamental gland expressed as a percentage of DML.

Lower beak (figs 4e, f) wide; rostrum with blunt tip; jaw edge rough, slightly serrated, jaw angle indistinct; blunt tooth on shoulder; no notch in hood; lateral wall without fold or ridge, roughly elongate rhomboidal with lower edge slightly concave, corner faintly produced; rostrum and hood light brown, posterior part of lateral wall and wings transparent. Radula (fig. 4c) seven series, each row with seven unicuspid teeth.

Gladius absent.

Spermatophores (figs 5a, b) small, five spermatophores from the holotype approximately 2–2.5 mm long (spermatophore length index 24–30), greatest width approximately 0.08–0.1 mm (spermatophore width index 3.4–4.8), sperm reservoir about 0.4–0.5mm (sperm reservoir index 19–22), structure complex, with spiral appearance in ejaculatory apparatus and the sperm mass, cement body 0.72–0.78 mm long (cement body index 30–36), connects to sperm reservoir by a narrow neck, oral end of cement body elongated funnel shaped.

Bursa copulatrix (figs 5c–f) open type, large, roughly ear-shaped, longer than wide; anteriorly extends medially towards midline, running antero-laterally just below right funnel locking cartilage, reaching posterior end of mantle cavity. Longitudinal opening of bursa close to mantle ventral midline,
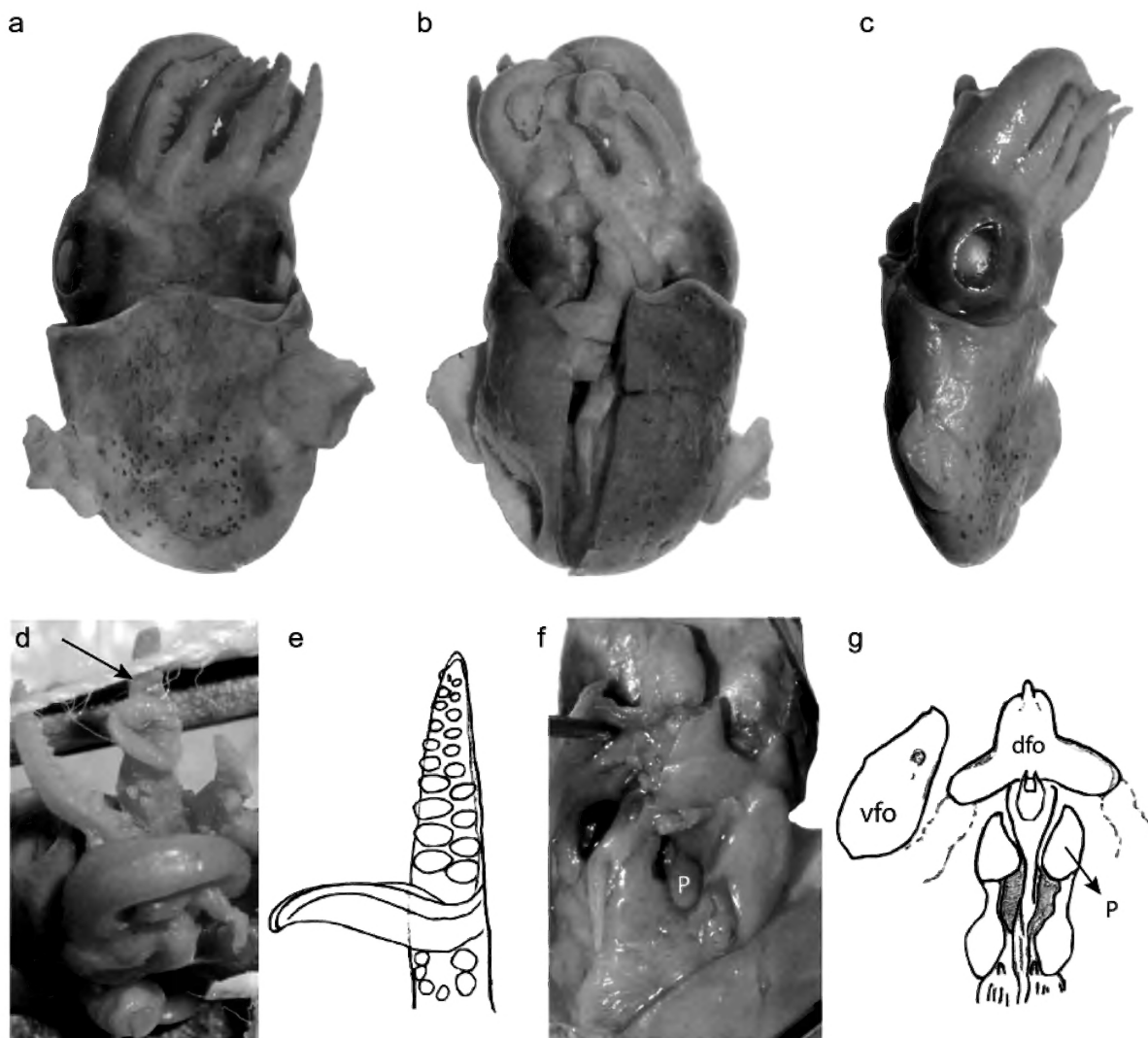
Figure 1. *Dextrasepiola taenia* n. gen. & n. sp., male: a, dorsal view, holotype (MOV F80458); b, ventral view (MOV F80458); c, lateral view (MOV F80458); d, hectocotylised arm (right arm I; MOV F80458); e, diagram of the hectocotylised arm showing tape-like modification, paratype 2 (MOV F74469; drawn by T. Okutani); f, inside mantle cavity, showing photophores (p) and other organs (MOV F80458); g, diagram of opened funnel and inside mantle cavity showing dorsal funnel organ (dfo), ventral funnel organ (vfo) and photophores (p; MOV F80458; drawn by T. Okutani).
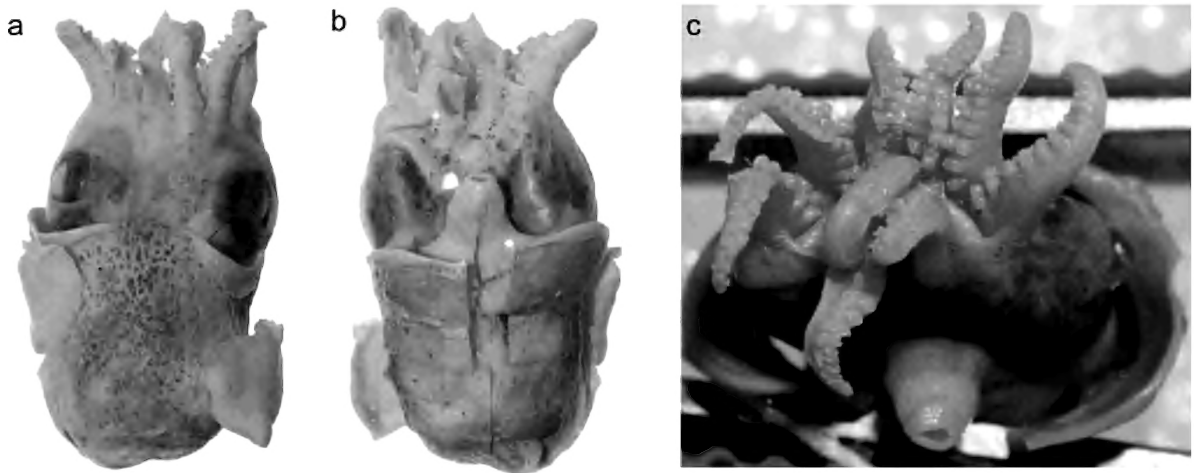
Figure 2. *Dextrasepiola taenia* n. gen. & n. sp., female, paratype 1 (MOV F91359): a, dorsal view; b, ventral view; c, oral view of arm crown showing sucker arrangements of female.
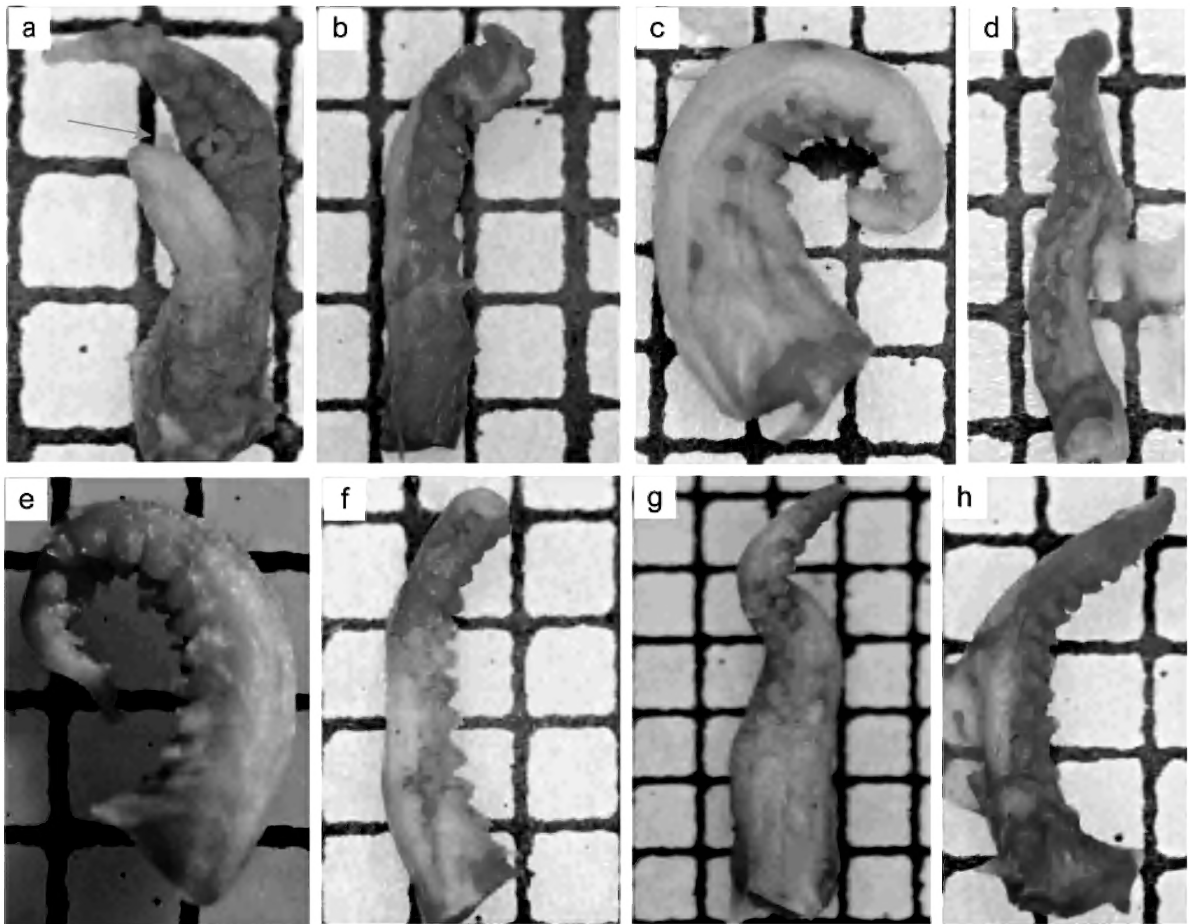

Figure 3. *Dextrasepiola taenia* n. gen. & n. sp. male, paratype 2 (MOV F74469). Oral view of arms (grids in background: 1 mm × 1 mm): a, right arm I, arrow points to remnant of a tiny sucker; b, right arm II; c, right arm III; d, right arm IV; e, left arm I; f, left arm II; g, left arm III; h, left arm IV.

running along long axis of bursa. Mature females with large nidamental gland, (nidamental gland index 36.6–54.4).

Alcohol-preserved specimens brown in colour, dorsal mantle surface lighter than ventral surface. Dark chocolate-brown chromatophores scattered over brown-coloured background on both dorsal and ventral surfaces of head and mantle, and along aboral surface of all arms. Surfaces of fins devoid of chromatophores and pigmented spots. Skin smooth, lacking sculpture or papillae.

Etymology: Species epithet *taenia* from Latin *taenia* meaning tape-like. The name denotes the tape-like structure in the copulatory apparatus on the hectocotylised arm of the males.

Distribution: Only known from Moreton Bay, Queensland, Australia (fig. 13).

Remarks: This is the only known species in the genus. Due to the poor preservation of the specimens, nearly all suckers are lost or are without sucker rings. The description of sucker ring dentition and spermatophores must wait until better materials are available.

The poor state of preservation resulted in distorted morphology of the specimens studied. This most certainly contributes to the wide range of the morphometric indices listed in Table 2.

Amutatiola n. gen.

Diagnosis: Small Sepiolinae with fins rounded with large anterior lobe, which do not reach the anterior mantle margin; fin length about 40–66% mantle length. Suckers biseriate on all arms. Tentacular club suckers in 4–8 longitudinal series. Nuchal commissure moderately wide, not reaching over the ocular globes, about 38–59% of mantle width. A pair of dumbbell-shaped or elongated kidney-shaped photophores on ventral surface of ink sac. Gladius absent. Ventral mantle margin slightly sinuate, without any deep funnel indentation. No arm in mature males hectocotylised. Some arm suckers in mature males grossly enlarged. Female bursa copulatrix closed type, pouch-like, opening at level of base of left gill.

Type Species: Amutatiola macroventosa n. gen., n. sp. by monotypy.

Etymology: Generic name *Amutatiola* is derived from Greek *a* meaning without or absent plus Latin *mutatus* meaning changed or altered; the ending *-ola* is the diminutive suffix of *sepiola* meaning a small cuttlefish. The name denotes the unique feature among the Sepiolinae of having no arm hectocotylised in males.
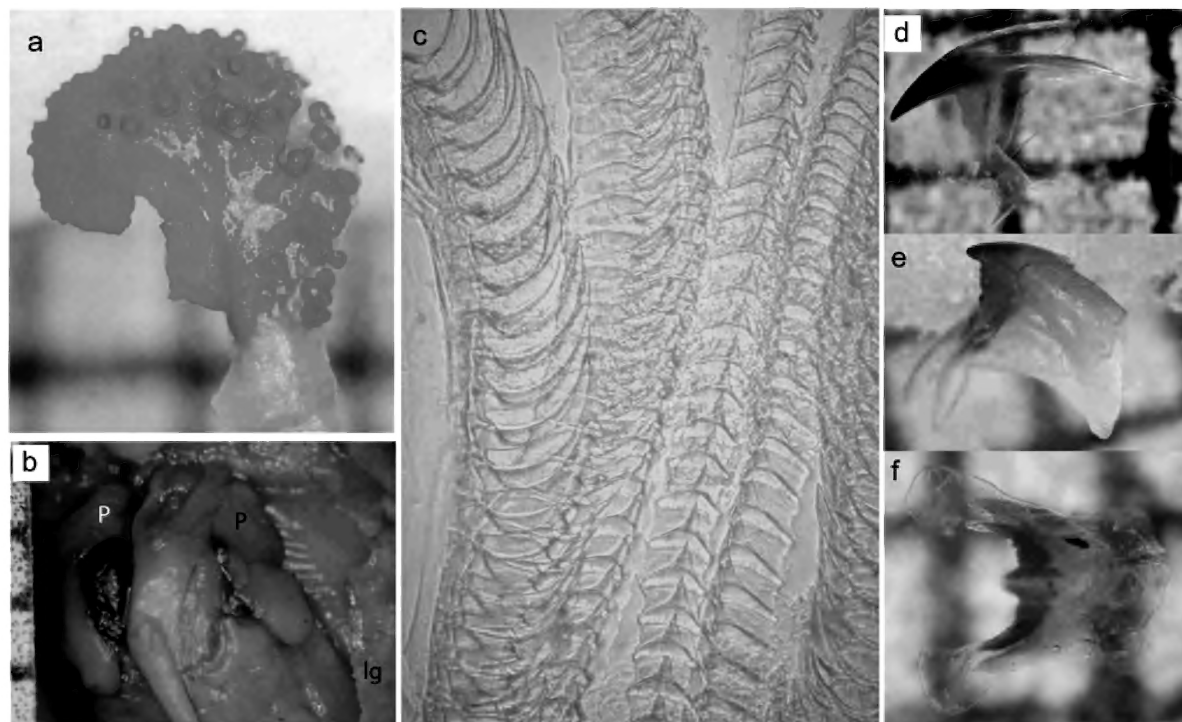

Figure 4. *Dextrasepiola taenia* n. gen. & n. sp. (grids in background: 1 mm × 1 mm): a, left tentacular club, female, paratype 3 (MOV F91361); b, inside mantle cavity: photophores (p), left gill (lg), male, holotype (MOVF80458); c, radula (paratype 1, MOV F91359); d, lateral view of upper beak (MOV F91361); e, lateral view of lower beak (MOV F91361); f, top view of lower beak (MOV F91361).
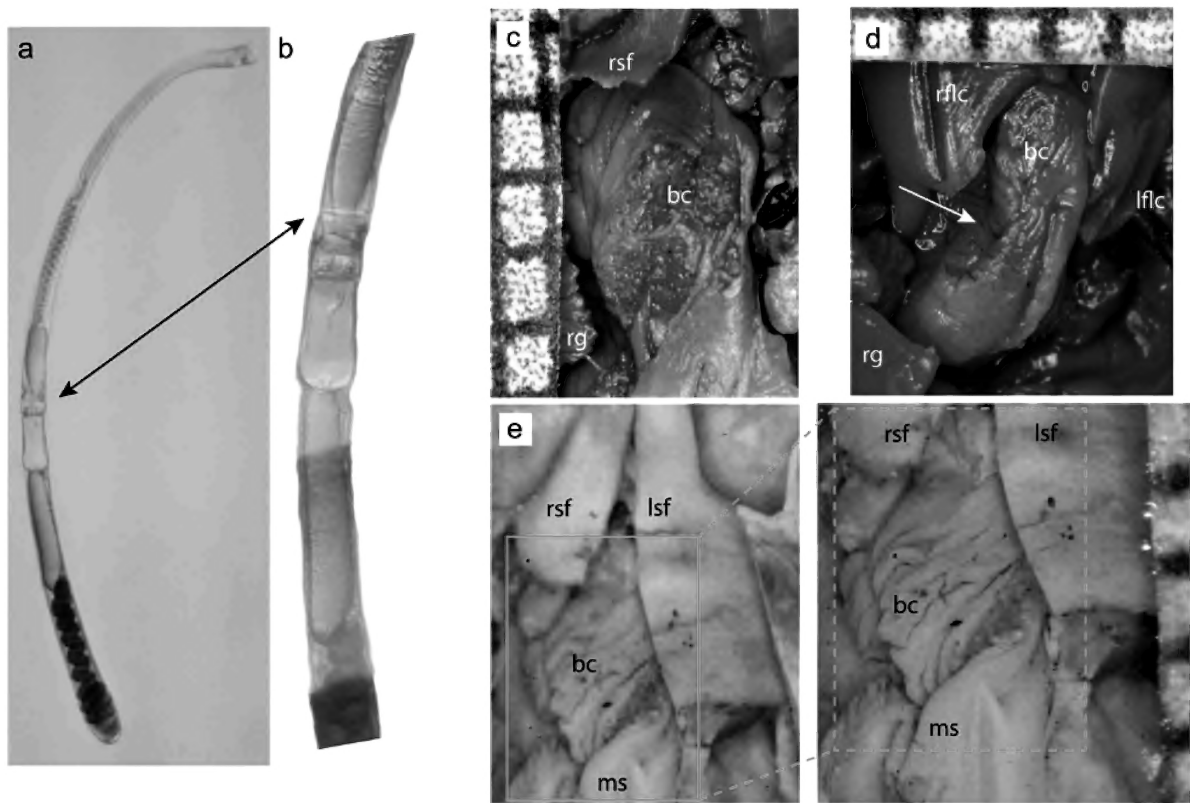
Figure 5. *Dextrasepiola taenia* n. gen. & n. sp. (grids in background: 1 mm × 1 mm): a, spermatophore from the holotype (MOV F80458); b, close-up of cement body; c, bursa copulatrix, paratype 1 (MOV F31359; bc: bursa copulatrix; rg: right gill; rsf: right side of funnel); d, bursa copulatrix, juvenile (MOV F31360; bc: bursa copulatrix; lflc: left funnel locking cartilage; rflc: right funnel locking cartilage; rg: right gill); e, bursa copulatrix, paratype 3 (MOV F31361; bc: bursa copulatrix; lsf: left side of funnel; ms: mantle septum; rsf: right side of funnel); f, close-up of a portion of e, arrow points to opening of bursa copulatrix.

Amutatiola macroventosa n. gen., n. sp.

Figures 6–13; Tables 3, 4

Material examined: Holotype: MOV F80081: south-east Tasmania, 42° 38.1' S, 148° 12.4' E, trawl depth 36–42 m, bottom depth 86–90 m, collected by CSIRO, FRV *Soela* SO1/85/124, 27 Feb 1985, 0331 hr, Rectangular Midwater Trawl with 8 m² mouth area, 1 male, 9.8 mm mantle length, mature (specimen #1).

Paratype 1: MOV F275293: Great Australian Bight, 32° 43' S, 126° 00' E–32° 45' S, 125° 59' E, 40–170 m, collected by CSIRO, FRV *Soela* SO3/80/32, 13 May 1980, 0100 hr, IYGPT, 1 female, 12.2 mm mantle length, mature (specimen #11).

Paratype 2: WAM 3091-83: west side of Irwin Reef, Port Denison, Western Australia, 29° 16' S, 114° 55' E; 7–8 m, collected by N. Sinclair, 4 Apr 1983, Rotenone Station, 1 male, 9.5 mm mantle length, mature (specimen #3).

Paratype 3: MOV F80083: south-east Tasmania, 42° 39.7' S, 148° 12.1' E, trawl depth 5–10 m, bottom depth 90–95 m, collected by CSIRO, FRV *Soela* SO1/85/104, 15 Feb 1985, 2034 hr, Rectangular Midwater Trawl with 8 m² mouth area, 1 male, 9.6 mm mantle length, mature (specimen #2).

Paratype 4: MOV F275294: Great Australian Bight, 33° 30' S, 131° 50.0' E–33° 30' S, 131° 53' E, 200–144 m, collected by FRV *Soela* SO3/80/1, 8 May 1980, 1 female, 12.8 mm mantle length, mature (specimen #9).

Paratype 5: MOV F158244: Luck Bay, western point off beach, Cape Le Grand National Park, Western Australia, 33° 59' S, 122° 13' E, 5 m, active over algae, collected by D. Rawlins, J. Finn and M. Norman, 26 April 1998, 1915 hr, hand net, 1 male, 8.8 mm mantle length, mature (specimen #4).

Paratype 6: MOV F275296: Luck Bay, western point off beach, Cape Le Grand National Park, Western Australia, 33° 59' S, 122° 13' E, 5 m, active over algae, collected by D. Rawlins, J. Finn and M. Norman, 26 April 1998, 1915 hr, hand net, 1 female, 6.2 mm mantle length, subadult (specimen #17).

Paratype 7: MOV F275295: Luck Bay, western point off beach, Cape Le Grand National Park, Western Australia, 33° 59' S, 122° 13' E, 5m, active over algae, collect. by D. Rawlins, J. Finn and M. Norman, 26 April 1998, 1915 hr, hand net, 1 male, 8.1 mm mantle length, mature (specimen #5).

Paratype 8: MOV F91362: Luck Bay, western point off beach, Cape Le Grand National Park, Western Australia, 33° 59' S, 122° 13' E, 5 m, active over algae, collected by D. Rawlins, J. Finn and M. Norman, 26 April 1998, 1915 hr, hand net, 1 male, 6.9 mm mantle length, mature (specimen #7).

Table 3. *Amutatiola macroventosa* n.gen. & n.sp. measurement, counts and indices of male specimens

Species	*Amutatiola macroventosa*						
Museum	MOV	MOV	WAM	MOV	MOV	MOV	MOV
Registration number	F80081	F80083	3091-83	F158244	F275295	F80087	F91362
Specimen number	1	2	3	4	5	6	7
Type status	Holotype	Paratype 3	Paratype 2	Paratype 5	Paratype 7	–	Paratype 8
Cruise	SO1/85	SO1/85	N. Sinclair, 4 Apr1983	–	–	–	–
Station number	124	104	4 Apr 1983, Rotenone Station.	–	–	–	–
Sex	male	male	male	male	male	male	male
Maturity	5	5	5	5	4	5	4
DML (mm)	9.8	9.6	9.5	8.8	8.1	8	6.9
VMLI	109.2	93.8	102.1	–	88	116.3	103.6
HLI	43.9	47.9	40	49.3	59.6	63.8	54.1
HWI	88.8	70.8	90.5	84.2	87.7	101.3	102
NCI	41.1	38.6	45.8	–	43.7	40.2	50.5
MWI	96.9	91.7	87.4	–	91.6	115	111.4
FuLI	69.4	62.5	70.5	–	81.2	61.3	85.5
FuWI	50	43.8	42.1	34.6	55.1	31.3	58.8
FFuI	60.3	66.7	68.7	–	77.8	61.2	79
FLI	62.2	58.3	53.7	–	54	63.8	64.9
FBLI	35.7	30.2	31.6	30.3	29.8	41.3	52.9
FWI	46.9	38.5	33.7	59.7	48.1	58.8	58.4
A_1LI	92.9	87.5	–	140.9	75.3	80	92.4
A_2LI	87.8	82.3	82.1	90.9	91	98.8	103.6
A_3LI	73.5	83.3	71.6	–	–	88.8	105.2
A_4LI	74.5	65.6	73.7	68.2	75.2	77.5	90.9
Arm formula	1.2.4.3.	1.3.2.4.	2.1.4.3.	–	2.1.3.4.	2.3.1.4.	3.2.1.4.
$A_{R1}LI$	84.7	91.7	76.8	102.3	72.8	100	88.4
TtLI	–	161.8	121.1	–	–	87.5	–
ClLI	24.5	21.9	29.5	22.7	32.1	28.8	26.1
ClRC	6	6	6	6	6–8	6–8	6–8
GLI	42.9	42.7	–	–	40	33.7	46.4
GWI	22.4	16.7	–	–	25.3	16.3	18.8
GiLC	21	21	–	–	17	16	16
A_1SC	21	20	19	20	14	28	16
A_2SC	30	30	30	32	33	27	28
A_3SC	–	–	27	–	24	–	24
A_4SC	29	29	27	21	24	26	22
$A_{R1}SC$	19	18	17	–	12	25	14
ClSI	2.4	1.6	1.9	0.6	1.6	2.3	1.9
A_1SI	21.4	17.6	19.8	18.6	20.4	11.9	24.2
A_2SI	4.7	9.7	5.1	7.3	17.4	–	6.7
A_3SI	13.7	8.4	14.5	17.2	20.3	–	20.4
A_4SI	4.1	4.8	8.1	5.6	6.3	–	7.4
SpLI	a:36.2; b:33.5; c:35.7; d:34.0	38.8	42.7	29.3	–	44.8	–
SpWI	a:6.2; b:6.7; c:5.7; d:6	6.7	5.4	6.6	–	7.0	–
SpRI	a:33.5; b:35.7; c:34; d:43.2	40.3	35.5	37.6	–	27.9	–
CBI	a:20.3; b:22; c:19.1; d:20	19.4	18.5	19.4	–	10.9	–

Note: Maturity 4, subadult – sexual characters well distinguished but gonads and accessory organs not completely developed; Maturity 5, adult – sexually mature with spermatophores in Needham's sac in males; ovaries, nidamental and oviducal glands fully developed and ripe, eggs sometimes in oviducts, in females; DML, dorsal mantle length (mm) – measured from anterior-most point of mantle to posterior end of mantle; VMLI, ventral mantle length index – ventral mantle length, measured from anterior border of mantle at ventral midline, to apex of mantle, expressed as a percentage of DML; HLI, head length index – dorsal length of head measured from point of fusion of dorsal arms to anterior tip of dorsal mantle expressed as a percentage of DML; HWI, head width index – greatest width of head at level of eyes expressed as a percentage of DML; NCI, nuchal commissure width index – width of nuchal commissure expressed as a percentage of width of mantle at the position of nuchal commissure; MWI, mantle width index – mantle width at mantle opening expressed as a percentage of DML; FuLI, funnel length index – length of funnel from anterior funnel opening to posterior border of funnel measured along ventral midline expressed as a percentage of DML; FuWI, funnel width index – width of funnel at junction of funnel and head just anterior to funnel locking cartilages expressed as a percentage of DML; FFuI, free funnel index – length of funnel from the anterior opening to the point of dorsal attachment to head expressed as a percentage of funnel length; FLI, fin length index – greatest length of a single fin expressed as a percentage of DML; FBLI, fin base length index – length of fin attachment to mantle expressed as a percentage of DML; FWI, fin width index – greatest width of a single fin expressed as a percentage of DML; A_1LI, arm I length index – length of arm I expressed as a percentage of DML; A_2LI, arm II length index – length of arm II expressed as a percentage of DML; A_3LI, arm III length index – length of arm III expressed as a percentage of DML; A_4LI, arm IV length index – length of arm IV expressed as a percentage of DML; $A_{R1}LI$, right arm I length index – length of right arm I expressed as a percentage of DML (only in males); TtLI, tentacle length index – total length of tentacular stalk and club expressed as a percentage of DML; ClLI, club length index – length of club, measured from proximal-most basal sucker to distal tip of club expressed as a percentage of DML; ClRC, club row count – number of longitudinal rows of suckers across width of club; GLI, gill length index – length of gill expressed as a percentage of DML; GWI, gill width index – greatest width of gill expressed as a percentage of DML; GiLC, gill lamellae count – number of lamellae on outer demibranch, excluding terminal lamella; A_1SC, sucker counts of arm I – total number of suckers or sucker stalks on arm I; A_2SC, sucker counts of arm II – total number of suckers or sucker stalks on arm II; A_3SC, sucker counts of arm III – total number of suckers or sucker stalks on arm III; A_4SC, sucker counts of arm IV – total number of suckers or sucker stalks on arm IV; $A_{R1}SC$, sucker counts of right arm I – total number of suckers or sucker stalks on right arm I (only in males); ClSI, club sucker index – diameter of largest club sucker expressed as a percentage of DML; A_1SI, arm I sucker index – diameter of largest sucker on arm I expressed as a percentage of DML; A_2SI, arm II sucker index – diameter of largest sucker on arm II expressed as a percentage of DML; A_3SI, arm III sucker index – diameter of largest sucker on arm III expressed as a percentage of DML; A_4SI, arm IV sucker index – diameter of largest sucker on arm IV expressed as a percentage of DML; SpLI, spermatophore length index – length of spermatophore expressed as a percentage of DML; SpWI, spermatophore width index – greatest width of spermatophore expressed as a percentage of spermatophore length; SpRI, sperm reservoir index – length of sperm reservoir expressed as a percentage of spermatophore length; CBI, cement body index – length of cement body expressed as a percentage of spermatophore length.

Table 4. *Amutatiola macroventosa* n.gen. & n.sp. measurement, counts and indices of female specimens

Species	Amutatiola macroventosa									
Museum	MOV	MOV	MOV	MOV	MOV	MOV	MOV	MOV	MOV	MOV
Registration number	F80084	F275294	F77100	F275293	F77100	F77100	F77100	F80084	F80087	F275296
Specimen number	8	9	10	11	12	13	14	15	16	17
Type status	–	Paratype 4	–	Paratype 1	–	–	–	–	–	Paratype 6
Cruise	Q/47	SO3/80	SO1/82	SO3/80	SO1/82	SO1/82	SO1/82	Q/47	–	–
Station number	51	1	1	32	1	1	1	51	–	–
Sex	female	female	female	female	female	female	female	female	female	female
Maturity	5	5	4	5	4	4	4	4	4–5	3
DML (mm)	13.2	12.8	12.6	12.2	11.9	11.6	10.6	10.3	9.2	6.2
VMLI	91.7	93	85.7	100	89.9	87.9	89.6	83.5	103.3	90.1
HLI	58.3	44.5	49.2	50.8	52.1	48.3	46.2	48.5	48.9	47
HWI	55.3	64.8	67.5	67.2	68.1	68.1	82.1	64.1	72.8	99.5
NCI	50	55.2	47.6	43	56.5	53.3	59	46.7	54	56.1
MWI	71.2	75	83.3	76.2	86.6	92.2	91.5	72.8	94.6	101.9
FuLI	58.3	62.5	62.2	59	63.1	64.5	74.2	50.5	65.2	89.3
FuWI	44.7	38.3	42.7	39.3	44.5	40.3	45.7	39.8	33.7	53.3
FFuI	79.2	55	63.8	69.4	63.9	60.2	57.2	71.2	66.7	67.8
FLI	49.2	39.8	52.4	50	67.2	53.4	56.6	48.5	64.1	62.6
FBLI	24.2	32.8	27	36.9	32.8	33.6	34	29.1	41.3	35
FWI	34.1	36.7	38.1	36.9	63	38.8	47.2	38.8	52.2	53.5
A_1LI	65.9	54.7	47.6	57.4	54.6	64.7	66	58.3	76.1	67.6
A_2LI	83.3	78.1	55.6	77.9	67.2	77.6	84.9	63.1	87	93.3
A_3LI	–	74.2	67.5	69.7	88.2	90.5	89.6	68	81.5	98.7
A_4LI	69.7	66.4	47.6	53.3	63	77.6	66	63.1	76.1	76.6
Arm formula	–	2.3.4.1.	3.2.4.=1.	2.3.4.1.	3.2.4.1.	3.2.=4.1.	3.2.4.=1.	3.2.=4.1.	2.3.4.=1.	3.2.4.1.
TtLI	–	132.8	–	–	–	–	–	–	108.7	–
ClLI	–	27.3	–	–	–	–	–	–	38	32.1
ClRC	–	68	–	–	–	–	–	–	6	68
GLI	40.9	33.6	38.1	38.5	31.9	35.3	40.6	25.2	42.4	35.3
GWI	20.5	14.1	22.2	19.7	16.8	18.1	12.3	15.5	23.9	18.3
GiLC	19	17	17	17	17	17	21	16	18	19
A_1SC	32	34	27	30	34	33	32	29	32	29
A_2SC	40	44	26	31	45	44	37	43	35	35
A_3SC	–	34	24	–	38	35	37	33	–	29
A_4SC	29	33	31	31	36	38	33	31	–	25
ClSI	–	1.2	–	–	–	–	–	–	2.8	2.9
A_1SI	3	3.4	4	3.6	4.2	4.3	4.7	4.3	–	5.3
A_2SI	3.5	3.4	3.9	3.6	4.1	4.2	4.6	4.3	–	5.8
A_3SI	3.3	3.4	3.3	3.8	3.5	3.6	4	3.9	–	5.3
A_4SI	3	3.4	3.2	2.7	3.4	3.4	3.8	2.9	–	4.5
NidGI	39.9	41.5	50.6	44	51.3	53.1	56.6	37.2	44.8	–

Note: Maturity 3, juvenile – young specimen in which some sexual characters are distinguished; Maturity 4, subadult – sexual characters well distinguished but gonads and accessory organs not completely developed; Maturity 5, adult – sexually mature with spermatophores in Needham's sac in males; ovaries, nidamental and oviducal glands fully developed and ripe, eggs sometimes in oviducts, in females; DML, dorsal mantle length (mm) – measured from anterior-most point of mantle to posterior end of mantle; VMLI, ventral mantle length index, measured from anterior border of mantle at ventral midline, to apex of mantle, expressed as a percentage of DML; HLI, head length index – dorsal length of head measured from point of fusion of dorsal arms to anterior tip of dorsal mantle expressed as a percentage of DML; HWI, head width index – greatest width of head at level of eyes expressed as a percentage of DML; NCI, nuchal commissure width index – width of nuchal commissure expressed as a percentage of width of mantle at the position of nuchal commissure; MWI, mantle width index – mantle width at mantle opening expressed as a percentage of DML; FuLI, funnel length index – length of funnel from anterior funnel opening to posterior border of funnel measured along ventral midline expressed as a percentage of DML; FuWI, funnel width index – width of funnel at junction of funnel and head just anterior to funnel locking cartilages expressed as a percentage of DML; FFuI, free funnel index – length of funnel from the anterior opening to the point of dorsal attachment to head expressed as a percentage of funnel length; FLI, fin length index – greatest length of a single fin expressed as a percentage of DML; FBLI, fin base length index – length of fin attachment to mantle expressed as a percentage of DML; FWI, fin width index – greatest width of a single fin expressed as a percentage of DML; A_1LI, arm I length index – length of arm I expressed as a percentage of DML; A_2LI, arm II length index – length of arm II expressed as a percentage of DML; A_3LI, arm III length index – length of arm III expressed as a percentage of DML; A_4LI, arm IV length index – length of arm IV expressed as a percentage of DML; TtLI, tentacle length index – total length of tentacular stalk and club expressed as a percentage of DML; ClLI, club length index – length of club, measured from proximal-most basal sucker to distal tip of club expressed as a percentage of DML; ClRC, club row count – number of longitudinal rows of suckers across width of club; GLI, gill length index – length of gill expressed as a percentage of DML; GWI, gill width index – greatest width of gill expressed as a percentage of DML; GiLC, gill lamellae count – number of lamellae on outer demibranch, excluding terminal lamella; A_1SC, sucker counts of arm I – total number of suckers or sucker stalks on arm I; A_2SC, sucker counts of arm II – total number of suckers or sucker stalks on arm II; A_3SC, sucker counts of arm III – total number of suckers or sucker stalks on arm III; A_4SC, sucker counts of arm IV – total number of suckers or sucker stalks on arm IV; ClSI, club sucker index – diameter of largest club sucker expressed as a percentage of DML; A_1SI, arm I sucker index – diameter of largest sucker on arm I expressed as a percentage of DML; A_2SI, arm II sucker index – diameter of largest sucker on arm II expressed as a percentage of DML; A_3SI, arm III sucker index – diameter of largest sucker on arm III expressed as a percentage of DML; A_4SI, arm IV sucker index – diameter of largest sucker on arm IV expressed as a percentage of DML; NidGI, nidamental gland index – length of nidamental gland expressed as a percentage of DML.

Other material: MOV F80087: Franklin Island, South Australia, 32° 27'S, 133° 40'E, sub-light, 4 Apr 1953, 1 male, 8.0 mm mantle length, mature; 1 female, 9.2 mm mantle length, subadult (specimens #6, 16).

MOV F80085: Great Australian Bight, 32° 43' S, 126° 00' E–32° 45' S, 125° 59' E, 40–170 m, collected by CSIRO, FRV *Soela* SO3/80/32, 13 May 1980, 0100 hr, IYGPT, 1 male, 6.6 mm mantle length, subadult; 9 males, 7.7–9.6 mm mantle length, mature; 3 females, 4.7–6.5 mm mantle length, juveniles.

MOV F80086: Great Australian Bight, 33° S, 126° E, 48–50 m, collected by CSIRO, FRV *Soela* S03/80/33, 13 May 1980, IYGPT, 1 male, 7.1 mm mantle length, subadult; 2 males, 8.5–9.8 mm mantle length, mature; 1 female, 12.2 mm mantle length, mature.

MOV F80084: Great Australian Bight, 33° 22' S, 125° 27' E – 33° 23' S, 125° 27' E, 64 m, collected by CSIRO, FRV *Courageous* Q47/51, 7 Apr 1979, 2 females, 10.3–13.2 mm mantle length, mature (specimens #8, 15).

MOV F77100: Bass Strait, 60 km west of Cape Frankland, Flinders Island, 39° 53' S, 147° 03' E, trawl depth 20–60 m, bottom depth 66–68 m, collected by CSIRO, FRV *Soela* SO1/82/1, 16 Jan 1982, 1 female, 5.6 mm mantle length, juvenile; 4 females, 10.6–12.6 mm mantle length, mature (specimens #10, 12, 13, 14; four larger specimens).

MOV F80082: Great Australian Bight, 33° 30' S, 131° 50.0' E–33° 30' S, 131° 53' E, 200–144 m, collected by FRV *Soela* SO3/80/1, 8 May 1980, 9 males, 4.8–7.6 mm mantle length, immature; 3 females, 5.4–6 mm mantle length, immature.

MOV F80080: Great Australian Bight, 32° 22' S, 131° 19' E–32° 17' S, 131° 18' E, 54–68 m, collected by CSIRO, FRV *Soela* SO3/81/41, 6 Aug 1981, 2130 hr, IYGPT, 2 females, 10.4–13.3 mm mantle length, mature.

MOV F158291: Port Victoria Jetty, South Australia, 34° 29' 45" S, 137° 28' 53" E, collected by J. Finn and Mark D. Norman, 21 May 1998, 1 female, 10.9 mm mantle length, mature.

Description: Mantle (figs 6a–c, 7, 8a–b) short dome-shaped with blunt posterior end, slightly longer than wide, muscular, studded by large chromatophores, fused with head dorsally. Anterior ventral mantle margin (figs 6b, 7b, 8b) shallowly concave with blunt lateral projections at position of mantle–funnel connectives, reaching level of posterior margin of eye lens. Head slightly narrower than mantle, head length about 50% of mantle length. Nuchal commissure moderately wide, width 38.6–50.5% of mantle width at commissure in males, 43–59% of mantle width at commissure in females, commissure does not reach beyond medial borders of bulbous eyes.
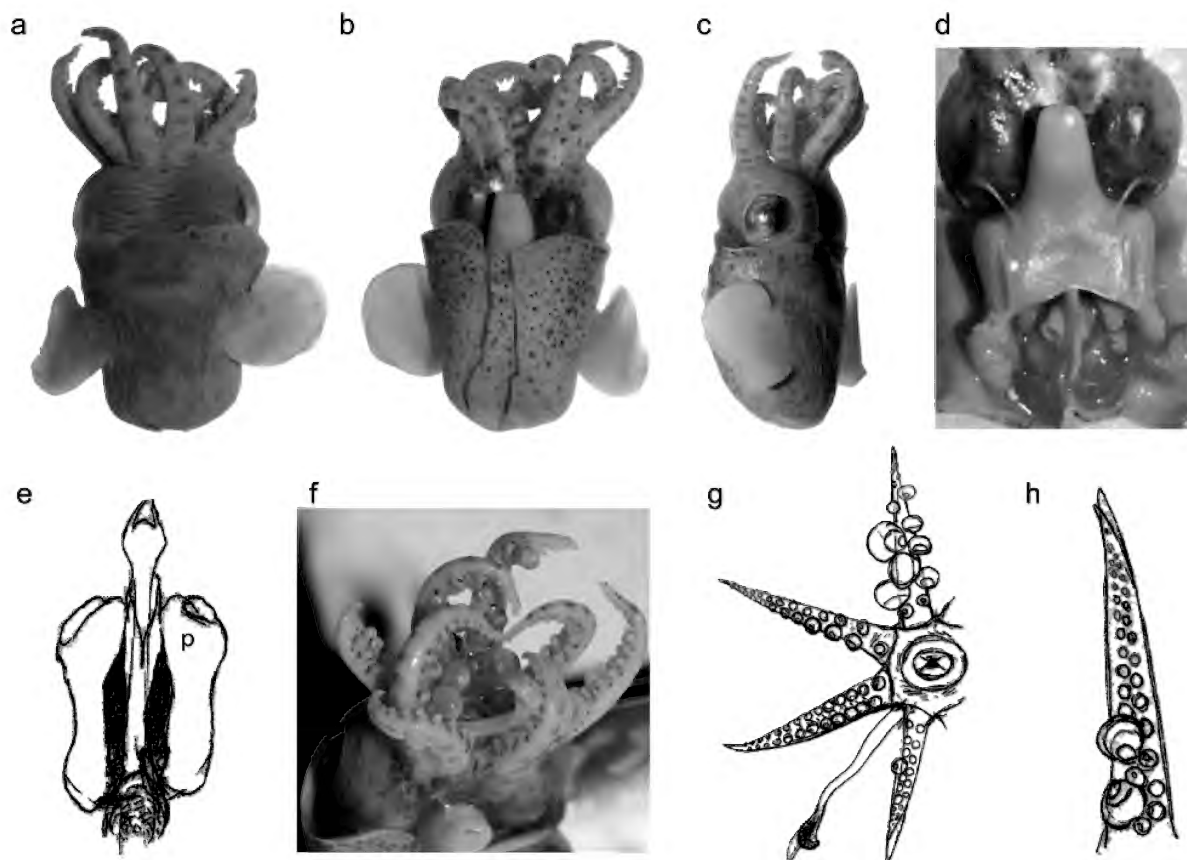
Figure 6. *Amutatiola macroventosa* n. gen. & n. sp. male, holotype (MOV F80081): a, dorsal view; b, ventral view; c, lateral view; d, inside mantle cavity showing funnel locking cartilages, partial photophores; e, diagram of photophores (p; drawn by T. Okutani); f, arm crown showing arm sucker arrangement; g, diagram of arm crown showing sucker arrangement (drawn by T. Okutani); h, diagram of arm IV showing sucker arrangement (drawn by T. Okutani).
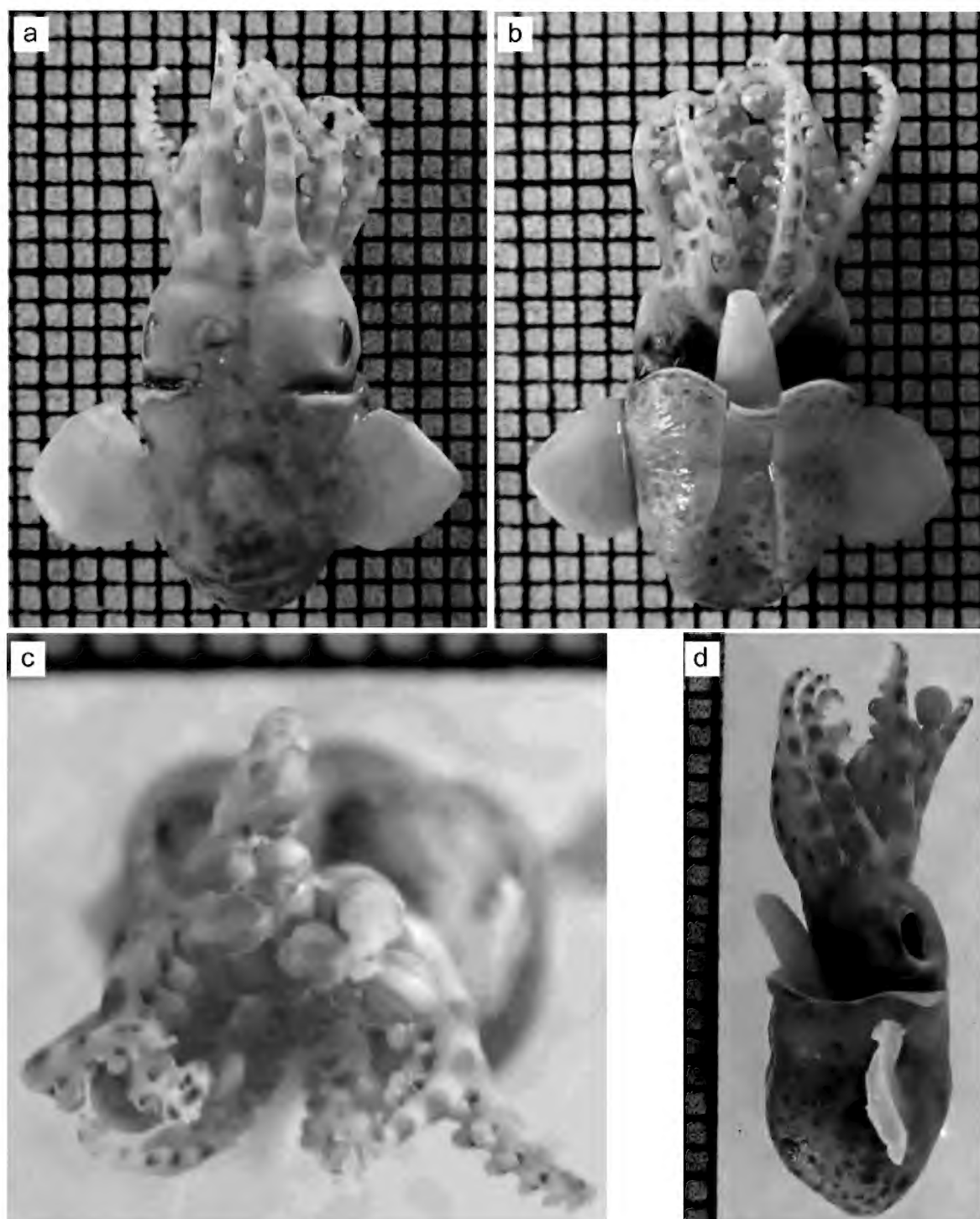
Figure 7. *Amutatiola macroventosa* n. gen. & n. sp. male, paratype 7 (MOV F275295; grids in background: 1 mm × 1 mm): a, dorsal view; b, ventral view; c, arm crown showing arm sucker arrangement; d, lateral view.
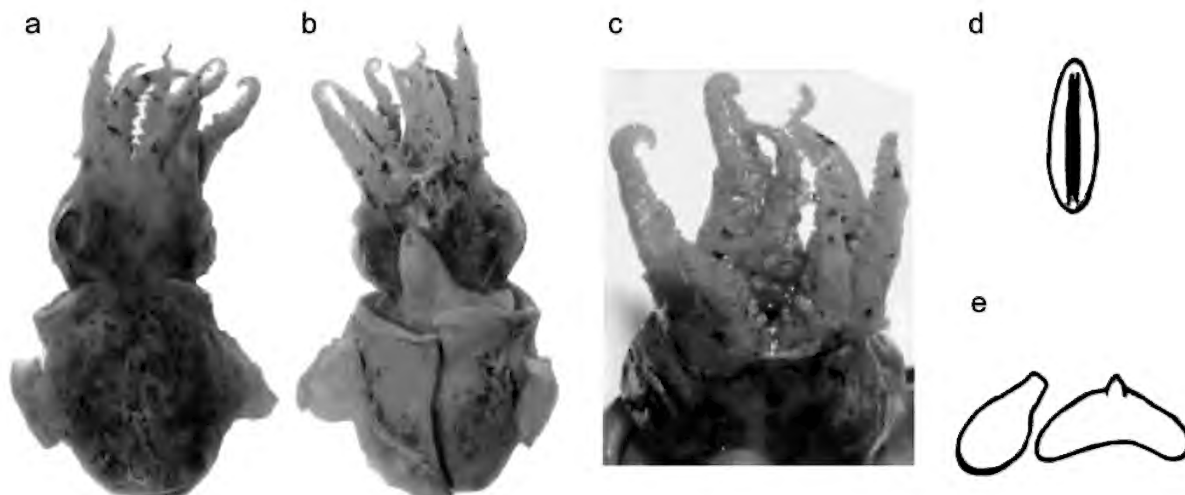
Figure 8. *Amutatiola macroventosa* n. gen. & n. sp.: a, dorsal view, female, paratype 1 (MOV F275293); b, ventral view, female, paratype 1 (MOV F275293); c, arm crown showing arm sucker arrangement, female, paratype 1 (MOV F275293); d, diagram of funnel locking cartilage, female, paratype 1 (MOV F275293; drawn by T. Okutani); e, diagram of funnel organs, male, paratype 3 (MOV F80083; drawn by T. Okutani).
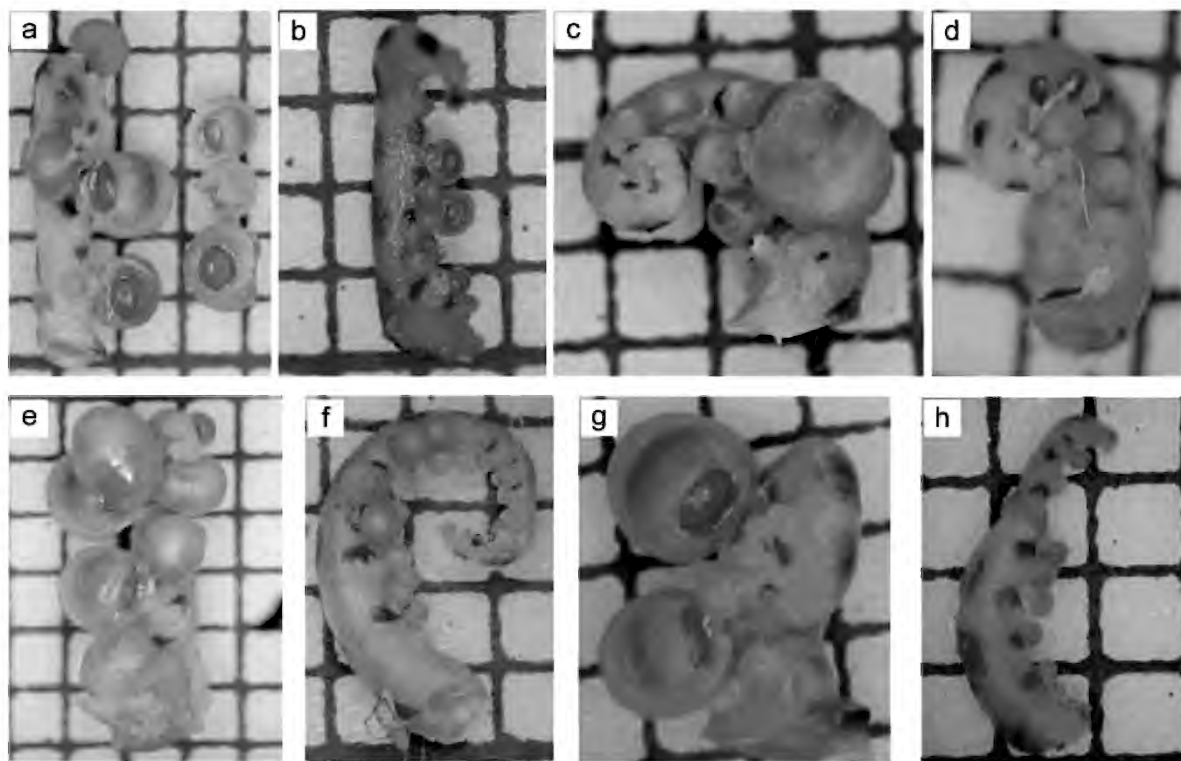
Figure 9. *Amutatiola macroventosa* n. gen. & n. sp. male, paratype 5 (MOV F158244). Oral views of arms (grids in background: 1 mm × 1 mm): a, right arm I; b, right arm II; c, right arm III; d, right arm IV; e, left arm I; f, left arm II; g, left arm III; h, left arm IV.

Head almost entirely occupied by a pair of large bulbous eyes with elliptical eye lid. Cornea membrane protecting eye attached to skin of head along dorsal margin. Olfactory papilla located behind posterior corner of eye orbit, ventral photosensitive vesicle not found. Funnel (figs 6b, d, 7b, d, 8b) long and slender, lacking pigmentation, reaching the level beyond anterior eye margin, and free from head for 55–80% of funnel length. Funnel connects to head by an oblique muscle band extending from beneath anterior end of funnel locking cartilage to ventro-posterior corner of eye.

Dorsal funnel organ (fig. 8e) broad V-shaped with a blunt papilla at the apex. A prominent funnel retractor muscle connected funnel near base with ventro-posterior periphery of eye. Ventral elements of funnel organ (fig. 8e) tear drop-shaped pad, narrower anteriorly. Funnel valve well developed on dorsal roof, tongue shaped, located well behind funnel aperture.

Funnel locking cartilage (fig. 8d) elongated oval with simple, slightly curved depression in middle, mantle locking cartilage long, low ridge.

Fins (figs 6a–c, 7a–b, d, 8a–b) circular in outline, attach to mantle at mid-point of mantle, meeting mantle smoothly posteriorly, anterior border of fins project forward prominently forming a deep cleft with mantle, border not reaching level of mantle margin, posterior borders of fins convex, less pronounced. Length of fin base about 33% of mantle length.

Arms moderately long, rounded aborally, flattened orally, lacking aboral keel and protective membranes. Arm formula inconsistent, in males arm I or II usually longest, arm III or IV usually shortest; in females, arm II or III longest, arm I or IV shortest. Arm suckers biserial with strong sexual dimorphism in sucker sizes and sucker ring dentitions. Web moderately pronounced between arms III and IV. No heteromorphism exists in morphology of right and left arms in males, specifically in the dorsal arms. Webs shallow between all arms except arms IV where no web exists, web D encloses base of tentacles in both sexes.

In males (figs 6f–h, 7, 9), arm I with up to 28 suckers, some suckers in proximal portion of arm enlarged: first to sixth proximal suckers on both dorsal and ventral series enormously enlarged, the third sucker on ventral series the largest, enlarged suckers on ventral series generally larger than dorsal series. Diameter of enlarged suckers exceed arm width. Arm II with up to 32 suckers, of which proximal second to seventh on ventral series slightly enlarged; no enlargement of suckers on dorsal series, suckers gradually reduced in size from proximal to distal end of arm II. Arm III with approximately 27 suckers, first to fourth proximal suckers on ventral series enormously enlarged (1.6 mm in diameter); no enlargement of suckers on dorsal
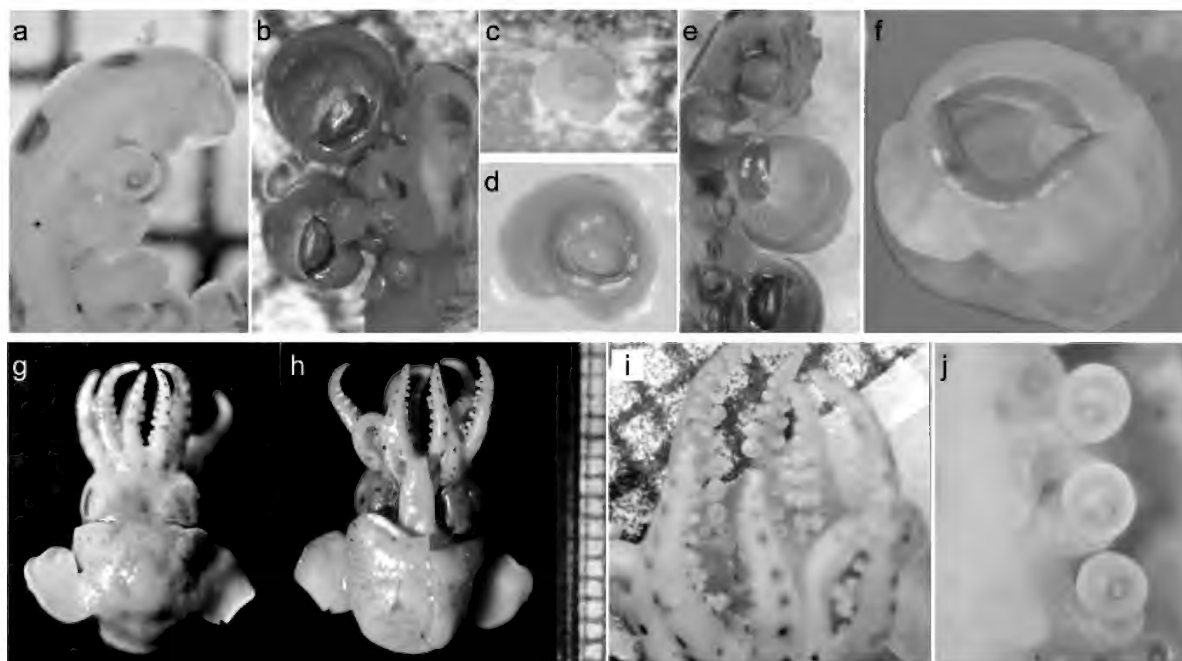

Figure 10. *Amutatiola macroventosa* n. gen. & n. sp. Sucker ring dentition (grids in background: 1 mm × 1 mm): a, left arm IV of male, paratype 5 (F158244) showing normal (non-enlarged) suckers near arm tip; b, right arm III of male, paratype 5 (F158244) showing sucker ring of enlarged suckers; c, d, normal sucker of left arm II of male, paratype 5 (F158244); e, left arm I of male, paratype 5 (F158244) showing enlarged suckers; f, an enlarged sucker of e showing sucker ring; g, dorsal view of female (F275296) showing non-enlargement of suckers; h, ventral view of female (F275296) showing non-enlargement of suckers; i, arm crown of female (F275296) showing non-enlargement of suckers; j, close-up of a portion of an arm of i showing sucker ring dentition.

series. Arm IV with approximately 29 normal suckers, no enlargement. Chitinous sucker rings of normal suckers almost at the same level as muscular rim of suckers, sucker ring margin minutely denticulated (figs 10a, c, d). Chitinous sucker rings of enlarged suckers (figs 10b, e, f) extended aborally beyond level of muscular sucker rims, chitinous ring often covered by thin, opaque membrane, sucker ring divided into 2 parts, distal 33–50% of sucker ring long, semicircular shape, proximal portion of sucker ring lower than distal portion, crescent shaped.

Females with more suckers than the corresponding arm in males. Arm I with up to 34 suckers, arm II with up to 45 suckers, arm III with up to 38 suckers and arm IV to 38 suckers. No enlarged sucker in females (figs 8c, 10g–j).

Chitinous sucker rings (figs 10i–j) similar to the non-enlarged suckers in males, sucker rings entire, with minutely denticulated margin.

Tentacle weak, longer than arms. Club slightly expanded, curled due to the presence of the dorsal web, small carpal suckers in 4 series, manal and dactyl suckers small, numerous in approximately 6–8 series, carpal and manal suckers much larger than dactylus suckers, in the central part of club, particularly those on dorsal 2 series slightly larger than others, suckers slightly diminish in size towards club margins and distally (fig. 11a). Sucker ring dentition of largest club sucker finely toothed around entire minute circle.

Gills with 16–21 lamellae per demibranch, plus a terminal
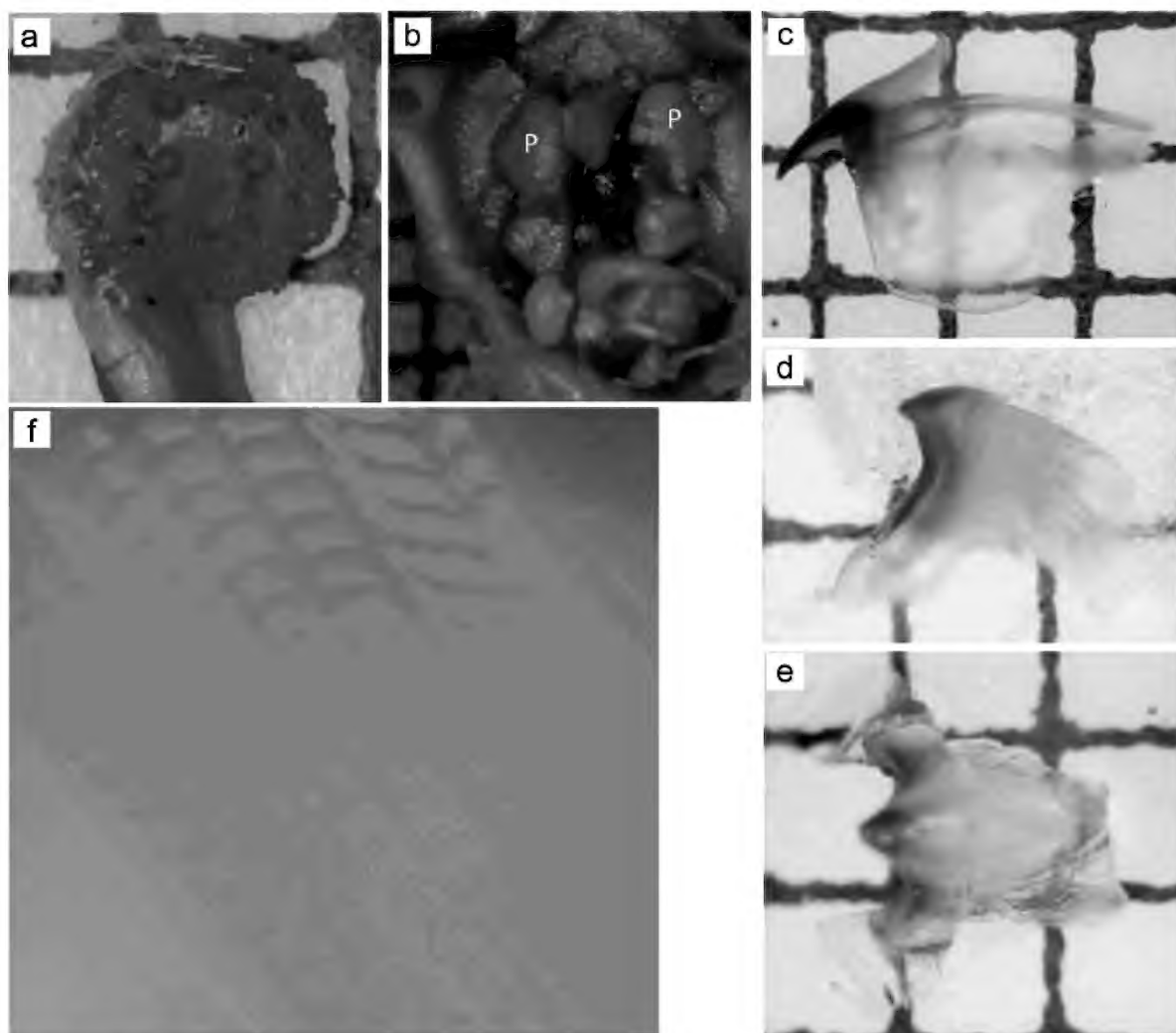
Figure 11. *Amutatiola macroventosa* n.gen. & n.sp. (grids in background: 1 mm × 1 mm): a, right tentacular club, male, paratype 5 (MOV F158244); b, photophores (p), male, paratype 5 (MOV F158244); c, lateral view of upper beak, female, paratype 1 (MOV F275293); d, lateral view of lower beak, female, paratype 1 (MOV F275293); e, top view of lower beak, female, paratype 1 (MOV F275293); f, radula, female, paratype 1 (MOV F275293).

lamella. A pair of yellowish photophores (figs 6e, 11b), opaque with both ends swollen, dumbbell-shaped or elongated kidney-shaped, on both sides of ink sac.

Upper beak (fig. 11c) rostrum slightly curved with pointed rostral tip; jaw angle obtuse; wing long, shoulder (cutting edge) nearly straight; lateral wall deep; rostrum dark brown to black, hood, shoulder and dorsal part of lateral wall light brown, posterior part of hood, most of lateral wall unpigmented, transparent.

Lower beak (figs 11d, e) wide; rostral tip blunt; jaw edge almost smooth, jaw angle indistinct; blunt tooth on shoulder; no notch in hood; lateral wall without fold or ridge, roughly elongate rhomboidal with lower edge concave, corner faintly produced; rostrum and hood light brown in colour, wings and posterior part of lateral wall transparent. Radula (fig. 11f) 7 series, each row with 7 unicuspid teeth.

Gladius absent.

Spermatophores (fig. 12a) small, 8 spermatophores from 5 individuals approximately 2.6–4.1mm long (spermatophore length index 29.3–42.7), greatest width approximately 0.17–0.25 mm (spermatophore width index 5.4–7), sperm mass moderately long, sperm reservoir about 0.97–1.5 mm (sperm reservoir index 27.9–43.2), structure simple, no obvious ornamental appearance, cement body approximately 0.39–0.75 mm long, connects to sperm reservoir by a narrow neck, oral end of cement body elongated funnel-shaped (cement body index 11–22), appearance of ejaculatory apparatus plain, without spiral appearance of the preceding species.

Bursa copulatrix closed type, pouch like (Bello, 2020; fig. 12b), opening at level of base of left gill, running dorsally, on a mature female (Paratype 1) anterior end width approximately 2 mm with slit-like opening approximately 1.1 mm long, length of pouch approximately 2.3 mm, some spermatangia visible at opening of bursa. Mature and maturing females with large nidamental gland, (nidamental gland index 37.2–56.6).

Alcohol-preserved specimens brown in colour, dorsal mantle surface slightly darker than ventral surface. Dark blackish brown chromatophores scattered over brown-coloured background on both dorsal and ventral surfaces of head and mantle, and along aboral surface of all arms. Surfaces of fins devoid of chromatophores and pigmented spots, except a semicircular patch of brown chromatophores along fin insertion on dorsal side of fin. Skin smooth, lacking sculpture or papillae.

Etymology: Species epithet *macroventosa* is derived from Greek *makros* meaning large plus Latin *ventosa* meaning suction cup or sucker. The name denotes the presence of the greatly enlarged suckers on some arms of mature males.

Distribution: Flinders Island, Bass Strait, and south-eastern Tasmania to South Australia and the Great Australian Bight to Port Denison, Western Australia (fig. 13).
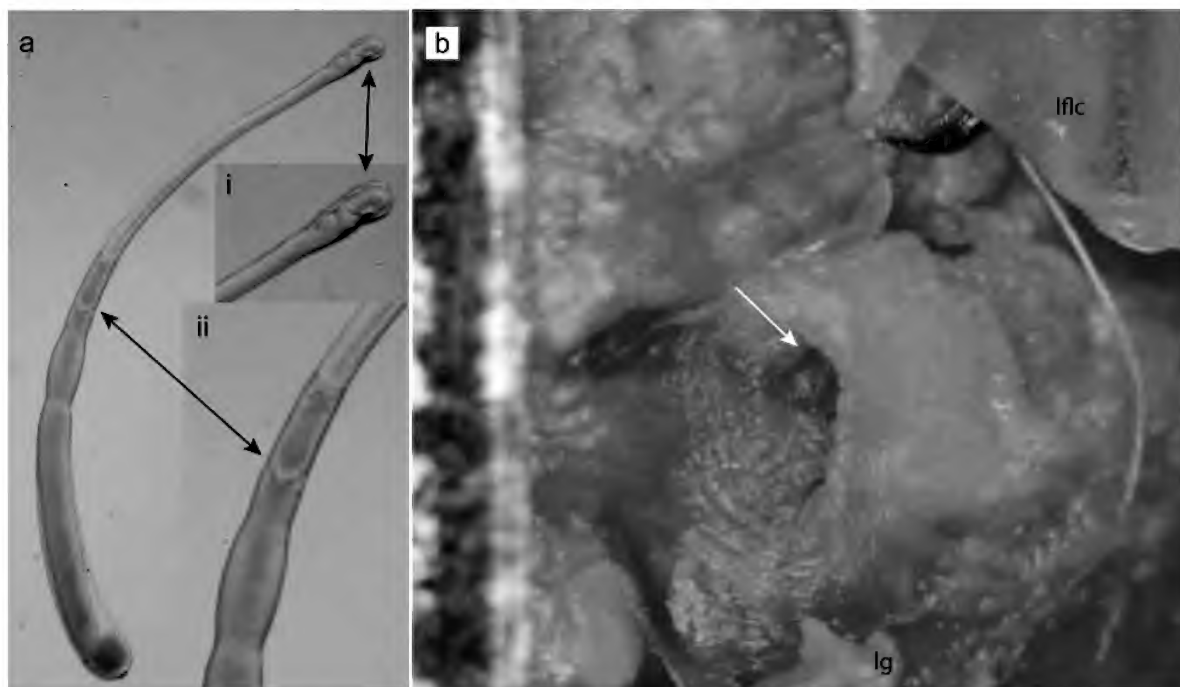

Figure 12. *Amutatiola macroventosa* n. gen. & n. sp.: a, spermatophore, holotype (MOV F80081) Spermatophore length, 3.55 mm (insets: i, close-up of oral cap; ii, close-up of cement body); b, Bursa copulatrix, paratype 1 (MOV F275293; black scale: 1 mm/division) (lflc: left funnel locking cartilage; lg: left gill); arrow points to the bursa copulatrix entrance.

Remarks: Apart from *Dextrasepiola taenia* n. sp. described earlier in this paper, all known species of the subfamily Sepiolinae have the left dorsal arm of maturing and mature males hectocotylised and sucker stalks of some suckers in the copulatory apparatus of the hetocotylus modified into horn-like, hook-like, papillae or laminae (Bello, 2020; Naef, 1912a, b; 1923; Nesis, 1982). The present species is unique in having enormously enlarged suckers and lacking a hectocotylised arm bearing highly modified sucker stalks in males. There are some species of Sepiolinae that carry enlarged suckers in hectocotylised arms (Bello, 2020; Naef, 1923), but none is so pronounced as in this species. The female has normal-sized suckers but more of them. In addition to sucker size, strong sexual dimorphism exists in the dentition of the sucker ring: the dentition of the sucker ring of enlarged suckers in males conspicuously differs from that of the females and the non-enlarged suckers in males.

The structure of the cement body and the sperm mass of the spermatophore of this species is simple in appearance, with no obvious ornamentation, as seen in the preceding species or in *Sepietta oweniana* (d'Orbigny in Férussac and d'Orbigny, 1841; cf. figs 5a, b, 12a; Øresland and Oxby, 2021, figs 59–61).

As in the preceding species, the ranges of the morphometric indices are wide (Tables 3–4). This is certainly due to the range of the state of specimens prior to and during fixation and preservation. With such a wide range of values, it is of dubious value to use them to delineate a specific index for the species.

Figure 13. Distributional map of *Dextrasepiola taenia* n. gen. & n. sp. (blue) and *Amutatiola macroventosa* n. gen. & n. sp. (red).

Table 5. Comparison of genera of Sepiolinae (after Bello, 2020 and present results)

	Sepiola Leach, 1817	Inioteuthis Verrill, 1881	Euprymna Steenstrup, 1887	Sepietta Naef, 1912	Rondeletiola Naef, 1921	Adinaefiola Bello, 2020	Boletzkyola Bello, 2020	Lusepiola Bello, 2020	Eumandya Bello, 2020	Dextrasepiola n.gen.	Amutatiola n.gen.
Fins	rounded; fin length about half mantle length	rounded; fin length about half mantle length	rounded; fin length half mantle length	rounded or bluntly angled laterally; fin length about half mantle length	bluntly angled laterally; fin length about half mantle length	rounded; fin length about half mantle length	rounded; fin length about half mantle length	rounded with large anterior lobe, may reach anterior mantle margin; fin length about 50–66% mantle length	rounded; fin length half mantle length	rounded with large anterior lobe, not reaching anterior mantle margin; fin length about 50–80% mantle length	rounded with large anterior lobe, not reaching anterior mantle margin; fin length about 40–66% mantle length
Arm suckers	biseriate on arms I to III and at least proximally on arm IV	biseriate on all arms	4 longitudinal series, exceptionally in 8 series	biseriate on all arms	biseriate on all arms	biseriate on all arms	biseriate on all arms	biseriate on all arms	biseriate on all arms	biseriate on all arms	biseriate on all arms
Club suckers	4–8 longitudinal series	8–10 longitudinal series	numerous minute suckers in a few tens of longitudinal series	12 or more longitudinal series	16 longitudinal series	8 longitudinal series	8 longitudinal series	4–8 longitudinal series	6–14 longitudinal series	4–8 longitudinal series	4–8 longitudinal series
Nuchal commissure (mantle-head occipital band)	narrow, not reaching over ocular globes	narrow, not reaching over ocular globes	broad, extending over ocular globes	narrow, not reaching over ocular globes	narrow, not reaching over ocular globes	narrow, not reaching over ocular globes	narrow, not reaching over ocular globes	narrow, not reaching over ocular globes	broad, extending over ocular globes	narrow, not reaching over ocular globes, about 25–40% of its width	moderately wide, not reaching over ocular globes, about 38–59% of its width
Photophores on ventral surface of ink-sac	one pair, kidney-shaped	absent	one pair, kidney-shaped	absent	one single, bipartite, oval-shaped	one pair, kidney-shaped	one single, cordiform	one pair, kidney-shaped	one pair, kidney-shaped	one pair, dumbbell-shaped	one pair, dumbbell-shaped or elongated kidney-shaped
Gladius	present, reduced	absent	absent	present, reduced	absent	present, reduced	absent	absent	absent	absent	absent
Ventral mantle margin	slightly sinuate, without any deep funnel indentation	slightly sinuate, without any deep funnel indentation	slightly sinuate, without any deep funnel indentation	slightly sinuate, without any deep funnel indentation	slightly sinuate, without any deep funnel indentation	with deep funnel indentation and markedly sinuate margin.	slightly sinuate, without any deep funnel indentation	slightly sinuate, without any deep funnel indentation	faintly sinuate or with slightly deep funnel indentation	slightly sinuate, without any deep funnel indentation	slightly sinuate, without any deep funnel indentation
Hectocotylized arm in male	left arm I, tripartite	left arm I, tripartite	left arm I, thicker than right arm I, bipartite	left arm I, tripartite	left arm I, tripartite	left arm I, tripartite	left arm I, tripartite	left arm I, tripartite	left arm I bipartite	right arm I, tripartite	No hectocotylized arm; some arm suckers in mature males grossly enlarged

	Sepiola Leach, 1817	*Inioteuthis* Verrill, 1881	*Euprymna* Steenstrup, 1887	*Sepietta* Naef, 1912	*Rondeletiola* Naef, 1921	*Adinaefiola* Bello, 2020	*Boletzkyola* Bello, 2020	*Lusepiola* Bello, 2020	*Eumandya* Bello, 2020	*Dextrasepiola* n.gen.	*Amutatiola* n.gen.
Basal part of hectocotylus	with three suckers, two ventral and one dorsal	with three suckers, two ventral and one dorsal	occupying 20–50% of arm, with regular suckers	with three or four suckers, two ventral and one or two dorsal	with three suckers, two ventral and one dorsal	either with three suckers, two ventral and one dorsal, or two ventral suckers only	with one incomplete transverse series of suckers (only ventral one is present)	with four regular suckers in two series	occupying 50–66% of arm, with regular suckers	with five suckers in two series	–
Copulatory apparatus	with transverse formation of two ventral and two dorsal modified suckerless pedicels, all four of them lengthened and fused with each other throughout their length (few additional dorsal modified pedicels may be present mesially to transverse formation)	broadly enlarged, ear-shaped, involving about six dorsal and seven ventral modified sucker pedicels; dorsal pedicels lengthened, rolled ventrally, joined by a broad web proximally crossing arm oral face to reach ventral formation of three horn-like pedicels, connected with each other by narrow web, so that a webbed structure delimits meso-proximally a hollow; proximal horn-like pedicels of ventral row followed distally by a void hence by about four deeply modified pedicels combined into a trough-like formation	1–3 modified pedicels lengthened papilla-like, may bear vestigial suckers, in third to fifth position of ventral sucker series	with transverse formation of two ventral and two dorsal modified suckerless pedicels of various degrees of development, all four of them fused at their bases, ventral-most one longest and hook-shaped	with transverse formation of two ventral and two dorsal modified suckerless pedicels all four of them fused at their bases, ventral-most strongly developed hook-like, others hardly developed, dorsal pedicels forming most part of transverse crest	with modified suckerless pedicels: two ventral pedicels horn- or tubercle-like, two dorsal pedicels separate from ventral ones, fused with each other and distally directed between two series of suckers of distal part, additional dorsal pedicels projecting toward right arm 1	with three ventral modified sucker-less pedicels enlarged and lengthened into thick, bluntly pointed horn-like structures	with modified sucker-less pedicels: two ventral pedicels horn-like, aligned, directed distally and slightly laterally, and two dorsal pedicels flattened, fused with each other and directed ventrally, adhering to oral arm surface and to base of both ventral horns to form a concave pad	pedicel of 3rd sucker in ventral series lengthened, papilla-like, may bear vestigial sucker at its tip, other suckers normal	long, fleshy, tape-like, formed by fusion of two adjoining sucker stalks, no trace of suckers on tape-like structure, no hook-like structure on arm	–

	Sepiola Leach, 1817	Inioteuthis Verrill, 1881	Euprymna Steenstrup, 1887	Sepietta Naef, 1912	Rondeletiola Naef, 1921	Adinaefiola Bello, 2020	Boletzkyola Bello, 2020	Lusepiola Bello, 2020	Eumandya Bello, 2020	Dextrasepiola n.gen.	Amutatiola n.gen.
Distal part of hectocotylus	with some enlarged suckers in dorsal series	with several enlarged suckers in ventral series, first one very large, laying on trough-like structure of copulatory apparatus	occupying 50–80% of arm distally, with lengthened columnar sucker pedicels, closely packed to form longitudinal palisades, bearing at tip embedded suckers that are partially covered by fleshy caps, number of palisades proximally equal to that of regular sucker rows but reduced toward arm extremity	with some proximal suckers of dorsal row enlarged, wide space between two sucker series	first two ventral suckers lacking, some proximal suckers enlarged in both series	with some enlarged suckers in either ventral or both series	with several suckers missing proximally in ventral row and four enlarged suckers in dorsal series	with sucker pedicels of both series leaf-like, lengthened, widened, triangular- or squarish-shaped, flattened proximo-distally, their bases inserted transversally on arm oral surface, except for distalmost suckers with regular short pedicels; in several preserved specimens distal part rotated towards right dorsal arm	occupying 33–50% of arm distally, with lengthened columnar sucker pedicels, closely packed longitudinally bearing reduced suckers and not connected with each other by any web	biserial suckers to arm tip (19 suckers in holotype, 23 suckers in paratype 2)	–
Female bursa copulatrix	roughly ear-shaped, devoid of cover	pouch-like	pouch-like	roughly ear-shaped, devoid of cover	roughly ear-shaped, devoid of cover	roughly ear-shaped, devoid of cover	pouch-like with wide opening	pouch-like	pouch-like	open type, roughly ear-shaped	closed type, pouch-like, opening at level of base of left gill
Type species	Sepiola rondeletii Leach, 1817, by monotypy	Inioteuthis japonica Verrill, 1881, by subsequent designation	Inioteuthis morsei Verrill, 1881, by subsequent designation	Sepiola oweniana d'Orbigny in Férussac & d'Orbigny, 1841, by monotypy	Sepietta minor Naef, 1912, by monotypy	Sepiola ligulata Naef, 1912, designated by Bello (2020)	Sepiola knudseni Adam, 1984, designated by Bello (2020)	Sepiola birostrata Sasaki, 1918, designated by Bello (2020)	Euprymna pardalota Reid, 2011, designated by Bello	Dextrasepiola taenia gen. nov., sp. nov. by monotypy.	Amutatiola macroventosa gen. nov., sp. nov. by monotypy

	Sepiola Leach, 1817	Inioteuthis Verrill, 1881	Euprymna Steenstrup, 1887	Sepietta Naef, 1912	Rondeletiola Naef, 1921	Adinaefiola Bello, 2020	Boletzkyola Bello, 2020	Lusepiola Bello, 2020	Eumandya Bello, 2020	Dextrasepiola n.gen.	Amutatiola n.gen.
Included species and Distribution	Sepiola rondeletii [NEA, MS]; S. affinis [MS]; S. atlantica [NEA, MS]; S. boletzkyi [AS]; S. bursadhaesa [CS]; S. intermedia [NEA, MS]; S. robusta [MS]; S. steenstrupiana [MS, RS, IO]; S. tridens [NS, NEA]	Inioteuthis japonica [Indo-Pac]; I. maculosa [Indo-Pac]	Euprymna morsei [north-western Pac]; E. albatrossae [western Pac]; E. berryi [north-western Pac]; E. brenneri [north-western Pac]; E. hoylei [Indo-Pac]; E. hyllebergi [eastern IO]; E. megaspadicea [north-western Pac]; E. penares [Indo-Pac]; E. scolopes [Central Pac]; E. stenodactyla [IO]; E. tasmanica [southern Australia]	Sepietta oweniana [EA, MS]; S. neglecta [NEA, MS]; S. obscura [MS, NEA]	Rondeletiola minor [EA, MS]; R. capensis [southern EA]	Adinaefiola ligulata [MS]; A. aurantiaca [NEA, western MS]; A. pfefferi [NEA]	Boletzkyola knudseni [EA]	Lusepiola birostrata [north-western Pac]; L. trirostrata [Indo-Pac]	Eumandya pardalota [northern Australia]; E. parva [north-western Pac]; E. phenax [Indo-Pac]	Dextrasepiola taenia n.gen., n.sp. [Australia]	Amutatiola macroventosa n.gen., n.sp. [Australia]

Note: AS, Aegean Sea; CS, Catalan Sea; EA, eastern Atlantic Ocean; IO, Indian Ocean; Indo-Pac, Indo-Pacific; MS, Mediterranean Sea; NEA, north-eastern Atlantic Ocean; NS, North Sea; Pac, Pacific Ocean; RS, Red Sea.

Discussion

Bello (2020) revised the subfamily Sepiolinae based on analyses of the structures of the hectocotylised arms, and split the old *Sepiola* Leach, 1817, into four genera: *Sepiola* Leach, 1817, *Adinaefiola* Bello, 2020, *Boletzkyola* Bello, 2020, and *Lusepiola* Bello, 2020. The genus *Euprymna* Steenstrup, 1887, was split into two genera: *Euprymna* and *Eumandya* Bello, 2020. According to Bello's (2020) revision, Sepiolinae includes nine genera, of which seven genera – *Sepiola, Adinaefiola, Boletzkyola, Inioteuthis, Lusepiola, Rondeletiola* and *Sepietta* – have a tripartite hectocotylus, and the remaining two genera – *Euprymna* and *Eumandya* – are characterised by the hectocotylus (left arm I) with sucker-stalks in its distalmost portion modified into a palisade-like structure.

Both new genera, *Dextrasepiola* and *Amutatiola*, share some basic features with the other members of Sepiolinae: mantle fused dorsally with head, biseriate arm suckers, bilobed kidney- or dumbbell-shaped visceral light organ (the latter two features are deemed plesiomorphic character states by Bello, 2020), reduced arm web, ventral mantle does not produce into a ventral shield (unlike in Heteroteuthinae) and small body size.

Dextrasepiola n. gen. also shares the same type of hectocotylisation with the tripartite-hectocotylus genera, but it conspicuously differs from the other because of its unique peculiarity that the right dorsal arm of the male is modified into a copulatory arm instead of the left one. In this genus, the copulatory apparatus is also unique in being formed by two suckerless stalks modified and fused into a tape-like structure. *Amutatiola* n. gen. is also unique among Sepiolinae in lacking an evident hectocotylised dorsal arm in male and instead having some arm suckers enormously enlarged. Table 5 shows the comparison of features of all 11 genera of Sepiolinae.

In a recent report, Sanchez et al. (2021) concluded that the subfamily Sepiolinae is split into Indo–Pacific and Atlantic–Mediterranean lineages, the former characterised by a closed type bursa copulatrix, and the latter by an open type bursa. The discovery of the *Dextrasepiola taenia* n. gen. and n. sp., (i.e. a sepioline genus and species with an open type bursa copulatrix) is not consistent with that systematic-biogeographic pattern.

With *Amutatiola macroventosa* n. gen. and n. sp., the lack of a normal sepioline hectocotylus in males is a unique feature which co-occurs with the enlargement of several suckers in the male arms. The enlargement of some suckers is also found in the mature males of several species of *Euprymna* (Norman and Lu, 1997), as well as in some Rossiinae and Heteroteuthinae (Nesis, 1982). Contrary to *Dextrasepiola taenia* n. gen. and n. sp., females of *Amutatiola macroventosa* n. gen. and n. sp. display a closed bursa copulatrix, which parallels the other Indo-Pacific sepioline genera and species.

Based on the present results and descriptions of the new sepioline genera and species, the definition of the subfamily Sepiolinae should be widened to include *Dextrasepiola* and *Amutatiola*. This can be done by amending the character state of Hectocotylisation for Sepiolinae in Table 1 to "left or right (in *Dextrasepiola*) dorsal arm hectocotylised or no hectocotylisation (in *Amutatiola*)" and by adding the character "bursa copulatrix" as "bursa copulatrix in female on left side of mantle cavity in all Sepiolinae except *Dextrasepiola* (on right side)". Subfamilies Heteroteuthinae and Rossinae do not have well-differentiated bursa copulatrix, spermatophores are implanted on the body or on a patch of wrinkled tissue near the opening of the oviduct (Hoving, et al., 2008, 2009; Naef, 1923).

References

Bello, G. 2013. Description of a new sepioline species, *Sepiola bursadhaesa* n. sp. (Cephalopoda: Sepiolidae), from the Catalan Sea, with remarks and identification key for the *Sepiola atlantica* group. *Scientia Marina* 77: 489–499.

Bello, G. 2020. Evolution of the hectocotylus in Sepiolinae (Cephalopoda: Sepiolidae) and description of four new genera. *European Journal of Taxonomy* 655: 1–53

Bello, G. and Salman, A. 2015. Description of a new sepioline species, *Sepiola boletzkyi* n.sp. (Cephalopoda: Sepiolidae), from the Aegean Sea. *European Journal of Taxonomy* 144: 1–12.

Heij A. de, and Goud J. 2010. *Sepiola tridens* spec. nov., an overlooked species (Cephalopoda: Sepiolidae) living in the North Sea and north-eastern Atlantic Ocean. *Basteria* 74: 51–62.

Hoving, H.J.T., Laptikhovsky, V., Piatkowski, U., and Önsoy, B. 2008. Reproduction in *Heteroteuthis dispar* (Rüppell, 1844) (Mollusca: Cephalopoda): a sepiolid reproductive adaptation to an oceanic lifestyle. *Marine Biology* 154: 219–230.

Hoving, H.J.T., Nauwelaerts, B., Van Genne, B., Stamhuis, E.J., and Zumholz, K. 2009. Spermatophore implantation in *Rossia moelleri* Steenstrup, 1856 (Sepiolidae; Cephalopoda). *Journal of Experimental Marine Biology and Ecology* 372: 75–81.

Lu, C.C. 2001. Cephalopoda. Pp.129–308 in: Wells, A. and Houston, H.W.K. (eds) *Zoological Catalogue of Australia*. Vol. 17.2. *Mollusca: Aplacophora, Polyplacophora, Scaphopoda, Cephalopoda*. CSIRO Publishing: Melbourne. xii, 353 pp.

Lu, C.C., and Boucher-Rodoni, R. 2006. A new genus and species of sepiolid squid from the waters around Tonga in the central South Pacific (Mollusca: Cephalopoda: Sepiolidae). *Zootaxa* 1310: 37–51.

Lu, C.C., and Dunning, M.C. 1998. Subclass Coleoidea Bather, 1888. Pp. 499–563 in: Beesley, P.L., Ross, G.J.B., and Wells, A. (eds) *Mollusca: The Southern Synthesis. Fauna of Australia*. Volume 5. CSIRO Publishing: Melbourne. Part A. xvi, 563 pp.

Lu, C.C., and Phillips, J.U. 1985. An annotated checklist of the Cephalopoda from Australian waters. *Occasional Papers of the Museum of Victoria* 2: 21–36.

Lu, C.C., and Roper, C.F.E. 1979. Cephalopods from deepwater dumpsite 106 (Western Atlantic): vertical distribution and seasonal abundance. *Smithsonian Contributions to Zoology* 288: 1–36.

Naef, A. 1912a. Teuthologische Notizen. 3. Die Arten du Gattungen *Sepiola* und *Sepietta*. *Zoologischer Anzeiger* 39: 262–271.

Naef, A. 1912b. Teuthologische Notizen. 7. Zur Morphologie und Systematik der *Sepiola*- und *Sepietta*- Arten. *Zoologischer Anzeiger* 40: 78–85.

Naef, A. 1923. Die Cephalopoden, Systematik. *Fauna und Flora des Golfes von Neapel* 35: 1–863. Israel Program for Scientific Translation: Jerusalem [English translation].

Nesis, K.N. 1982. *Cephalopods of the world*. English Translation from Russian. Levitov, B.S. (Transl.), Burgess, L.A. (ed.) (1987). T.F.H. Publications: Neptune city. 351 pp.

Norman, M.D., and Lu, C.C. 1997. Redescription of the southern dumpling squid *Euprymna tasmanica* and a revision of the genus *Euprymna* (Cephalopoda: Sepiolidae). *Journal of the Marine Biological Association of the United Kingdom* 77: 1109–1137.

Øresland, V., and Oxby, G. 2021. *A photo-illustrated dissection guide for bobtail squids*. Divers and Scientists West Coast Sweden, Guide No.1. 122 pp.

Roper, C.F.E., and Voss, G.L. 1983. Guidelines for taxonomic descriptions of cephalopod species. *Memoirs of the National Museum of Victoria* 44: 48–63.

Sanchez, G., Fernández-Álvarez, F.Á., Taite, M., Sugimoto, C., Jolly, J., Simakov, O., Marlétaz, F., Allcock, L., and Rokhsar, D. 2021. Phylogenomics illuminates the evolution of bobtail and bottletail squid (order Sepiolida). *Communications Biology* 4: 819.

Sanchez G., Jolly J., Reid A., Sugimoto C., Azama C., Marlétaz F., Simakov O., and Rokhsar D.S. 2019. New bobtail squid (Sepiolidae: Sepiolinae) from the Ryukyu islands revealed by molecular and morphological analysis. *Communications Biology* 2: 465.

Lower Devonian *Zosterophyllum*-like plants from central Victoria, Australia, and their significance

Fearghus R. McSweeney FGS[1,*], Jeff Shimeta[2], John S⊤. J.S. Buckeridge FGS[1,3]

[1] Earth and Oceanic Systems Group, RMIT University, GPO Box 2476, Melbourne, VIC 3001, Australia
[2] Centre for Environmental Sustainability and Remediation, School of Science, RMIT University, Melbourne, Australia
[3] Museums Victoria, VIC 3001, Australia
* Correspondence: Fearghus McSweeney, tidal75@gmail.com

Abstract
McSweeney, F.R., Shimeta, J., and Buckeridge, J.S. 2022. Lower Devonian *Zosterophyllum*-like plants from central Victoria, Australia, and their significance. *Memoirs of Museum Victoria* 81: 25–41.

Three specimens belonging to Zosterophyllaceae are described. Two of these possess bilateral symmetry and are the first to be described with this arrangement from the Lower Devonian of Victoria. One of these specimens is similar to *Zosterophyllum fertile*, and the other cf. *Zosterophyllum* sp. A. is unusual in possessing vascularised long stalks. The third specimen described cf. *Zosterophyllum* sp. B. from Ghin Ghin Road, near Yea possesses a small spike and has sporangia that appear vertically elliptical and similar to some South China taxa. All the specimens are significantly different to previous zosterophyll taxa described from Victoria.

Keywords
Victoria, *Baragwanathia* flora, *Platyzosterophyllum*, zosterophyll, systematics.

Introduction

The Wilson Creek Shale Formation of Victoria is notable for providing a link between the lithologies of the Mount Easton and Darraweit Guim Provinces (fig. 1) of the Melbourne Zone (VandenBerg, 1988: 114) and for being the type formation of *Baragwanathia longifolia* Lang and Cookson, 1935. Furthermore, it provides a useful approximate marker delineating the Silurian from Devonian rocks, as it has been dated as mid Pragian–Emsian (Carey and Bolger, 1995; Mawson and Talent, 1994). This paper examines three zosterophylls, two of which come from the Wilson Creek Shale and are the first to be described with bilateral symmetry in Victoria and are the first to be described from this formation. The third specimen is from the base of the Humevale Formation near Yea.

The first zosterophyll described from Victoria was *Zosterophyllum australianum* Lang and Cookson, 1930, from the Centennial Beds at North Road Quarry near Walhalla, now considered to be part of the Norton Gully Sandstone Formation (Douglas and Jell, 1985: 161). Lang and Cooksons' (1930: 148) work on *Z. australianum* confirmed an earlier assumption (Lang, 1927: 449–450) that the reinform appendages of *Zosterophyllum* were sporangia, with the presence of in situ spores. Additionally, Cookson (1935: pl. 10, figs 9–15) described *Z. australianum* from Mount Pleasant and Halls Flat Roads near Alexandra, also considered part of the Norton Gully Sandstone (VandenBerg, 1975, 1988). Hao and Wang (2000)

reassigned Cookson's (1935) *Z. australianum* specimens to *Z. ramosum*, primarily based on different sporangial morphological characteristics. The *Zosterophyllum ramosum* type locality occurs near Zhichang village in the Posongchong Formation, Yunnan, China (Hao and Wang, 2000).

Tims (1980), in her unpublished thesis, described and gave informal manuscript names to three zosterophylls in Victoria: *Zosterophyllum minutum* from Boola Formation at Tyers, *Pluricaulis biformis* from the Yea Formation at Limestone Road and *Chamaecaulon tylosus* from the Wilson Creek Shale on Frenchmans Spur Track near Matlock. *Zosterophyllum minutum* was subsequently redescribed and assigned to *Gippslandites minutus* McSweeney et al., 2020. Additionally, McSweeney et al. (2020) described another zosterophyll, *Parazosterophyllum timsiae*, from the base of the Humevale formation on Ghin Ghin Road, Yea.

Stratigraphic setting

Humevale Siltstone. The Humevale Formation was proposed by Williams (1964: 277) as a sequence of primarily siltstones about 5 km south-west of Tommy's Hut at Humevale and is found throughout much of the Darraweit Guim Province (fig. 1) of the Melbourne Zone (Edwards et al., 1997: fig. 6; VandenBerg, 1988: table 4.1). Williams (1964) delineated the upper and lower parts of the Humevale Formation with two sandstone units: the Clonbinane and Flowerdale Members, respectively. Above the

Clonbinane Member near the base of the Humevale Formation, Williams (1964: 276) added the Mount Phillipa Member, a sandstone unit noted for numerous *Nucleospira* sp. and rhynchonellids. Garratt and Wright (1988: 650) subdivided the Humevale Formation based on brachiopod faunal successions, with *Notoparmella plentiensis* Garratt, 1980, above the base of the Humevale Formation in the Whittlesea area, and the appearance of *Boucotia janaea* Garratt, 1980, near the top of the sequence. However, Talent et al. (2001: 151) suggested *B. janaea* maybe *B. australis* Gill, 1942. Edwards et al. (1997: 22) considered the Clonbinane and Mount Phillipa Members to be part of the Dargile Formation, and the Flowerdale Member to be part of the Norton Gully Sandstone, while retaining the Humevale Siltstone. At Ghin Ghin Road, the fossil exposure P4 (loc 1 in Garratt, 1978) according to Rickards and Garratt (1990: fig. 2) is at the base of the Humevale Formation, and Pridoli, upper Silurian; thus, slightly younger than the exposure at Limestone Road, south-east of Yea, which they consider to be Ludlovian, with both interpretations based on graptolites. This Ludlovian–Pragian, upper Silurian age for the exposures in the Yea area by Garratt (1978), Rickards and Garratt (1990), and Rickards (2000) is contentious, primarily due to the relatively advanced plant architectures for this time and the similarity of some of the flora to younger exposures elsewhere in Victoria, such as the Wilson Creek Shale (Banks, 1980; Cleal and Thomas, 1999; Edwards et al., 1979 Hueber, 1983, 1992). Edwards et al. (1997: 22) placed much of the lithology of Yea, including both Limestone Road and Ghin Ghin Road exposures, in the lithologically variable Norton Gully Sandstone. VandenBerg (*pers. comm.* June 2021) mapped the Yea area in 2008 (unpublished) confirming much of Edwards et al. (1997), and found Yea to be predominantly Norton Gully Sandstone with a narrow band of the Wilson Creek Shale near the Yea anticline. In this paper, we retain the Humevale Siltstone, because this new information on the Yea lithology needs to be published. However, we find Edwards et al. (1997) and VandenBerg's argument cogent and so use a conservative interpretation of the age of the exposure at Ghin Ghin Road, giving it a Pragian–Emsian, Lower Devonian.

Wilson Creek Shale. The Wilson Creek Shale occurs in both the Darraweit Guim and Mount Easton provinces of the Melbourne Zone (fig. 1) and part of the Jordan River Group (VandenBerg, 1973, 1988). Lithologically, the Wilson Creek Shale consists of black shale that changes from cream to grey on weathering and is interpreted as representing once deep anoxic quiescent marine conditions (Edwards et al., 1997; VandenBerg et al., 2006). Sandstone beds are prevalent towards the top of the formation and are construed as representing the growing influence of turbidity currents late in the sequence (Edwards et al., 1997). Siltstone occurs primarily in the basal and upper portions of the formation, and limestone is found to interfinger with the Coopers Creek Formation at Jacobs Creek, north of Tyers (Edwards et al., 1997; VandenBerg, 1988; VandenBerg et al., 2006). The Wilson Creek Shale conformably overlies the Humevale Siltstones, Eldon Sandstone, Whitelaw Siltstone and Boola Formation, and conformably underlies the Norton Gully Sandstone, Easts Lookout Siltstone (fig. 2),

Marshall Creek Member and Yeringberg Formation, albeit large scale strike faulting is common according to VandenBerg (1988) and VandenBerg et al. (2006). Lang and Cookson (1935) described – in addition to *Baragwanathia longifolia* – *Yarravia oblonga*, *Y. subsphaerica* and *Hostinella* sp. as occurring in the Wilson Creek Shale. Tims (1980) described numerous informal species in her thesis as occurring in the Wilson Creek Shale, especially at Frenchmans Spur Track and Coles Clearing on the Thomson River. Following her thesis, she described two rhyniophytoids, *Salopella australis* and *S. caespitosa*, and the trimerophyte *Dawsonites subarcuatus* as occurring in the Wilson Creek Shale at Frenchmans Spur Track, about 10 km west of Matlock (Tims and Chambers, 1984). Recently, *Salopella laidae* was described from Limestone Road by McSweeney et al. 2021c.

In the first half of the twentieth century, the lithological sequence that would be later assigned to the Wilson Creek Shale (Edwards et al., 1997; Thomas, 1953; VandenBerg, 1975, 2006) was believed to be early Ludlow, upper Silurian, based on Elles's assignation (Lang and Cookson, 1935: 422). Jaeger (1966) reassigned the graptolites to the Lower Devonian based on the occurrence of the monograptids *Uncinatograptus thomasi* (=*Monograptus thomasi thomasi*) Jaeger, 1966, throughout the formation, and *Neomonograptus notoaequabilis* (=*M. aequabilis notoaequabilis*) Jaeger and Stein, 1969, in the upper half of the formation (Lenz, 2013). *Neomonograptus notoaequabilis* extends into the overlying Norton Gully Sandstone according to VandenBerg et al. (2006). Furthermore, both *Eognathodus sulcatus sulcatus* and *Polynathus dehiscens* occur in the Coopers Creek Limestone that inter-fingers the Wilson Creek Shale at Tyers, indicating a mid Pragian–Emsian age (Carey and Bolger, 1995; Mawson and Talent, 1994).

Material and methods

The specimens cf. *Zosterophyllum* sp. A. (NMV P256740) and cf. *Z. fertile* (NMV P50040) were found by J. D. Tims on Frenchmans Spur Track near Matlock in the Wilson Creek Shale in the 1970s, with the former referred to in Tims (1980: fig. 4.4.19) indirectly, whereby she described three *Hedeia* (=*Yarravia*) sp., which occur on the same plane. Tims (1980) noted the specimen cf. *Zosterophyllum* sp. A. was loaned to H. P. Banks but made no reference to the associated zosterophyll. The specimen cf. *Zosterophyllum* sp. A. (McSweeney et al. 2021a) was given to the lead author by Prof. Dianne Edwards of Cardiff University in March 2019. The specimen cf. *Z. fertile* was originally assigned to *Zosterophyllum* sp. by Tims (1980: 91). The final specimen cf. *Zosterophyllum* sp. B. (NMV P256742) was found as float by the lead author at location P4 on Ghin Ghin Road, near Yea, on 8 August 2012, at location P4 on Ghin Ghin Road, about 8 km north north-west of Yea Township (37° 13' S, 145° 38' E). P4 is equivalent to loc. 1 in Garratt (1978: fig. 2).

Dégagement had been undertaken on cf. *Zosterophyllum* sp. A. to the right of the spike on the part. Further dégagement as per Fairon-Demaret et al. (1999) was carried out by the lead author to better expose sporangia two, four and five, and around the basal region of the fertile axis, and to expose part

of the axis near the base and apex of the specimen. Samples taken from sporangia two and four of cf. *Zosterophyllum* sp. A. did not reveal any preserved spores, and samples of the basal axial region of the fertile axis did not yield any anatomical features when viewed under a low vacuum on a FEI Quanta 200 ESEM. Dégagement was performed on the distal and proximal parts of the spike of cf. *Z. fertile* by Tims (1980: 91) to expose sporangia in those areas, but no further dégagement was carried out because the specimen was fragile. Dégagement of cf. *Zosterophyllum* sp. B. was undertaken by the lead author around the spike, but no additional parts of the zosterophyll were found. A veneer of iron-oxide coating the surfaces was removed and mounted onto a stub and examined under a low vacuum on a FEI Quanta 200 ESEM. No spores or internal anatomy were uncovered.

Photographs of cf. *Zosterophyllum* sp. A., cf. *Z.* sp. B. and cf. *Z. fertile* were taken using a AxioCamMRc5 camera attached to a Zeiss microscope and a Leica M205 C microscope with Leica Application Suite software version 3.8.0. Images were Z-stacked to improve depth of field using Adobe Photoshop CC 2017. ImageJ software was used to take morphological measurements. Rodney Start of Museums Victoria took images of cf. *Zosterophyllum* sp. A. on 5 December 2019 using a Canon EOS 5D Mark III camera and cross-polarised light circular filter with flash strip-lights to enhance contrast. All photographs had contrast enhanced using Adobe Photoshop CC 2017 and were arranged using Adobe Illustrator CC 2017.

Institutional abbreviation

NMV P, Museum Victoria Palaeontology Collection, Melbourne, Australia
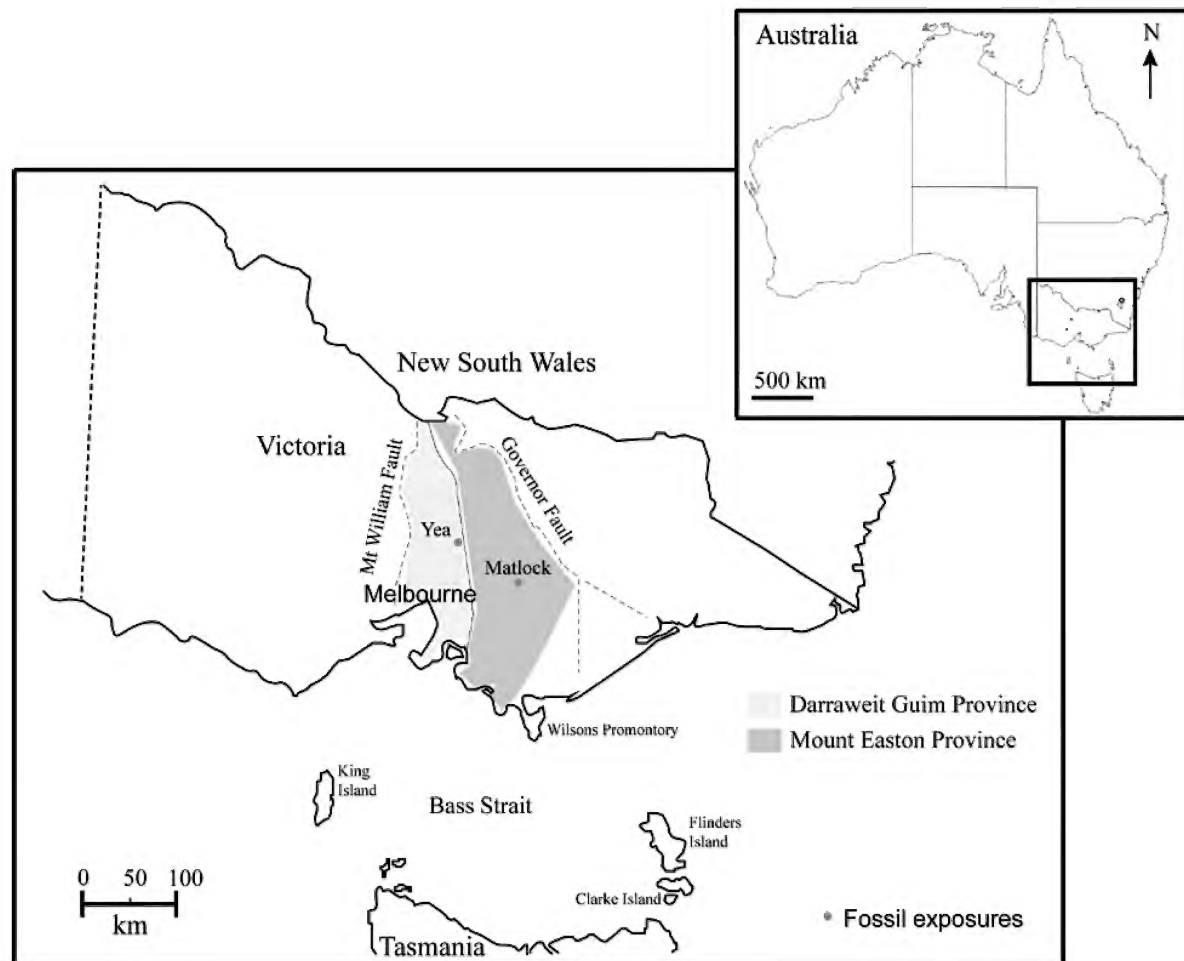
Figure 1. Location of Matlock in the Mount Easton Province and Yea in the Darraweit Guim Province of the Melbourne Zone in Victoria, Australia. Source: after Moore et al. (1998: fig. 2).

Systematic palaeontology

Division Tracheophyta

Class Zosterophyllopsida Hao and Xue, 2013

Order Zosterophyllales Banks, 1968

Family Zosterophyllaceae Banks, 1968

Remarks. Initially, *Zosterophyllum* were separated into two groups, *Platy-zosterophyllum* and *Eu-zosterophyllum*, by Croft and Lang (1942: 145), but Hueber (1972: 121) split *Zosterophyllum* into two subgenera, *Platyzosterophyllum* and *Zosterophyllum*. The distinguishing character of *Platyzosterophyllum* is the arrangement of sporangia in row(s) of one, two or three along the fertile axes, while the sporangia of *Zosterophyllum* are arranged helically (Croft and Lang, 1942; Edward, 1975; Gensel, 1982; Hueber, 1972). Furthermore, *Platyzosterophyllum* often possess circinate vernation (Croft and Lang, 1942; Edward, 1975; Gensel, 1982; Hueber, 1972). The specimens cf. *Zosterophyllum* sp. A. and cf. *Z. fertile* described herein possess bilateral symmetry, but lack enough characteristics to unequivocally assign to *Platyzosterophyllum*.

cf. *Zosterophyllum fertile* Leclercq, 1942

Figure 3a–c

Material examined. NMV P50040.1 and P50040.2, part and counterpart, respectively.

Locality. Occurs on a road cutting on Frenchmans Spur Track, approximately midway between Big River Road to the north-north-west, Warburton Road to the east and Frenchmans Spur Track, ~10 km west of Matlock, central Victoria.

Horizon and age. Wilson Creek Shale Formation, middle Pragian–Emsian, Lower Devonian (Carey and Bolger, 1995; Mawson and Talent, 1994).

Description. The specimen consists of part and counterpart of one partial spike with basal and apical regions missing and preserved as a carbonised compression. The axis is ~1.0 mm wide and 10.0 mm long and unbranched, and the spike up to 6.8 mm wide. Eight sporangia are borne alternately in two rows. The sporangia are attached by recurved stalks; some are perpendicular to ~60° to the fertile axis and curve sharply distally to at most 90°. The convex margins of some of the
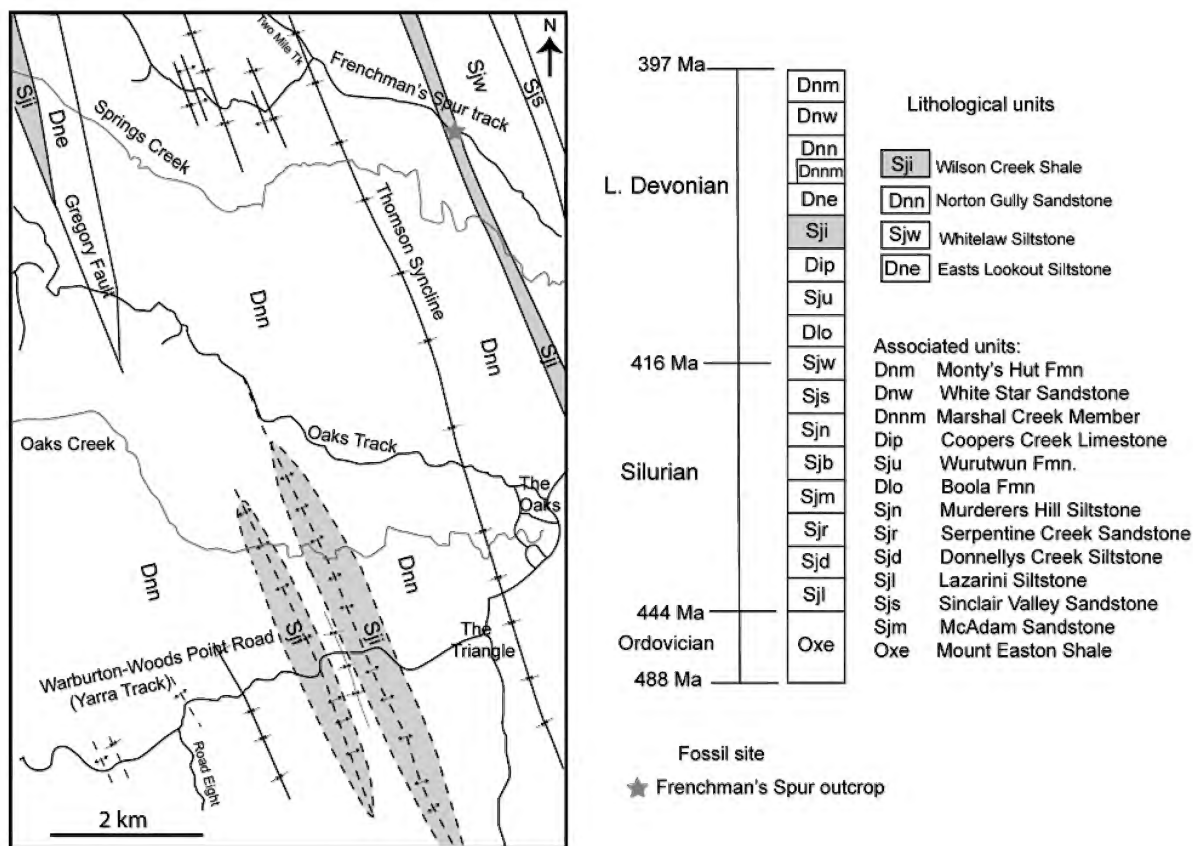
Figure 2. Location of the Wilson Creek Shale outcrop on Frenchmans Spur Track, 10 km west of Matlock. Geological map showing the location of Frenchmans Spur outcrop at the star, north of Springs Creek. Source: Map after Willman et al. (2006).

sporangia possess a thickened/darker/border, here interpreted as likely pertaining to dehiscence (fig. 3, sporangia 6, 7). An adaxially orientated basal lobe occurs on some sporangia (fig. 3b, central arrows).

Remarks. The sporangia are in two rows with no clear demarcation between the attachment of the stalk and the basal region of the sporangia. The specimen bears some resemblance to Edwards' (1969a: fig. 1b) South Wales *Z.* cf. *fertile*. Edwards' (1969a) specimens are from the Old Red Sandstone Brecon Beacons and Llanover Quarries, South Wales (Pragian–Emsian Lower Devonian age) and were placed in *Z.* cf. *fertile*, because the original diagnosis was based on only a single specimen from Belgium (Leclercq, 1942) such that further specimens from both Wales and Belgium were thought necessary to determine specific affinity with confidence. Wellman et al. (2000) recorded the earliest occurrence of *Z.* cf. *fertile* from the Anglo-Welsh Basin as being mid-Lochkovian (Lower Devonian). The fructification of Edwards' (1969a) specimens, while incomplete, were 1.0 cm high and 3.0 mm wide, which is comparable in height but over two times smaller than the Victorian specimen, which reached 6.8 mm wide. Edwards' (1972) *Z. fertile*, also based on an incomplete spike but with a significant proportion preserved, was 7.2 cm high and 3.0 mm wide, while Wellman et al.'s (2000) *Z.* cf. *fertile* reached 2.0 cm in height and 3.5 mm wide. Axial width for Leclercq's (1942) holotype measured 1.0–1.5 mm wide and conforms to the Victorian specimen. However, the Victorian specimen's axis, where visible, was found to be ~1.0 mm wide. The widest axial width for *Z. fertile* was found by Edwards (1972: 78) for a specimen from the Lower Old Red Sandstone of Forfar, Scotland, with an axial width of 3.0 mm, decreasing only slightly to 2.8 mm wide, while the specimens of *Z.* cf. *fertile* from Brecon Beacons Quarry, according to Edwards (1969a: 924), showed greater range, 0.8–2.5 mm wide.

The stalks for Leclercq (1942), Edwards (1969a, 1972) and Wellman et al. (2000) range between 0.3–0.5 mm wide and 1.0–1.8 mm long. The Victorian cf. *Z. fertile* stalks are broadly similar, 0.5–0.7 mm wide and up to ~2.0 mm long.

The sporangial shape in face view for the Victorian specimen is reniform (fig. 3, sporangium 8), similar to Wellman et al. (2000), while Leclercq (1942) described it as elongate–reniform, and Edwards (1969a) for *Z.* cf. *fertile* described it as irregular. The sporangia examined by Leclercq (1942), Edwards (1969a, 1972) and Wellman et al. (2000) were all in the range of 2.0–2.5 mm wide and 1.6–3.1 mm high. The sporangial dimensions of cf. *Z. fertile* are difficult to ascertain due to their poor preservation.

Edwards (1969a: 924) found the longest fructification of *Z.* cf. *fertile*. It had eight sporangia but lacked an apical region. Due to the lack of a complete spike herein and poor preservation resulting in equivocal characters, the Victorian specimen was placed in cf. *Z. fertile*, it being conceivable that given better preservation the plant might be placed it outside the defining characteristics of *Zosterophyllum*.

cf. *Zosterophyllum* sp. A

Gen. et sp. indet.

Figures 4–9

Material examined. NMV P256740.1 and P256740.2, part and counterpart, respectively.

Locality. Frenchmans Spur Track, ~10 km west of Matlock, central Victoria.

Horizon and age. Wilson Creek Shale, middle Pragian–Emsian, L. Devonian (Carey and Bolger, 1995; Mawson and Talent, 1994).
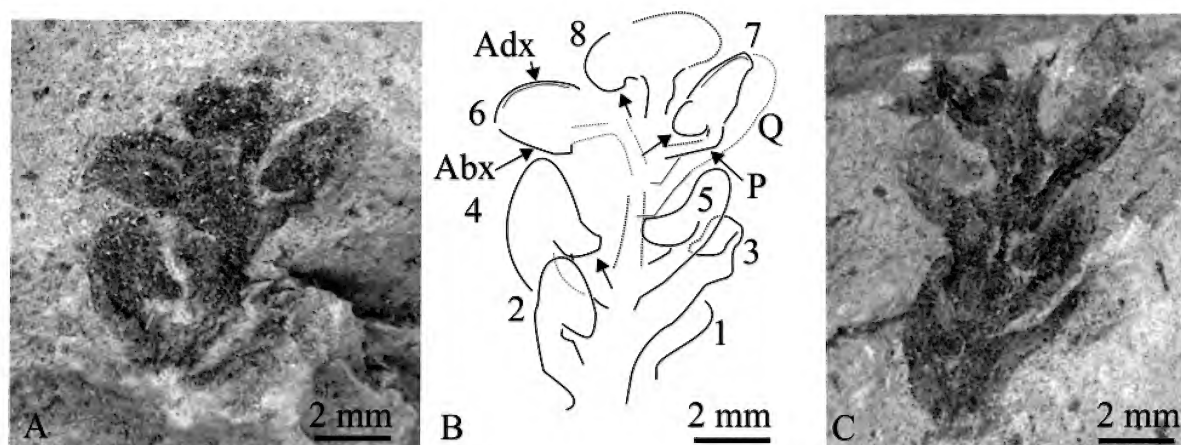

Figure 3. cf. *Z. fertile*, from the Wilson Creek Shale Formation on Frenchmans Spur, 10 km west of Matlock: a, part (NMV P50040.1); b, line drawing of partial spike. Abx = abaxial valve, Adx = adaxial valve, Q = ?poorly preserved sporangium, P = stalk, which is normal to the fertile axis before turning upwards. Central arrows pointing to lobes; c, counterpart (NMV P50040.2). Note. Counterpart image reversed to be in the same orientation as the part.

Description. The specimen consists of a longitudinally elongate lax spike with its apical region missing. The basal half of the spike contains about a third of the total sporangia in two rows (figs 4, 5a), and distally, the sporangia are more closely arranged (?helically) but the insertion points are not clear. The naked fertile axis is unbranched, 1.3–2.6 mm wide, curving basally, the spike slightly decreases in width acropetally. The lax spike is 10 mm wide and up to at least 45 mm long, consisting of 20 sporangia arranged on long vascularised stalks up to 2.0 mm long and 1.0–1.3 mm wide, at acute angles 15°–45° to the vertical, before the stalks reorientate towards the apex of the spike just beneath each sporangium. There is very little vertical overlap of sporangia. Some fine protuberances and depressions emanating from the vascular trace (fig. 6) are interpreted here as representing insertions of further stalks. The junction between sporangium and stalk is unknown. The sporangia are circular to reniform in face view, 0.95–3.7 mm wide and 0.5–

2.3 mm high, with weakly developed lobes (fig. 7) and a narrow border visible on distal margin of some sporangia, such as sporangia two, 10 (figs 7, 8) and 12, are 0.13–0.15 mm wide and is interpreted as likely pertaining to dehiscence. Sporangia one and two are longitudinally elliptical and are interpreted to be infolded, such that half the abaxial valve is visible (fig. 8). Vascular trace 0.34–1.3 mm in the fertile axis, 0.17–0.21 mm on the stalks. There are two sporangia in close proximity to the spike, but they are clearly orientated at an angle to indicate they may come from another axis in their vicinity (fig. 5a).

The vascular trace is conspicuous in that it is preferentially preserved compared with cortical tissue (fig. 4), the cortex being preserved as a grey film in the surrounding matrix. The stalk of sporangium one (fig. 8) is inserted almost perpendicular to the fertile axis and is bent such that most of the stalk is parallel to the fertile axis before curving upwards, just beneath the basal region of the sporangium. Several poorly preserved axes lie
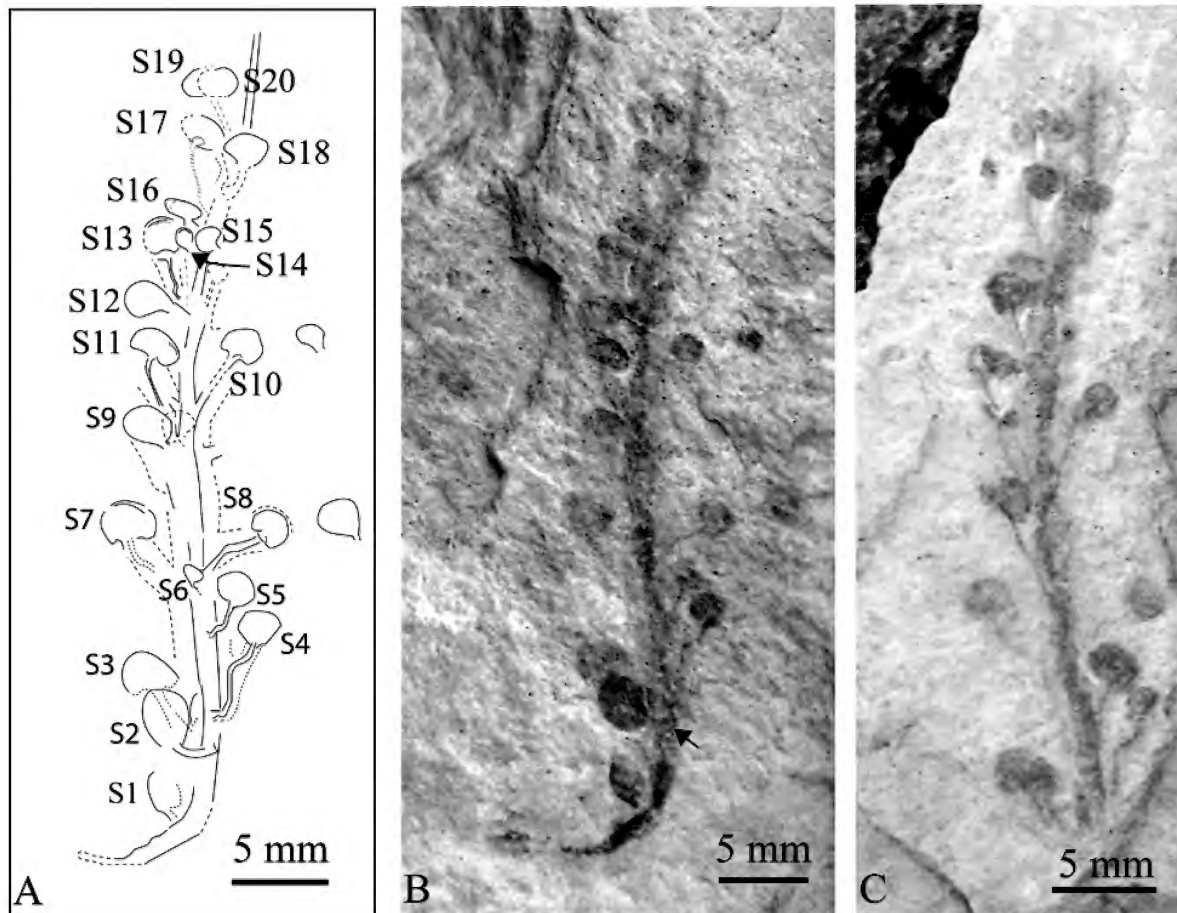
Figure 4. cf. *Zosterophyllum* sp. A. from the Wilson Creek Shale Formation on Frenchmans Spur, 10 km west of Matlock: a, line drawing, dotted lines are from faint remains of compression. S=Sporangium; Q=Poorly preserved sporangium or sporangium likely not belonging to same spike; b, part NMV P256740.1. Arrow at stalk, which has been pushed across fertile axis; c, counterpart, NMV P256740.2 with part of basal region of spike missing. Note. Counterpart image reversed to be in the same orientation as the part.

beneath the spike but are too poorly preserved and lack direct connection to warrant further consideration. However, the subtending axis to the spike aligns with an axis 4 mm wide (figs. 8, 9) and is suggestive of derivation from the same spike. This suggests the linear aerial extent of cover of the plant was at least 45 mm wide. Furthermore, the horizontal orientation of this axis to the spike is suggestive of a rhizomatous system, but it remains equivocal due to the absence of reticulum axes and H- and K-branching (*sensu* Hao et al., 2010: fig. 3; Walton, 1964: fig. 1). To the right of the apical region of the spike on the part, there are at least four axes that do not possess any attached sporangia, and beneath these axes towards the middle of the spike, a poorly preserved axis is visible with two sporangia (fig. 9) not directly attached to it but with their sporangial stalks orientated towards it, suggesting it was once attached. The alignment of these axes with the spike may indicate a tuft habit, but without clear evidence of additional spikes, its habit remains inexplicit.

Remarks. The description is based on one specimen – 45 mm high, part and counterpart with one spike (fig. 4) with sporangia laxly arranged on vascularised long stalks – preserved as a fine film of carbonaceous material lacking anatomy. The specimen occurs with three specimens of *Yarravia* sp. Lang and Cookson, 1935, on the same plane (McSweeney et al. 2021a: fig. 5a–d). The limits of the fertile axis and stalks are defined by grey film on each side of a much darker vascular trace. The fine slender nature of the darkened linear structures below the stalks are too narrow to support a sporangium, such that it seems parsimonious for the original widths of the axes to be defined by these ghosted grey areas. Lele and Walton (1961: 471), when

describing axes prepared from acetate transfers, found the xylem to appear as a preferentially preserved dark bands (and to be about one sixth the axial width) and noted the vascular traces were often displaced from their central position. This, they postulated, was likely due to decay of the cortex prior to burial during early digenesis. This would help explain the convoluted nature of the vascular trace herein (figs. 4–6), indicating the structure of the axes had already started to break down before becoming fully fossilised.

The specimen possesses depressions and protuberances along parts of its fertile axis, which is especially noticeable midway along the spike (fig. 6). These are interpreted as likely insertion points for some axes of sporangia and follows Edwards' (1975: 255) interpretation of a similar feature on *Z. myretonianum*. Xue (2009: 507), in describing *Z. minorstachyum*, suggested that small conical protuberances along the axes may reflect parasitism. This possibility was considered, but the irregularities on the vascular trace are primarily depressions in areas noticeably lacking sporangia, and in some cases appear to be the basal-most attachment of the stalk to the fertile axis' vascular trace. Additionally, we did not consider areas lacking in sporangia to be indicative of a deciduous spike, as seen with *Z. deciduum* from the Emsian, Lower Devonian of Belgium (Gerrienne, 1988). While it is plausible that once the more mature proximal sporangia has dehisced and subsequently abscised, plants would be better served by losing some sporangia in this region to concentrate energy on immature sporangia in the distal region of the spike. However, the specimen still possesses large proximal sporangia and only some sporangia appear to be missing, suggesting that
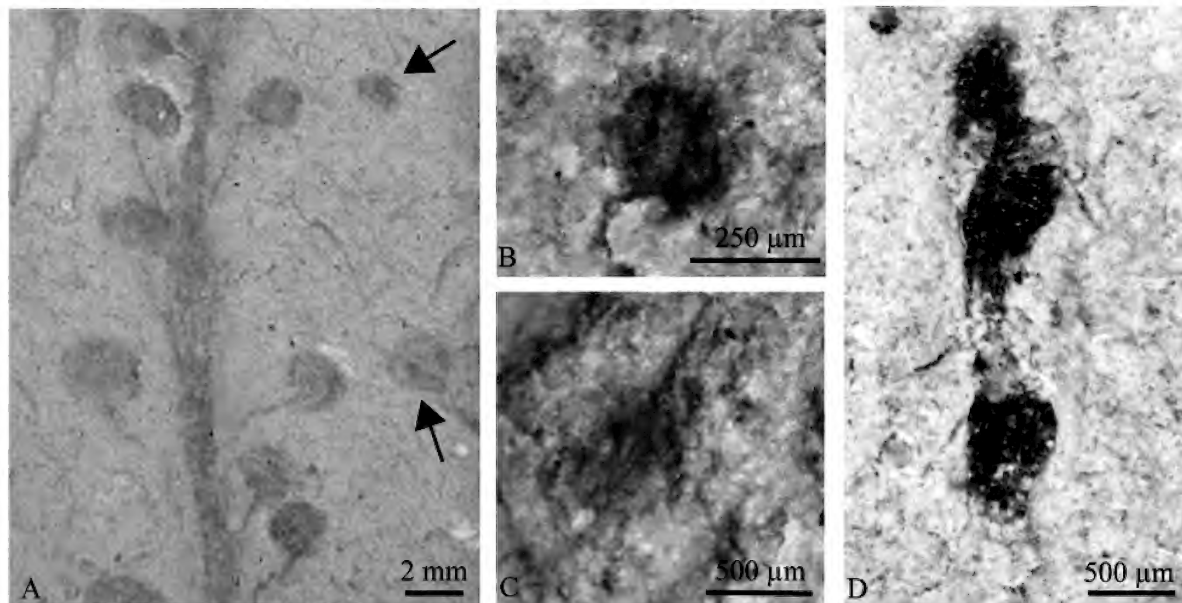

Figure 5. cf. *Zosterophyllum* sp. A. (part, NMV P256740.1): a, two isolated sporangia at arrows (pre-dégagement) with basal region of both sporangia orientated away from the spike; b–d, on the reverse of the slab, isolated sporangia with much similar dimensions and weakly developed sporangial lobes. Image a taken by Rodney Start © Museums Victoria.

they may have been lost, most likely as a result of excision due to the biostratinomy phase (Jackson, 2010: 5) of fossilisation. The absence of a junction at the axial–sporangial interface does not mean it never existed because it may have been destroyed during fossilisation. When examining Llanover specimens of *Zosterophyllum* from the Old Red Sandstone of South Wales, Edwards (1969a: 924) found organs could be superimposed and amalgamated into the surrounding tissue during preservation, resulting in them been indistinguishable.

The specimen described herein is atypical in comparison with most *Zosterophyllums* because of paucity of folded sporangia seen in lateral view with only two proximal sporangia so preserved. Furthermore, the sporangia rarely overlap each other, with one instance occurring in the proximal region of the spike where sporangium two has been pushed onto the basal region of sporangium three (fig. 4b, arrow at stalk of sporangium two) and distally for sporangia 19 and 20 (fig. 4).

Comparison with other taxa. The sporangia of the specimen are borne alternatively in two rows on opposite sides of the axis, akin to *Platyzosterophyllum*, and so the specimen was compared to *Platyzosterophyllum* first. However, some *Platyzosterophyllum* possess sporangia emanating from two rows on one side of the axis, such as *Z.* cf. *fertile* in Wellman et al. (2000: 181) and are noticeably more compact. The stalks of *Z. fertile* are perpendicular to the fertile axis, before sharply turning towards the apex, such that they are borne in an upright to slightly recumbent position (Wellman et al. 2000: 181). This characteristic of recurved stalks perpendicular to the fertile axis is also seen in *Z. spectabile* Schweitzer, 1979, according to Gensel (1982: 662). However, the specimen clearly differs

from these taxa because the stalks are orientated at acute angles of 15°–45° without any noticeable change in orientation, other than immediately below each sporangium, where they sharply reorientate upright and parallel to the fertile axis (figs 5a, 6, 7a). Furthermore, the sporangia of *Z. fertile* are oblate (Wellman et al. 2000: 183), being almost linear along the margins, while the specimen's sporangia are rounded to reniform. The dimensions of both taxa also differ slightly, with *Z. fertile* possessing stalks that are much narrower than the 1.0–1.2 mm width for the specimen, with *Z. fertile* at most reaching 0.5 mm wide (Edwards, 1972) but generally (including for *Z.* cf. *fertile*) 0.3–0.4 mm wide (Edwards, 1969a; Leclercq, 1942; Wellman et al., 2000). The sporangial dimensions for *Z. fertile* are, in part, similar to the specimen, with the sporangia of *Z. fertile* up to 2.3 mm wide (Edwards, 1972), and for *Z.* cf. *fertile* specimens the sporangial dimensions were 2.0–2.3 mm wide (Edwards, 1969a; Leclercq, 1942; Wellman et al., 2000). The specimen's sporangial widths vary more greatly on the same spike and range between 0.95–3.7 mm wide, suggesting the plant was not mature. In comparison with the Welsh specimen, *Z. llanoveranum*, sporangia are arranged in 1–2 alternative rows but differs from the specimen with sporangia borne close together and in the distal region of the spike, sometimes helically arranged (Edwards, 1969b). This could not be confirmed here because the stalk insertion points are lacking.

Edwards (1975: 263) cautioned against the use of the arrangement of the sporangia on the spike as a definitive characteristic with which to delineate species. Edwards noted bilateral symmetry basally in the spike with the distal part
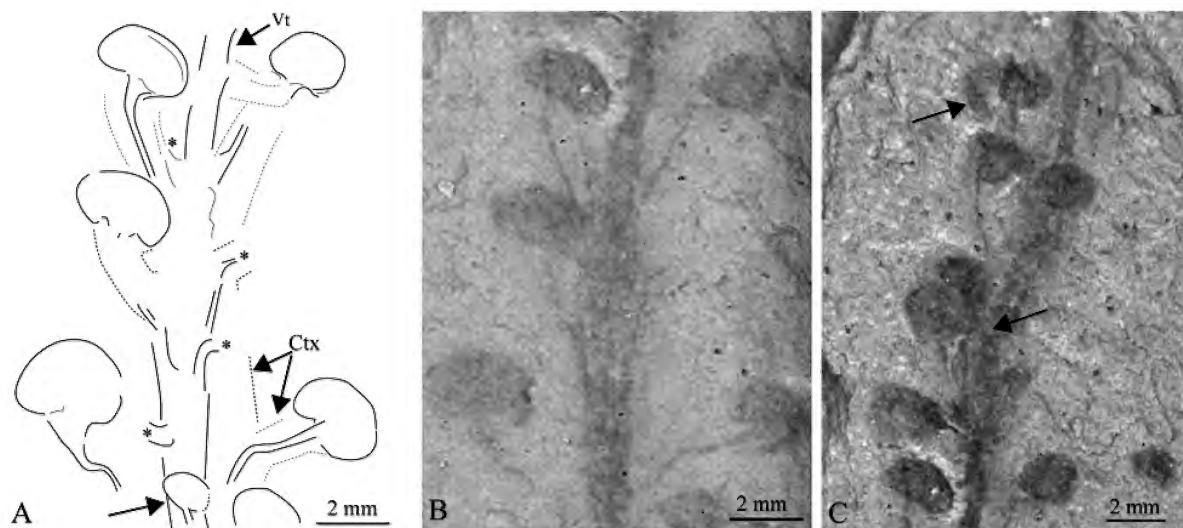

Figure 6. cf. *Zosterophyllum* sp. A. (part, NMV P256740.1): a, line drawing of medial region of the spike seen in B; b, the cortex (Ctx) is represented by a tincture of light grey in comparison to a darker coloured vascular trace (Vt). Some perturbations and depressions (*) likely represent additional stalks. Note small proximal sporangia (at arrow) in a central position on the fertile axis; c, distal part of spike – lower arrow at stalk that has been pushed across the fertile axis. At the upper arrow sporangium with no stalk, partially behind another sporangium. Smaller sporangia more centrally located suggests distal part of spike may be helically inserted. Images taken by Rodney Start © Museums Victoria.

helically arranged in some specimens of *Z. myretonianum* and attributed it to the compression of widely spaced spirally arranged sporangia, giving this misleading appearance (Edwards, 1975: 261). Furthermore, Gerrienne (1988: 328) made similar observations, adding that the difference may also be due to different ontogenetic stages of individual spikes, and Gensel (1982) noted for *Z. divaricatum*, sporangia bending and twisting of sporangia to one side.
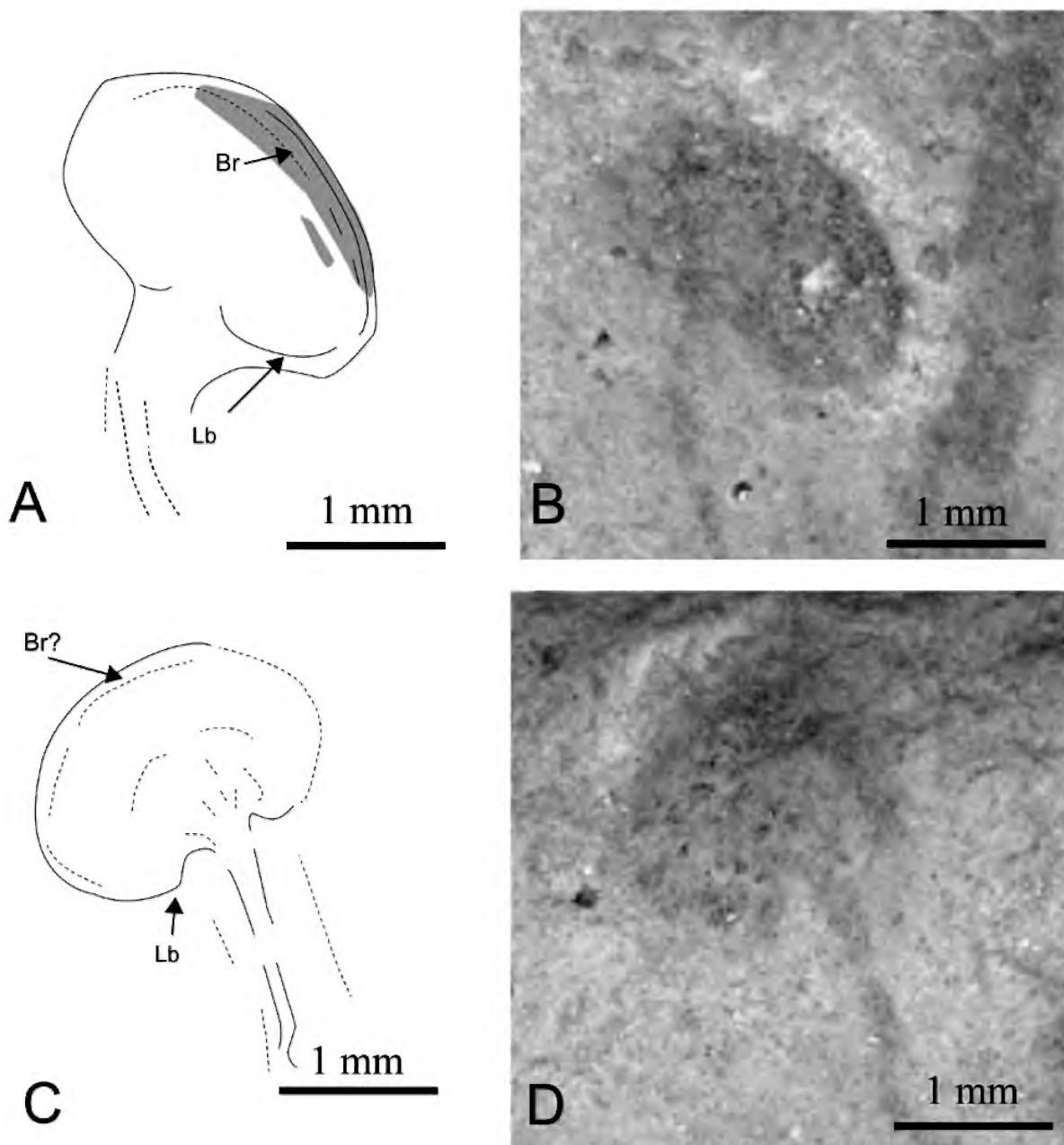

Figure 7. cf. *Zosterophyllum* sp. A. (part, NMV P256740.1). Interpretative line drawings: a, c, sporangia in b, d, respectively. The sporangia have weakly developed lobes (Lb), and a lack of a clear junction between the stalk and sporangium. A fine border (Br) is visible only alone distal margins.
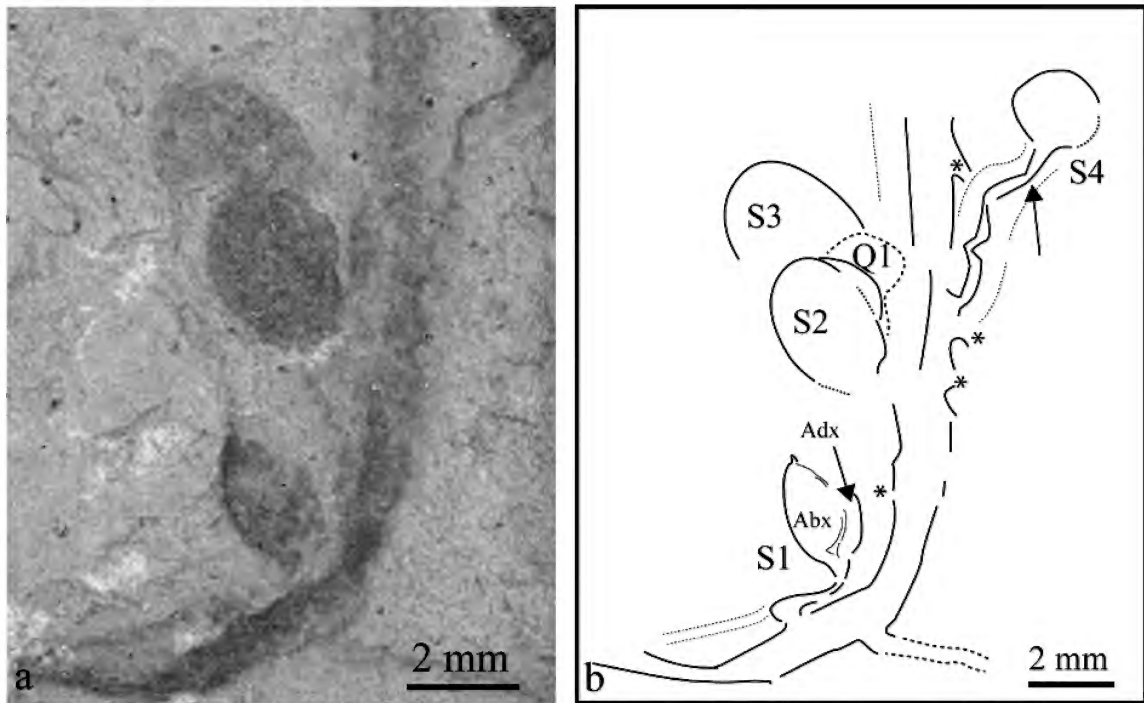
Figure 8. cf. *Zosterophyllum* sp. A. (part, NMV P256740.1): a, proximal region of spike; b, interpretative line drawing. Sporangia one and two (S1–2) appear infolded, with both abaxial (Abx) and partial adaxial (Adx) valves visible in sporangia and two perturbations and depressions (*) possibly representative of additional stalks that were not preserved. Q1, shadowing of possible sporangium, and upper arrow shows change in orientation of stalk beneath sporangium four.
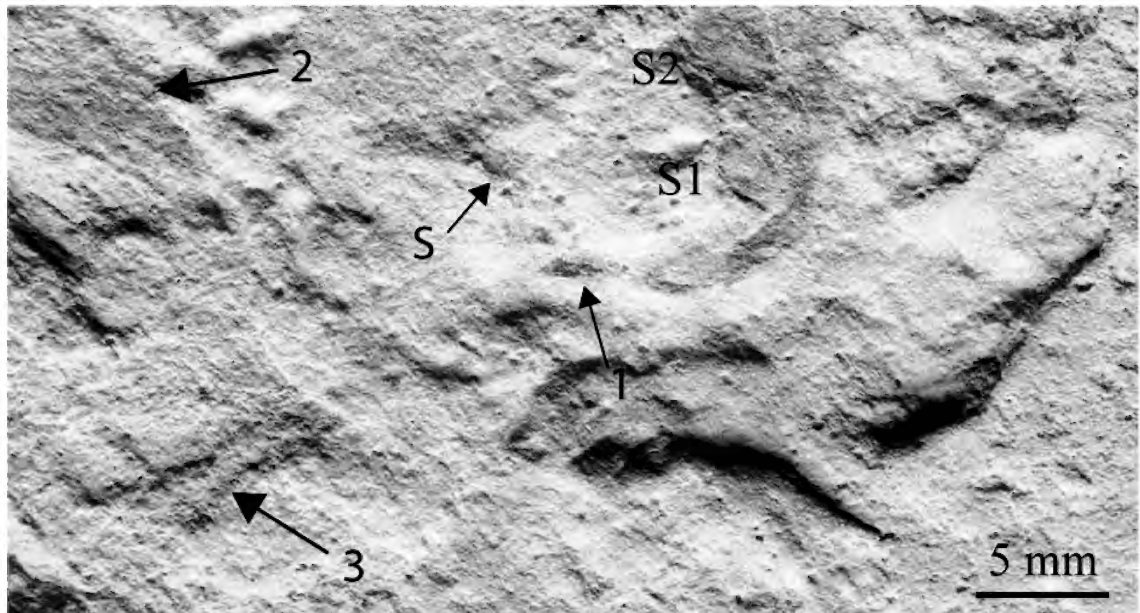
Figure 9. cf. *Zosterophyllum* sp. A. (part, NMV P256740.1). Proximal region of spike with sporangia one (S1) and two (S2) visible and fertile axis curving into ?rhizomatous region (arrow 1) and possibly extending out towards axes (arrows 2 and 3). Isolated sporangium (S) in same orientation as sporangia in spike. Image taken by Rodney Start © Museums Victoria.

In comparison with species within the subgenus *Zosterophyllum* with reniform sporangia, the specimen is closest to *Z. bifurcatum* Li and Cai, 1977; *Z. deciduum*; *Z. myretonianum* Lang, 1927; *Z. ramosum*; *Z. rhenanum*; *Z. yunnanicum* Hsü, 1966; and *Z. shengfengense*, all of which have sporangia in approximately the same size range.

Zosterophyllum myretonianum is one of the best studied *Zosterophyllum* to date (Edwards, 1975; Lang, 1927; Lele and Walton, 1961). Edwards (1969: 261) noted when examining *Z. myretonianum* from Aberlemno, Scotland, that they possessed spikes with different levels of sporangial packing, such that the specimens could be divided into compact, intermediate and laxly arranged spikes. The sporangial–stalk interface of *Z. myretonianum*, according to Edwards (1975), possesses a dome-like region at the point of insertion on the sporangium of some of the specimens, which produces its reniform shape. It is noticeable that in *Z. myretonianum*, despite different stages in development, the orientation of the sporangial stalk remains largely constant, with the sporangial stalk inserted at almost 90° (Edwards, 1975) to the fertile axis before curving upwards immediately with the sporangium held erect. This clearly differs from the specimen where the sporangial stalks extend from the fertile axis, curving upwards only just beneath the sporangium and in some cases attached to the sporangium at an angle, thus producing a splayed appearance. *Zosterophyllum bifurcatum* possess well-developed lobes and much narrower stalks than the specimen reaching up to 0.6 mm wide according to Li and Cai (1977) and Hao and Xue (2013). *Zosterophyllum rhenanum* also possess well-developed sporangial lobes and has a noticeable junction between sporangium and stalk, and a large border of 0.6 mm (Hao and Xue, 2013; Schweitzer, 1979). *Zosterophyllum deciduum* has weakly developed sporangial lobes (Gerrienne, 1988: 322), similar to the specimen, but the sporangial stalks were wide (0.4–0.75 mm) near the fertile axis and narrow (0.1–0.3 mm) near the sporangium (Gerrienne, 1988: 320), with the contact between the sporangium and subtending stalk producing a clear junction with no evidence of widening beneath the sporangia (Gerrienne, 1988: 331). These characteristics are at odds with what is observed with the specimen where sporangial stalks remain parallel in width before widening into the base of the sporangium. Furthermore, *Z. deciduum* bifurcates both below and within its fertile parts (Gerrienne, 1988).

In comparison with *Zosterophyllum* from the South China plate with similar sporangial dimension, *Zosterophyllum shengfengense* from the Lochkovian, Lower Devonian of Xitun Formation, Yunnan, China, differs from the specimen in not possessing any sporangial basal lobes, and shorter stalks, 0.5–0.8 mm wide and 0.8–1.6 mm long (Hao et al., 2010; Hao and Xue, 2013). Furthermore, *Zosterophyllum shengfengense* (Hao et al., 2010: 222), like *Z. myretonianum* (Lele and Walton, 1961: 471), possess tubercles proximally on the plant, unlike the specimen (Hao et al., 2010: fig. 2a). *Zosterophyllum yunnanicum* from the Xujiachong Formation, Yunnan, possess crowded spikes with up to 50 sporangia circular to elliptical in face view, dehiscence zone up to 0.5 mm wide, stalks 0.3–0.9 mm wide and 0.6–3.0 mm long

inserted an acute angle to the fertile axis and widening into the bases of sporangia (Edwards et al., 2015: 223). The stalks emanate perpendicular to the spike, based on Edwards et al. (2015: pl. 4, figs 1, 2) and immediately reorientate producing 30°–40° to the fertile axis (Wang, 2007: 528). This reorientation of the stalks near the fertile axis differs significantly from the specimen, where the stalks reorientate only just beneath each sporangium. Furthermore, *Z. yunnanicum* produces a dome-like structure at the stalk–sporangium interface (Edwards et al., 2015).

Comparison with known Victorian zosterophyll taxa. Only four zosterophylls have thus far been described from Victoria. These include *Z. australianum* Lang and Cookson, 1930; *Z. ramosum* Hao and Wang, 2000; *Parazosterophyllum timsiae* McSweeney et al., 2020; and *Gippslandites minutus* McSweeney et al., 2020. Both *Z. australianum* and *Z. ramosum* occur in the Norton Gully Sandstone Formation of Victoria and are younger than the specimen, which is currently only known from the underlying Wilson Creek Shale. *Zosterophyllum australianum* occurs at North Road Quarry, Walhalla, Victoria, and Yunnan (Posongchong Formation), China (Hao and Xue 2013; Lang and Cookson 1930). *Zosterophyllum australianum* possess sporangia that are noticeably larger than the specimen and are longitudinally elliptical or fan-shaped, 2.8–8.0 mm wide and 2.2–5.0 mm high, with short stalks inserted on the fertile axis at 90° (Hao and Xue, 2013; Lang and Cookson, 1930). *Zosterophyllum ramosum* occur at Mount Pleasant and Halls Flat Road, Alexandra (Cookson, 1935; Hao and Wang, 2000). Mount Pleasant Road is the type locality of *Yarravia (Hedeia) corymbosa* Cookson, 1935, and cf. *Baragwanathia longifolia*, cf. *Yarravia oblonga*, cf. *Hostinella* and *Pachytheca* sp. have been found by Cookson (1935) to occur with *Z. ramosum* (McSweeney et al., 2021a, b). *Zosterophyllum ramosum* was originally called *Z. australianum* by Cookson (1935: pl. 10, figs 9–12), but was later reinterpreted by Hao and Wang (2000: 31) to be a new species *Z. ramosum*, which also occurs in Yunnan (Posongchong Formation), China. *Zosterophyllum ramosum* possess circular to reniform sporangia similar to the specimen, but the sporangia are larger, being 1.6–6.0 mm wide and 1.9–5.5 mm high, on stalks up to 5.0 mm inserted on the fertile axis at 15°–35° (Hao and Wang, 2000; Hao and Xue, 2013). Both *Z. ramosum* and *Z. australianum*, according to Hao and Xue (2013: fig. 6.5), possess apple-shaped Za-type sporangium with extended thickened margins, a character not found in the specimen. *Parazosterophyllum timsiae* is from Ghin Ghin Road, Yea, in the base of the Humevale Formation and based on Rickards & Garratt (1990) Pridoli, upper Silurian–Pragian, Lower Devonian, and may be either coeval or older than the specimen and differ significantly from the specimen with its spike terminating lateral branch (McSweeney et al., 2020). *Gippslandites minutus* is from an outcrop of the Boola formation (Lochkovian–Pragian, L. Devonian) near Boola Quarry, Tyers, Victoria (Tims, 1980; McSweeney et al., 2000). The Boola formation is slightly older than the Wilson Creek Shale, which overlies the Boola formation at Coopers Creek according to Edwards et al. (1997: 39). *Gippslandites minutus* differs from the specimen because its sporangia are much smaller, 0.6–2.6

mm wide and 0.3–1.9 mm high, and differ significantly from *Zosterophyllum* spp. with anisovalvate sporangia (McSweeney et al., 2020).

The defining characteristic of the specimen is primarily the angle of insertion of the vascularised stalks and no overlap between vertical adjacent sporangia. As noted by Edwards (1975: 264), the most useful characters in species delimitation within *Zosterophyllum* are stalk and sporangial characters. It is clear that the specimen differs from zosterophylls from Victoria primarily on sporangial morphology and symmetry. As the sporangial stalks were likely longer in life when turgid and prior to degradation resulting in convoluted vascular trace, the lack of vertical overlap of sporangia and vascularisation of the stalks, and clear demarcation of insertion points on the fertile axis means the specimen cannot be readily put into the subgenus *Platyzosterophyllum*, and is thus assigned to cf. *Zosterophyllum* sp. A. until better material becomes available to allow for further assessment of its phylogenetic and taxonomic position.

cf. *Zosterophyllum* sp. B.

Gen. et sp. indet.

Figures 10, 11

Material. NMV P256742.1 and P256742.2 (P4-5 field note identifier), part and counterpart, respectively.

Locality. P4 is equivalent to Loc. 1 in Garratt (1978: fig. 2), and occurs on Ghin Ghin Road, 8 km northwest of Yea township, central Victoria.

Horizon and age. Humevale Siltstone, Pragian–Emsian, Lower Devonian (Edwards et al., 1997; Garratt, 1978; Rickards, 2000; Rickards and Garratt, 1990; VandenBerg et al. 2000; VandenBerg pers. comm. June 2021).

Description. Single specimen, comprising compact spike, with part and counterpart preserved in semi-relief as an iron oxide coated impression and cast, only gross morphological features are visible (fig. 10). The spike measures 21 mm high and 10 mm
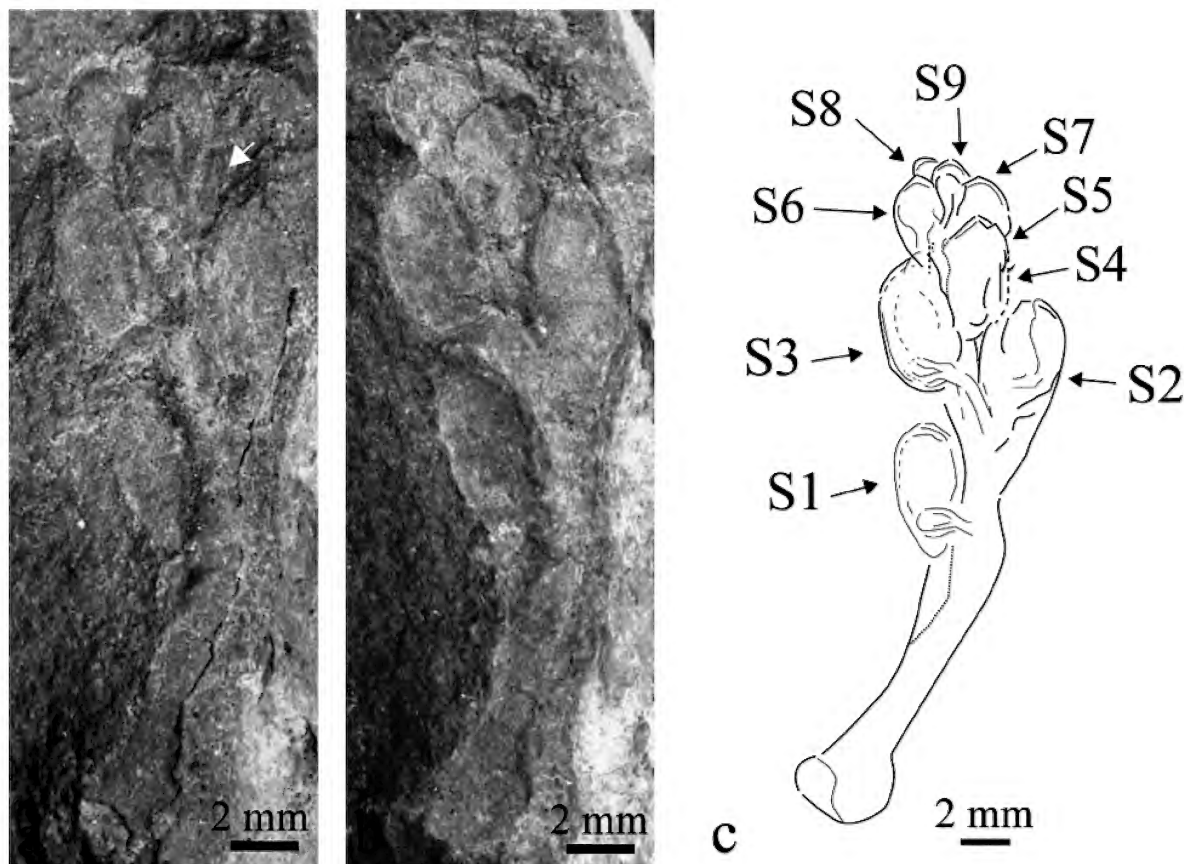
Figure 10. cf. *Zosterophyllum* sp. B, from the Humevale Siltstone, Ghin Ghin Road, Yea: a, part (NMV P NMV P256742.1); b, counterpart (NMV P NMV P256742.2) respectively; c, line drawing, with S1–9 (sporangia one to nine). Note: Part image reversed to be in the same orientation as the counterpart. Note. Arrow in part, points to sporangium 4, which is obscured in the counterpart.
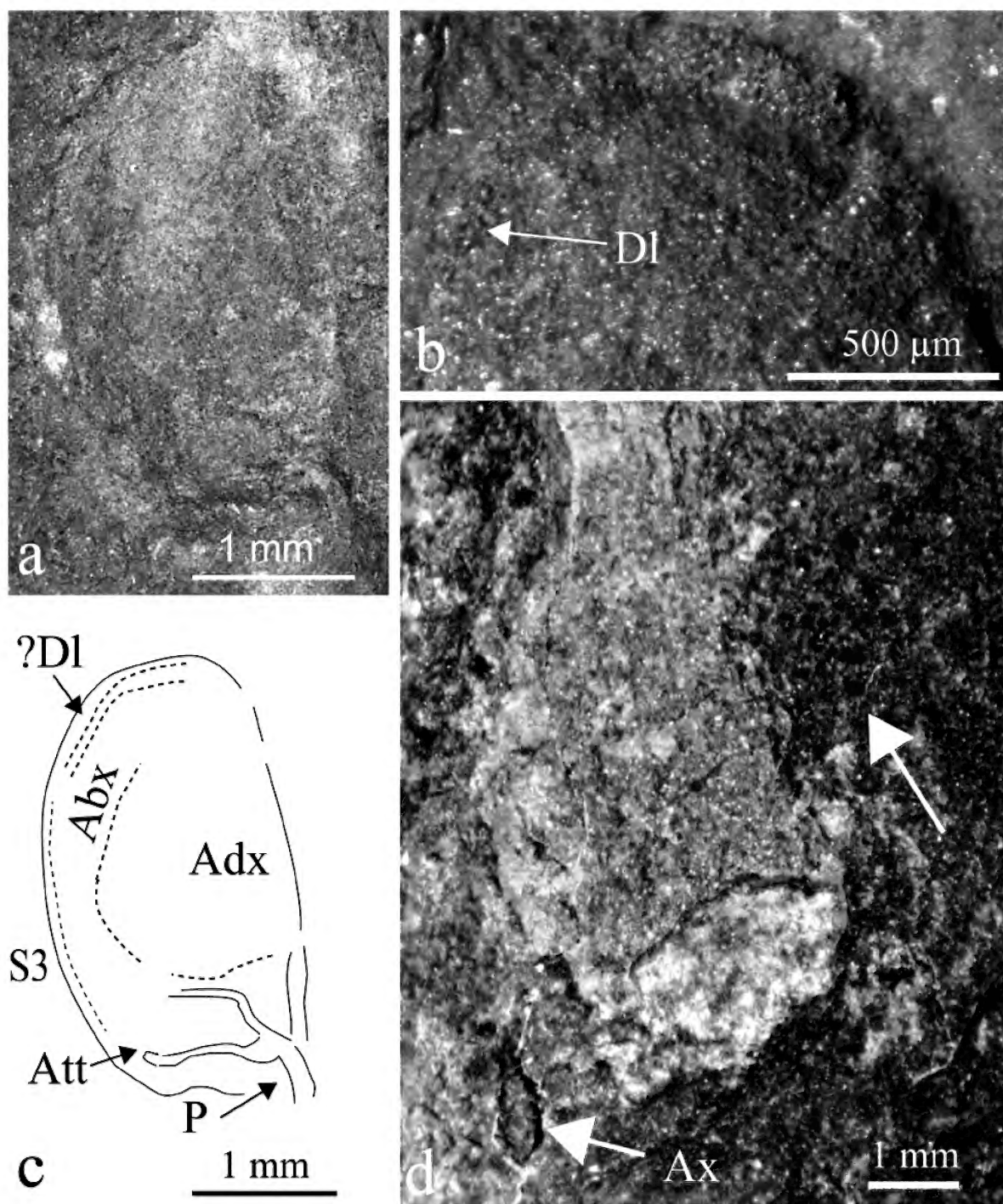
Figure 11. cf. *Zosterophyllum* sp. B. NMV P256742.1: a, c, (line drawing) sporangium 3 (counterpart) in-folded, with stalk attachment widening out in basal region of sporangium. Poorly defined dehiscence zone (zone) and line; b, sporangium one (counterpart) with border visible; d, basal oval structure (part), with what appears to be a much smaller spike emanating from it (at arrow), and a poorly preserved axis beneath the oval structure.

wide, with at least nine sporangia arranged helically, becoming more compact distally. The fertile naked axis measures 1.5–3.75 mm wide, narrowing distally before terminating in sporangium nine. Sporangia in face view (1.2–3.0 mm wide and 3.9–4.3 mm long) occur in the distal part of the spike and are circular to oblong. Proximally, sporangia one to three are in lateral view, being longitudinally elliptical and infolded. Sporangia are inserted at an angle of ~20°. Proximally on the spike there is an elliptical (lateral view) junction at the point of attachment (face view) on the abaxial valve between the stalk and the sporangium. The stalks are decurrent, narrowing slightly before widening distally at the base of the sporangium. The sporangia possess a dehiscence zone along their entire distal margins, with a border 0.1–0.2 mm wide gradually tapering proximally towards the stalk attachment.

Remarks. There is a notable disparity in size between the much larger proximal sporangia (S1–5) and distal sporangia (S6–9), suggesting the spike may be immature. Sporangia one–three are in a lateral position and are infolded, a common feature seen especially in laterally placed sporangia of *Zosterophyllum*. It suggests that the sporangia may have originally had relatively flat bodies, as proposed by Lang (1927) when explaining this feature in *Zosterophyllum myretonianum*. The points of attachment of the stalk to the sporangia are visible on sporangia one and three (Figs 11a, c), with the stalks widening into the base of the sporangia. The attachment is elliptical, and it is possible that the raised regions defining the elliptical region, which appear partially raised, may reflect the splitting of the attachment at the base of the sporangium, possibly feeding each of the valve. However, the preservation is too poor and this remains equivocal. The attachment occurs on the adaxial side of the valve, but the demarcations between both valves are faint or absent on the sporangia. Most of the distal sporangia show the stalk centred beneath the sporangium, with a gradual widening of the stalk into the valve. Sporangium seven, which is in face-view, appears to show the widening of the distal part of the stalk on the lower part of a valve, producing a sub-circular zone of attachment. Sporangium five, while poorly preserved, is in side view and greatly compressed laterally with the projecting edge of the border visible in the apex, and a fine stalk is present in the basal region. The adaxial valve only appears marginally darker than the surrounding matrix and is convex, while the upper valve is flatter and delimited by its iron-oxide colouration. Sporangia four and six also appear to show a slight separation at the distal-most region of the valves. This may be a result of compression as the sporangia are small relative to the proximal sporangia, suggesting they were not fully mature.

The dehiscence line can be seen along the distal margins of the proximal sporangia, visible down to the stalk attachment (fig. 11c) but is only visible on some of the distal sporangia. There is a dehiscence zone beside the dehiscence line no wider than 0.2 mm and is clearest on the proximal sporangia.

The proximal part of the fertile axis expands into an oval-shaped body (fig. 11d) that measures 3.74 mm wide and 5.80 mm high. The point where the axis starts increasing in diameter was taken as the start of this structure because there is no other way to differentiate it from the axis. The oval body is similar to the corm-like structure found basally on

Horneophyton lignieri Barghoorn and Darrah (= *Hornea lignieri* Kidston and Lang, 1920). However, because no anatomy is preserved, its nature remains equivocal and may be a quirk of preservation. A small, fine, faint linear structure (fig. 11d) appears to emanate from the oval body, but remains equivocal because sampling did not reveal any organic remains and high magnification did not reveal any morphological characters.

The specimen fits into the class Zosterophyllopsida based on the presence of naked axes, cauline sporangia made up of two valves that dehisce along their distal margins, and vascularized stalks (Croft and Lang, 1942). The Zosterophyllopsida includes two orders, Zosterophyllales and Gosslingiales, and because this specimen possessed a terminal sporangium, it has been assigned to order Zosterophyllales. Numerous characteristics are notably absent, such as H- or K-branching and circinate vernation. Because the sporangia were not in rows, the specimen was excluded from the subgenus *Platyzosterophyllum* and tentatively placed into the subgenus *Zosterophyllum*. However, it was difficult to determine the true morphological outline of the sporangia, with some of the distal sporangia appearing slightly longer than wider. Furthermore, the absence of sporangia proximally in face view added to the uncertainty of whether the sporangia were slightly vertically elongate. Distally, the sporangia are poorly preserved with no unequivocal demarcation of both the valves and junctions between the valves and their subtending stalks. For the subgenus *Zosterophyllum*, the sporangia are reinform, fan-shaped and isovalved, and are excluded if anisovalvate or vertically longer than wide according to Edwards et al. (2016) and Edwards and Li (2018a). Additionally, the presence of an oval region at the proximal end of the fertile axis added further doubt to its true assignation, and so the specimen was placed into cf. *Zosterophyllum* sp.

cf. *Zosterophyllum* sp. B differs from known *Zosterophyllum* spp. from Victoria (*Z. australianum* and *Z. ramosum*), despite the limited characters available for comparison. *Zosterophyllum australianum* possess horizontally elliptical sporangia with large, thickened margins (0.4–1.1 mm wide) and sporangia far larger than cf. *Zosterophyllum* sp. B., reaching up to 8.0 mm wide and 5.0 mm high (Hao and Xue, 2013; Lang and Cookson, 1930). Additionally, the stalks of *Z. australianum* are inserted at an angle of ~90°, in contrast to ~20°° in cf. *Zosterophyllum* sp. B. *Zosterophyllum ramosum*, like *Z. australianum*, possess much larger sporangia, reaching up to 6.0 mm wide and 5.5 mm high, and are circular to reinform in shape (Hao and Wang, 2000).

In comparison with other zosterophylls with vertically elongate sporangia outside the subgenus *Zosterophyllum*, cf. *Zosterophyllum* sp. B. appears distinct, despite the paucity of available characters with which to compare. For example, *Guangnania cuneata* Wang and Hao, 2002, possess anisovalvate upright sporangia, but differ from cf. *Zosterophyllum* sp. in the spike not being compact, the sporangia being much longer than wide (3.9–6.2 mm high and 1.5–1.9 mm wide) and not possessing a terminal sporangium. *Yunia dichotoma* Hao and Beck, 1991, from the Zhichang section of the Posongchong Formation, differs from cf. *Zosterophyllum* sp. B in the morphology of the sporangia, which are elongate–elliptical to ovoid, but the sporangia did not form spikes (Hao and Beck,

1991). Additionally, the axes of *Y. dichotoma* possess small spines (Hao and Beck, 1991). *Huia recurvata* Geng, 1985, of the Posongchong Formation, Yunnan, China, produced sporangia that were ovate to ovoid 2D to 3D (Hao and Xue, 2013: 70). *Huia recurvata* differs in having adaxially reflected closely arranged sporangia as opposed to the crowded arrangement seen in cf. *Zosterophyllum* sp. B., with sporangia 3–5 mm wide and 6–10 mm high (Hao and Xue, 2013).

Primarily, because the specimen lacks unequivocal evidence as to the characteristics of the sporangia, such as whether the sporangia are longer than wide, it has been placed in cf. *Zosterophyllum* sp. B.

Discussion

The term sporangial stalk is used with regards to cf. *Zosterophyllum* sp. A. for convenience, similar to Edwards (2006: 96), but it is possible they represent lateral branches with sessile sporangia, as proposed by Hueber (1992: 480) in his examination of zosterophyll sporangial and based on his hypothesis that some cooksonioids were the progenitor of this group. The presence of a vascular trace in the sporangial stalk of cf. *Zosterophyllum* sp. A. adds credence to Hueber's hypothesis (category 3) and has been observed with *Z. divaricatum* (Gensel, 1982: 654), *Z. myretonianum* (Edwards, 1975: 262; Lang, 1927: 450), and according to Niklas and Banks (1990: 278), *Z. rhenanum* and *Z. longhaushanense*. Niklas and Banks (1990: 277) proposed two patterns of fertile growth within zosterophylls governed by apical meristematic growth and speculated the difference in symmetry for *Z. myretonianum*, *Z. fertile* and *Z. llanoveranum* was due to uncanalised growth and that the nature of the apices (terminate and non-terminate) was the key to determining the type of meristematic growth. Interestingly Niklas and Banks (1990: 278), in discussing bilateral symmetry, postulated that the stalks were not the same as fertile axes and the lateral cluster of initials producing the stalks and sporangia would likely result in limited to no vascularisation of the stalk. This limited vascularisation of lateral axes appears to occur with cf. *Zosterophyllum* sp. A., whereby the apical initials of lateral axes were limited to just a single axis before terminating in a sporangium.

Both cf. *Zosterophyllum* sp. A. and cf. *Z. fertile* possess sporangia arranged in rows on their spikes, and this is the first time this arrangement has been described for Victorian Devonian flora. The zosterophyll assemblages from China, particularly those from the Pragian Posongchong Formation of the South China Plate, have predominantly been of sporangia inserted helically into the spike (Hao & Xue, 2013). Only three cases of sporangia occurring in rows in spikes have been recorded: *Zosterophyllum longhuashanense* Li and Cai, 1977; *Distichophytum* sp.; and *Amplectosporangium* (*Oricilla*) *unilaerale* Edwards and Li, 2018 (Edwards and Li, 2018; Hao and Xue, 2013). Another, *Ornicephalum* (*Zosterophyllum*) *sichuanense* Edwards and Li (2018: 100), superficially appears to show two-rowed sporangia. The geographical location of Victoria during the Pragian–Emsian, Lower Devonian, approximately 30° south of the equator, far from both the South China Plate and other known *Zosterophyllum* localities, suggests

two of the specimens described herein may be new taxa. The palaeocontinental positioning of Victoria and the South China Plate during the Lower Devonian is based on the work of Mitchell et al. (2012) and Torsvik and Cocks (2019), and is summarised in McSweeney et al. (2020). Australia and South China have only two species in common thus far – *Z. australianum* and *Z. ramosum* – and the specimens described herein further add to the hypothesis of limited floristic exchange, as espoused by Xue et al. (2018: 98).

Conclusion

This study has confirmed the first occurrence of bilateral symmetry in Victoria. Despite the dearth of fossil evidence, three additional forms – cf. *Zosterophyllum* sp. A, cf. *Z*. sp. B. and cf. *Z. fertile* – indicate greater diversity in the region during the Silurio–Devonian than previously known. However, forms with better preservation are required to determine their taxonomic positions with certainty.

Disclosure Statement

No potential conflict of interest was reported by the authors.

References

Banks, H.P. 1980. Floral assemblages in the Siluro-Devonian. Pp. 1–24 in: Dilcher, D.L. and Taylor, T.N. (eds), *Biostratigraphy of fossil plants: successional and palaeoecological analyses*. Dowden, Hutchinson and Ross: Stroudsburg, PA, USA.

Carey, S.P., and Bolger, P.F. 1995. Conodonts of disparate Lower Devonian zones, Wilson Creek Shale, Tyers-Walhalla area, Victoria, Australia. *Alcheringa* 19(1): 73–86.

Cleal, C.J., and Thomas, B.A. 1999. *Fossils illustrated 3: Plant fossils: the history of land vegetation*. Boydell Press: Woodbridge, Suffolk, UK, 200 pp.

Cookson, I.C. 1935. On plant remains from the Silurian of Victoria, Australia, that extend and connect hitherto described. *Philosophical Transactions of the Royal Society of London Series B* 225: 127–148.

Croft, W.N., and Lang, W.H. 1942. The Lower Devonian flora of the Senni Beds of Monmouthshire and Breconshire. *Philosophical Transactions of the Royal Society of London B* 231: 131–163.

Douglas, J.G., and Jell, P.A. 1985. Two thalloid (probably algal) species from the Early Devonian of Central Victoria. *Proceedings of the Royal Society of Victoria* 97(3): 157–162.

Edwards, D. 1969a. *Zosterophyllum* from the Old Red Sandstone of South Wales. *New Phytologist* 68: 923–931.

Edwards, D. 1969b. Further observations on *Zosterophyllum llanoveranum* from the Lower Devonian of South Wales. *American Journal of Botany* 56(2): 201–210.

Edwards, D. 1972. A *Zosterophyllum* fructification from the Lower Old Red Sandstone of Scotland. *Review of Palaeobotany and Palynology* 14: 77–83.

Edwards, D. 1975. Some observations on the fertile parts of *Zosterophyllum myretonianum* Penhallow from the Lower Old Red Sandstone of Scotland. *Transactions of the Royal Society of Edinburgh* 69: 251–265.

Edwards, D. 2006. *Danziella artesiana*, a new name for *Zosterophyllum artesianum* from the Lower Devonian of Artois, northern France. *Review of Palaeobotany and Palynology* 142: 93–101.

Edwards, D., Bassett, M.G., and Rogerson, E.C.W. 1979. The earliest vascular land plants: continuing the search for proof. *Lethaia* 12: 313–324.

Edwards, D., Yang, N., Hueber, F.M., and Li, C-S. 2015. Additional observations on *Zosterophyllum yunnanicum* Hsü from the Lower Devonian of Yunnan, China. *Review of Palaeobotany and Palynology* 221: 220–229.

Edwards, D., and Li, C-S. 2018. Diversity in affinities of plants with lateral sporangia from the Lower Devonian of Sichuan Province, China. *Review of Palaeobotany and Palynology* 258: 98–111.

Edwards, J., Olshina, A., and Slater, K.R. 1997. Nagambie and part of Yea 1:100 000 map geological report. *Geological Survey of Victoria Report* 109, 145 pp.

Fairon-Demaret, M., Hilton, J., and Berry, C.M. 1999. Surface preparation of macrofossils (dégagement). Pp. 33–35 in: Jones, T.P. and Rowe, N.P. (eds), *Fossil plants and spores: modern techniques*. Geological Society: London.

Garratt, M.J. 1978. New evidence of a Silurian (Ludlow) age for the earliest *Baragwanathia* flora. *Alcheringa* 2: 217–224.

Garratt, M.J. 1980. Silurio–Devonian Notanopliidae (Brachiopoda). *Memoirs of the National Museum* 41: 15–45.

Garratt, M.J., and Wright, A.J. 1988. Late Silurian to Early Devonian biostratigraphy of southeastern Australia. Pp. 103–146 in: McMillan, N.J., Embrey, A.F., and Glass, D.J. (eds), *Devonian of the world*. Volume 3. Canadian Society of Petroleum Geologists: Calgary, Canada.

Gensel, P.G. 1982. A new species of *Zosterophyllum* from the early Devonian of New Brunswick. *American Journal of Botany* 69(5): 651–669.

Gerrienne, P. 1988. Early Devonian plant remains from Marchin (north of Dinant Synclinorium, Belgium), I. *Zosterophyllum deciduum* sp. nov. *Review of Palaeobotany and Palynology* 55: 317–335.

Gill, E.D. 1942. On the thickness and age of the type Yeringian strata, Lilydale, Victoria. *Proceedings of the Royal Society of Victoria* 54: 21–52.

Hao, S.-G., and Beck, C.B. 1991. *Yunia dichotoma*, a Lower Devonian plant from Yunnan, China. *Review of Palaeobotany and Palynology* 68: 181–195.

Hao, S.-G., and Wang, D.-M. 2000. Two species of *Zosterophyllum* Penhallow (*Z. australianum* Lang and Cookson, *Z. ramosum* sp. nov.) from the Lower Devonian (Pragian) of southeastern Yunnan, China. *Acta Palaeontologica Sinica* 39 (sup.): 26–41.

Hao, S.-G., and Xue, J. 2013. *The early Devonian Posongchong flora of Yunnan – a contribution to an understanding of the evolution and diversity of vascular plants*. Science Press: Beijing, China, 366 pp.

Hao, S.-G., Xue, J., Guo, D., and Wang, D. 2010. Earliest rooting system and root: shoot ratio from a new *Zosterophyllum* plant. *New Phytologist* 185: 217–225.

Hao, S.-G., Xue, J., Liu, Z., and Wang, D. 2007. *Zosterophyllum* Penhallow around the Silurian–Devonian boundary of northeastern Yunnan, China. *International Journal of Plant Science* 168(4): 477–489.

Hueber, F.M. 1972. *Rebuchia ovata*, its vegetative morphology and classification with the Zosterophyllophytina. *Review of Palaeobotany and Palynology* 14: 113–127.

Hueber, F.M. 1983. A new species of *Baragwanathia* from the Sextant Formation (Emsian), Northern Ontario, Canada. *Botanical Journal of the Linnean Society* 86: 57–79.

Hueber, F.M. 1992. Thoughts on the early lycopsids and zosterophylls. *Annals of the Missouri Botanical Garden* 79: 474–499.

Jackson, P.N.W. 2010. *Introducing palaeontology – a guide to ancient life*. Dunedin Academic Press Ltd: Edinburgh, Scotland. 152 pp.

Jaeger, H. 1966. Two late *Monograptus* species from Victoria, Australia and their significance for dating the *Baragwanathia* flora. *Proceedings of the Royal Society of Victoria* 79: 393–413.

Kidston, R., and Lang, W.H. 1920. On Old Red Sandstone plants showing structure, from the Rhynie chert bed, Aberdeenshire. II. Additional notes on *Rhynia gwynne-vaughanii* with descriptions of *Rhynia major* n. sp. and *Hornea lignieri* n. g., n. sp. *Transactions of the Royal Society of Edinburgh* 52: 603–627.

Lang, W.H. 1927. Contributions to the study of the Old Red Sandstone Flora of Scotland. VI. On *Zosterophyllum myretonianum*, Penh., and some other plant-remains from the Carmyllie Beds of the Lower Old Red Sandstone. VII. On a specimen of *Pseudosporochnus* from the Stromness Beds. *Earth and Environmental Science Transactions of the Royal Society of Edinburgh* 55(2): 443–455.

Lang, W.H., and Cookson, I.C. 1930. Some fossil plants of Early Devonian type from the Walhalla Series, Victoria, Australia. *Philosophical Transactions of the Royal Society of London Series B* 219: 133–163.

Lang, W.H., and Cookson, I.C. 1935. On a flora, including vascular land plants, associated with *Monograptus*, in rocks of Silurian age from Victoria, Australia. *Transactions of the Royal Society of London, B* 224: 421–449.

Leclercq, S. 1942. Quelques plantes fossiles recueillies dans le Dévonien inférieur des environs de Nonceveux (bordure orientale du bassin di Dinant). *Annales de la Société Géologique de Belgique* 65: 193–211. (French)

Lele, K.M., and Walton, J. 1961. Contributions to the knowledge of *Zosterophyllum myretonianum* Penhallow from the Lower Old Red Sandstone of Angus. *Transactions of the Royal Society of Edinburgh* 64: 469–475.

Lenz, A.C. 2013. Early Devonian graptolites and graptolite biostratigraphy, Arctic Islands, Canada. *Canadian Journal of Earth Sciences* 50(11): 1097–1115.

Li, X.X., and Cai, C.Y. 1977. Early Devonian *Zosterophyllum* remains from Southwest China. *Acta Palaeontologica Sinica* 16: 12–34. (Chinese)

Mawson, R., and Talent, J.A. 1994. Age of an Early Devonian carbonate fan and isolated limestone clasts and megaclasts, East-Central Victoria. *Proceedings of the Royal Society of Victoria* 106: 31–70.

McSweeney, F.R., Shimeta, J., and Buckeridge, J.S. 2020. Two new genera of early Tracheophyta (Zosterophyllaceae) from the upper Silurian–Lower Devonian of Victoria, Australia. *Alcheringa* 44(3): 379–396.

McSweeney, F.R., Shimeta, J., and Buckeridge, J.S. 2021a. *Yarravia oblonga* Lang & Cookson, 1935 emend. from the Lower Devonian of Victoria. *Alcheringa* 45 (3), 299–314. 10.1080/03115518.2021.1958257

McSweeney, F.R., Shimeta, J., and Buckeridge, J.S. 2021b. Lower Devonian (Pragian–Emsian) land plants from Alexandra, Victoria, Australia: an early window into the diversity of Victorian flora from southeastern Australia. *Alcheringa* 45 (3), 315–328. 10.1080/03115518.2021.1971297

McSweeney, F.R., Shimeta, J., and Buckeridge, J.S. 2021c. Early land plants from the Lower Devonian of central Victoria, Australia, including a new species of *Salopella*. *Memoirs of Museum Victoria* 80, 193–205. 10.24199/j.mmv.2021.80.11.

Mitchell, R.N., Kilian, T.M., and Evans, D.A. 2012. Supercontinent cycles and the circulation of absolute palaeolongitude in deep time. *Nature* 482: 208–212.

Moore, D.H., VandenBerg, A.H.M., William, C.E., and Magart, A.P.M. 1998. Palaeozoic geology and resources of Victoria. *AGSO Journal of Australian Geology & Geophysics* 17: 107–122.

Niklas, K.J., and Banks, H.P. A reevaluation of the Zosterophyllophytina with comments on the origins of lycopods. *American Journal of Botany* 77(2): 274–283.

Rickards, R.B. 2000. The age of the earliest club mosses: the Silurian *Baragwanathia* flora in Victoria, Australia. *Geological Magazine* 137(2): 207–209.

Rickards, R.B., and Garratt, M.J. 1990. Pridoli graptolites from the Humevale Formation at Ghin Ghin and Cheviot, Victoria, Australia. *Proceedings of the Geological Society* 48(1): 41–46.

Schweitzer, H.J. 1979. Die Zosterophyllaceae des rheinischen Unterdevons. *Bonner Palaeobotanische Mitteilungen* 3: 1–32. (German)

Talent, J.A., Gratsianova, R.T. and Yolkin, E.A. 2001. Latest Silurian (Pridoli) to Middle Devonian (Givetian) of the Asio-Australia hemisphere; rationalization of brachiopod taxa and faunal lists; stratigraphic correlation chart. *Courier Forschungsinstitut Senckenberg* 236: 1–221.

Thomas, D.E. 1953. Tanjilian Fossils. *Mining and Geological Journal* 5(2): 27.

Tims, J.D. 1980. *The early land flora of Victoria*. PhD thesis, University of Melbourne, Victoria, Australia. 233 pp. (unpublished)

Tims, J.D., and Chambers, T.C. 1984. Rhyniophytina and Trimerophytina from the early land flora of Victoria, Australia. *Palaeontology* 27(2): 265–279.

Torsvik, T.H., and Cocks, L.R.M. 2019. The integration of palaeomagnetism, in the geological record and mantle tomography in location of ancient continents. *Geological Magazine* 156: 1–19.

VandenBerg, A.H.M. 1973. Geology of the Melbourne District. Pp. 14–30 in: McAndrew, J., and Marsden, M.A.H. (eds), *Regional guide to Victorian geology*. 2nd ed., School of Geology, University of Melbourne: Melbourne.

VandenBerg, A.H.M. 1975. Definitions and descriptions of Middle Ordovician to Middle Devonian rock units of the Warburton District East Central Victoria. *Geological Survey of Victoria Unpublished Report* 1976/6.

VandenBerg, A.H.M. 1988. Silurian–Middle Devonian. Pp. 103–141 in: Douglas, J.G. and Ferguson, J.A. (eds), *Geology of Victoria*. 2nd ed., Geological Society of Victoria: Melbourne.

VandenBerg, A.H.M., Cayleym, R.A., Willman, C.E., Moreland, V.J., Seymon, A.R., Osborne, C.R., Taylor, P., and Sandford, A.C. 2006. Walhalla-Woods Point-Tallangallook special map area geological report. *Geological Survey of Victoria* 127. GeoScience Victoria, Department of Primary Industries: Melbourne.

Wang, D.-M. 2007. Two species of *Zosterophyllum* from South China and dating of the Xujiachong Formation with a biostratigraphic method. *Acta Geologica Sinica* 81(4): 525–538.

Wang, D.-M., and Hao, S.-G. 2002. *Guangnania cuneata* gen. et sp. nov. from the Lower Devonian of Yunnan Province, China. *Review of Palaeobotany and Palynology* 122: 13–27.

Walton, J. 1964. On the morphology of *Zosterophyllum* and some other early Devonian plants. *Phytomorphology* 14: 155–160.

Wellman, C.H. Habgood, K., Jenkins, G., and Richardson, J.B. 2000. A new plant assemblage (microfossil and megafossil) from the Lower Old Red Sandstone of the Anglo-Welsh Basin: its implication for the palaeoecology of early terrestrial ecosystems. *Review of Palaeobotany and Palynology* 109: 161–196.

Williams, G.E. 1964. The geology of the Kinglake district, central Victoria. *Proceedings of the Royal Society of Victoria* 77(2): 273–328.

Willman, C.E., Taylor, D.H., Morand, V.J., and VandenBerg, A.H.M. 2006. *Matlock 1:50 000 geological map*. Geological Survey of Victoria. GeoScience Victoria. Department of Primary Industries: Melbourne.

Xue, J. 2009. Two Zosterophyll plants from the Lower Devonian (Lochkovian) Xitun Formation of Northeastern Yunnan, China. *Acta Geologica Sinica* 83(3): 504–512.

Xue, J., Huang, P., Wang, D., Xiong, C., Liu, L., and Basinger, J.F. 2018. Silurian–Devonian terrestrial revolution in South China: Taxonomy, diversity, and character evolution of vascular plants in a palaeogeographical isolated, low-latitude region. *Earth-Science Reviews* 180: 92–125.

Taungurungia gen. nov., from the Lower Devonian of Yea, central Victoria, Australia

Fearghus R. McSweeney FGS[1,2,*], Jeff Shimeta[2], John St. J.S. Buckeridge FGS[1,3]

[1] Earth and Oceanic Systems Group, RMIT University, GPO Box 2476, Melbourne, VIC 3001, Australia
[2] School of Science, RMIT University, Melbourne, VIC 3001, Australia
[3] Museums Victoria, VIC 3001, Australia
* To whom correspondence should be addressed. Email: tidal75@gmail.com

Abstract   McSweeney, F.R., Shimeta, J. and Buckeridge, J.S. 2022. *Taungurungia* gen. nov., from the Lower Devonian of Yea, central Victoria, Australia. *Memoirs of Museum Victoria* 81: 43–53.
    This paper records a new genus *Taungurungia*, which is the first new taxon with emergences to be described from the Lower Devonian of Victoria. The fossil is preserved primarily as a compression and impression, and lacks internal anatomy. The fossil extends our knowledge of known variations within early land plants, with most characteristics, such as emergences and H- or K-branching, redolent of affinities with the zosterophylls. However, having a large ovate terminal sporangium, the fossil adds to taxa that in some cases have been provisionally allied to the zosterophylls with elongate sporangia; this further demonstrates the need for reassessment of the Zosterophyllopsida.

Keywords   embryophytes, zosterophyll, emergences, Lower Devonian, Victoria

Introduction

Banks (1968, 1975) recognised three subdivisions from the Psilophytales: the Rhyniophytina, Zosterophyllophytina and Trimerophytina. Subsequently, these have been raised to higher taxonomic ranks by many workers (Hao and Xue, 2013; Kenrick and Crane, 1997). Herein, we examine a new form similar to Zosterophyllopsida *sensu* Hao and Xue (2013). Zosterophyllopsida have sporangia that have a width to height ratio ≥1 and are reniform, globose or rounded in face view (Banks, 1968, 1975). However, some rare exceptions have been noted where the sporangia are longer than wide (Edwards et al., 2016; Edwards and Li, 2018; Hao and Beck, 1991; Hao and Xue, 2013; Wang and Hao, 2002). The specimen described herein augments taxa with longer-than-wide sporangia and is significant because little is known about these aberrations and their taxonomic significance. Four Zosterophyllopsida species are known from Victoria: *Zosterophyllum australanium* Lang and Cookson, 1930; *Z. ramosum* Hao and Wang, 2000; *Parazosterophyllum timsiae* McSweeney et al., 2020; and *Gippslandites minutus* McSweeney et al., 2020. But none of these Zosterophyllopsida resemble the specimen descibed below. Furthermore, axes with emergences are rare in Devonian Victorian flora and have only been described by Cookson (1935) and McSweeney et al. (2021) from the Norton Gully Sandstone Formation of Alexandra; axes resembling *Psilophyon* were noted by Williams (1964: 285) at location A82 on Kerridale Road, Homewood, near Yea.

Locality, stratigraphy and age

Location F103 (*sensu* Garratt, 1980) occurs in the Norton Gully Sandstone Formation according to Edwards et al. (1997, 1998) and VandenBerg et al. (2000). Garratt (1980: 590) did not record any fossils at F103. The Norton Gully Formation is found throughout the Mount Easton Province and parts of the Darraweit Guim Province (fig. 1) according to Edwards et al. (1997: fig. 6; VandenBerg et al. 2000: fig. 2.106). The exposure is on the northern side of the Goulburn Valley Highway (fig. 2) and consists of a sequence of siltstones that are indicative of quiescent conditions during deposition. The Norton Gully Sandstone Formation is considered to be Emsian age by Morand and Fanning (2006) and, based on the occurrence of *Uncinatograptus thomasi* (Jaeger, 1966), is considered to be Pragian and possibly Emsian age by Lenz (2013). Therefore, a late Pragian–Emsian, (Lower Devonian) age is given herein to account for these minor disparities.

Material and methods

NMV P257028.1 (part) and NMV P257028.2 (counterpart) were found *in situ* in January 2015 by the lead author with Michael Garratt. These buff yellow fine-grained siltstones easily split along bedding planes, with the fossil preserved as an iron-stained mould and cast with some carbonaceous film.

The specimen was photographed (figs 3a, b, 4a, 5, 6, 7a) by Rod Start of Museums Victoria on 17 March 2020, using cross-polarised light (circular filter) with a Canon 5DSR camera fitted
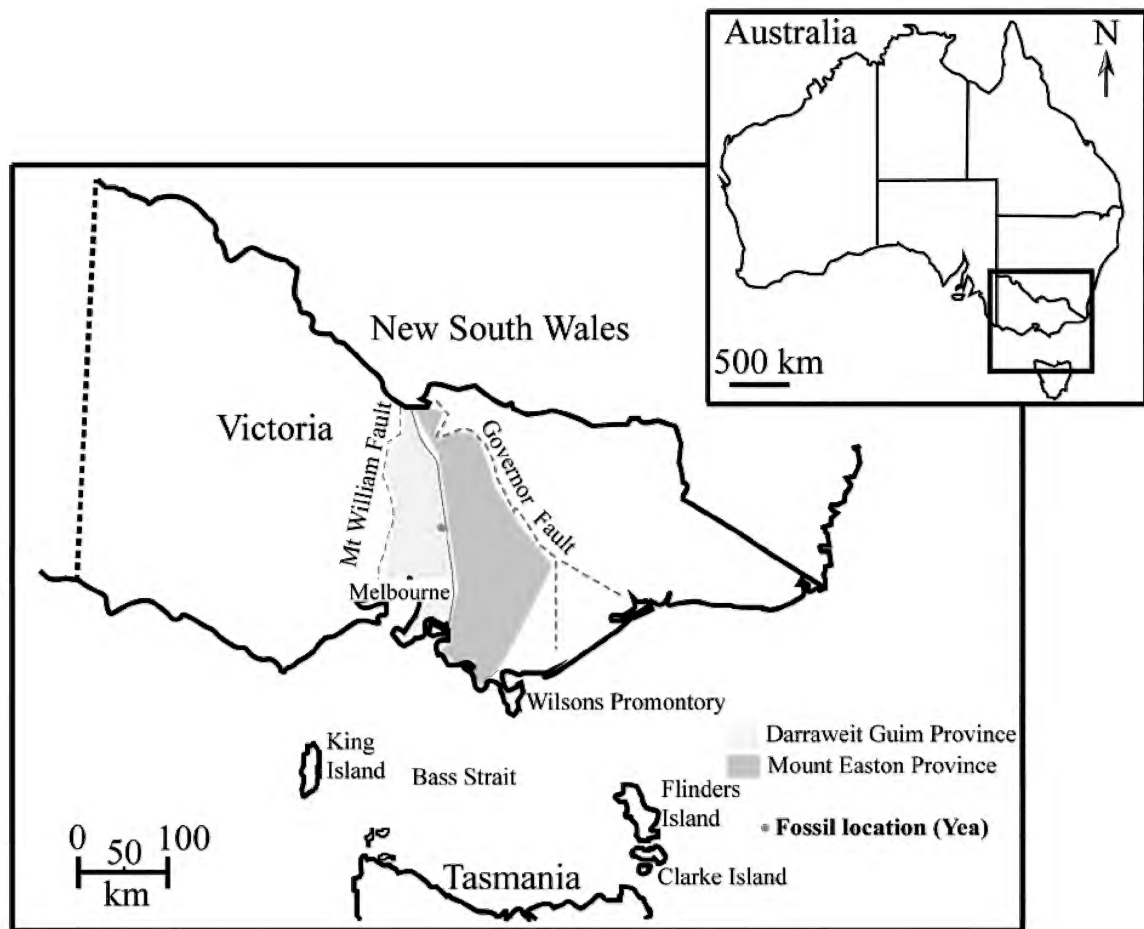
Figure 1. Map of Victoria, Australia, showing the fossil location of Yea within the Melbourne Zone. Source: adapted from Moore et al. (1998: fig. 2).
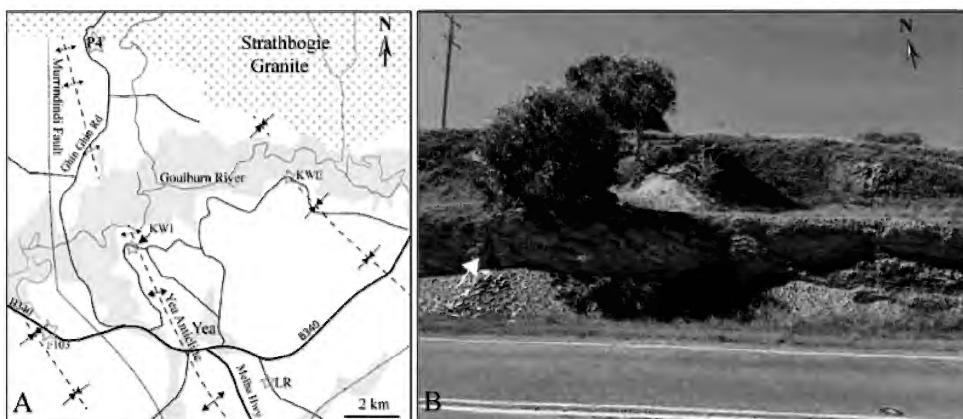

Figure 2. Goulburn Valley Highway fossil location F103 (Garratt 1980): a, F103 located about 5 km west of Yea; b, part of F103 exposure (37° 12' 30" S; 145° 21' 56" E) with arrow at location where *Taungurungia garrattii* gen. et sp. nov. was found *in situ*. Map after Garratt (1978) and positioning of Strathbogie Batholith after VandenBerg (1997).

with an EF 100 mm f/2.8L macro lens. Flash strip-lights were used to enhance contrast. The remaining images were taken using an AxioCamMRc5 camera attached to a Zeiss SteREO Discovery V8 stereomicroscope. Images were Z-stacked to improve depth of field using Adobe Photoshop CC 2017. ImageJ software (Image J1.52d, Wayne Rasband, USA, http://imagej. nih.gov/ij) was used to take measurements. Extensive dégagement (primarily following Fairon-Demaret et al., 1999) was undertaken by the lead author, mainly on NMV P257028.1, with a sample removed from an uncovered axis for analysis in low-vacuum mode on a FEI Quanta-200 scanning electron microscope at the RMIT Microscopy and Microanalysis Facility. No anatomical information was obtained. Dégagement of the distal region of one of the daughter axes on the counterpart (NMV P257028.2) revealed terminal small fusiform bodies along the axis (fig. 7a pre-dégagement; fig. 7b post-dégagement). Dégagement above the large terminal sporangium (fig. 3 pre-dégagement; fig. 4d post-dégagement) revealed small fusiform bodies near an axis that was poorly preserved. This dégagement was undertaken by gently loosening the overlying matrix above the spike by gently tapping the steel needle on the matrix to remove grains and work down to the fossil. Dégagement of proximally curved axis revealed additional minute fusiform bodies (fig. 7c, d post-dégagement).

Institutional abbreviations

NMV P, Museums Victoria Palaeontology Collection, Melbourne, Australia. The specimen NMV P257028.1 and NMV P257028.2, part and counterpart respectively, are housed in the Palaeontological section, Museums Victoria, Melbourne.

Systematic palaeobotany

Class. *Insertae sedis*

Genus. *Taungurungia* McSweeney, Shimeta and Buckeridge gen. nov.

Diagnosis: Terete axes with deltoid to elongate emergences. Fertile axes terminate in single large sessile ovate sporangium partially sunken into the axis with a curved junction between the axis and sporangium. Branching anisotomous and ?H- or K-branching in basal regions. Small fusiform to elliptical bodies (buds/sterile sporangia) occur on axes including the distal regions and on slender lateral axes, some with short stalks.

Etymology: Named for the indigenous Taungurung people.

Type species: *Taungurungia garrattii* McSweeney, Shimeta and Buckeridge gen. et sp. nov.

Taungurungia garrattii McSweeney, Shimeta and Buckeridge, sp. nov.

Figures 3–10

Species diagnosis: As for genus. Plant at least 185 mm high with axes at least 7.8 mm wide. Emergences up to 1.5 mm wide and 3.4 mm long. Mature axes terminate in a single ovate sporangium at least 7.5 mm wide and at least 15.5 mm long. Small fusiform

to elliptical bodies (buds/sterile sporangia) 0.5 mm wide and 1 mm long, some with short stalks occurring on all axes.

Etymology: Named for Michael Garratt in recognition of his work in Palaeozoic palaeontology, especially on brachiopods.

Holotype: NMV P257028.1 (part; F103-1p) and NMV P257028.2 (counterpart; F103-1cp), part and counterpart respectively.

Locality: The exposure occurs on the Goulburn Valley Highway (B340) 5 km west of Yea and was designated F103 by Garratt (1980). 37° 12' 30" S; 145° 21' 56" E.

Stratigraphy and age: Norton Gully Sandstone Formation, late Pragian–Emsian, Lower Devonian.

Taungurungia garrattii sp. nov.

Description (based on one specimen part and counterpart): The specimen consists of six parent axes that are 2.4–7.5 mm wide and taper gently acropetally; three of these axes are poorly preserved. The axes are oxidised and golden to yellow in coloration, with a vascular trace evident in parts of the axes, most notably proximally measuring 1.6 mm wide. Three of the larger axes terminate in a single sessile large ovate sporangium (fig. 3a). One is poorly preserved with only part of its apical region preserved (fig. 3b). The largest sporangium is 7.5 mm wide and 15.5 mm long and is ovate, reaching its maximum width 6.4 mm up from its base (figs 3, 4a, b). The sporangium does not possess a stalk, appears sessile and is partially embedded in the axis with a curved junction. Another large sporangium occurs low on the specimen (figs 3, 5) and is 14.7 mm long and 5.6 mm wide and is missing part of its cast basally. This sporangium sits with part of its basal region embedded into its subtending axis, again with a curved junction. The distal region of this sporangium is more elongate. These two sporangia have two fractures running transversely at an oblique angle. There is no evidence of a bounded region along these fractures to indicate they are related to dehiscence. Additionally, there is no evidence of a marginal rim preserved on any of the sporangia.

Emergences are 0.6–1.5 mm wide and 1.3–3.4 mm long, varying in morphology according to length (fig. 6) and more occur on the largest axis than the other axes. The smaller emergences are deltoid, and the larger emergences are elongate and perpendicular to the parent axes. One elongate emergence extends perpendicular to the parent axis for about 0.3 mm before re-orientating at about 45° to the axis (fig. 6d). One of the deltoid emergences has a fine vascular trace 0.07 mm wide along its length (fig. 6b).

Fusiform bodies (figs 7, 8) up to 0.5 mm wide and 1 mm long occur on the axes, most occurring distally but in two instances are found to occur in discrete areas of no more than 8 mm long and 2 mm wide on the sides of the main parent axes (fig. 8a, b). Dégagement of the distal region of one of the daughter axes revealed fine fusiform bodies with short stalks (fig. 7a, b). Additionally, similar fusiform bodies were found to occur on the narrow lateral axes that emanate from the main parent axes at almost right angles (fig. 7e), and on the counterpart, faint impressions of numerous fusiform bodies were found on the large central terminal sporangium (fig. 4c). Dégagement

above the main large terminal sporangium revealed more of these fusiform bodies extending beyond the large sporangium (figs 4d, 9). There is no connection between the small fusiform bodies and the large terminal sporangium.

Three types of branching are evident. The first is where a parent axis branches anisotomously and is only seen once, occurring 33 mm from its apex producing a daughter axis 2.9 mm wide that tapers to 1.5 mm wide (figs 3, 7a). The daughter axis and distal region of the parent axis both appear lax. The second type of branching occurs along the sides of the parent axes and consists of narrow lateral axes usually branching perpendicular from the parent axis. These narrow lateral axes are about 0.2 mm wide and up to 2–3 mm long and are sparsely distributed on the parent axes; some occur just beneath the large terminal sporangium of the central axis (fig. 7e). None of these narrow lateral axes branch, and they possess two to three fusiform bodies interpreted as dormant buds or sterile sporangia, one of which is always terminal. One large example of a lateral axis occurs proximally off one of the parent axes and is 15 mm long, varying in width from 0.3–1.1 mm, curving orthotropically with a terminal fusiform body 0.24 mm wide and 0.53 mm long (fig. 7c, d). A third type of branching occurs basally on the central axis with an oblique axial extension forming an approximate K-branch (fig. 3a), with some smaller protuberances, possibly remnants of fusiform bodies (fig. 8c), close to each other. The acroscopic part of this vegetation is similar in morphology to the distal regions of the two large terminal sporangia. A portion of axis was extracted from a poorly exposed axis (fig. 3) within the matrix, revealing longitudinal structures possibly indicative of the cell's original orientation (fig. 10).

Comments: The location of sporangia has been used by many workers (Edwards et al., 1989; Gensel 1992; Kenrick and Edwards, 1988; Niklas and Banks, 1990) to differentiate zosterophylls into either the Gosslingiales or Zosterophyllales. Zosterophyllales have both lateral and terminal sporangia. However, the presence of emergences suggests affinities with the Gosslingiales; but Gosslingiales lacks terminal sporangia (Hao and Xue, 2013). Additionally, the sporangia of *Taungurangia garrattii* are not reniform or globose as in zosterophylls, which precludes assignation to *Zosterophyllum* (Edwards et al., 2016; Gensel, 1992: 455). Instead, the terminal sporangia are noticeably elongate and lack a thickened zone bounding a dehiscence line as seen in most zosterophylls (Hao and Xue, 2013). The apparent limited branching and single terminal elongate sporangium suggests rhyniophytes affinities, but while branching appears limited, numerous slender axes emanate from the parent axes. Based on the primary characteristics – notably the presence of emergences, K- or H-branching, conspicuous large terminal elongate sporangium and noticeably sparse branching – we provisionally place *Taungurangia garrattii* in the Class *incertae sedis*.

We believe the small fusiform bodies may represent buds or sterile vestigial sporangia (figs 7, 8). This is a similar conundrum to the original consideration of what were originally believed to be sporangia along the axes of *Sawdonia ornata* (Dawson) Hueber but were later found to be buds/arrested apices (Gensel and Berry, 2016: 619; Hueber, 1992: fig. 3). We found no fusiform bodies of intermediary size with the large terminal sporangia; instead, they are all broadly the same size. Furthermore, most of the fusiform bodies have
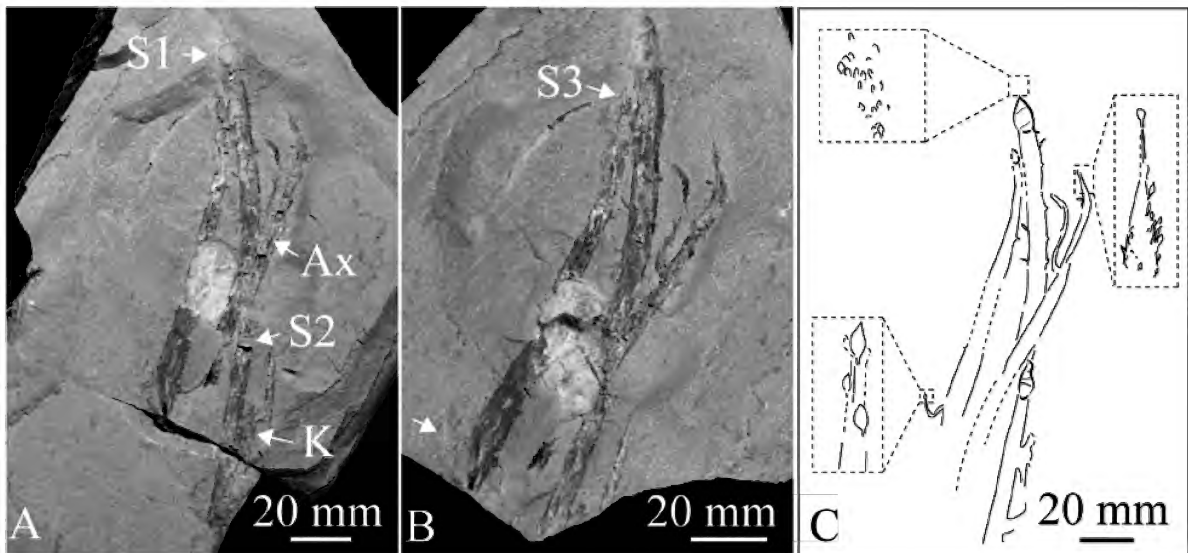

Figure 3. *Taungurungia garrattii* gen. et sp. nov., holotype: a, part specimen (NMV P257028.1) with lower arrow at K-branching. Terminal ovate sporangia at S1 and S2. At Ax is an axis that goes into the matrix. K- or H-branching at lower arrow; b, counterpart (NMV P257028.2). At upper arrow S3 is poorly preserved sporangium. Lower arrow points the axis curving upwards which is visible in fig. 7c, d close-up after dégagment. The counterpart image is reversed to be in the same orientation as the part; c, line-drawing without small bud/sterile sporangial bodies included. Images a and b were taken by Rodney Start © Museums Victoria.
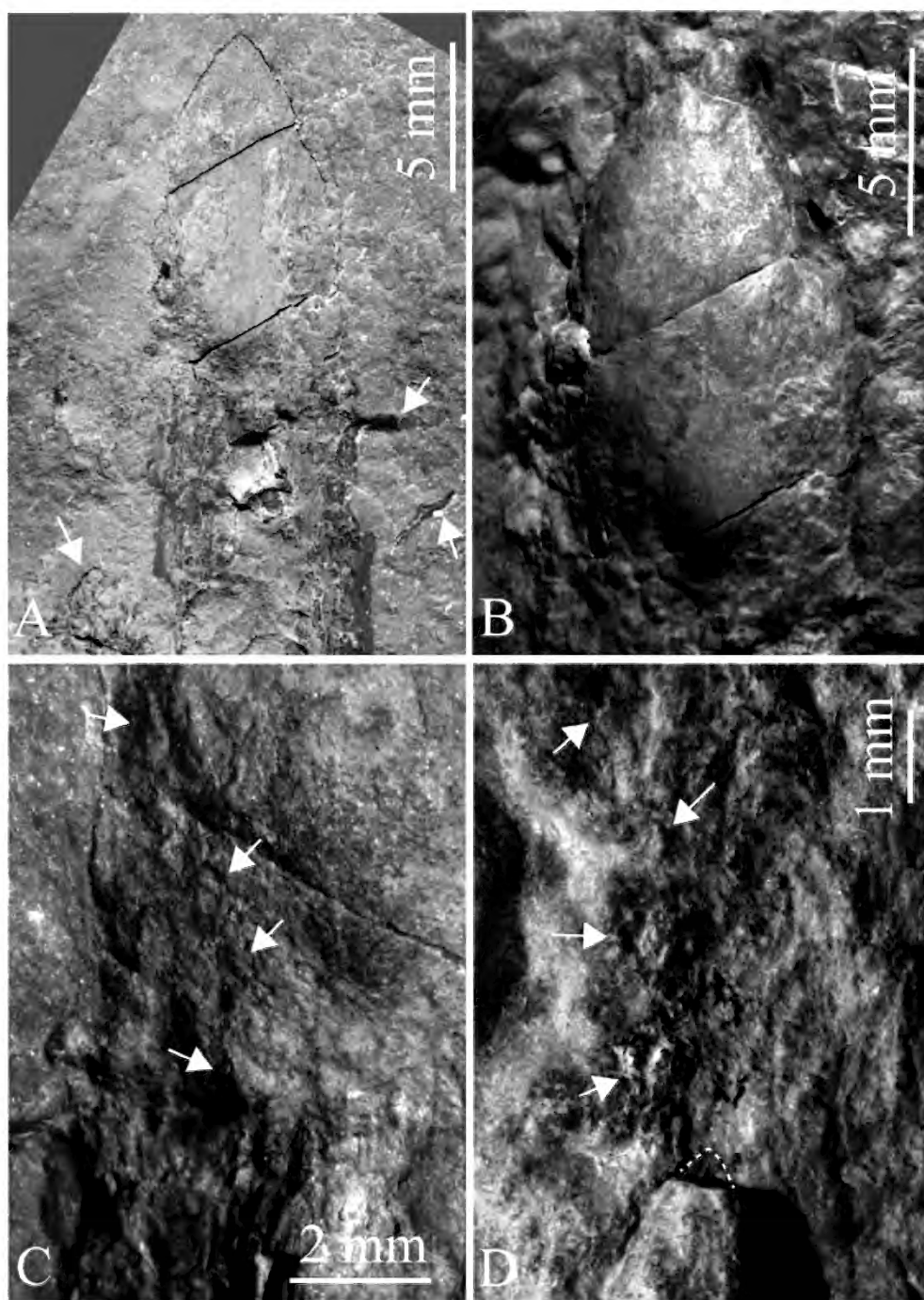
Figure 4. *Taungurungia garrattii* gen. et sp. nov., holotype, part specimen NMV P257028.1: a, ovate sporangium pre-dégagement. Left arrow is at apex of poorly preserved sporangium. Right arrows are at two lateral axes close to the base of the sporangium. Close-up of lower axis in fig. 7e; b, post-dégagement, reveals sporangium preserved in relief; c, faint impressions at arrows of fusiform bodies (buds/sterile sporangia) on counterpart. Lower arrow shows a fusiform body attached directly to the axis at the junction with the sporangium; d, dégagement above the sporanium revealed numerous small fusiform bodies (buds/sterile sporangia) at arrows similar to c. Tip of sporangium disintegrated during dégagement, positioning highlighted with dotted line. Image a taken by Rodney Start © Museums Victoria.

Figure 5. *Taungurungia garrattii* gen. et sp. nov., holotype, part specimen NMV P257028.1. Large sporangium low down on the specimen. The apex is slightly curved (upper arrow) and more elongate then the sporangium in fig. 4. Branching visible (lower arrow). Note: the sporangium appears partly embedded in its subtending axis. Image taken by Rodney Start © Museums Victoria.

narrow subtending axes that clearly differ from the large sporangia, which are sessile. If these fusiform bodies were to grow to a similar size as the terminal sporangia, they would likely have caused the plant to become unstable because they occur on narrow lateral axes and at the end of daughter axes.

The oblique region of extended vegetation (?K- or H-branching) seen basally is indicative of creeping vegetation, such as that seen with *Discalis longistipia* Hao (1989: 159) and other zosterophylls (Walton, 1964). Branching frequency and pattern from the emergences could not be determined. The lax appearance of the daughter axes (fig. 7a) could be interpreted as being almost recurved, a similar pattern of growth as circinate axes (Lyon and Edwards, 1991: 327) associated with indeterminate growth (Niklas and Banks, 1990). However, we consider this lax appearance to be due to partial wilting because there is no evidence of recurved growth on the smaller axes, which would be expected for this characteristic.

Comparison to other taxa

The specimen described herein has some similarities to *Halleophyton zhichangense* Li and Edwards, 1997, from the Zhichang section of the Posongchong Formation, Yunnan, China, in that rhomboidal depressions (Li and Edwards, 1997: fig. 5) are found on the axes and bear a passing resemblance to the depressions found on the sporangium mould (fig. 4c). However, *H. zhichangense* has much smaller sporangia, which are ellipsoidal and globose, 1.9–3.3 mm long and 1.7–3.1 wide (Li and Edwards, 1997).

Elongate-ovoid sporangia are characters of rhynialeans, but the presence of emergences and ?K- or H-branching suggests affinities with the zosterophylls. Elongate sporangia occurring on taxa with presumed affinities to the zosterophylls broadly similar to *T. garrattii* comprises six species (Table 1) that lived on the South China plate. Five of these (*Guangnania cuneata* Wang and Hao, 2002, *Guangnania minor* Edwards et al., 2016, *Sichuania uskielloides* Edwards and Li, 2018, *Baoyinia sichuanensis* Edwards and Li, 2018 and *Yunia Guangnania* Hao and Xue,
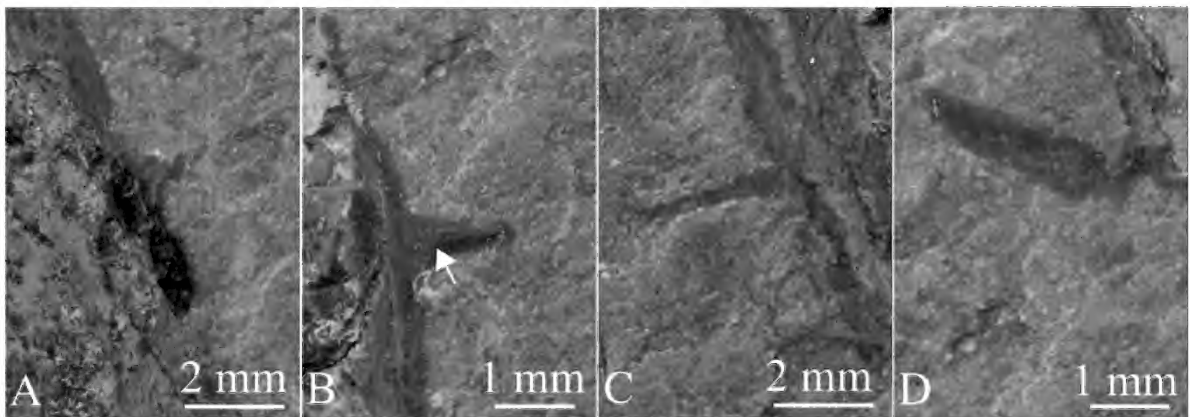

Figure 6. *Taungurungia garrattii* gen. et sp. nov. holotype, part specimen NMV P257028.1: a–d, ontogenetic changes in morphology and orientation of emergences. In image b, arrow at possible vascular trace extending out to tip. Images were taken by Rodney Start © Museums Victoria.

2013) have naked axes and therefore *T. garrattii* can be easily distinguished from them. *Yunia dichotoma* Hao and Beck, 1991, does have emergences in the form of sparely distributed spines and therefore differs from *Taungurungia garrattii*. Additionally, *Y. dichotoma* differs from *T. garrattii* because it has a marginal rim on the sporangia; this character is also found with *Ramoferis amalia* Hao and Xue, 2011, and *Baoyinia sichuanensis* (Edwards and Li, 2018). *Ramoferis amalia* also differs from *T. garrattii* in having ovoid to pear-shaped sporangia (Hao and Xue, 2011).

The sporangia of *Y. dichotoma* differ from those of *T. garrattii* in that they are elliptical to ovoid with rounded apices (Hao and Beck, 1991). The sporangia of these six taxa are also noticeably much smaller than *T. garrattii*. The largest sporangia *G. cuneata*, 2.8 mm wide and 9.6 mm long (Edwards et al., 2016; Wang and Hao, 2002), is much smaller than the largest sporangium of *T. garrattii*, which is 7.5 mm wide and 15.5 mm long. Additionally, the largest axial width for these six taxa (Table 1) is 5.0 mm for *Y. dichotoma* (Hao

Table 1. Zosterophyllopsida *sensu* Hao and Xue (2013) with longer than wide sporangia in comparison to *Taungurungia garrattii gen.* et sp. nov.

Taxon	Age; formation; type location	Axial width	Emergences type; width (basally) and length	Sporangia (face view)	Comment	Source(s)
Guangnania cuneata **Wang and Hao, 2002**	Pragian, Lower Devonian; Posongchong Formation; Daliantang, Yunnan, China	W: 0.6–3.0 L: 80	None	Elongate-cuneate W: 1.2–2.8 L: 3.5–9.6	Found also in the Xujiachong Formation. Lose spikes, stalks at least 5.2 mm long. Nonterminate	Wang and Hao (2002); Edwards et al. (2016: table 3)
G. minor **Edwards et al., 2016**	Loch–Pragian, Lower Devonian; Pingyipu Group, Yanmenba section; North Sichuan, China	W: 1.2–1.4 L: 155	None	Elongate-cuneate W: 1.2–1.9 L: 1.7–3.2	Sporangia helically arranged in terminal spikes	Edwards et al. (2016: table 3)
Sichuania uskielloides **Edwards and Li, 2018**	Loch–Pragian, Lower Devonian; Pingyipu group, Yanmenba section; North Sichuan, China	W: 1.2–2.3 (spike) L: >45	None	Elliptical-oval W: 2.8–4.8 L: 4.0–6.0	Sporangia laterally flattened; stalks up to 1.5 mm wide. Spike lax	Edwards and Li (2018)
Baoyinia sichuanensis **Edwards and Li, 2018**	Loch–Pragian, Lower Devonian; Pingyipu group, Yanmenba section; North Sichuan, China	W: 2–3 (spike axis)	None	Ovoid W: 2.5–3.5 L: 4.0–7.5	Stalks up to 2 mm wide. Sporangia isovalvate occurring in clusters; no vegetative parts	Edwards and Li (2018)
Yunia dichotoma **Hao and Beck, 1991**	Pragian, Lower Devonian; Posongchong Formation, Zhichang section; Yunnan, China	W: 5.0 L: 90	Axial spines W: 0.5–1.4 L: 0.6–1.5	Elongate-elliptical to ovoid W: 1.3–3.5 L: 2.2–5.1	Peripheral border; axes sparsely covered in small spines	Hao and Beck (1991); Hao and Xue (2013: 119)
Y. Guangnania **Hao and Xue, 2013**	Pragian, Lower Devonian; Posongchong Formation; Daliantang, Yunnan, China	W: 3.5–4.0 L: 50	None	Elongate-elliptical W: 2.2–4.8 L: 5.0–8.3	Peripheral border; stalks <1 mm long; sporangia scatted spirally; isotomous branching	Hao and Xue (2013: 122)
Taungurungia garrattii gen. **et sp. nov.**	Late Pragian–Emsian, Lower Devonian; Norton Gully formation; Yea, central Victoria, Australia	W: 2.4–7.5 L: 185	Deltoid-elongate W: 0.6–1.5 L: 1.3–3.4	Ovate W: 5.3–7.5 L: 14.4–15.5	No stalk evident on large sporangia; fusiform and elliptical bud/sterile sporangia c. W: 0.5 L: 1.0	Herein

Note: All dimensions are in mm; L, length; W, width

and Beck, 1991), and the longest specimen is for *G. minor,* attaining a height of at least 155 mm (Edwards and Li, 2018). In both cases, *T. garrattii* is noticeably larger, with its axes up to at least 7.5 mm wide and 185 mm long.

The emergences on *T. garrattii* are broadly similar in morphology to those of *Crenaticaulis* Banks and Davis, 1969, and in some respects to those of *Forania* Jensen and Gensel, 2013, in that they are deltoid and elongate-triangular (Banks
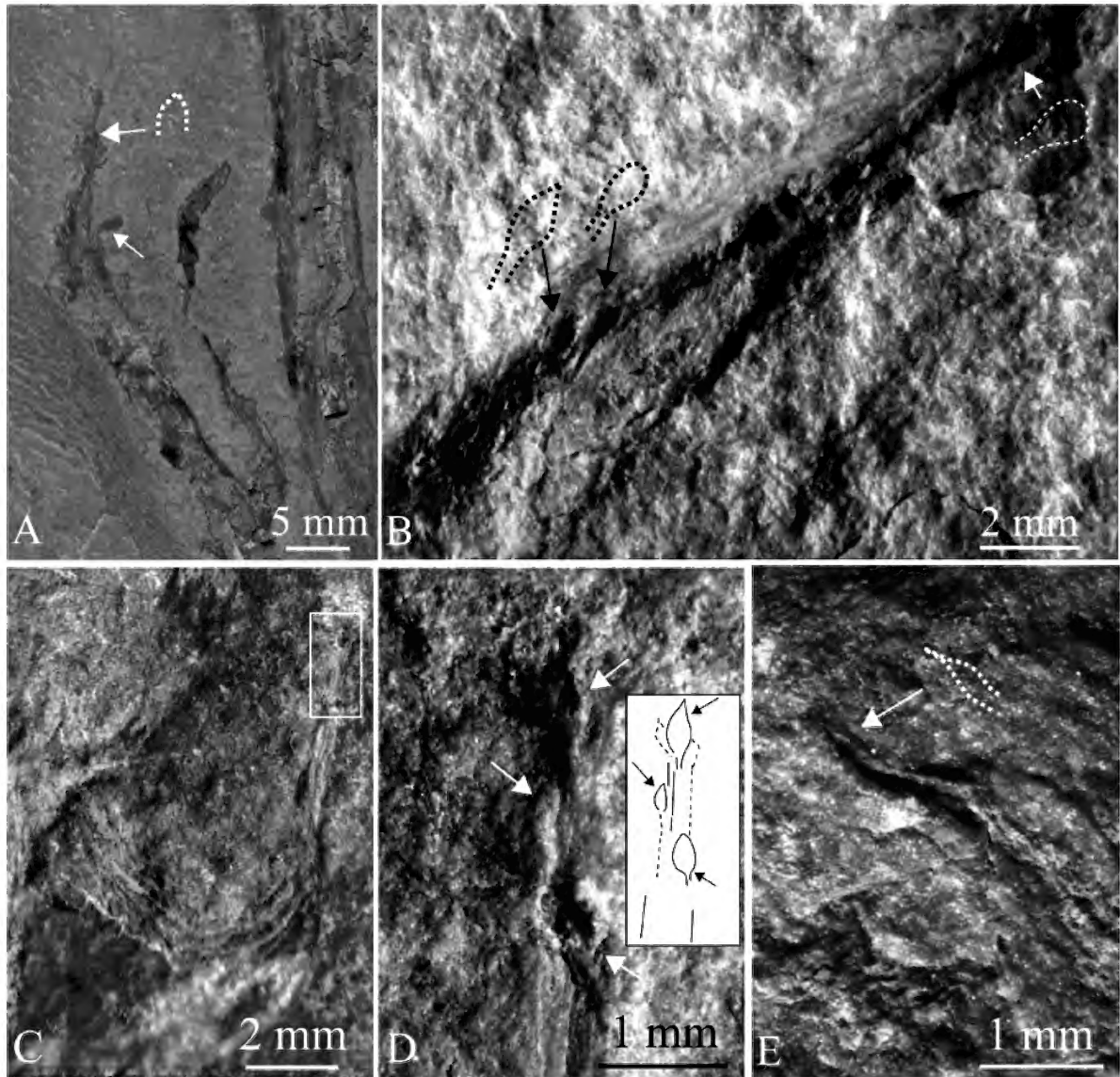

Figure 7. *Taungurungia garrattii* gen. et sp. nov. holotype, fusiform bodies (buds/sterile sporangia). Some of these are highlighted with enlarged dotted outlines near them: a, anisotomous branching with terminal partial fusiform body (upper arrow). Emergence or branching (lower arrow); b, post-dégagement, several fusiform bodies with short subtending axes are visible along the edge of the axis. Distally the axis narrows and terminates in an elongate rounded body (Arrow on right); c, curved axis displaying negative geotropism. Close-up (rectangular region) is in (d); d, distal part of curved axis possesses minute fusiform bodies (at arrows). An insert highlights the morphology. Evidence of determinate growth can be seen as the axis is terminated by one of these fusiform bodies; e, fine axis emanating about 4 mm on the same axis subtending the large central terminal sporangium, with arrow at small terminal body. All images are from the counterpart (NMV P257028.2). Image a was taken by Rodney Start © Museums Victoria. Images b–e were taken with a unidirectional light source.
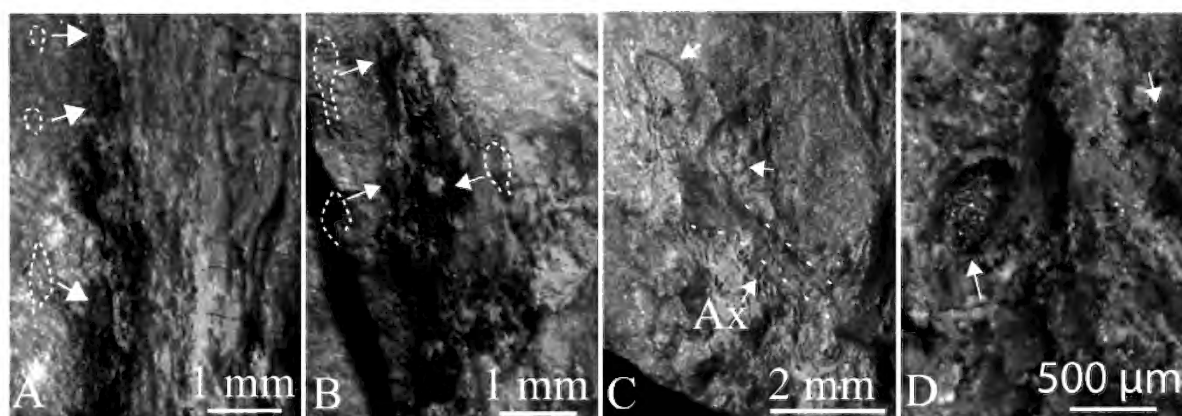
Figure 8. *Taungurungia garrattii* gen. et sp. nov. holotype, fusiform to elongate rounded (buds/sterile sporangia) bodies with some highlighted with enlarged dotted outlines beside them: a, b, on the side of axes in carbonised matter; c, faint axis (Ax) with ?fusiform bodies; d, close-up of fusiform bodies (arrows) on one of the large parent axes. No clear dehiscence lines are present. A short narrow stalk is subtending the sporangium on the left. Images a, b and d are from the counterpart (NMV P257028.2).
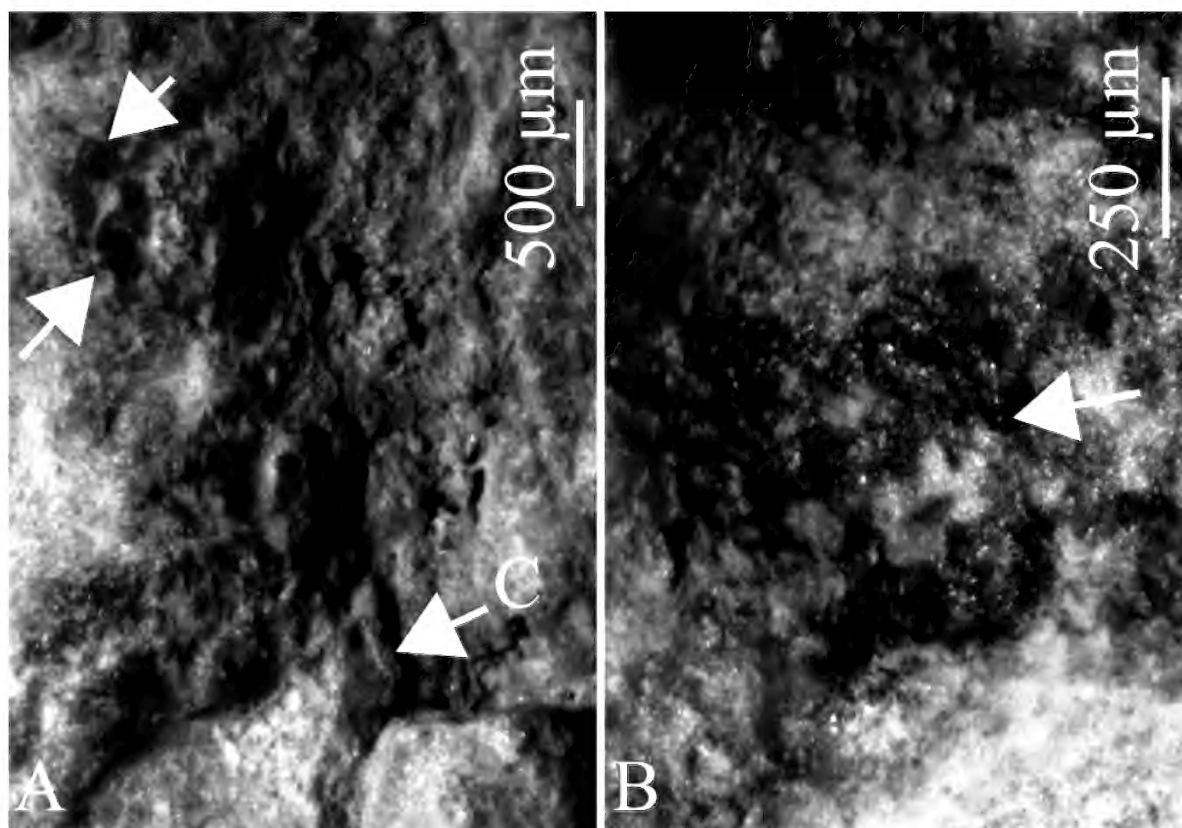

Figure 9. *Taungurungia garrattii* gen. et sp. nov. holotype, part specimen, NMV P257028.1 close-up of fusiform to elongate rounded (buds/sterile sporangia) body: a, immediate area above and right of the main terminal sporangium with some poorly preserved casts of fusiform bodies evident at the arrows. An ovate body (arrow c) pre-dégagement; b, the same ovate body post-dégagement. Its shape may represent partial compression because it is slightly dipping down into the matrix from its subtending axis. At arrow evidence of possible dehiscence line.

and Davis, 1969; Jensen and Gensel, 2013). However, *Crenaticaulis* emergences are biseriate, continuous and in 1–2 rows per side, while the emergences of *Forania* are biseriate and discontinuous (Jensen and Gensel, 2013: table 1). With *T. garrattii*, the emergences appear scattered and change significantly with maturity.

Discussion

Hueber (1992: 479) noted zosterophylls as having sporangia that were either reinform or globose, and that this morphology remained the same throughout their history while exhibiting variations in axial morphology. Thenceforth, several genera such as *Guangnania, Baoyinia* and *Yunia* from the South China Plate have been described as having noticeably elongate sporangia, but with characters indicative of affinities with the zosterophylls. This suggests that zosterophylls exhibited far more variation in sporangial morphology, or that these taxa may represent a separate group(s), as suggested by Hao and Xue (2013: 119) for *Guangnania* and *Yunia*. This paper describes the first known occurrence of elongate sporangia in association with zosterophyll characters in Australia. However, it cannot be assumed they have a common ancestor because the elongate sporangia may be an analogous structure brought about by homoplasy. Anatomical evidence in the form of xylem anatomy would be required to better determine their suprageneric positioning. Unfortunately, xylem structures have only been found in one taxon, namely *Yunia dichotoma*, which differs from zosterophylls (and lycophytes) in showing centrarch maturation rather than exarch, and similar in having G-type

tracheidal structure (Hao and Beck, 1991), which is similar to *Huia gracilis* Wang and Hao, 2001. However, *Huia gracilis* is considered by Wang and Hao (2001) as a questionable rhyniopsid based on stalk length and its ovate sporangia, despite the present of a loose spike and K- or H-branching, while Kenrick and Crane (1997: 172) consider *H. gracilis* a basal lycopsid. Differing rates of evolutionary change within Zosterophyllopsida and Rhyniopsida may have also played a role in certain characters evolving to a point outside their respective classes while maintaining other characters for extended periods, resulting in modular evolution.

Conclusions

In this paper we describe the first taxon from Victoria with emergences and an unusually large terminal elongate sporangium. We did not assign *T. garrattii* to Zosterophyllopsida because anatomical information for sporangial dehiscence, xylem type and spike is required to better determine its suprageneric positioning.

Disclosure statement

No potential conflict of interest was reported by the authors.
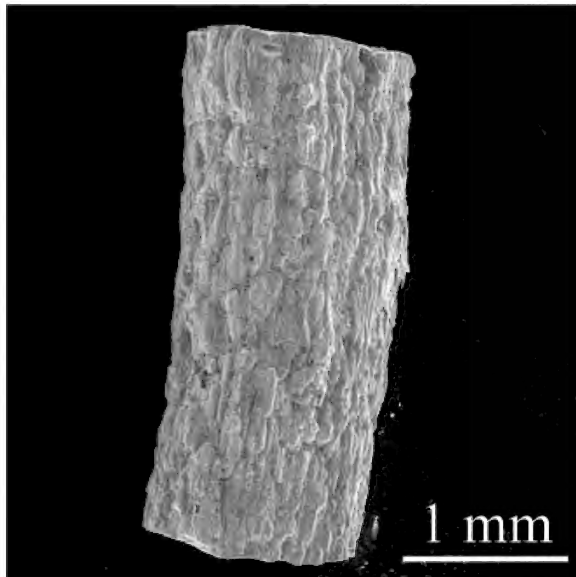

Figure 10. *Taungurungia garrattii* gen. et sp. nov. holotype, counterpart, P257028.2. Micrograph of an axis (part specimen) with longitudinal structures, possibly indicative of cell orientation. Taken using an FEI Quanta 200 scanning electron microscope in low vacuum mode.

References

Banks, H.P. 1968. The early history of land plants. Pp. 73–107 in: Drake, E.T. (ed), *Evolution and environment: a symposium presented on the occasion of the one hundredth anniversary of the Foundation of the Peabody Museum of Natural History at Yale University*. Yale University Press: New Haven.

Banks, H.P. 1975. Reclassification of Psilophyta. *Taxon* 24: 401–413.

Banks, H.P., and Davis, M.R. 1969. *Crenaticaulis*, a new genus of Devonian plants allied to *Zosterophyllum*, and its bearing on the classification of early land plants. *American Journal of Botany* 56(4): 436–449.

Cookson, I.C. 1935. On plant remains from the Silurian of Victoria, Australia, that extend and connect floras hitherto described. *Philosophical Transactions of the Royal Society Series B* 225: 127–148.

Edwards, D., and Kenrick, P. 1986. A new zosterophyll from the Lower Devonian of Wales. *Botanical Journal of the Linnean Society* 92: 269–283.

Edwards, D., and Li, C.-S. 2018. Further insights into the Lower Devonian terrestrial vegetation of Sichuan Province, China. *Review of Palaeobotany and Palynology* 253: 37–48.

Edwards, D., Geng, B.-Y., and Li, C.-S. 2016. New plants from the Lower Devonian Pingyipu Group, Jiangyou County, Sichuan Province, China. *PLoS One* 11(11): e0163549.

Edwards, D., Kenrick, P., and Carluccio, L.M. 1989. A reconsideration of cf. *Psilophyton princeps* (Croft & Lang, 1942), a zosterophyll widespread in the Lower Old Red Sandstone of South Wales. *Botanical Journal of the Linnean Society* 100: 293–318.

Edwards, J., Olshina, A., and Slater, K.R. 1997. Nagambie and part of Yea 1:100 000 map geological report. *Geological Survey of Victoria Report* 109: 1–145.

Edwards, J., Wohlt, K.E., Slater, K.R., Olshina, A., and Hutchinson, D.F. 1998. Heathcote and parts of Woodend and Echuca 1:100 000 map area geological report. *Geological Survey of Victoria Report* 108: 1–215.

Fairon-demaret, M., Hilton, J., and Berry, C.M. 1999. Surface preparation of macrofossils (dégagement). Pp. 33–35 in: Jones, T.P. and Rowe, N.P. (eds), *Fossil plants and spores: modern techniques*. Geological Society: London.

Garratt, M.J. 1978. New evidence for a Silurian (Ludlow) age for the earliest *Baragwanathia* flora. *Alcheringa* 2(3): 217–224.

Garratt, M.J. 1980. Silurian to Early Devonian stratigraphy faunas and depositional history of central Victoria. PhD thesis (unpublished), University of Wollongong, New South Wales, Australia.

Gensel, P.G. 1992. Phylogenetic relationships of the zosterophylls and lycopsids: evidence from morphology, paleoecology, and cladistic methods of inference. *Annals of the Missouri Botanical Garden* 79: 450–473.

Gensel, P.G., and Berry, C.M. 2016. Sporangial morphology of the Early Devonian zosterophyll *Sawdonia ornata* from the type locality (Gaspé). *International Journal of Plant Science* 177(7): 618–632.

Hao, S.-G. 1989. A new zosterophyll from the Lower Devonian (Siegenian) of Yunnan, China. *Review of Palaeobotany and Palynology* 57: 155–171.

Hao, S.-G., and Beck, C.B. 1991. *Yunia dichotoma*, a Lower Devonian plant from Yunnan, China. *Review of Palaeobotany and Palynology* 68: 181–195.

Hao, S.-G., and Wang, D.-M. 2000. Two species of *Zosterophyllum* Penhallow (*Z. australianum* Lang and Cookson, *Z. ramosum* sp. nov.) from the Lower Devonian (Pragian) of southeastern Yunnan, China. *Acta Palaeontologica Sinica* 39: 26–41.

Hao, S.-G., and Xue, J. 2011. A new zosterophyll plant, *Ramoferis* gen. nov., from the Posongchong Formation of Lower Devonian (Pragian) of Southeastern Yunnan, China. *Acta Geologica Sinica* 85: 765–776.

Hao, S.-G., and Xue, J. 2013. *The early Devonian Posongchong flora of Yunnan – a contribution to an understanding of the evolution and diversity of vascular plants*. Science Press: Beijing. 366 pp.

Hueber, F.M. 1992. Thoughts on early lycopsids and zosterophylls. *Annals of the Missouri Botanical Garden* 79: 474–499.

Jaeger, H. 1966. Two late *Monograptus* species from Victoria, Australia and their significance for dating the *Baragwanathia* flora. *Proceedings of the Royal Society of Victoria* 79: 393–413.

Jensen, D.P., and Gensel, P.G. 2013. *Forania plegiospinosa*, gen. et sp. nov.: a zosterophyll from the Early Devonian of New Brunswick, Canada, with a novel emergence type. *International Journal of Plant Science* 174(4): 687–701.

Kenrick, P., and Crane, P.R. 1997. *The origin and early diversification of land plants: a cladistic study*. Smithsonian Institution: Washington, D.C.

Kenrick, P., and Edwards, D. 1988. A new zosterophyll from a recently discovered exposure of the Lower Devonian Senni Beds in Dyfed, Wales. *Botanical Journal of the Linnean Society* 98: 97–115.

Lang, W.H., and Cookson, I.C. 1930. Some fossil plants of Early Devonian type from the Walhalla Series, Victoria, Australia. *Philosophical Transactions of the Royal Society of London B* 219: 133–163.

Lenz, A.C. 2013. Early Devonian graptolites and graptolite biostratigraphy, Arctic Islands, Canada. *Canadian Journal of Earth Sciences* 50(11): 1097–1115.

Li, C.-S., and Edwards, D. 1997. A new microphyllous plant from the Lower Devonian of Yunnan Province, China. *American Journal of Botany* 84: 1441–1448.

Lyon, A.G., and Edwards, D. 1991. The first zosterophyll from the Lower Devonian Rhynie Chert, Aberdeenshire. *Transactions of the Royal Society of Edinburgh: Earth Sciences* 82: 323–332.

McSweeney, F.R., Shimeta, J., and Buckeridge, J.S. 2020. Two new genera of early Tracheophyta (Zosterophyllaceae) from the upper Silurian–Lower Devonian of Victoria, Australia. *Alcheringa* 43(3): 379–396.

McSweeney, F.R., Shimeta, J. and Buckeridge, J.S. 2021. Lower Devonian (Pragian–Emsian) land plants from Alexandra, Victoria, Australia: An early window into the diversity of Victorian flora from southeastern Australia. *Alcheringa* 45 (3), 315-328.

Morand, V.J., and Fanning, C.M. 2006. SHRMIP zircon dating results for various rocks from Victoria, 2006. *Geological Survey of Victoria Technical Report* 2006/2.

Moore, D.H., VandenBerg, A.H.M., William, C.E., and Magart, A.P.M. 1998. Palaeozoic geology and resources of Victoria. *AGSO Journal of Australia Geology and Geophysics* 17, 107–122.

Niklas, K.J., and Banks, H.P. 1990. A re-evaluation of the Zosterophyllophytina with comments on the origin of lycopods. *American Journal of Botany* 77(2): 274–283.

Rickards, R.B. 2000. The age of the earliest club mosses: the Silurian *Baragwanathia* flora in Victoria, Australia. *Geological Magazine* 137(2), 207–209.

Rickards, R.B., and Garratt, M.J. 1990. Pridoli graptolites from the Humevale Formation at Ghin Ghin and Cheviot, Victoria, Australia. *Proceedings of the Yorkshire Geological Society* 48: 41–46.

VandenBerg, A.H.M. 1975. Definitions and descriptions of Middle Ordovician to Middle Devonian rock units of the Warburton District East Central Victoria. *Geological Survey of Victoria* 1975/6: 1–52.

VandenBerg, A.H.M. 1988. Silurian–Middle Devonian. Pp. 103–141 in: Douglas, J.G., and Ferguson, J.A., (eds), *Geology of Victoria* 2nd ed. Victorian Division, Geological Society of Australia: Melbourne.

VandenBerg, A.H.M. 1997. *Melbourne Geological Map* 1: 250 000, 2nd ed, Department of Natural Resources and Environment: Fitzroy.

VandenBerg, A.H.M., Willman, C.E., Maher, S., Simons, B.A., Cayley, R.A., Taylor, D.H., Morand, V.J., Moore, D.H., and Radojkovic, A. 2000. The Tasman Fold Belt System in Victoria. Geology and mineralisation of Proterozoic to Carboniferous rocks. *Geological Survey of Victoria Special Publication*. Department of Natural Resources and Environment: Melbourne. 973 pp.

Walton, J. 1964. On the morphology of *Zosterophyllum* and other early Devonian plants. *Phytomorphology* 14: 155–160.

Wang, D.M., and Hao, S.-G. 2001. A new species of vascular plants from Xujiachong Formation (Lower Devonian) of Yunnan Province, China. *Review of Palaeobotany and Palynology* 114: 157–174.

Wang, D.M., and Hao, S.-G. 2002. *Guangnania cuneata* gen. et sp. nov. from the Lower Devonian of Yunnan Province, China. *Review of Palaeobotany and Palynology* 122: 13–27.

Williams, G.E. 1964. The geology of the Kinglake district, central Victoria. *Proceedings of the Royal Society of Victoria* 77(2): 273–328.

New species of *Paratya* (Decapoda: Atyidae) from Australian inland waters – linking morphological characters with molecular lineages

Phillip J. Suter[1,*], Julia H. Mynott[1] and Megan Crump[1]

[1] Centre for Freshwater Ecosystems, Department of Ecology, Environment and Evolution, La Trobe University, Albury–Wodonga Campus, Victoria, Australia
* To whom correspondence should be addressed. Email: p.suter@latrobe.edu.au

Abstract

Suter, P.J., Mynott, J.H. and Crump, M. 2022. New species of Paratya (Decapoda: Atyidae) from Australian inland waters – linking morphological characters with molecular lineages. *Memoirs of Museum Victoria* 81: 55–122.

The taxonomic history of the atyid shrimp *Paratya* in Australia has been one of confusion due to the high morphological variability in material collected from its wide range of distribution. Early research concluded that all material should be considered a single species, *P. australiensis* Kemp, pending an acceptable revision. After morphological examination of material throughout the known distribution, others concluded that only a single species occurred in Australia. Molecular studies have recognised at least 10 distinct lineages. In the current study, fresh material was collected, and molecular sequencing was undertaken from a single leg from each specimen. Having confirmed the 10 lineages, the specimens were dissected for morphological examination. These lineages are recognised as distinct species and morphological descriptions are provided for seven new species: *Paratya walkeri* n. sp., *P. spinosa* n. sp., *P. williamsi* n. sp., *P. whitemae* n. sp., *P. strathbogiensis* n.sp., *P. gariwerdensis* n. sp. and *P. rouxi* n. sp. A new combination, *P. arrostra* Riek, is raised from sub-species to species, *P. tasmaniensis* Riek is reinstated and *P. australiensis* Kemp is redescribed. A key based on morphology is included.

Introduction

The freshwater Atyid shrimps in the genus *Paratya* Miers, 1882 (Miers, 1882), are widespread throughout streams in the eastern Pacific with *P. borealis* Marin, 2018, in the Russian far east (Marin, 2018); *P. marteni* Roux, 1925, in the Lesser Sunda Islands, Indonesia (Chace, 1997); *P. boninensis* Satake and Cai, 2005, *P. improvisa* Kemp, 1917, and *P. compressa* (Marin, 2018; Page et al., 2005a; Satake and Cai, 2005); *P. norfolkensis* Kemp, 1917, in Norfolk Island (Page et al., 2005a); *P. caledonica*, *P. cf intermedia* Roux, 1926, and *P. cf typa* Roux, 1926, in New Caledonia (Page et al., 2005a); *P. curvirostris* (Heller, 1862) in New Zealand (Page et al., 2005a); and *P. australiensis* Kemp, 1917, in Australia (Kemp, 1917; Williams, 1981; Williams and Smith, 1979). Using mitochondrial sequences of *COI* and 16S ribosomal DNA, Page et al. (2005a) examined the dispersal of *Paratya* throughout the South Pacific and hypothesised that these shrimp dispersed via oceanic currents and using the amphidromous life cycle of some of the species.

The Australian shrimps of the genus *Paratya* are widespread throughout eastern Australia, from Queensland to South Australia and Tasmania (Cook et al., 2006; Williams, 1977; Williams and Smith, 1979; fig. 1). The first species of *Paratya* from Australia, *Paratya australiensis*, was described by Kemp (1917).

Since first being described, the taxonomic history of *Paratya* in Australia has been one of confusion due to the high morphological variability in material collected from a wide range of locations. Two authors (Calman, 1926; Roux, 1926) recognised that animals in their collections were not typical in appearance to *P. australiensis*, and Calman (1926) suggested they may represent a distinct local race based on the examination of rostral characters.

Roux (1926) compared specimens from populations from the Horton River near Bingara, North Yanco near Narrandera, Jamberoo on the southern coast of New South Wales, the Nepean River, Parramatta and Marrickville in Sydney, and Middle Harbour in Port Jackson. Importantly, he noted two forms from North Yanco: one with a long rostrum with two postorbital spines and 5–8 ventral rostral spines, and a second with a short rostrum with no postorbital spines and 1–3 ventral rostral spines. Roux (1926) noted that he could not separate samples into regional races, even though the North Yanco sample suggests two taxa because samples from the Sydney area also had specimens with a short rostrum but with postorbital spines. Riek (1953) recognised five taxa and described two new species and two subspecies *Paratya australiensis*, *P. australiensis arrostra*,

P. atacta, *P. atacta adynata* and *P. tasmaniensis*. Walker (1973), in an unpublished honours thesis, suggested all Riek's taxa were conspecific. Williams (1977) considered Riek's revision to be "inadequate and cannot be accepted as a serious taxonomic statement" (p. 403) and "pending an acceptable revision, all Australian forms of *Paratya* are regarded as belonging to a single species, *P. australiensis*" (p. 403). In a subsequent paper by Williams and Smith (1979), all Riek's taxa were formally synonymised with *Paratya australiensis* Kemp.

Williams and Smith (1979) re-described *P. australiensis* and designated a neotype from Riek's material from close to the type location of "Clyde near Sydney", because Kemp's (1917) original type material no longer exists (Williams and Smith, 1979, p. 817). The variability of morphology was documented by these authors (Smith and Williams, 1980; Williams and Smith, 1979) from examination of specimens from populations throughout the known geographical distribution and from a single population in Cardinia Creek near Melbourne, Victoria. They concluded that only a single highly variable species (*Paratya australiensis*) occurred in Australia.

A series of papers on the genetic characteristics of *Paratya* (Baker et al., 2004; Cook et al., 2007; Hancock et al., 1998; Page et al., 2005b) culminated in the paper by Cook et al. (2006), which demonstrated nine distinct lineages over the geographical range of *Paratya*. The nine lineages consisted of widespread lineages (4, 6 and 8), lineages from only a single river (3, 5 and 7) and lineages from geographically adjacent rivers (1, 2 and 9). A further lineage was discovered in south-west Victoria by McClusky (2007). Cook et al. (2006) suggested that there may be defining morphological differences present among the lineages.

This study's aims were to link morphological and molecular data to find distinguishing morphological characters that enable the identification of the separate lineages of *"Paratya australiensis"* and to revise the taxonomy of *Paratya* in Australia.

Specifically, the aims of this study were to:
- use molecular data to assign individual specimens to lineages
- discover morphological diagnostic characters for females and males separately to allow for the morphological identification of the lineages and eliminate any sexual dimorphism of character expression
- test the hypotheses that where molecular differences are present, there are corresponding morphological differences present.

Methods

Study site locations: Study site locations were selected based on information provided by Cook et al. (2006) relating to the location of individual lineages and based on specimens kindly provided by J. Devine from Sydney Water, B. Cook (Queensland), C. Madden (South Australia), J. Conallin (New South Wales), B. Mos and personal collections. Collectors are identified by their initials: B. Cook (BC), Sydney Water (SW), Environment Protection Authority, Victoria (Vic EPA), C. Madden (CM), J. Conallin (JC), J. Mynott (JM), M. Crump (MC), J. Hawking (JH), B. Mos (BM), T. Walker (TW), T. Curmi (TC), S. Oeding (SO), L. Shuveral (LS), B. Kroll (BKr), J. Webb (JW), D. Black (DB), A. Clements (AC), P. S. Lake (PSL), B. Knott (BK) and P. Suter (PS).

Morphology: Terminology of anatomical structures is after Raabe and Raabe (2008). Specimens were examined under a stereo dissecting microscope. The appendages from one side of the body only were dissected with the pereiopods, pleopods, telson, antennae, stylocerite, scaphocerite and mouthparts all mounted on slides using Euparal for further examination.

Measurements were obtained using an eyepiece graticule calibrated with a 5 mm micro-ruler to determine scale.

Standard measurements, as illustrated by von Rintelen and Cai (2009), were used throughout. Carapace length was measured from the anterior margin of the carapace to the posterior of the eye orbit; rostral length was measured from the eye orbit to the apex of the rostrum, rostral depth was the maximum depth; length of ventral spine row was from the posterior base of the posterior spine to the anterior base of the most anterior spine; stylocerite and scaphocerite lengths were from the base of each structure to the apex; pereiopod and mouthpart measurements were the maximum length of each segment made on the external margins; width measurements were the maximum width of the segment; total pereiopod length was by addition of length of each segment; telson length was from the base to the apex but not including the terminal spines and the width was maximum width at base.

Measurements were compared directly and after being corrected for body size using the carapace length to compensate for variation related to the size (and age) of an individual. Only mature females were used in the analysis due to the presence of known sexual dimorphisms and the limited number of mature males in the collections. Females were determined by the presence of the broad thelycum located on the 8th thoracic segment; the short lanceolate endopod of the first pleopod, which is similar in shape to the exopod; and the absence of the appendix masculina on pleopod 2. All measurements are reported in the descriptions as the holotype character measure with the range of expression (i.e. maximum and minimum) in parentheses.

Segment ratios for pereiopods were for all segments and exopod length with the carpus length, with the carpus length in parentheses. The antennal peduncle measurement ratios were all compared with the apical segment length (3as). The maxilliped 2 comparisons were the ratios of the apical, mid and basal segments and exopod lengths to the basal segment length with the basal segment length given in parentheses. Segment ratios for maxilliped 3 were the ratios of the apical, mid and basal segments and exopod lengths to the mid segment length with the mid segment length given in parentheses.

All maps were prepared using Cartographica. (www.macgis.com).

Laboratory methods: Genetic techniques were used to assess the relationships within the species *Paratya australiensis* and to determine taxonomic resolution of the previously identified *Paratya* lineages in Cook et al. (2006) and McClusky (2007). Total genomic DNA was extracted using two methods.

Figure 1. Maps: a, distribution of *Paratya* in Australia. Sources include data from Cook et al. (2006); Baker et al. (2004), Cook (2006), Hurwood et al. (2003), McCluskey (2007) and data from this study; b, distribution of *Paratya* specimens analysed in this study. Maps created in Cartographica.

The first DNA extraction method was a standardised proteinase-K/Chelex solution following the protocol of Webb and Suter (2010). Leg tissue was removed from each specimen and placed in 100 μL of Chelex solution (5% Chelex (weight:volume), 0.2% SDS, 10 mM Tris pH 8 and 0.5 mM EDTA) and 10 μL of 20 mg/mL proteinase-K. Specimens were incubated overnight in solution at 55 °C, removed and centrifuged at 1500 rpm for 5 minutes before being placed in a thermocycler for 5 minutes at 95 °C to deactivate the proteinase-K. The extracted DNA was then diluted 1:5 with 1X TE (20 μL DNA extraction: 80 μL TE).

The second DNA extraction method was a Qiagen DNeasy blood and tissue kit following standard protocols (Qiagen Handbook, 2006 www1.qiagen.com/literature/). A region of the cytochrome c oxidase subunit 1 gene (*COI*) was amplified using Folmer primers (HCO2198 and LCOI490 (Folmer et al., 1994). All primers were M13-tailed to facilitate sequencing. Polymerase chain reaction conditions for the *COI* fragment used the following protocol: 60 seconds at 94 °C; 5 cycles of 60 seconds at 94 °C, 90 seconds at 45 °C and 90 seconds at 72 °C; 35 cycles of 60 seconds at 94 °C, 60 seconds at 50 °C and 60 seconds at 72 °C; and a final cycle of 4 minutes at 72 °C. Polymerase chain reaction preparations of 40 μL were made either with: (i) 4 μL buffer reagent, 2 μL 50 mM MgCl$_2$, 0.8 μL of each primer, 0.1 μL Platenium taq polymerase (Invitrogen, Melbourne), 1 μL of DNA template and 13.3 μL of ddH$_2$O, or with (ii) 20 μL Taq mastermix (Qiagen), 1 μL DNA template, 0.8 μL of each primer and 17.4 μL of RNA-free water (Qiagen). Polymerase chain reaction products were sent to Macrogen Inc. (Seoul, Republic of Korea) for purification and sequencing.

Sequence data from previous studies were downloaded from GenBank (Baker et al., 2004; Cook et al., 2006; Hurwood et al., 2003; McClusky 2007) to form a backbone for lineages (Supplementary Table 1). Outgroup sequences were downloaded from GenBank for *Caridina* and other *Paratya* species. Data generated in this study were assembled in DnaBaser version 2.91.5 (Heracle BioSoft SRL, Romania, www.DnaBaser.com) with mismatches, if present, assessed visually. Alignments were generated using MUSCLE (Edgar, 2004) in MEGA version 10.1.8 (Kumar et al., 2018) and translated to protein sequences to check for stop codons. All sequences were trimmed to 434 base pairs to match the sequence length of GenBank data. All new sequences from this study have been deposited on GenBank with the identifiers OL420759–OL420929.

Phylogenetic analysis: Genetic analyses were performed in MEGA version 10.1.8 with base composition for the 383 sequences (in-group only) showing an AT bias overall and particularly at the third codon position (overall: A = 25.5%, T = 34.2%, C = 21% and G = 19.3% (AT = 59.7%); third codon position AT = 77.8%). A test of homogeneity showed that overall, the sequences were predominantly homogenous with the first codon position showing an equal amount of homogeneity and heterogeneity between the sequences. The estimated transition:transversion ratio was R = 3.12. A maximum likelihood test of model selection returned T92+G+I

as the best model, with T92+G as the second best. Neighbour-joining analysis was performed in MEGA version 10.1.8 on 397 sequences using the Tamura 3-parameter model with gamma = 0.81, rates among sites homogeneous and 2000 bootstrap pseudo-replicates.

Distances were also assessed in MEGA Version 10.1.8 using the un-corrected p-distance with default assumptions.

Results

Phylogenetic analysis: Genetic data from previous studies were used to form a backbone for previously identified lineages (Baker et al., 2004; Cook et al., 2006; Cook et al., 2002; McClusky, 2007). The ingroup for the analyses included 383 sequences with the backbone comprising 198 sequences (Supplementary Table 1). Ten lineages had been observed in previous studies, 185 sequences generated in this study were analysed against the 10-lineage backbone to assess morphological variation among lineages. Molecular data (fig. 2) showed monophyletic support for all 10 lineages, with sequence data from this study associated with each lineage. Inter- and intra-specific variations were consistent with the values recorded by Cook et al. (2006). Species boundaries were determined by molecular divergences following Costa et al. (2007) and Hebert et al. (2003) and the examination of morphological differences between lineages. The combined approach supports the designation of the lineages as species.

Paratya australiensis and *P. gariwerdensis* show lower support values (fig. 2) due to the presence of sub-clades that are predominantly composed of a small set of sequences from the backbone set. Distance data further reflects the variation, with *P. gariwerdensis* showing a maximum intraspecific distance of 4.8% (Table 1) and inter-specific variation ranging from 4.6–9.7%. Sequences generated in this study for *P. gariwerdensis* aligned in well-supported clades (bootstrap values 84–96%). *Paratya australiensis* shows less divergence distance between sequences, with a maximum intra-specific distance of 2.8%, which is marginally higher than the maximum intra-specific distance for Decapoda (2.57%; Costa et al., 2007), and as stated by Hebert et al. (2003), intra-specific variation is rarely greater than 2%.

Paratya arrostra, *P. whitemae* and *P. tasmaniensis* also showed high intra-specific variation with maxima of 4.1–4.8% (Table 1). These three species have widespread distributions. *Paratya arrostra* comprised five well-supported sub-clades (fig. 3, supplementary fig. 1). Sub-clade E contained the bulk of the sequence data and most of the sequences generated in this study. Sub-clade E showed very little sequence divergence, despite associated specimens occurring over a large geographic area from South Australia, Victoria, New South Wales and Queensland. Sub-clade A included three sequences from this study that were located from the Clarence River catchment near Coffs Harbour, New South Wales, to the Richmond River catchment near Ballina, New South Wales. Subclade B included two sequences from this study from northern Queensland at Tinaroo. Sub-clades C (n = 2) and D (n = 4) comprised haplotypes from Cook et al. (2006).

Figure 2. Neighbour-joining analysis of *Paratya* using Tamura-3-parameter, gamma distribution shape parameter of 0.81, homogenous pattern among lineages and 2000 bootstrap pseudoreplicates. Bootstrap values >72% displayed. Sequence data from Cook et al. (2006); Baker et al. (2004), Cook (2006), Hurwood et al. (2003), McCluskey (2007) and this study.
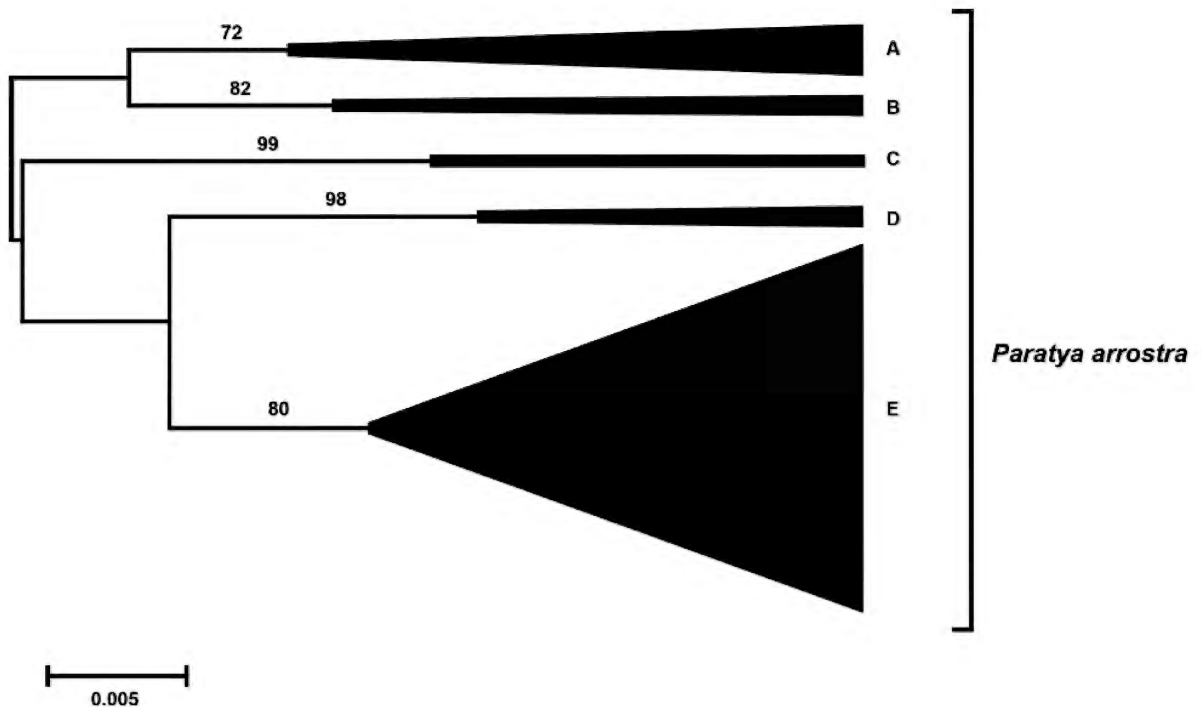
Figure 3. Sub-tree of *Paratya arrostra* Riek, 1953, showing supported subclades. Themajority of material collected across a wide geographical area in this study grouped within a single clade (E), which is equivalent to Lineage 4B in Cook et al. (2006). Previous haplotypes from Cook et al. (2006) form the other sub-clades, but no specific geographical information is known for these sequences. Sub-clades A and B contain some specimens from this study.
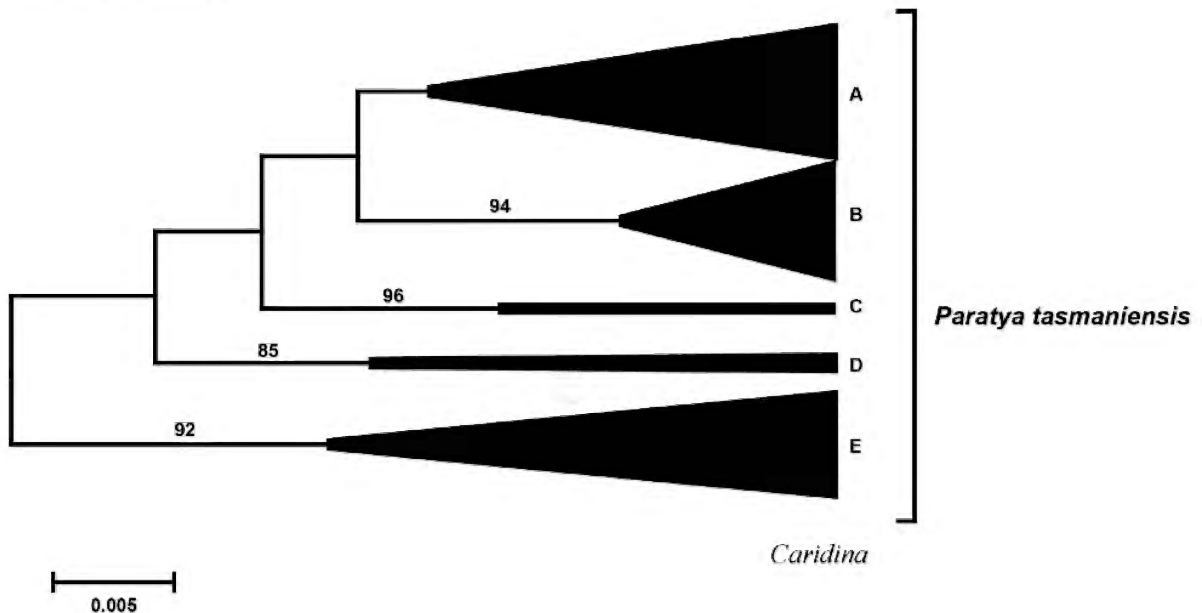
Figure 4. Sub-tree of *Paratya tasmaniensis* Riek, 1953, showing supported sub-clades. Sub-clade A predominantly has material from Tasmania but with a single specimen collected at Hamilton, Victoria. Sub-clade B contains specimens from the Glenelg River catchment, south-west Victoria through to the Hastings River in New South Wales. Sub-clade E contains sequences from Cook (2006) from the Strathbogie area, and sub-clades C and D are from Cook et al. (2006) and McCluskey (2007).

Table 1. Divergence distances for the *Paratya* species recognised in this study and linked to lineages from previous studies. Inter– and intra–specific pairwise p–distances for the CO1 fragment from MEGA version 10.1.8

	P. australiensis Lineage A Baker/Cook 1		*P. walkeri* Cook 2		*P. spinosa* Cook 3		*P. arrostra* McClusky C/Cook 4		*P. williamsi* Lineage D Baker/Cook 5		*P. whitemae* Lineage B BakerMcClusky A/Cook 6		*P. strathbogiensis* Cook 7		*P. tasmaniensis* Lineage C Baker/Cook 8/McClusky B		*P. rouxi* Cook 9		*P. gariwerdensis* McClusky D	
	min	max	min	max	min	max	min	max	min	max	min	max	min	max	min	max	min	max	min	max
P. australiensis Lineage A Baker/Cook1	0.000	**0.028**																		
P. walkeri Cook 2	**0.025**	0.051	0.002	0.012																
P. spinosa Cook 3	**0.030**	0.058	**0.030**	0.039	0.000	0.012														
P. arrostra McClusky C/Cook 4	0.052	0.078	0.059	0.081	0.055	0.081	0.000	**0.048**												
P. williamsi Lineage D Baker/Cook 5	0.039	0.058	0.044	0.051	0.041	0.046	0.076	0.097	0.000	0.002										
P. whitemae Lineage B BakerMcClusky A/Cook 6	0.044	0.067	0.039	0.069	0.044	0.074	0.048	0.078	0.058	0.071	0.000	**0.041**								
P. strathbogiensis Cook 7	0.046	0.062	0.053	0.060	0.044	0.058	0.067	0.085	0.055	0.060	0.053	0.071	0.000	0.005						
P. tasmaniensis Lineage C Baker/Cook 8/McClusky B	0.044	0.074	0.055	0.081	0.048	0.076	0.065	0.097	0.060	0.076	0.053	0.085	0.060	0.078	0.000	**0.048**				
P. rouxi Cook 9	0.055	0.071	0.060	0.067	0.051	0.062	0.065	0.085	0.074	0.076	0.055	0.078	0.078	0.083	0.065	0.083	0.000	0.002		
P. gariwerdensis McClusky D	0.048	0.078	0.053	0.071	0.055	0.081	0.062	0.097	0.062	0.081	0.051	0.088	0.046	0.058	0.062	0.094	0.078	0.097	0.002	**0.048**

Paratya tasmaniensis comprised five well-supported sub-clades (fig. 4, supplementary fig. 2). Sub-clade A and B had sequences from this study associated with the backbone material. Sub-clade C (n = 2) and D (n = 4) comprised haplotypes from McClusky (2007) and Cook et al. (2006). Sub-clade E comprised sequences from Cook (2006) with specimens collected from the Granite Creeks area of the Strathbogie Ranges, Victoria.

Paratya whitemae comprised one well-supported and three poorly supported sub-clades (supplementary fig. 3). The well-supported sub-clade contained only sequences from the backbone data (Cook et al., 2006; Hurwood et al., 2003; McClusky, 2007). The bulk of sequences for this species showed very little divergence and comprised one sub-clade, the other sub-clades showed more divergence within the clade.

Paratya walkeri, *P. spinosa* and *P. australiensis* showed low minimum inter-specific variation between each other but were well supported in the neighbour-joining analysis and morphologically. *Paratya spinosa* had 3% divergence from both *P. australiensis* and *P. walkeri*. However, *P. australiensis* and *P. walkeri* had a minimum inter-specific divergence of 2.5% (Table 1). This is consistent with the inter-specific variation within the Atyidae where Chen et al. (2020) observed inter-specific variation as low as 3.3% (3.3–33%) in *Caridina* from China, while Christodoulou et al. (2012) reported 5.9% (5.9–28.7%) variation in *Atyaephyra* and Shih et al. (2019) reported 2.17% (2.17–53%) variation in *Neocaridina*.

Systematics

Genus *Paratya* Miers, 1882

Paratya australiensis Kemp 1917

Diagnosis: Rostrum longer or shorter than carapace, usually slender and pointed; dorsally armed with 11–34 teeth of which 0–4 are postorbital spines; ventrally with 1–14 large serrations; dorsal edge straight or very slightly concave.

Eyes well developed, darkly pigmented.

Carapace with supraorbital spine large and distinct, antennal spine smaller; pterygostomian spine indistinct, but pterygostomium angle quite acute; hepatic spine absent.

Antenna 1 length about half body length. Peduncle with numerous finely setose spines in row near lateral, ventral and distal margins and along medial edge; lateral distal angle of first segment with prominent acute process or stylocerite that reaches to distal border of peduncle segment.

Antenna 2 longer than body. Peduncle first segment without setae, overlapping second segment dorsally, with prominent tooth at outer distal angle; second segment with short row of setae dorsally; third segment with group of setae at inner distal angle. Scaphocerite with regular row of setose spines on inner and distal margins; outer margin extending to a sharp point overreached by lamella. Flagellum long and slender.

Maxillipeds 1 exopod flagellum distinct, well developed and with numerous long setose spines on all margins, approximately half the length of the caridean lobe; caridean lobe broad with numerous short setose spines on outer margins and a few on body of lobe; epipodite small. Maxilliped 2 exopod long and narrow, several setose spines of various

lengths near tip and basally. Epipodite with podobranch.

Maxilliped 3 basal segment curved, apical segment with large terminal claw, medial distal margin with broad teeth-like spines, largest in basal third, outer margin with broad tooth-like spines longest in basal third; several transverse spine rows near base; mid and basal segments with several short simple spines. Exopod long and narrow, with several long setose spines near tip and several short setose spines near base. Epipodite with basal conical projection.

Pereiopods 1–5 all possessing an exopodite, only pereiopods 1–4 with epipodite. Pereiopods 1 and 2 with propodus and dactylus forming chelae each with a terminal tuft of setae. Dactylus of pereiopod 3 and 4 with a prominent terminal claw and strong spines on medial margin; dactylus of pereiopod 5 with prominent terminal claw and very regular, comb-like row of numerous small spines on medial margin.

Pleopod 1 male with endopod about half length of exopod, narrowly ovate at base, usually excavated distally with numerous long setose spines laterally and medial spines.

Pleopod 2 appendix masculina present in males, absent in females. Appendix interna long and narrow about one-fifth of length of endopod and exopod, distal margin with long setae. Peduncle with short and long spines.

Telson long and tapers towards posterior, dorsal surface with 2–3 pairs of strong sub-marginal teeth-like spines, posterior margin with 1 pair of spine-like teeth and 6–14 long strong terminal spines.

Paratya australiensis Male neotype

This species was fully described by Williams and Smith (1979) and the description given below adds a morphotype from the Shoalhaven R and the morphometric characters for direct comparisons of all species recognised in this revision.

Paratya australiensis Kemp

Figure 5

Paratya australiensis Kemp (1917); primary type material no longer exists

P. australiensis Riek (1953)

P. australiensis Williams and Smith (1979); neotype male selected from material named by Riek (1953) AM P28693. Neotype examined by MC

Lineage A (Baker et al., 2004)

Lineage 1 (Cook et al., 2006)

Numerous authors referred to *P. australiensis* in both taxonomic (Calman, 1926; Kemp, 1917; Roux, 1926; Smith and Williams, 1980; Williams, 1977; Williams and Smith, 1979) and ecological studies (Baker et al., 2004; Balcombe et al., 2007; Boulton, 2003; Bunn and Hughes, 1997; Chessman and Robinson, 1987; Hancock, 1998; Hancock and Bunn, 1997; Hancock and Bunn, 1999; Hancock et al., 1998; Hart et al., 1991; Hladyz et al., 2012; Hughes et al., 2003; Hughes et al., 1995; Hurwood et al., 2003; Kefford et al., 2004; Marchant et al., 1999; Marchant et al., 1984; Metzeling, 1993; Piola et al., 2008; Reidet al., 2008; Richardson and Humphries, 2010; Smith and Williams, 1980; Walsh and Mitchell, 1995; Williams, 1977), but these ecological studies recognised only a single species from the taxonomic decision by Williams and Smith (1979). Based on current knowledge, these identifications should be revisited.
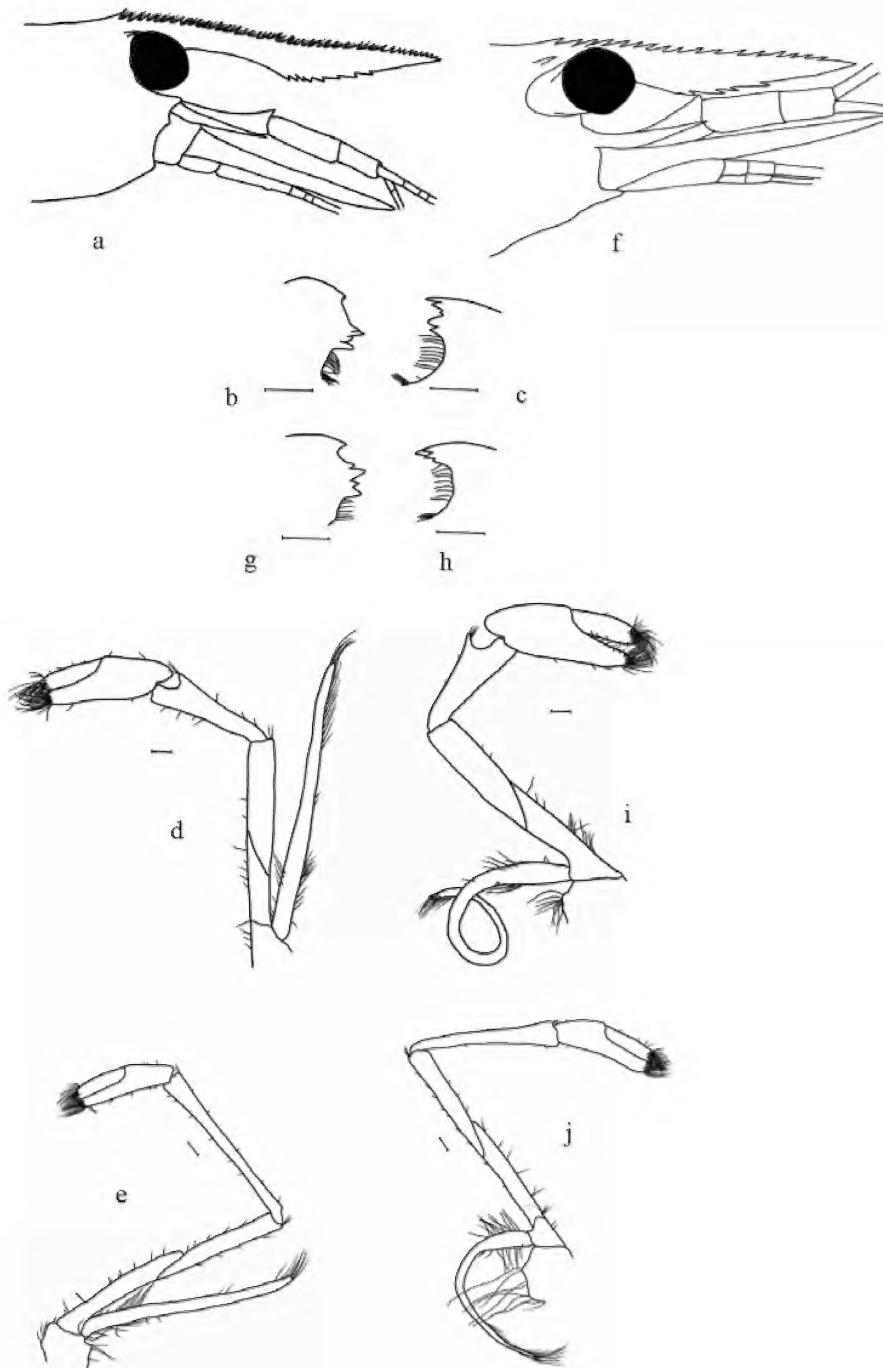
Figure 5. *Paratya australiensis*: a–e, *P. australiensis* Kemp; f–j, *P. australiensis* Shoalhaven morphotype; a, rostrum; b, left mandible incisors; c, right mandible incisors; d, first pereiopod; e, second pereiopod; f, rostrum; g, left mandible incisors; h, right mandible incisors; i, first pereiopod; j, second pereiopod. Scale lines 0.2 mm.

Material Examined: New South Wales: Neotype male AM P28693 Seven Hills, Sydney: Hawkesbury R at Powells Lane, –33.569 S, 150.745 E, 9 March 2011 (SW); Hawkesbury R at North Richmond, –33.589 S, 150.715 E, 9 March 2011 (SW); Hawksbury R at Wilberforce, –336018 S, 150.8245 E, 21 April 2011 (SW) Nepean R at Penrith Weir, –33.746 S, 150.682 E, 14 April 2011 (SW); Warragamba R upstream of Nepean R confluence, –33.8589 S, 150.611 E, 18 April 2011 (SW); Bedford Ck, Blue Mountains, –33.75 S, 150.4474 E, May 2011 (SW) MC32; Bungonia Ck at Bungonia, –34.8528 S, 149.9437 E, no date (SW), Shoalhaven R at Hillview, –35.1826 S, 149.9541 E, no date (SW); Boro Ck at Marlowe upper Shoalhaven R, –35.3426 S, 149.7386 E, no date (SW); Hacking R at McKell Ave, –34.1524 S, 151.0284 E, 5 May 2011 (SW); South Ck at Richmond Rd, –33.6775 S, 150.8121 E, 30 May 2011 (SW).

Williams and Smith (1979) fully illustrated *P. australiensis*, and these have not been duplicated here. Some comparative characters of the two morphotypes are provided (fig. 5).

Diagnosis: P. australiensis differs from all other species by the following combination of characters: rostrum long, extending beyond antennular peduncle and scaphocerite in Sydney streams, dorsal edge very slightly concave, dorsally armed with 16–28 teeth, 1–3 postorbital spines, ventrally with 4–7 large serrations over a length of 0.60–1.5 mm, distal half of ventral edge more or less straight; left mandible with 4–5 teeth separated by finely ridged notch from a less distinct apical tooth; right mandible with 4 teeth in in 2 separate incisor processes; scaphognathite of maxilla 2 rounded apically almost extending to apex of upper endite; maxilliped 1 with exopod flagellum distinct, well developed and with numerous long setose spines on all margins, approximately four-fifths length of caridean lobe; exopod of maxilliped 2 1.70–2.77 times longer than endopod, epipodite with podobranchs extending just to base of third segment of endopodite; maxilliped 3 with medial distal margin of apical segment of endopod with 9–11 broad teeth-like spines, outer margin with 2–4 broad teeth-like spines plus 2–4 smaller spines, exopod long and narrow, tip over-reaching distal end of basal endopod segment; pereiopod 1 with long carpus and long slender chelae, exopod extending to mid carpus–base of propodus; pereiopod 2 with exopod extending to apex of merus; dactylus of pereiopod 3 with prominent terminal claw and 7–11 strong spines on medial margin, exopod extends to mid merus; dactylus of pereiopod 4 prominent terminal claw and 6–11 spines on medial margin, exopod extends to mid-apical third of merus; dactylus of pereiopod 5 with prominent terminal claw and very regular comb-like row of 55–80 small spines on medial margin, exopod extends to mid merus.

Shoalhaven R morphotype: Rostrum extends beyond peduncle, but not beyond scaphocerite, dorsally armed with 16–17 spines, 0 postorbital spines, ventrally with 2–5 spines over a length of 0.60–1.5 mm.

Carapace*:* length 4.1–8.0 mm.

Rostrum (Williams and Smith, 1979; fig. 1a): long, 4.0–5.6 mm, extending beyond both antennular peduncle and scaphocerite in specimens from the Sydney area (fig. 5a) but slightly shorter and not extending beyond the scaphocerite in specimens from the upper Shoalhaven system (fig. 5f), rostral length 0.62–1.24 times length of carapace, dorsal edge very

slightly concave, with slight upwards curve, moderately slender to broad and pointed, rostrum 6.75–9.33 times longer than wide; dorsally armed with 16–25 teeth, ratio of rostral spines to rostral length is 3.15–4.90 with 1–3 post orbital spines in the Sydney morphotype (fig. 5a) or 0 post orbital spines in the Shoalhaven morphotype (fig. 5f); ventrally with 2–6 large serrations over a length of 0.6–1.5 mm all anterior to widest point; distal half of ventral edge more or less straight, ratio of ventral rostral spines length to rostral length = 0.13–0.28 and 3.20–8.00 times more dorsal spines than ventral spines; rostral length 0.92–1.5 times length of scaphocerite.

Antenna 1 (Williams and Smith, 1979; fig. 1, b, c) peduncle 3.40–4.54 mm long, not quite reaching distal tip of scaphocerite, length 0.90–1.07 times as long as scaphocerite. Stylocerite 1.40–2.80 mm long, length 6.89–13.33 longer than width, 0.33–0.43 times carapace length, reaching beyond distal border of peduncle segment, almost to end of acute process on the lateral distal angle of the first segment (fig. 5f).

Antenna 2 (Williams and Smith, 1979; fig. 1d) second segment of peduncle 1.00–1.94 mm long, 0.29–0.44 times length of scaphocerite, 2.53–3.80 times longer than wide. Scaphocerite 3.40–4.72 mm long, 0.60–0.85 times carapace length, 2.76–4.25 times as long as wide.

Mouthparts (Williams and Smith, 1979; figs 1e–i, 2a–c). Left mandible (fig. 5b, g) with 4–5 teeth separated by finely ridged notch from a less distinct apical tooth; spine row immediately below incisor process of 6–10 rugose spines (lifting spines); spine row above molar process of approximately over 20 sparsely setose spines. Right mandible (fig. 5c, h) with 4 teeth separated into 2 incisor groups of 2 teeth, apical and third teeth largest, teeth 2 and 4 shorter; spine row immediately below teeth with 8–10 spines, each finely setose basally; spine row above molar process. Molar process ridged.

Maxilla palps, with 1 long, setose terminal spine and 1–2 simple sub–terminal ones, inner distal angle may be slightly acute.

Maxilla 2 scaphognathite rounded apically almost extending to apex of upper endite. Palps small, terminal parts narrow with 1–2 setose spines.

Maxilliped 1 palp with broad base, short narrow distal lobe, several long setose spines on distal margins. Exopod flagellum distinct, well developed and with numerous long setose spines on all margins, approximately half to four-fifths the length of the caridean lobe.

Maxilliped 2 endopod length 0.68–1.32 mm; exopod long and narrow, length 1.73–2.80 mm, exopod 1.70–2.77 times longer than endopod. Epipodite with podobranchs extending just to base of third segment of endopodite.

Maxilliped 3 endopod length 3.07–7.54 mm, 1.70–2.77 times longer than exopod; with 3 distal segments of similar length; basal segment curved; apical segment with large terminal claw, medial distal margin with 9–11 broad teeth-like spines, largest in basal third, outer margin with 2–4 broad teeth-like spines and 2–4 smaller spines, longest in basal third. Exopod long and narrow, length 1.80–3.62 mm, tip over-reaching distal end of basal endopod segment.

Thoracic appendages (Williams and Smith, 1979; figs 2d, e, 3a–c). Pereiopod 1 (fig. 5d, i). 3.45–5.49 mm long, 0.68–0.91 times length of carapace. Chelae short to long and slender, 1.09–1.93 mm long, propodus 2.55–3.46 times as long as wide, 1.88–2.21 times longer than dactylus; palm length 1.58–1.91 times width and 1.00–1.38 times dactylus length (fig. 5d, i). Carpus long, 1.47–3.08 times longer than greatest width. Segment ratios compared with carpus length 0.54–0.78 : 1.04–1.71 : 1.00 (0.92–1.36) mm : 0.99–1.45 : 0.35–0.84 : 2.21–3.27. Exopod extending to mid carpus–base of propodus.

Pereiopod 2 (fig. 5e, j). length 5.04–9.58 mm, 1.00–1.47 times carapace length. Chelae long and slender 1.11–1.76 mm long, approximately two-thirds carpus length, 3.59–4.14 times as long as wide, palm length 1.71–1.98 times width and 0.82–1.31 times dactylus length (fig. 5e, j). Propodus length 1.61–2.07 times longer than dactylus. Carpus 5.76–8.16 times as long as greatest width, slightly broader distally, distal margin with small excavation. Segment ratios 0.30–0.38 : 0.56–0.72 : 1.00 (1.73–2.84) mm : 0.58–0.96 : 0.34–1.00 : 0.83–1.49. Exopod extending to apex of merus.

Pereiopod 3 slightly longer than pereiopod 2 and more slender, length 5.7–10.08 mm, 1.19–1.60 times carapace length. Dactylus with prominent terminal claw and 7–11 strong spines on medial margin. Propodus length 3.23–4.56 times longer than dactylus, length 9.81–14.3 times as long as wide with 12–15 spines on inner margin. Merus with 1 strong spine on medial margin and 1 near ventral distal margin. Segment ratios 0.38–0.54 : 1.62–1.79 : 1.00 (1.07–1.88) mm : 1.60–2.11 : 0.50–0.77 : 1.60–1.74. Exopod extends to mid merus.

Pereiopod 4 similar to pereiopod 3, 6.09–9.60 mm long, 1.20–1.52 times carapace length. Dactylus with prominent terminal claw and 6–11 spines on medial margin. Propodus length 3.92–4.94 times longer than dactylus, length 10.74–16.50 longer than wide, with 11–17 spines on medial margin; merus with 1 or 2 strong spines on medial margin and 1 near ventral distal margin. Segment ratios 0.37–0.44 : 1.67–1.90) : 1.00 (1.16–1.80) mm : 1.64–2.01 : 0.54–0.82 : 1.18–1.87. Exopod extends to mid-apical third of merus.

Pereiopod 5 similar length to pereiopods 3 and 4, 5.85–9.79 mm long, 1.21–1.57 times carapace length. Dactylus with prominent terminal claw and very regular comb-like row of 55–80 small spines on medial margin. Propodus length 2.83–3.60 times longer than dactylus, length 9.57–16.54 times longer than wide with 8–16 medial teeth. Carpus approximately half propodus length with 1 large spine near distal margin. Merus with 1 strong medial spine and 0–1 distal spines; ischium less than half length of propodus; segment ratios 0.52–0.74 : 1.83–2.09 : 1.00 (1.15–1.85) mm : 1.33–1.90 : 0.58–0.99 : 1.22–1.69. Exopod extends to mid merus.

Abdomen (Williams and Smith, 1979; figs 3d–f, 4a–c). Pleopods peduncle of first pleopod short, 0.23–0.33 times length of carapace, 2.62–3.33 times width, exopod 1.05–1.6 times peduncle length, endopod 0.42–0.83 times peduncle length; second pleopod peduncle short, 0.29–0.44 times length of carapace, 2.31–3.5 times width, exopod 1.00–1.58 times peduncle length, endopod slightly shorter 1.00–1.55 times peduncle length. Length of first peduncle 0.93–1.38 times length of second peduncle length.

Telson length 3.00–4.48 mm, 0.55–0.73 times carapace length, 2.35–3.28 times as long as greatest width, and tapering distally. Dorsal surface with 2 pairs of strong submarginal teeth-like spines. Posterior margin convex with 1 pair of teeth-like spines outermost, 6 long, strong setose spines, and 2 short, simple spines.

Uropods approximately equal to telson length.

Males (Williams and Smith, 1979; fig. 3d–f). Smaller than females, carapace length 5.25 mm; endopod of pleopod 1 strongly excavated with 12 short external spines on medial margin and 17 long setae on inner margin.

Comments: Lineage 1 specimens are consistent with the neotype of *P. australiensis* described and illustrated by Williams and Smith (1979) from Seven Hills near Sydney. Kemp (1917) described *Paratya australiensis* from Clyde, Sydney, but, as the type was missing, Williams and Smith (1979) attempted to find material from the type locality, but were unsuccessful. They selected a specimen from Riek's (1953) collection from the Seven Hills site as the neotype. Both locations (Seven Hills and Clyde) are in the Parramatta R system and are only 10 km apart (Williams and Smith, 1979). The material examined in this study was from adjacent catchments. *P. australiensis* appears restricted to coastal catchments in the Sydney area and in the Shoalhaven catchment. *P. australiensis* does not have an overlapping distribution with *P. walkeri*, *P. spinosa*, *P. strathbogiensis* and *P. gariwerdensis* but it does overlap with *P. arrostra*, *P. williamsi*, *P. whitemae* and *P. tasmaniensis*. *P. whitemae* has been found at the same locality as *P. australiensis*, and both occur in the Hawksbury R and Nepean R.

P. australiensis can be clearly distinguished from the species possessing a short rostrum (*P. arrostra* and *P. rouxi*) by the rostrum extending beyond the peduncle compared with the rostrum that does not extend beyond the peduncle, and characters listed in Table 2.

P. australiensis can be distinguished from all the long rostrum species by the combination of characters listed in Table 3. Main characters include the number of dorsal rostral spines; the number of ventral rostral spine; palm length to width of second cheliped; carpus of pereiopod 1 long; the length of the lower rostral spine row; number of long terminal spines of telson; scaphognathite of maxilla 2 long almost extending to end of endite; right mandible with 2 pairs of incisors (Table 3). The presence of two morphotypes of *P. australiensis* is similar to the observations made on another Australian atyid shrimp, *Australatya*, by Choy et al. (2019).

Paratya walkeri n. sp.

Figures 6–8

http://zoobank.org/urn:lsid:zoobank.org:act:E03B305A-0EDD-4ABD-92E8-566AE860E9E0

Lineage 2 (Cook et al., 2006)

Type material: Holotype New South Wales. Dingo Ck, –30.3103 S, 152.9822 E, 24 May 2015 (BM) PS9. Body in ethanol and antennae, mouthparts, pereiopods and abdominal structures dissected, mounted on 2 slides. Accession Ref. PS9. Australian Museum (AM) Ref No. P.105600.001.

Table 2. Characters that distinguish all *Paratya* species with a long rostrum which extends beyond the antennal peduncle

Character	*Paratya australiensis* L1	*Paratya walkeri* L2	*Paratya spinosa* L3	*Paratya arrostra* L4B	*Paratya williamsi* L5	*Paratya whitemae* L6	*Paratya strathbogiensis* L7	*Paratya tasmaniensis* L8	*Paratya gariwerdensis* LD
Carapace length (mm)	4.1–8.0	5.75–6.25	5.70–6.20	5.10–7.00	4.85–6.00	4.5–6.6	5.6–6.5	5.40–7.50	3.6–4.1
Rostrum longer than carapace	–	+	–/=	+/–	+/=	=	–	+	–
Rostrum extends beyond scaphocerite	+/–	+	+	+/–	=	+	+	+	–
Number of dorsal rostral spines	16–17 or 16–28	24–30	28–30	22–34	21–27	20–34	21–24	22–29	26–28
Number of post-orbital spines	0 or 1–3	2–4	1–3	2–3	2–3	1–4	1–2	2–4	2
Number of ventral rostral spines	2–5 or 4–7	14–16	8–10	4–11	1–5	4–14	4–6	4–13	7–10
Number of ventral spines posterior to greatest depth of rostrum	0	1–2	0–1	0–1	0–1	1–2	0	0	2–3
Length of ventral rostral spine row (mm)	0.6–1.5	2.75–4.00	1.65–3.00	1.10–2.20	0.10–2.00	1.30–2.80	1.30–1.80	2.10–3.40	1.30–1.50
First pereiopod carpus length	Long, 1.73–2.84 mm	Short, 1.25–1.35 mm	Short, 1.12–1.28 mm	Short, 1.01–1.40 mm	Short, 1.05–1.10 mm	Short, 0.87–1.40 mm	Short, 1.13–1.47 mm	Short to long, 1.00–2.67 mm	Very short, 0.88–0.90 mm
First pereiopod chelae shape	Short to long and slender	Long and broad	Short and broad	Short and slender	Short and broad	Short and broad	Short and broad to long and slender	Short and broad to long and slender	Short and broad
First pereiopod Propodus length/carpus length	1.04–1.71	1.30–1.44	1.29–1.43	1.08–1.84	1.27–1.44	1.14–1.49	1.19–1.31	1.25–1.41	1.26–1.33
First pereiopod propodus length/width	2.55–3.46	2.64–3.04	2.68–2.87	2.50–3.47	2.28–3.02	2.48–3.84	2.86–3.26	2.95–3.43	2.44–3.07
First pereiopod palm length/palm width	1.58–1.91	1.48–1.65	1.44–1.79	1.13–1.90	1.36–1.70	1.56–2.25	1.42–2.14	1.60–1.83	1.39–1.67
Second pereiopod palm length/palm width	1.71–1.98	1.50–1.61	1.45–1.82	1.13–2.08	1.50–1.56	1.50–2.50	2.00–2.22	1.80–3.35	1.22–1.53
Second pereiopod propodus length/dactylus length	1.61–2.07	1.56–2.06	1.53–1.77	1.43–1.98	1.76–1.80	1.39–1.91	1.67–1.81	1.57–2.06	1.77–2.04
Dactylus 3 teeth	7–11	7–10	7–9	9–11	5–7	7–11	8–13	9–11	6–7
Dactylus 4 teeth	6–11	7–8	7–9	8–12	5–6	8–11	9–12	8–12	7–8
Dactylus 5 comb	55–80	53–62	44–60	70–91	49–66	81–94	64–80	70–85	70–80
Telson length/carapace length	0.55–0.73	0.64–0.74	0.63–0.71	0.51–0.76	0.67–0.72	0.58–0.83	0.57–0.66	0.59–0.70	0.67–0.70
Number of long terminal spines of telson	6	9–10	6–10	7–13, (usually 11–12)	8	8–10	8–12	8–12	6–7
Right mandible incisors	Incisors paired each with 2 teeth, 1 and 3 large, 2 and 4 shorter	Incisors single with 4 teeth, tooth 2 largest, 1, 3, 4 shorter	Incisors single with 4–5 teeth, all large and of equal size	Incisors single 1 and 3 large, 2 and 4 slightly shorter	Incisors single with 4 teeth, 3 and 4 teeth largest 1 and 2 shorter	Incisors single with 3–4 teeth, 2 central teeth largest, 1 and 4 shorter	Incisors paired outer with 2 teeth 1 and 3 large with 2 very short, 4 large, 3 and separated	Incisors single with 4–5 teeth, tooth 3 largest, 1, 2 and 3 smaller	Incisors single with 4 teeth, 1, 2 and 4 smaller than 3
Maxilla 2 scaphognathite	Rounded apically, not truncated	Truncated	Rounded apically, not truncated	Rounded apically, not truncated	Truncated	Rounded apically, not truncated	Truncated	Truncated	Truncated
Distribution	NSW Sydney streams (Parramatta and Shoalhaven rivers)	NSW northern coastal rivers (Tweed and Clarence rivers)	NSW northern coastal rivers (Tweed River)	Widespread, Murray–Darling Basin SA, Coastal streams Vic, north-east NSW, south-east Qld.	NSW, Kangaroo Valley, Shoalhaven catchment	Coastal streams of NSW and Vic, south-east Qld	Vic, streams in the Strathbogie Ranges	Tasmanian, SA, Vic and NSW coastal, inland streams of the Murray–Darling Basin	South-west Vic in streams draining the Grampian Mountains

Note: L1, L2, L3 etc. refer to the lineage of previous publications mentioned in the text.

Table 3. Characters that distinguish all *Paratya* species with a short rostrum that does not extend beyond the antennal peduncle

Character	*Paratya rouxi* (L9)	*Paratya arrostra* (4B)	*Paratya arrostra* (4C)
Carapace length (mm)	4.90–5.30	3.1–7.0	5.5–6.3
Rostrum shorter than carapace	+	+	+
Number of dorsal rostral spines	11–19	19–25	16–19
Number of post-orbital spines	0	2–3	0–1 spine displaced posteriorly and separate from rostral spines
Number of ventral rostral spines	1–3	3–7	4–5
Length of ventral rostral spine row (mm)	<0.4	>0.4	>0.4
Antenna 1 stylocerite and peduncle process	Extends just to basal third of process	Extends almost to end of process	Extends almost to end of process
First pereiopod carpus length	Long, length 7.0–9.3 times width	Long, length 6.2–8.8 times width	Short, length 5.2–5.9 times width
First pereiopod chelae shape	Slender	Slender	Broad/robust
First pereiopod Propodus length/carpus length	1.2–1.4	1.1–1.8	1.4–2.1
Telson length/carapace length	0.67–0.71	0.44–0.60	0.44–0.60
Number of long terminal spines of telson	10–12	7–13 (usually 11–12)	7–13 (usually 11–12)
Right mandible Incisors	Paired incisors, each with 2 large teeth	Single incisor of 4–5 large teeth	Single incisor with 4–5 large teeth
Maxilla 2 scaphognathite	Truncated, shorter than endite	Rounded apically, not truncated, almost reaching apex of endite	Rounded apically not truncated, almost reaching apex of endite
Distribution	Inland Murray–Darling catchment, NSW	Widespread, Vic, NSW, Qld, SA	South-east Qld

Note: L9, 4B and 4C refer to lineages of Cook et al. (2006).

Paratypes: New South Wales. 5 specimens in ethanol same data as holotype; Accession Ref. PS23, PS8 Genbank Registration OL420929; body in ethanol and other structures dissected, mounted on 2 slides each; AM Ref No. P.105601; 3 specimens in alcohol.

Material Examined: New South Wales: Dingo Ck, –30.3103 S, 152.9822 E, 24 May 2015 (BM).

Diagnosis: P. walkeri differs from all other species by the following combination of characters: rostrum long, extending beyond both antennular peduncle and scaphocerite, dorsal edge very slightly concave, dorsally armed with 24–30 teeth, 2–4 postorbital spines, ventrally with 14–16 large serrations over a length of 2.75–4.00 mm, extending from just posterior of greatest depth; distal half of ventral edge straight; left mandible with 3 teeth separated by a notch from 2 less distinct apical teeth; right mandible with 4 teeth in a single incisor process; scaphognathite of maxilla 2 truncated distally not extending to apex of upper endite; maxilliped 1 with exopod flagellum distinct, well developed and with numerous long setose spines on all margins, approximately two-thirds length of caridean lobe; exopod of maxilliped 2 1.09–2.13 times longer than endopod, maxilliped 3 with medial distal margin of apical segment of endopod with 6–12 broad teeth-like spines, outer margin with 2 broad teeth-like spines, exopod long and narrow, tip over-reaching distal end of basal endopod segment; pereiopod 1 with long carpus and long, robust chelae, exopod extending to mid to apex of carpus; pereiopod 2 with exopod extending to mid-apex of merus; dactylus of pereiopod 3 with prominent terminal claw and 7–10 strong spines on medial margin, exopod extends to mid merus; dactylus of pereiopod 4 prominent terminal claw and 7–8 spines

on medial margin, exopod extends to apical third of merus; dactylus of pereiopod 5 with prominent terminal claw and very regular comb-like row of 53–60 small spines on medial margin, propodus with 8–11 medial spines; exopod extends to basal third to mid third of merus. Telson with 9–10 long terminal spines.

Carapace length 6.25 mm (5.75–6.25).

Rostrum long, 6.3 mm (5.75–6.60), extending beyond both antennular peduncle and scaphocerite (fig. 6a), rostral length 1.08 (0.95–1.15) times longer than carapace, dorsal edge curved upwards to tip, broad and pointed, rostral length 9.00 (6.76–9.00) times greater than width; dorsally armed with 29 (24–30) teeth, ratio of rostral spines to rostral length is 4.60 (4.17–4.60); 4 (2–4) postorbital spines; ventrally with 16 (14–16) large serrations (fig. 6a) over a length of 4.00 mm (2.75–4.00), 2 (1–2) spines posterior to widest point; ratio of ventral spine length to rostral length is 0.63 (0.42–0.63) and 1.81 (1.60–2.14), more dorsal spines than ventral spines; rostral length 1.42 (1.25–1.42) times length of scaphocerite.

Antenna 1 peduncle 3.88 (3.40–4.70) mm long, not reaching distal tip of scaphocerite (fig. 6b), 0.87 (0.81–0.91) times length of scaphocerite. Stylocerite 2.88 (2.18–2.88) mm long, length 11.50 (7.25–11.50) longer than wide, 0.46 (0.36–0.46) times carapace length, reaching beyond distal border of peduncle segment to mid or apex of broad acute process on distal angle of first segment.

Antenna 2 (fig. 6c) apical segment of peduncle 1.55 (1.55–1.60) mm long, 0.35 (0.34–0.35) length of scaphocerite, 2.70 (2.56–2.70) longer than wide. Scaphocerite 4.45 (4.45–4.70) mm long, 0.71 (0.71–0.82) times length of carapace, 3.30 (3.24–3.68) longer than wide.
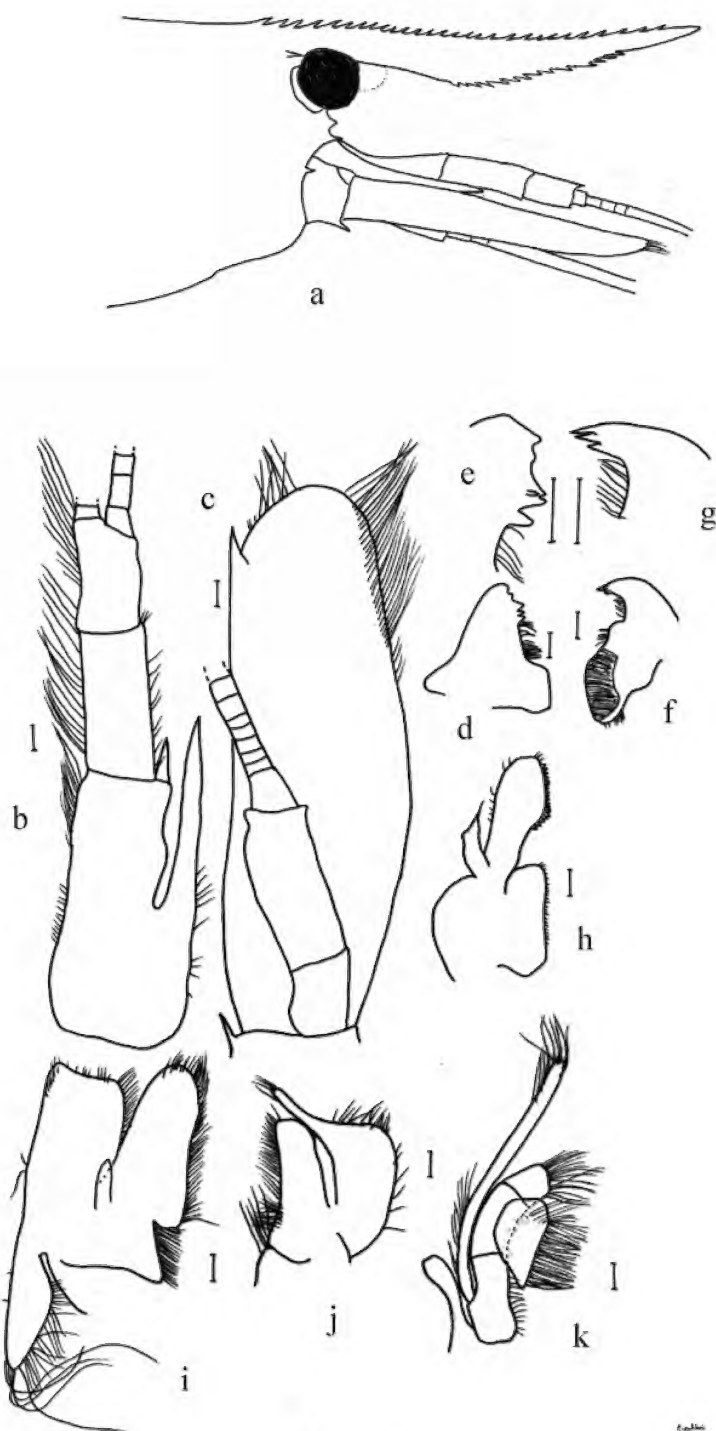
Figure 6. *Paratya walkeri* sp. nov.: a, head region and rostrum; b, antenna 1 peduncle and stylocerite; c, scaphocerite; d, left mandible; e, enlarged incisors; f, right mandible; g, enlarged incisors; h, maxilla 1; i, maxilla 2; j, maxilliped 1; k, maxilliped 2. Scale lines 0.2 mm.
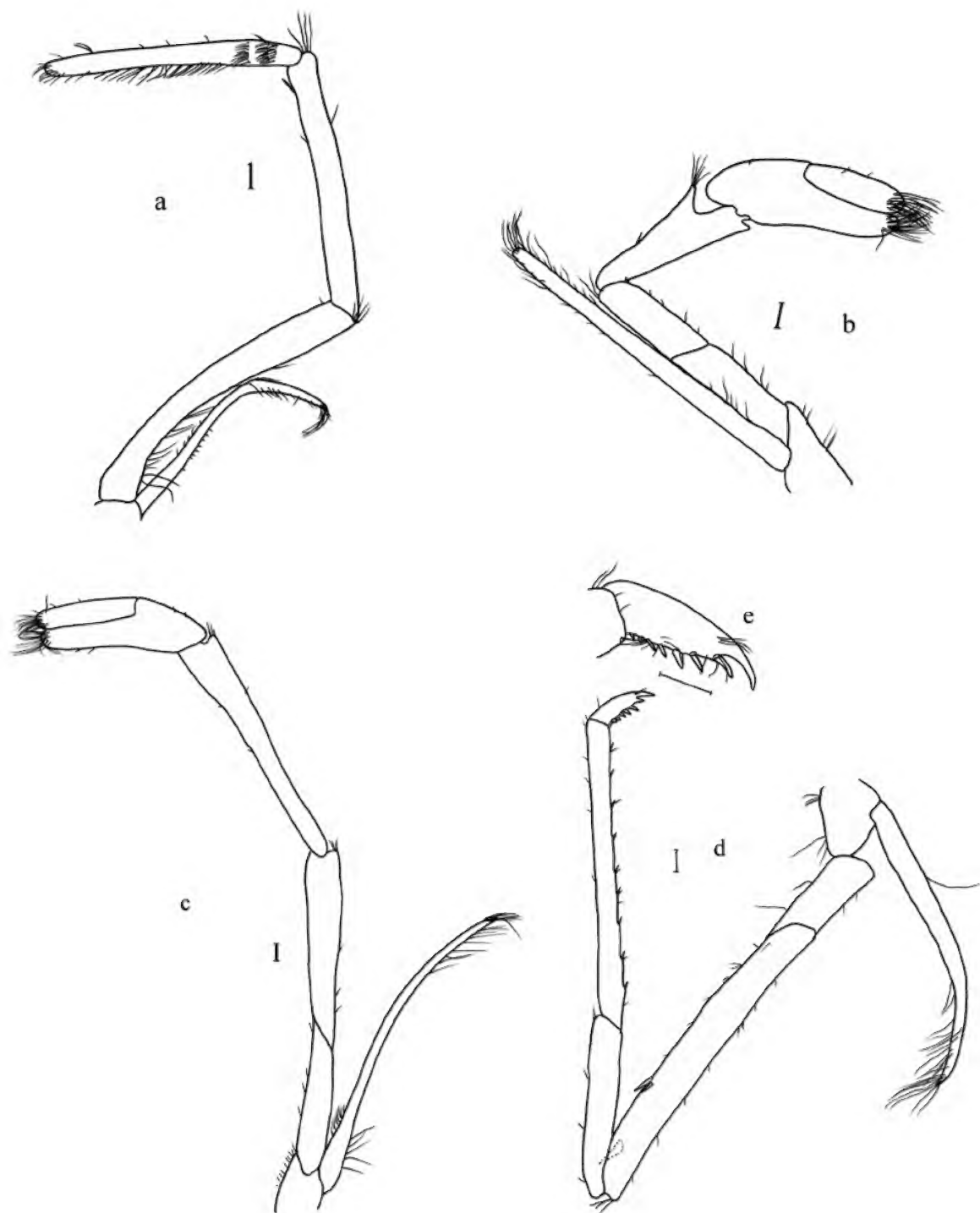
Figure 7. *Paratya walkeri* sp. nov.: a, maxilliped 3; b, pereiopod 1; c, pereiopod 2; d, pereiopod 3; e, dactylus. Scale lines 0.2 mm.
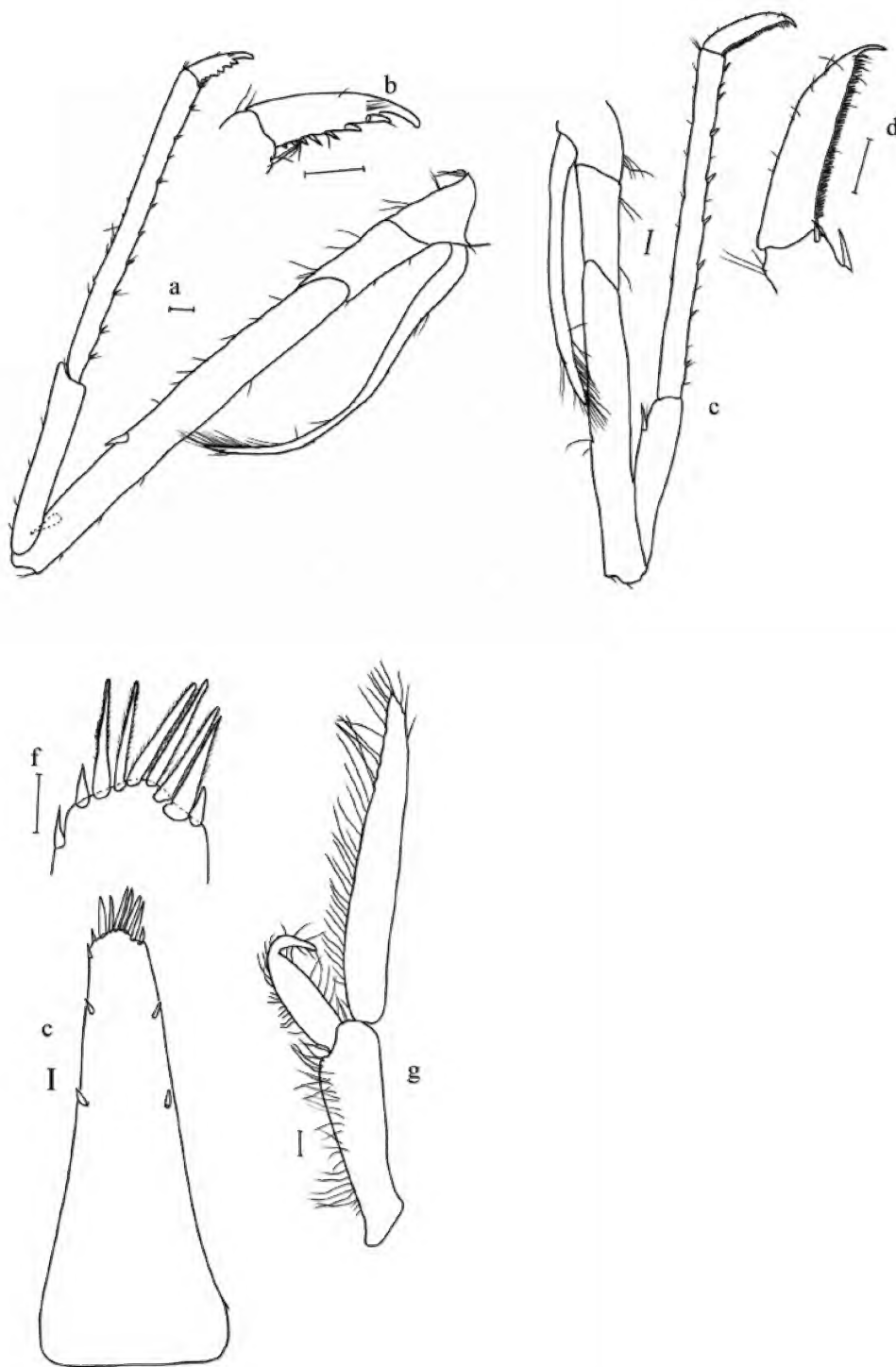
Figure 8. *Paratya walkeri* sp. nov.: a, pereiopod 4; b, dactylus 4; c, pereiopod 5; d, dactylus 5; e, telson; f, telson terminal spines; g, pleopod 1 of female. Scale lines 0.2 mm.

Mouthparts. Left mandible (fig. 6d, e) with 3 teeth separated by a notch from 2 less distinct apical teeth; spine row immediately below incisor process of 6 rugose spines (lifting spines); spine row above molar process of approximately over 20 sparsely setose spines. Right mandible (fig. 6f, g) with 4 teeth in a single incisor process with tooth 2 largest; spine row immediately below teeth with 7 lifting spines; spine row above molar process. Molar process ridged.

Maxilla 1 (fig. 6h) as for *P. australiensis*.

Maxilla 2 scaphognathite truncated distally (fig. 6i), not extending to apex of upper endite.

Maxilliped 1 (fig. 6j) palp with broad base, short narrow distal lobe, and several long setose spines on distal margins. Exopod flagellum distinct, well developed, longer than *P. australiensis* with numerous long setose spines on all margins, approximately Two-thirds to equal length of caridean lobe.

Maxilliped 2 (fig. 6k) endopod 1.14 (1.11–1.30) mm long, exopod long and narrow 2.35 (1.43–2.38) mm long, exopod 2.03 (1.09–2.13) times longer than endopod. Epipodite with podobranch.

Maxilliped 3 (fig. 7a) endopod length 7.38 (7.05–7.58) mm, 2.68–2.69 times longer than exopod, with 3 distal segments of similar length; basal segment curved, apical segment with large terminal claw, medial distal margin with 7 (6–12) broad teeth-like spines, largest 1 in basal third, outer margin with 1 apical tooth-like spine and 1 paired sub-apical setae. Epipodite with basal conical projection.

Thoracic appendages. Pereiopod 1 (fig. 7b) 5.20 (5.12–5.28) mm long, 0.83 (0.83–0.92) times carapace length. Chelae long and broad or short and broad, 1.75 (1.75–1.85) mm long, propodus 3.04 (2.64–3.04) times longer than wide, 2.00 (1.85–2.18) times longer than dactylus, 1.30 (1.30–1.44) times longer than carpus; palm length 1.48 (1.48–1.65) times width and 1.03 (1.03–1.32) dactylus length. Carpus long 2.45 (2.00–2.45) times as long as greatest width, broadening distally, distal margin excavate. Segment ratios 0.65 (0.65–0.78) : 1.30 (1.30–1.44) : 1.00 (1.35 [1.25–1.35] mm) : 1.15 (1.15–1.24) : 0.41 (0.38–0.42) : 2.50 (2.50–2.68). Exopod extending to mid to apex of carpus.

Pereiopod 2 (fig. 7c) 7.45 (7.15–7.48) mm long, 1.19 (1.18–1.30) times carapace length. Chelae long and slender 1.70 (1.58–1.68) mm long, nearly two-thirds length of carpus, 2.96 (2.96–3.53) times longer than wide, palm length 1.61 (1.50–1.61) times width and 1.12 (0.70–1.12) times dactylus length. Propodus 2.06 (1.56–2.06) times longer than dactylus. Carpus 7.69 (6.79–7.69) times as long as greatest width, slightly broader distally, distal margin with small excavation. Segment ratios 0.33 (0.33–0.43) : 0.68 (0.66–0.68) : 1.00 (2.50 [2.38–2.50] mm) : 0.80 (0.78–0.82) : 0.49 (0.49–0.57) : 1.36 (1.30–1.41). Exopod extending to apex of merus to base of carpus.

Pereiopod 3 (fig. 7d, e) distinctly longer than pereiopod 2 and more slender 8.65 (8.55–9.70) mm long, 1.38 (1.38–1.69) times carapace length. Dactylus with prominent terminal claw and 7 (7–10) strong spines on medial margin (fig. 7e). Propodus length 5.26 (4.28–5.33) times longer than dactylus, length 15.13 (13.78–15.13) times longer than wide with 9 (7–10) spines on inner margin. Merus with 1 strong spines on medial margin and 1 near ventral distal margin; segment

ratios 0.33 (0.32–0.40) : 0.68 (0.66–0.68) : 1.00 (1.65 [1.63–1.80] mm) : 0.80 (0.78–0.82) : 0.49 (0.50–0.57 : 1.36 (1.30–1.41). Exopod extends to mid merus.

Pereiopod 4 (fig. 8a, b) similar to pereiopod 3, 9.35 (9.18–9.35) mm long, 1.50 (1.50–1.60) times carapace length. Dactylus with prominent terminal claw and 7 (7–8) spines on medial margin (fig. 8b). Propodus length 4.44 (3.97–4.44) times longer than dactylus, length 13.33 (11.90–14.40) times longer than wide, with 11 (10–13) spines on medial margin; merus with only 1 strong spine on medial margin and 1 near ventral distal margin. Segment ratios 0.35 (0.39–0.49) : 1.83 (1.70–2.00) : 1.00 (1.75 [1.63–1.75] mm) : 1.85 (1.85–2.15) : 0.56 (0.51–0.62): 1.70 (1.67–1.75). Exopod extends to middle third of merus.

Pereiopod 5 (fig. 8c, d) similar length to pereiopods 3 and 4, 9.15 (9.08–9.28) mm long, 1.46 (1.46–1.61) times longer than carapace. Dactylus with prominent terminal claw and very regular, comb–like row of 53 (53–62) small spines on medial margin (fig. 8d). Propodus length 4.25 (3.68–4.25) times longer than dactylus, length 17.00 (15.00–17.00) times longer than wide with 8 (8–11) long medial teeth and setae on external margin. Carpus with 1 large spines near distal margin. Merus with 1 strong medial spine and 1 distal spine; segment ratios 0.47 (0.47–0.60) : 2.00 (2.00–2.19) : 1.00 (1.70 [1.63–1.70] mm) : 1.76 (1.72–1.82) : 0.62 (0.61–0.69) : 1.61 (1.43–1.61). Exopod extends to mid merus (basal third to mid third of merus).

Abdomen. Pleopod peduncle of first pleopod short, 0.26 (0.26–0.37) times length of carapace length, 2.36 (2.36–4.30) times width, exopod 0.73 (0.73–1.40) times peduncle length, endopod 0.70 times peduncle length (fig. 8g); second pleopod peduncle short, 0.36 (0.29–0.36) times length of carapace, 2.64 (1.67–2.64) times width, exopod 1.29 (1.29–1.54) times peduncle length, endopod slightly shorter 1.13 (1.13–1.46) times peduncle length.

Telson (fig. 8e, f) length 4.00 (4.00–4.25) mm, 0.64 (0.64–0.74) times carapace length, 3.64 (2.86–3.64) times as long as greatest width, tapering distally. Dorsal surface with 2 pairs of strong submarginal teeth-like spines. Posterior margin convex with 1 pair of teeth-like spines outermost, 7 (7–8) long, strong setose spines (fig. 8f).

Uropods approximately equal to telson length.

Males unknown.

Etymology: Named after Dr Terry Walker whose study of *Paratya* in Tasmania (Walker, 1973) initiated subsequent taxonomic and morphometric studies (Smith and Williams, 1980; Williams, 1977; Williams and Smith, 1979) and who has encouraged this morphological study.

Comments: Paratya walkeri may be confused with *P. australiensis*, *P. arrostra* and *P. whitemae* due to the very long rostrum that is slightly concave. *P. walkeri* can be differentiated from all the long rostrum species by the combination of characters in Table 2, including the number of dorsal rostral spines (24–30), number of post orbital spines (2–4), number of ventral spines (14–16) over a length of 2.75–4.00 mm; dactylus 4 with 7–8 medial spines; 1–2 ventral rostral spines posterior to maximum rostrum width.

Distribution: P. walkeri is restricted to the northern coastal rivers of New South Wales in the Tweed R and Clarence R catchments. Cook et al. (2006) recorded this species only in the Tweed R; we recorded it in the Manning R system but not at the Tweed R site. It is possible that *P. walkeri* and *P. spinosa* may coexist.

Paratya spinosa n. sp.

Figures 9–11

http://zoobank.org/urn:lsid:zoobank.org:act:2EBBA831-3594-4725-A47F-530AA42CC609

Lineage 3 (Cook et al., 2006)

Type Material: Holotype New South Wales. Korrumbyn Ck, Tributary of Tweed R, Mt Warning, –28.4 S, 153.3 E, no date (BC). Body in ethanol and antennae, mouthparts, pereiopods and abdominal structures dissected, mounted on 2 slides. Accession Ref. MC11. AM Ref No. P.105602.001.

Paratypes: New South Wales. Details as for holotype, Accession Ref. MC17 Genbank Registration OL420818, MC13 bodies in ethanol and other structures dissected, mounted on 2 slides each and 2 whole specimens.

Material Examined: New South Wales: Korrumbyn Ck, Tributary of Tweed R, Mt Warning, –28.4 S, 153.3 E, no date (BC).

Diagnosis: P. spinosa differs from all other species by the following combination of characters: rostrum long, extending beyond both antennular peduncle and scaphocerite, dorsal edge straight, dorsally armed with 28–30 teeth, 3 postorbital spines, ventrally with 9–10 large serrations over a length of 1.65–3.00 mm, all forward of greatest depth; distal half of ventral edge straight; left mandible with 4 teeth separated by finely ridged notch from a less distinct apical tooth; right mandible with 4–5 teeth in a single incisor process with all teeth large; scaphognathite of maxilla 2 rounded apically extending to apex of upper endite; maxilliped 1 with exopod flagellum distinct, well developed and with numerous long setose spines on all margins, approximately half length of caridean lobe; exopod of maxilliped 2 1.06–1.20 times longer than endopod; maxilliped 3 with medial distal margin of apical segment of endopod with 8–13 broad teeth-like spines, outer margin with 1–2 broad teeth-like spines, exopod long and narrow, tip over-reaching distal end of basal endopod segment; pereiopod 1 with long carpus and short and broad chelae; pereiopod 2 with exopod extending to apex of merus; dactylus of pereiopod 3 with prominent terminal claw and 7–9 strong spines on medial margin, exopod extends to apex of merus; dactylus of pereiopod with a prominent terminal claw and 6–12 spines on medial margin, exopod extends to mid merus; dactylus of pereiopod 5 with prominent terminal claw and very regular comb–like row of 44–60 small spines on medial margin, exopod extends to basal third of merus.

Carapace length 6.20 (5.70–6.20) mm.

Rostrum (fig. 9a) long 6.20 (5.70–6.05) mm, extending beyond both antennular peduncle and scaphocerite, rostral length 0.81 (0.81–1.16) times longer than carapace, dorsal edge straight, moderately slender and pointed; rostral length, 6.25 (6.25–8.25) greater than width; dorsally armed with 28 (28–30) teeth, ratio of rostral spines and rostral length is 5.60

(4.24–5.60), with 1-3 postorbital spines (fig. 9a); ventrally with 9 (8–10) large serrations over a length of 1.65 (1.65–3.0) mm, 1 or 2 spines posterior of greatest depth, distal half of ventral edge straight, ratio of ventral spine length and rostral length is 0.33 (0.33–0.45) with 3.11 (3.00–3.11) times more dorsal spines than ventral spines; rostral length 1.11 (1.11–1.83) times length of scaphocerite.

Antenna 1 (fig. 9b) peduncle 4.45 (3.78–4.56) mm long, not quite reaching distal tip of scaphocerite, length 0.99 (0.89–1.27) times length of scaphocerite. Stylocerite 2.53 (2.2–2.53) mm long, length 7.21 (7.21–9.17) times longer than width, 0.41 (0.39–0.41) times carapace length, reaching beyond distal border of peduncle segment almost to end of broad acute process on distal angle of first segment.

Antenna 2 (fig. 9c) second segment of peduncle 1.50 (1.25–1.68) mm long, 0.33 (0.29–0.47) times length of scaphocerite, 2.50 (2.38–3.23) times longer than wide scaphocerite 4.50 (3.60–4.50) mm long, 0.73 (0.63–0.73) times carapace length, 2.90 (2.57–2.93) times as long as wide.

Mouthparts. Left mandible (fig. 9d, e) with 4 teeth separated by finely ridged notch from a less distinct apical tooth; spine row immediately below incisor process of 10 rugose spines (lifting spines); spine row above molar process of approximately over 20 sparsely setose spines. Right mandible (fig. 9f, g) with 4–5 teeth in a single incisor process, all teeth large and of equal length; spine row immediately below teeth with 9 spines each finely setose basally; spine row above molar process. Molar process ridged.

Maxilla 1 (fig. 9h) palps short, truncate, with 1 long, setose terminal spine and 1 small, simple subterminal one, inner distal angle rounded.

Maxilla 2 palps small, but longer than *P. australiensis*, terminal parts narrow and with 1 sub-apical setose spine. Scaphognathite rounded apically, extending to apex of upper endite (fig. 9i).

Maxilliped 1 (fig. 9j) palp with broad base, short narrow distal lobe, and several long setose spines on distal margins. Exopod flagellum distinct, well developed and with numerous long setose spines on all margins, approximately half length of caridean lobe.

Maxilliped 2 (fig. 9k) endopod 1.19 (1.19–1.26) mm long; exopod long and narrow, length 1.43 (1.33–1.43) mm, exopod 1.06–1.20 times longer than endopod. Epipodite with podobranch.

Maxilliped 3 (fig. 10a) endopod length 4.03 (3.62–6.33) mm, 2.41 (2.41–2.54) times longer than exopod; with 3 distal segments of similar length; basal segment curved, apical segment with large terminal claw, medial distal margin with 9 (8–13) broad teeth-like spines, largest in basal third, outer margin with 1 apical broad tooth–like spines. Exopod long and narrow 1.67 (1.43–2.64) mm long, tip extends beyond distal end of basal endopod segment.

Thoracic appendages. Pereiopod 1 (fig. 10b) 4.98 (4.68–4.98) mm long, 0.80 (0.80–0.82) times carapace length. Chelae short and broad (fig. 10b), 1.65 (1.60–1.68) mm long, propodus 2.87 (2.68–2.87) times as long as wide, 1.83 (1.83–1.97) times longer than dactylus 1.29 (1.29–1.43) times longer than carpus; palm length 1.47 (1.44–1.79) palm width and
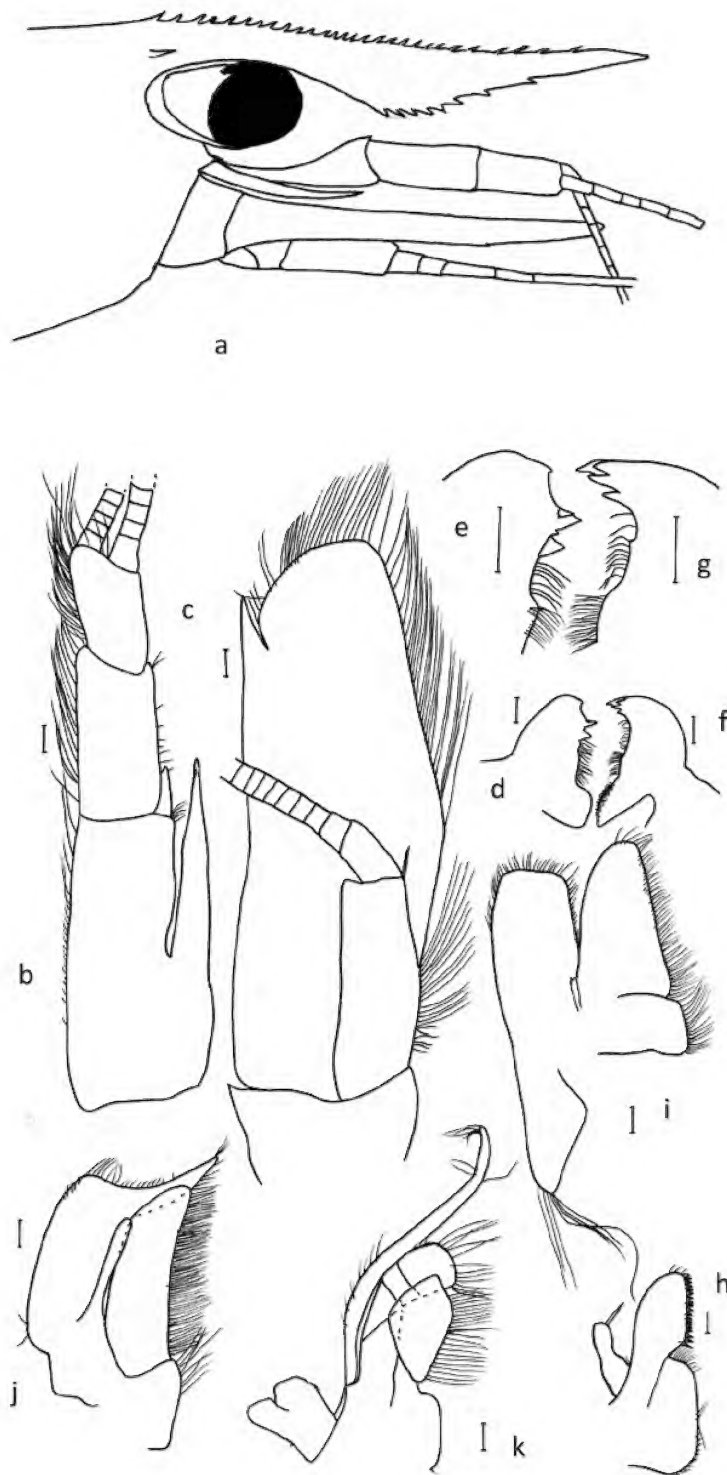
Figure 9. *Paratya spinosa* sp. nov.: a, head region and rostrum; b, antenna 1 peduncle and stylocerite; c, scaphocerite; d, left mandible; e, enlarged incisors; f, right mandible; g, enlarged incisors; h, maxilla 1; i, maxilla 2; j, maxilliped 1; k, maxilliped 2. Scale lines 0.2 mm.
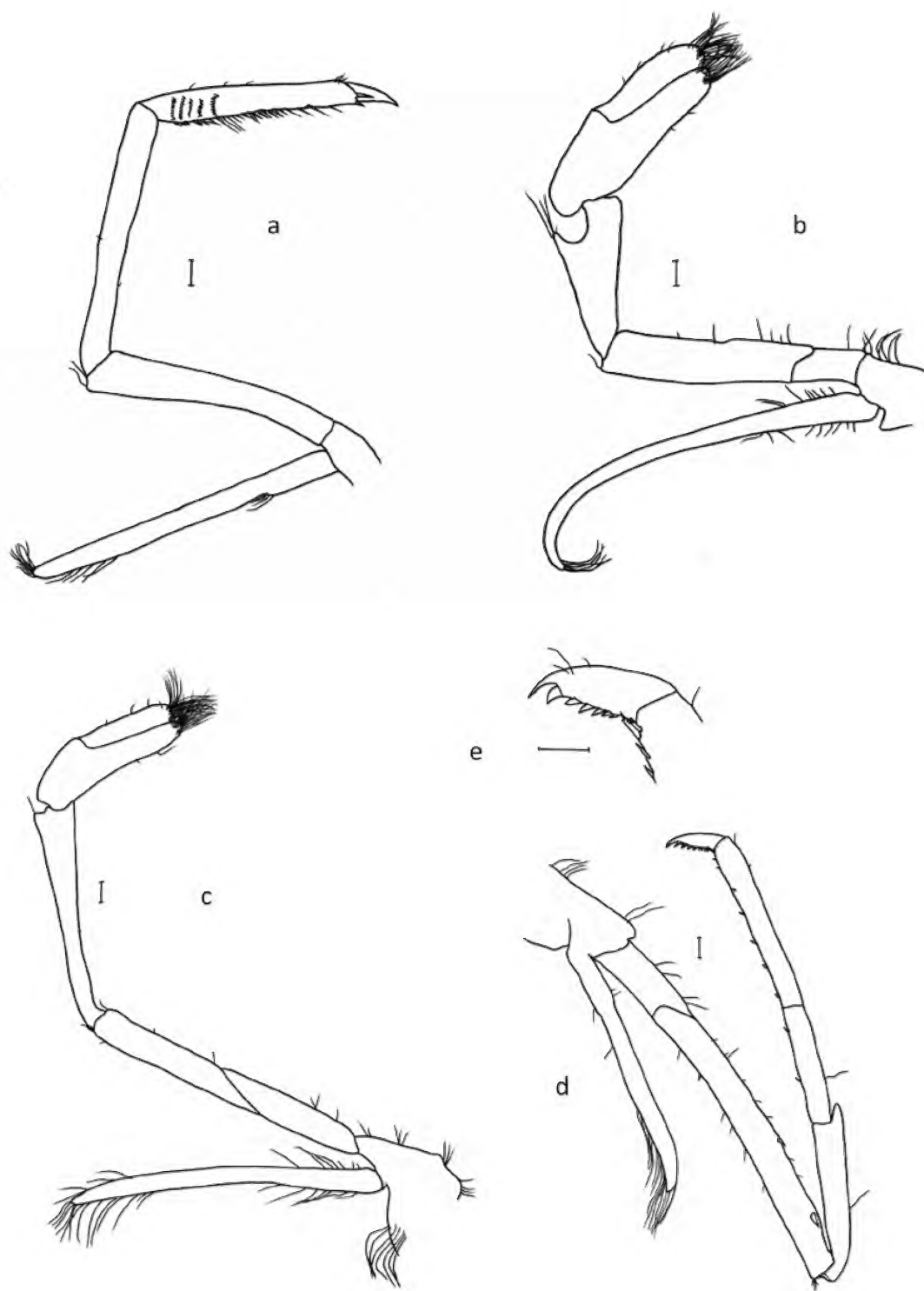
Figure 10. *Paratya spinosa* sp. nov.: a, maxilliped 3; b, pereiopod 1; c, pereiopod 2; d, pereiopod 3; e, dactylus 3. Scale lines 0.2 mm.
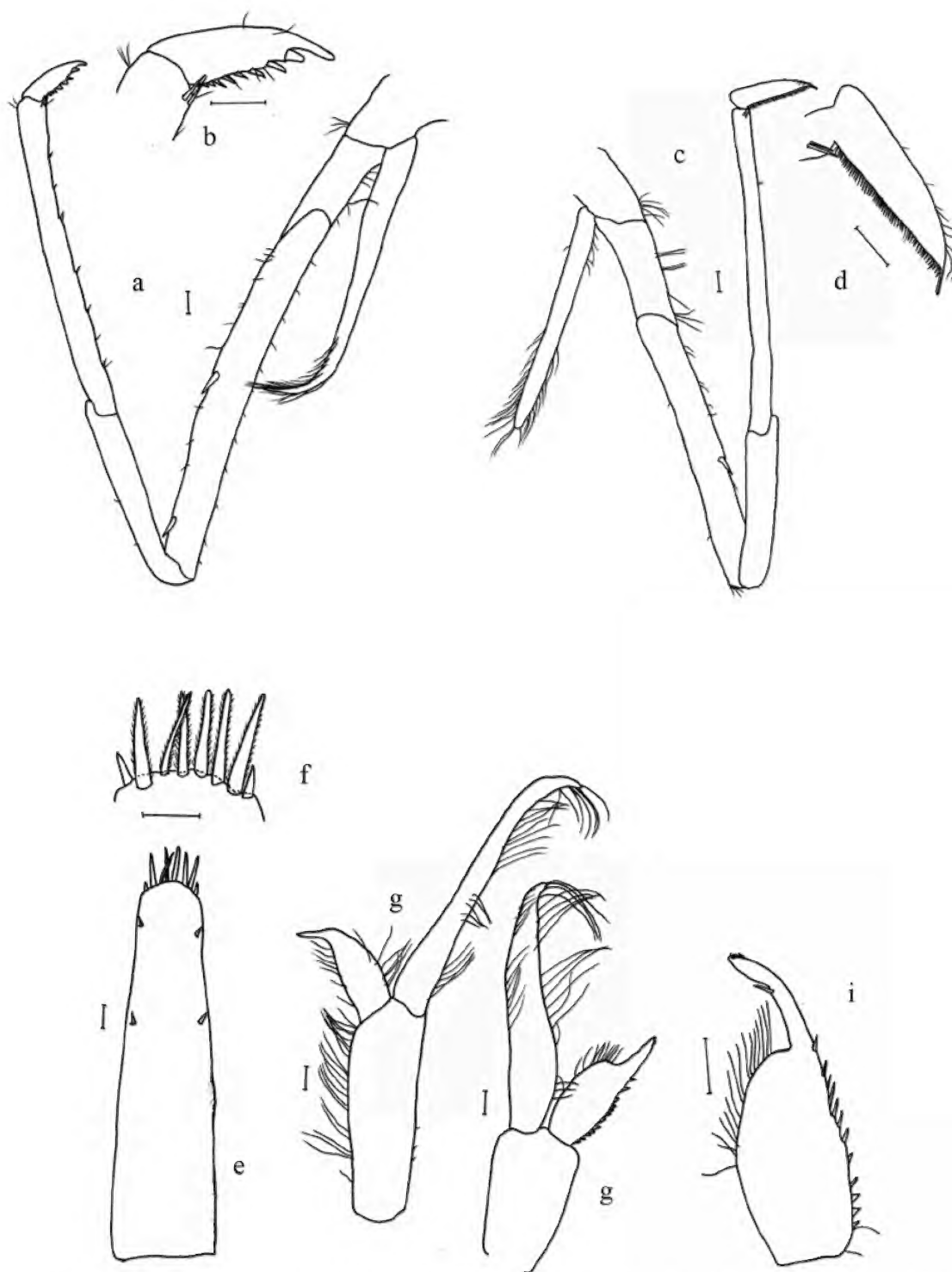
Figure 11. *Paratya spinosa* sp. nov.: a, pereiopod 4; b, dactylus 4; c, pereiopod 5; d, dactylus 5; e, telson; f, telson terminal spines; g, pleopod 1 of female; h, pleopod 1 of male; i, endopod 1 of male. Scale lines 0.2 mm.

0.94 (0.93–1.06) times dactylus length. Carpus long 2.32 (2.27–2.50) times longer than greatest width, broadening distally, distal margin excavate. Segment ratios 0.71 (0.68–0.74) : 1.29 (1.29–1.43) : 1.00 (1.30 [1.12–1.28] mm) : 1.20 (1.18–1.30) : 0.41 (0.41–0.45) : 2.55 (–). Exopod extending to mid carpus.

Pereiopod 2 (fig. 10c) 7.05 (6.71–7.05) mm long, 1.14 (1.11–1.18) times carapace length. Chelae long and slender 1.55 (1.50–1.55) mm long (fig. 10c), 3.10 (3.00–3.19) times longer than wide, 0.65 (0.65–0.69) times carpus length; palm length 1.80 (1.45–1.82) times longer than palm width, 0.77 (0.53–0.77) times length of dactylus. Propodus length 1.77 (1.53–1.77) times longer than dactylus. Carpus 7.38 (5.60–7.38) times longer than greatest width, slightly broader distally with small excavation. Segment ratios 0.36 (0.36–0.45) : 0.65 (0.65–0.69) : 1.00 (2.40 [2.18–2.40] mm) : 0.80 (0.80) : 0.49 (0.49–0.59) : 1.41 (1.41–1.43). Exopod extending to apex of merus.

Pereiopod 3 (fig. 10d, e) distinctly longer than pereiopod 2 and more slender 9.08 (7.48–9.08) mm long, 1.46 (1.31–1.46) times carapace length, dactylus with prominent terminal claw and 9 (7–9) strong spines on medial margin (fig. 10e). Propodus length 4.56 (4.56–4.80) times longer than dactylus, length 12.30 (10.67–12.30) times longer than wide with 8 (6–8) spines on inner margin, outer margin lacks spines. Carpus with 1 large subapical spine. Merus with 1 strong spine on medial margin and 1 near ventral distal margin; segment ratios 0.44 (0.34–0.44) : 1.98 (1.64–1.98) : 1.00 (1.55 [1.55–1.56] mm) : 2.35 (1.58–2.35) : 0.52 (0.52–0.57) : 1.65 (–). Exopod extends to mid merus.

Pereiopod 4 (fig. 11a, b) similar length to pereiopod 3, 9.08 (7.68–9.20) mm long, 1.46 (1.35–1.52) times carapace length. Dactylus with prominent terminal claw and 7 (7–8) spines on medial margin (fig. 11b). Propodus length 4.96 (4.11–4.96) times longer than dactylus, 12.90 (9.74–13.33) longer than wide, with 10 (6–12) spines on medial margin, outer margin without spines; carpus with large subapical spine; merus with 1 strong spine on medial margin and 1 near ventral distal margin. Segment ratios 0.40 (0.37–0.40) : 1.98 (1.50–1.98) : 1.00 (1.63 [1.63–1.65] mm) : 2.09 (1.69–2.20) : 0.51 (0.49–0.56) : 1.71 (1.71–1.82). Exopod extends to mid merus.

Pereiopod 5 (fig. 11c, d). Slightly longer than pereiopods 3 and 4, 9.65 (8.45–9.65) mm long, 1.56 (1.48–1.56) times carapace length. Dactylus with prominent terminal claw and very regular, comb–like row of numerous (44–55) small spines on medial margin (fig. 11d). Propodus length 3.92 (–) times longer than dactylus, length 14.50 (12.6–14.50) times longer than wide with 7 (5–11) long medial teeth, external margin lacking spines. Carpus without large spines near distal margin. Merus with 1 strong medial spine and lacking a distal spine; segment ratios 0.55 (–) : 2.16 (1.56–2.16) : 1.00 (1.68 [1.50–1.81] mm) : 1.85 (1.57–2.23) : 0.75 (0.54–0.75) : 1.67 (1.21–1.92). Exopod extends to mid merus.

Abdomen. Pleopods peduncle of first pleopod short, 0.40 (0.33–0.40) times length of carapace, 4.17 (3.08–4.17) times longer than wide, exopod 1.14 (1.14–1.43) times peduncle length, endopod (fig. 11g), (0.53–0.58) times peduncle length; second pleopod peduncle short, 0.43 (0.37–0.43) times length

of carapace, 2.94 (2.81–3.00) times longer than wide, exopod 1.13 (1.13–1.29) times peduncle length, endopod slightly shorter 1.06 (1.06–1.22) times peduncle length. Length of first peduncle 1.06 (1.06–1.13) times length of second peduncle.

Telson (fig. 11e, f) length 4.41 (3.7–4.41) mm, 0.71 (0.63–0.71) times carapace length, 3.14 (2.98–3.14) times longer than greatest width and tapering distally. Dorsal surface with 1–2 pairs of strong submarginal teeth-like spines. Posterior margin convex with 1 pair of teeth-like spines outermost, 7 (6–10) long, strong setose spines (fig. 11f).

Uropods approximately equal to telson length.

Males smaller than females, carapace length 4.5 mm; with endopod of pleopod 1 strongly excavate apically with 12 external spines on medial margin and 15 long setae on inner margin (fig. 11i).

Etymology: Spinosa after the very spiny rostrum with 28–30 dorsal spines and 9–10 ventral spines.

Comments: P. spinosa is most similar to *P. tasmaniensis* but may co-occur with *P. walkeri. P. spinosa* can be distinguished from all other long rostrum species by the combination of characters listed in Table 2 including the number of dorsal rostral spines (28–30); number of ventral rostral spines (9–10); right mandible incisors with 4–5 teeth; shape of scaphognathite of maxilla 2.

P. spinosa has a restricted distribution in streams of the northern coastal streams in New South Wales (Tweed R catchment) while *P. tasmaniensis* is widespread in Tasmania, coastal Victoria, New South Wales and Queensland and in the Murray-Darling catchment in New South Wales and South Australia. Cook et al. (2006) recorded lineage 3 in the Clarence R system but we recorded *P. spinosa* only in the Tweed R system. It is possible that both *P. spinosa* and *P. walkeri* may coexist in the Tweed R.

Paratya arrostra (Riek), 1953 comb. nov.

Figures 12–14

Paratya australiensis arrostra Riek, 1953; in part = rostrum mid length (fig. 12a)
Terrors Ck, Dayboro, Queensland. Types examined by MC.
Paratya atacta Riek 1953; in part = rostrum very long, comb. Nov. (fig. 12c)
Upper Nerang R, southern Queensland
Paratya atacta adynata Riek 1953; in part = rostrum mid length, comb. Nov. (fig. 12b). Small creek in upper reaches of Middle Harbour, Sydney, New South Wales
P. australiensis Williams and Smith (1979); neotype male selected from material named by Riek (1953), AM P28693.
Paratya australiensis Gan et al. (2016); determination of the mitogenome of *Paratya australiensis*.
Lineage 4 (Cook et al., 2006)
Lineage C (McClusky, 2007)

Material Examined: Victoria: Hughes Ck at Hughes Ck Rd, –37.0075 S, 145.3212 E, 28 September 2011 (PS, JM, MC); King Parrot Ck at Flowerdale, –37.2953 S, 145.2905 E, 28 September 2011 (PS, JM, MC); Goulburn R past Loch Gary at flood markers, –36.2411 S, 145.2866 E, 28 September 2011 (JM, MC); Yea R at Glenburn, –37.4239 S, 145.4210 E, 28 September (PS, JM, MC);
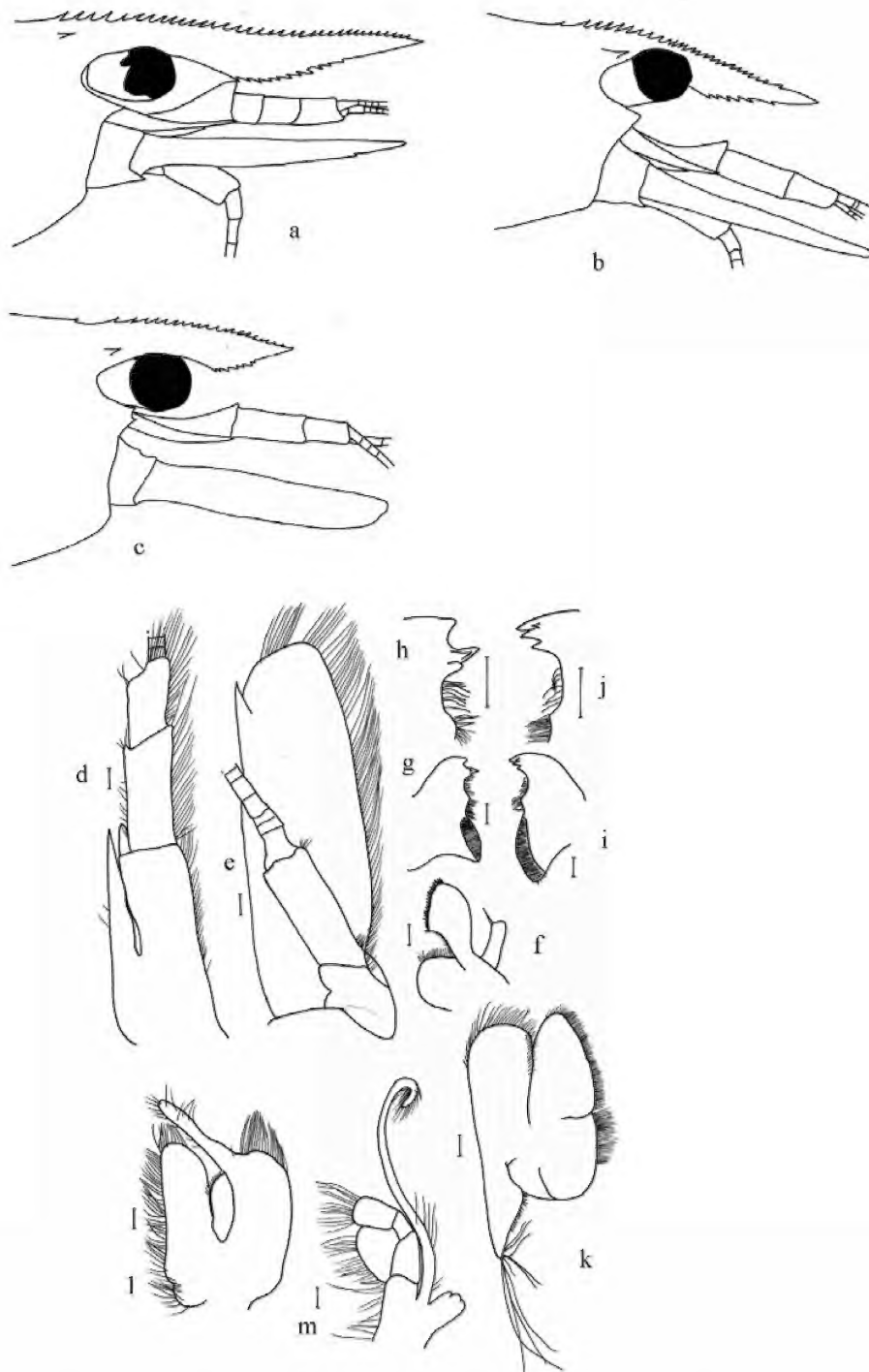
Figure 12. *Paratya arrostra* Riek: a, head region and rostrum of lineage 4 long; b, head region and rostrum of lineage 4 short; c, head region and rostrum of lineage 4c; d, antenna 1 peduncle and stylocerite; e, scaphocerite; f, maxilla 1; g, left mandible; h, enlarged incisors; i, right mandible; j, enlarged incisors; k, maxilla 2; l, maxilliped 1; m, maxilliped 2. Scale lines 0.2 mm.
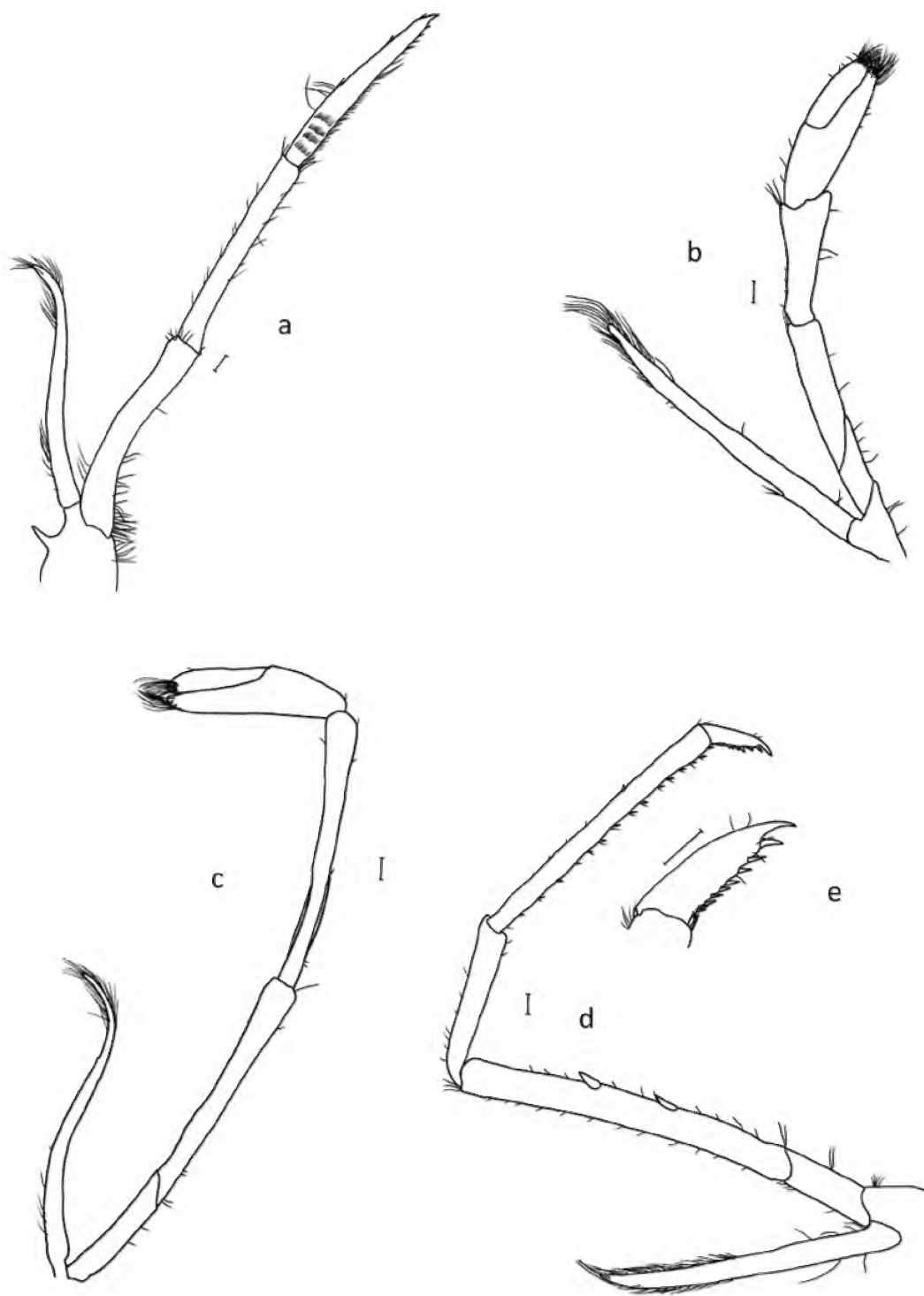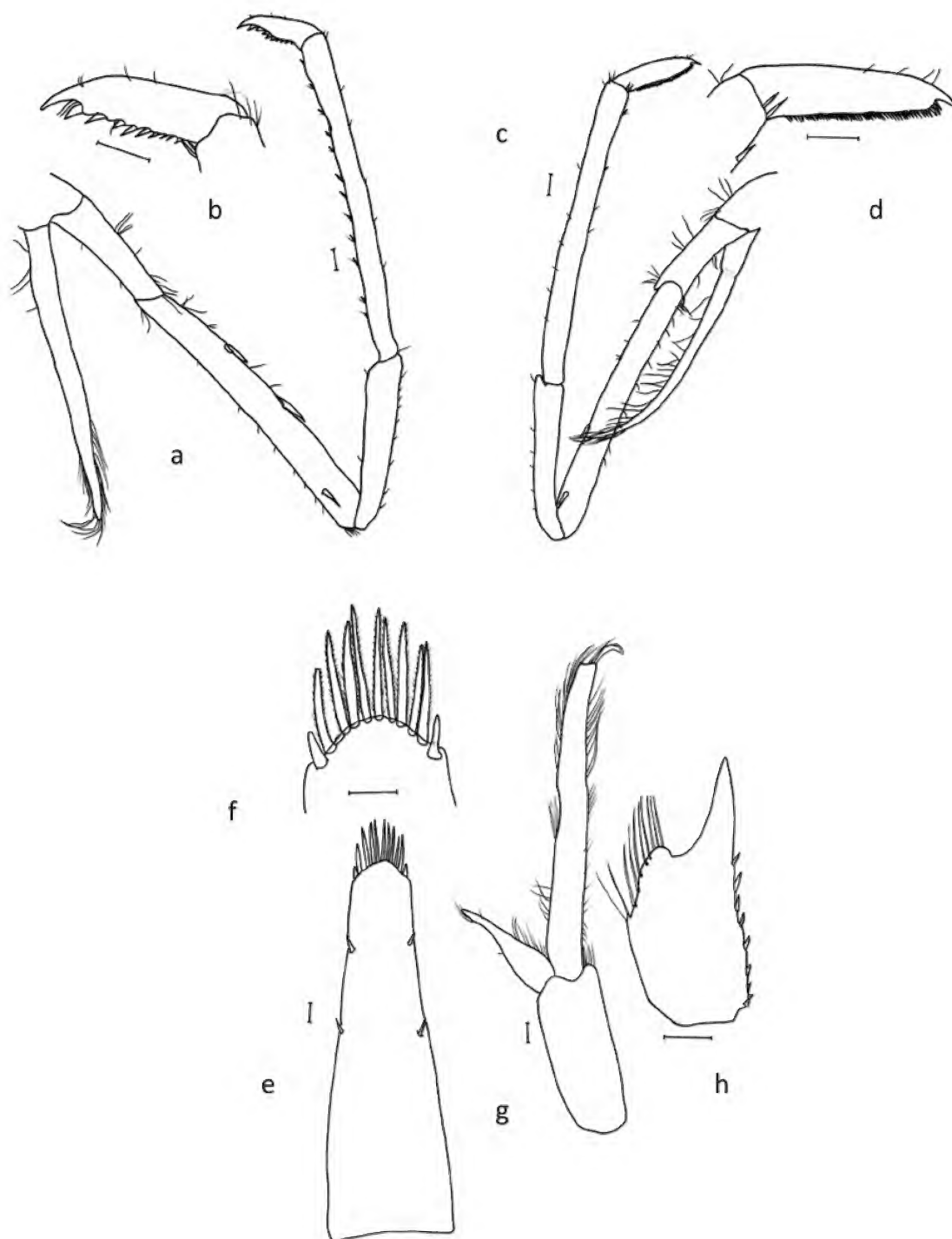
Figure 13. *Paratya arrostra* Riek: a, maxilliped 3; b, pereiopod 1; c, pereiopod 2; d, pereiopod 3; e, dactylus 3. Scale lines 0.2 mm.

Figure 14. *Paratya arrostra* Riek: a, pereiopod 4; b, dactylus 4; c, pereiopod 5; d, dactylus 5; e, telson; f, telson terminal spines; g, pleopod 1 of female; h, endopod 1 of male. Scale lines 0.2 mm.

Wimmera R downstream of Dimboola Weir, −36.4557 S, 142.0167 E, 6 March 2012 (Vic EPA); Ovens R near Wangaratta, −36.3371 S, 146.3191 E, August 2010 (JM, MC, JM).

New South Wales: Wakool Reserve, −35.4963 S, 144.4541 E, June 2011 (JC); Bagnall's Lagoon, Albury, −36.070 S, 146.854 E, April 2011 (PS); Murray R below Lake Hume, −36.0998 S, 147.0228 E, 12 August 2010 (JW, MC, JM); Hawksbury R at Windsor Bridge, −33.6023 S, 150.8233 E, 10 November 2011 (SW); Hawksbury R at Wilberforce, −33.6020 S, 150.8241 E, 10 September 2011 (SW); Hawksbury R at Sackville Ferry, −33.5003 S, 150.8746 E, 19 September 2020 (SW); Hawksbury R North Richmond, −33.5684 S, 150.7485 E, 9 March 2011 (SW); South Ck Richmond Rd, −33.6775 S, 150.8121 E, 30 March 2011 (SW); McCarrs Ck, −33.6410 S, 151.2780 E, 13 September 2011 (SW); Nepean R at Sharpes Weir, −34.0384 S, 150.6793 E, 15 September 2011 (SW); Nepean R at Grove Rd, −34.0415 S, 150.6964 E, 2 April 2011 (SW); Nepean R at Wallacia Bridge, −33.8655 S, 150.6374 E, 18 April 2011 (SW); Nepean R at Maldon Weir, −34.2034 S, 150.6301 E, 5 April 2011 (SW); Lachlan R, Newell Highway at Forbes, −33.3956 S, 147.9903 E, 3 November 2011 (PS, JM, MC); Lachlan at Cargellico −32.2033 S, 146.3589 E, Jun 1999 (PS, TC); Lachlan R at Glenmore, −33.4413 S, 145.5377 S, July 1999, (PS, TC); Lachlan R at Goolagong, −33.6060 S, 148.4324 E, July 1999 (PS, TC); Lachlan R at Condobolin, −33.0915 S, 147.1476 E, July 1999 (PS, TC); Macquarie R at Dubbo, −32.2470 S, 148.5990 E, 23 September 2010 (PS, MC); Murrumbidgee R at Wagga Wagga, −35.1041 S, 147.3751 E, 11 November 2003 (PS); Billabong Ck at Coree, −35.3556 S, 145.5041 E, 24 June 2001 (PS, LS); Billabong Ck at Moulamein, −35.0913 S, 144.0334 E, 2 April 2001 (PS, LS); Billabong Ck at Urana, −35.3598 S, 146.0942 E, 14 May 2001 (PS, LS); Billabong Ck at Walbundrie, −35.6971 S, 146.7253 E, 14 May 2001 (PS, LS); Billabong Ck at Wanganella, −35.2124 S, 144.3150 E, 2 April 2001 (PS, LS); Way Way Ck, −30.7680 S, 152.9427 E, 24 May 2016 (BM); Maguire Ck −28.8367 S, 153.3364 E Jun 2020 (SO); Maguire Ck −28.8367 S, 153.3364 E (BM); Tucki Tucki Ck, −28.8225 S, 153.3362 S, June 2020 (SO); Pinebrush Ck, −30.1306 S, 153.1328 E (BM); Small creek in upper reaches of Middle Harbour, Sydney, type locality for *P. atacta adynata* Riek 1953; Wattamollaa Ck on Clinton Park Rd Kangaroo Valley, −34.7371 E, 150.5929 S, 27 September 2017 (PS, JM, JH); Kangaroo R at Hampden Bridge, −34.7272 S, 150.5218 E, 26 September 2017 (PS, JM, JH); Stream on Broger Rd Shoalhaven catchment, −34.7105 S, 150.6827 E, 27 September 2017 (PS, JM, JH); Stream on Jarretts Rd – Upper Kangaroo Valley Rd, −34.7036 S, 150.5880 E, 27 September 2017 (PS, JM, JH); Brogers Ck in Shoalhaven catchment, −34.7105 S, 150.6827 E, 27 September 2017 (PS, JM, JH); Orara R at Nana Glen, −30.1328 S, 153.0077 E, no date, (BK); Brogo R at Brogo, −36.5402 S, 149.8265 E, 10 March 1999; Williams R at Coreei Bridge Dungog, −32.3968 S, 151.7631 E, 30 October 2011 (PS, JM, MC); The Falls at Forest Falls Retreat Johns R, −31.709 S, 152.6612 E, 31 October 2011 (MC, JM, PS); The Cascades at Forest Falls Retreat Johns R, −31.70 S,152.655 E, 31 October 2011 (MC, JM, PS); Lake Yarrunga at Bendeela recreation area −34.7398 S, 150.4705 E, 27 September 2017 (PS, JM, JH).

South Australia: Brenda Park wetland south of Morgan, −34.0818 S, 139.6743 E, 8 November 2011 (CM).

Queensland: Terrors Ck, Dayboro, type locality for *P. australiensis arrostra* Riek 1953; Upper Nerang R, southern Queensland, type locality for *P. atacta* Riek 1953; Kilcoy Ck, upper Brisbane R, −26.94 S, 152.568 E, no date (BC); Boar Pocket Ck, Tinaroo, −17.1708 S, 145.6447 E, 20 October 2017 (BM, BKr).

Diagnosis: P. arrostra differs from all other species by the following combination of characters: rostrum variable, long, extending beyond antennular peduncle or extending beyond both the antennular peduncle and scaphocerite, or short not extending beyond the peduncle or intermediate extending beyond peduncle but not the scaphocerite; dorsal edge slightly concave or straight, dorsally armed with 22–34 teeth, 2–3 postorbital spines, ventrally with 3–11 large serrations over a length of 0.40–2.20mm; distal half of ventral edge straight or curved; left mandible with 2–5 (usually 4–5) teeth separated by a smooth angular notch from a distinct apical tooth; right mandible with 4 teeth in 2 separate incisor processes; scaphognathite of maxilla 2 rounded apically extending to apex of upper endite; maxilliped 1 with exopod flagellum distinct, well developed and with numerous long setose spines on all margins, over half length of caridean lobe; exopod of maxilliped 2 2.18–3.45 times longer than endopod, epipodite with long podobranchs extending just to basal third of third segment of endopodite; maxilliped 3 with medial distal margin of apical segment of endopod with 6–8 broad teeth-like spines, outer margin with 2 broad teeth-like spines, exopod long and narrow, tip over-reaching distal end of basal endopod segment; pereiopod 1 with long carpus and long slender chelae, exopod extending to mid to apex of carpus; pereiopod 2 with exopod extending to apex of merus or base of carpus; dactylus of pereiopod 3 with prominent terminal claw and 9–11 strong spines on medial margin, exopod extends to mid merus to base of carpus; dactylus of pereiopod 4 prominent terminal claw and 8–12 spines on medial margin, exopod extends to mid merus; dactylus of pereiopod 5 with prominent terminal claw and very regular comb-like row of 70–90 small spines on medial margin, exopod extends to mid merus.

Morphotypes of P. arrostra: P. arrostra specimens with a very short rostrum not extending beyond the second segment of the antennular peduncle and only to mid scaphocerite (Lineage 4C) can be distinguished from all other species of *Paratya* by this short rostrum, dorsal edge straight and curved down at end, dorsally armed with 16–19 spines, 0–1 postorbital spines, with postorbital separated from other rostral spines, ventrally with 4–5 large serrations over a length of 0.60–1.2 mm, extending from posterior of greatest depth; distal half of ventral edge straight (Table 3).

P. arrostra with the shorter rostrum which does not extend beyond the scaphocerite (lineage 4B) can be distinguished from all other species of *Paratya* by the following combination of characters: 3–7 ventral spines on rostrum extend over a length of less than 1.80 mm; rostral length approximately equal to scaphocerite length 0.73–1.24; exopod of pereiopod 1, 2 and 3 extending to mid merus to base of carpus.

P. arrostra specimens with the longer rostrum character that extends beyond the end of the scaphocerite (Lineage 4B, 4E) differs from all other species of *Paratya* by the following combination of characters: 4–11 ventral spines extending over a length of 0.6–2.2 mm; rostral length 1.14–1.31 times longer than scaphocerite length; carpus of pereiopod 1 short; chelae of pereiopod 1 long and slender (Table 3).

Carapace length 5.10–7.00 mm.

Rostrum variable length either (i, lineages 4B, 4E) long, extending beyond antennular peduncle and to or beyond the end of the scaophocerite (fig. 12a), dorsally slightly concave, moderately slender; length 5.7–7.0 mm, 1.04–1.08 times length of carapace; dorsally armed with 23–34 teeth, ratio of

rostral spines to length 4.6–6.67; 2–3 postorbital eye spines (fig. 12a), ventrally with 4–11 large serrations over a length of 1.10–2.2 mm, extending from posterior of, or from, greatest depth (fig. 12a), distal half of ventral edge straight or curved, ratio of ventral spines to rostral length is 0.11–0.34; rostral length 7.86–8.83 times depth, length 1.14–1.31 times length of scaphocerite or (ii lineage 4B) rostrum short, length 2.50–5.30 mm, rostrum not extending beyond antennular peduncle (fig. 12b); 0.63–0.91 times length of carapace, dorsal edge straight and may be angled downwards (fig. 12b); dorsally armed with 22–29 teeth, ratio of rostral spines to length 4.34–7.60, 2–3 postorbital eye spines (fig. 12b), ventrally with 3–7 large serrations over a length of 0.4–1.8mm all forward of greatest depth (fig. 12b), distal half of ventral edge straight; rostral length/depth 6.33–8.83, length 0.73–1.24 times length of scaphocerite or (iii lineage 4C) rostrum very short 3.10–3.50 mm, not extending beyond the second segment of the antennular peduncle (fig. 12c) and only to half scaphocerite, rostral length 0.49–0.60 times length of carapace, shape broad and pointed, dorsal edge straight and curved down at end; dorsally armed with 16–19 teeth (fig. 12c), ratio of dorsal spines to length is 5.15–5.43 and 3.40–4.00 times more spines than ventral spines; 0–1 postorbital eye spines, when present spine distinctly posterior and separated from other rostral spines (fig. 12c); ventrally with 4–5 large serrations over a length of 0.60–1.20 mm, extending from posterior of greatest depth, ratio of ventral spines to rostral length is 0.18–0.34; distal half of ventral edge straight; rostral length/depth, 5.17–6.60; length 0.80–0.90 times length of scaphocerite.

Antenna 1 (fig. 12d) peduncle not quite reaching distal tip of scaphocerite, but similar length to scaphocerite itself, 0.42–1.06 times as long as scaphocerite; lateral distal angle of first segment with prominent blunt process at outer distal margin with small acute tooth on outer margin of segment but may be absent in some variations. Stylocerite 1.84–2.48 mm long, length 7.21–9.17 longer than width, 0.39–0.41 times carapace length, reaching beyond distal border of peduncle segment (fig. 12d) almost to end of acute process on distal angle of first segment (fig. 12d).

Antenna 2 (fig. 12e) second segment length 1.25–1.68mm long, 0.23–0.34 times length of scaphocerite, 2.00–3.36 longer than width. Scaphocerite 3.70–5.10 mm long, 0.64–0.94 times carapace length and 2.73–4.00 times as long as wide.

Mouthparts. Left mandible (fig. 12g, h) with 2–5 (usually 4–5) teeth separated by smooth angular notch from a distinct acute apical tooth; spine row immediately below incisor process of 8–10 rugose spines (lifting spines); spine row above molar process of approximately over 20 sparsely setose spines. Right mandible (fig. 12i, j) with 4 teeth in 2 separate incisor processes with first and third teeth largest and second and fourth smaller; spine row immediately below teeth with 8–10 spines each finely setose basally; spine row above molar process. Molar process ridged.

Maxilla 1 as for *P. australiensis* (fig. 12f).
Maxilla 2 as for *P. australiensis* (fig. 12k).
Maxilliped 1 as for *P. australiensis* (fig. 12l).
Maxilliped 2 (fig. 12m) endopod length 0.44–1.11 mm; exopod long and narrow, length 2.07–2.69 mm, exopod 2.18–

3.45 longer than endopod. Epipodite with long podobranch extending to basal third of third segment of endopodite.

Maxilliped 3 (fig. 13a) endopod length 5.72–7.23 mm, 2.20–2.75 times longer than exopod, with 3 distal segments of similar length; basal segment curved, apical segment with large terminal claw, medial distal margin with 6–8 broad teeth-like spines, largest 2 or 3 in basal half, outer margin with 2 long teeth-like spines in apical third. Exopod long and narrow 2.33–3.07 mm, tip over-reaching distal end of basal endopod segment.

Thoracic appendages. Pereiopod 1 (fig. 13b) length 3.51–5.23 mm, 0.66–0.89 times carapace length. Chelae short and slender (fig. 13b), 1.14–2.08 mm long, propodus 2.50–3.47 times as long as wide, 1.72–3.06 times longer than dactylus, 1.08–1.84 times longer than carpus; palm length 1.13–1.90 times palm width and 0.78–2.09 times dactylus length. Carpus long, 1.95–2.76 times as long as greatest width, broadening distally, distal margin excavate. Merus approximately one-third longer than carpus, parallel-sided. Ischium about one-quarter length of merus. Segment ratios 0.59–0.75 : 1.08–1.84 : 1.00 (1.01–1.40) mm : 1.14–1.84 : 0.40–0.50 : 1.65–3.16. Exopod extending to mid-apex of carpus.

Pereiopod 2 (fig. 13c) length 5.49–7.69 mm, 0.99–1.99 times carapace length. Chelae long and slender (fig. 13c) 1.15–1.63 mm long, half to two-thirds length of carpus, 2.87–4.20 times as long as wide; palm length 1.13–2.08 times longer than wide and 1.05–2.00 longer than dactylus. Propodus length 1.43–1.98 times longer than dactylus. Carpus 6.20–8.81 times as long as greatest width, slightly broader distally, distal margin with small excavation. Merus shorter than carpus, parallel-sided. Ischium about half as long as merus. Segment ratios 0.28–0.43 : 0.50–0.62 : 1.00 (2.29–2.72) mm : 0.73–0.88 : 0.30–0.46 : 1.14–1.22. Exopod extending to apex of merus to base of carpus.

Pereiopod 3 (fig. 13d, e) distinctly longer than pereiopod 2 and more slender 7.27–9.24 mm long, 1.28–1.57 times carapace length. Dactylus with prominent terminal claw and 9–11 strong spines on medial margin (fig. 13e). Propodus length 3.58–4.80 times longer than dactylus, length 11.61–15.77 times longer than wide with 6–13 spines on inner margin. Merus longer than propodus with 1–5 strong spines (usually 2) on medial margin and 1 near ventral distal margin; ischium approximately one-quarter to one-third length of propodus; segment ratios 0.36–0.51 : 1.60–1.88 : 1.00 (1.39–1.75) mm : 1.25–2.05 : 0.46–0.86 : 1.32–1.70. Exopod extends to mid-merus to base of carpus.

Pereiopod 4 (fig. 14a, b) similar to pereiopod 3, 7.69–9.81 mm long, 1.29–1.67 times carapace length. Dactylus with prominent terminal claw and 8–12 spines on medial margin (fig. 14b). Propodus length 3.05–5.00 times longer than dactylus, length 11.11–13.44 times longer than wide, with 11–16 spines on medial margin; merus with 1–3 strong spine on medial margin and 1 near ventral distal margin. Segment ratios 0.37–0.52 : 1.59–1.79 : 1.00 (1.49–1.93) mm : 1.83–2.38 : 0.50–0.68 : 1.35–1.50. Exopod extends to mid merus.

Pereiopod 5 (fig. 14c, d) similar length to pereiopods 3 and 4, 7.85–9.19 mm long, 1.37–1.56 times carapace length. Dactylus with prominent terminal claw and very regular,

comb-like row of numerous (70–91) small spines on medial margin (fig. 14d). Propodus length 2.97–3.91 times longer than dactylus, length 11.94–18.62 times as long as wide with 9–13 long medial spines and external margin without spines. Carpus approximately half propodus length without any large spines near distal margin. Merus similar length to propodus, with 1 strong medial spine and 1 distal spine; ischium one-third length of propodus; segment ratios 0.46–0.65 : 1.79–1.97 : 1.00 (1.52–1.80) mm : 1.54–1.97 : 0.47–0.66 : 1.29–1.61. Exopod extends to mid to apical third of merus.

Abdomen. Pleopods peduncle of first pleopod short, 0.26–0.37 times length of carapace length, 2.40–3.45 times width, exopod 1.29–1.81 times peduncle length, endopod 0.63–0.69 times peduncle length (fig. 14g); second pleopod peduncle short, 0.31–0.47 times length of carapace, 2.47–3.67 times width, exopod 1.09–1.35 times peduncle length, endopod slightly shorter 0.91–1.27 times peduncle length. Length of first peduncle 1.18–1.28 times length of second peduncle. Peduncle of pleopod 5 0.20–0.28 times length of carapace, 1.68–2.31 times width; exopod length 1.57–1.93 times peduncle length; endopod 1.22–1.57 times peduncle length; exopod length 1.14–1.29 times endopod length.

Telson (fig. 14e, f) length 3.10–4.10 mm, 0.51–0.76 times carapace length, 2.36–3.75 times as long as greatest width, and tapering distally, Dorsal surface with 0–2 pairs of strong submarginal teeth-like spines; posterior margin convex with 1 pair of teeth-like spines outermost, 7–13 (usually 11–12) long, strong setose spines (fig. 14f).

Uropods approximately equal to telson length, exopod 1.05–1.33 times telson length, length 2.84–3.19 times width; endopod 0.98–1.29 times telson length, length 3.28–4.25 times width.

Males smaller than females, carapace length 4.36 mm; endopod of first pleopod strongly excavated apically with 9–10 external spines and 10–14 long setae on inner margin (fig. 14h).

Comments: This is the most variable species of Paratya showing distinct rostral characteristics from rostrum shorter than the peduncle, rostrum longer than peduncle but not extending beyond the scaphocerite and rostrum long extending beyond the scaphocerite. Riek (1953) observed these distinct groups and described them as species or subspecies based on morphological character expression only. Williams and Smith (1979) considered all the taxa described by Riek were synonyms of P. australiensis. With the development of molecular techniques, it is now possible to recognise that these variants are all a single taxon and the taxon P. australiensis arrostra Riek is here raised to species level. Genetically, all Lineage 4 specimens have low intraspecific variation, and although Lineage 4C can be reliably identified morphologically (Table 3), it is slightly more difficult to reliably define lineages 4A, 4B, 4D and 4E (Cook et al., 2006) morphologically (Table 2) on the limited material we have been able to analyse. The presence of different morphotypes in this species is similar to the observations by Choy et al. (2019) in the Australian atyid shrimp Australatya.

P. arrostra is widely distributed through the Murray–Darling Basin, south-eastern coastal streams in Victoria and New South Wales, north-eastern New South Wales coastal streams, and south-eastern and northern Queensland (fig. 32a). Lineage 4A has been recorded from northern coastal streams in Queensland but we do not have any specimens of this lineage. Lineage 4C is restricted to south-eastern Queensland in the catchments of the Maroochy R, Mary R and Brisbane R. We have recorded P. arrostra to occur at sites in South Australia with P. rouxi and P. tasmaniensis; with P. rouxi, P. whitemae and P. strathbogiensis in Murray–Darling Basin rivers and with P. whitemae in coastal rivers.

Gan et al. (2016) defined the complete mitogenome of a species designated as P. australiensis from the Lodden R at Baringhup, Victoria. The mitochondrial genome is 15,990 base pairs in length (GenBank accession number: KM978917) and has 37 mitochondrial genes (13 protein-coding genes, 2 rRNAs and 22 tRNAs) and a non-coding region of 1006 base pairs (Gan et al. (2016). This genome (strain APR12) was analysed with the total GENBANK Paratya data (Supplementary Table 1) and the species used by Gan et al. (2016) was embedded with P. arrostra.

Paratya williamsi n. sp.

Figures 15–17

http://zoobank.org/urn:lsid:zoobank.org:act:F299988B-DF09-4765-A01E-B28875339C5D

Lineage 5 (Cook et al., 2006)

Type Material: Holotype New South Wales. Kangaroo R Hampden Bridge, −34.7272 S, 150.5218 E, 26 September 2017 (PS, JM, JH). Body in ethanol and antennae, mouthparts, pereiopods and abdominal structures dissected, mounted on 2 slides. AM Ref No. P.105603.001; Accession Ref. PS103, Genbank Registration OL420884.

Paratypes: New South Wales. Kangaroo R Hampden Bridge, −34.7272 S, 150.5218 E, 26 September 2017 (PS, JM, JH) Accession Ref. PS98, AM Ref No. P.105.603, Kangaroo Valley R on Gerringong Ck Rd, −34.6868 S, 150.6013E, Accession Ref. PS99, AM Ref No. P.105603, 27 September 2017 (PS, JM, JH), bodies in ethanol and other structures dissected, mounted on 2 slides each.

Material Examined: New South Wales: Hampden Bridge, −34.7272 S, 150.5218 E, 26 September 2017 (PS, JM, JH); Kangaroo Valley R on Gerringong Ck Rd, −34.6868 S, 150.6013 E, 27 September 2017 (PS, JM, JH).

Diagnosis: Paratya williamsi differs from all other species by the following combination of characters: rostrum long, 4.80–5.20 mm, extending beyond antennular peduncle and to end of scaphocerite, rostral length 0.84–1.03 times longer than carapace, dorsal edge curved upwards to tip, narrow and pointed, rostrum 7.16–9.60 times longer than wide, dorsally armed with 21–27 teeth, ratio of rostral spines to rostral length is 4.38–5.38, with 2–3 postorbital spines; ventrally with 1–5 short serrations over a length of 0.10–2.00 mm, 1 spine posterior to greatest depth, distal half of ventral edge straight, ratio of ventral spine length to rostral length is 0.21–1.00 and 4.40–21.00 more dorsal spines than ventral spines; rostral length 1.15–1.34 times length of scaphocerite. Left mandible with 4–5 teeth separated by a notch from 3 less distinct apical
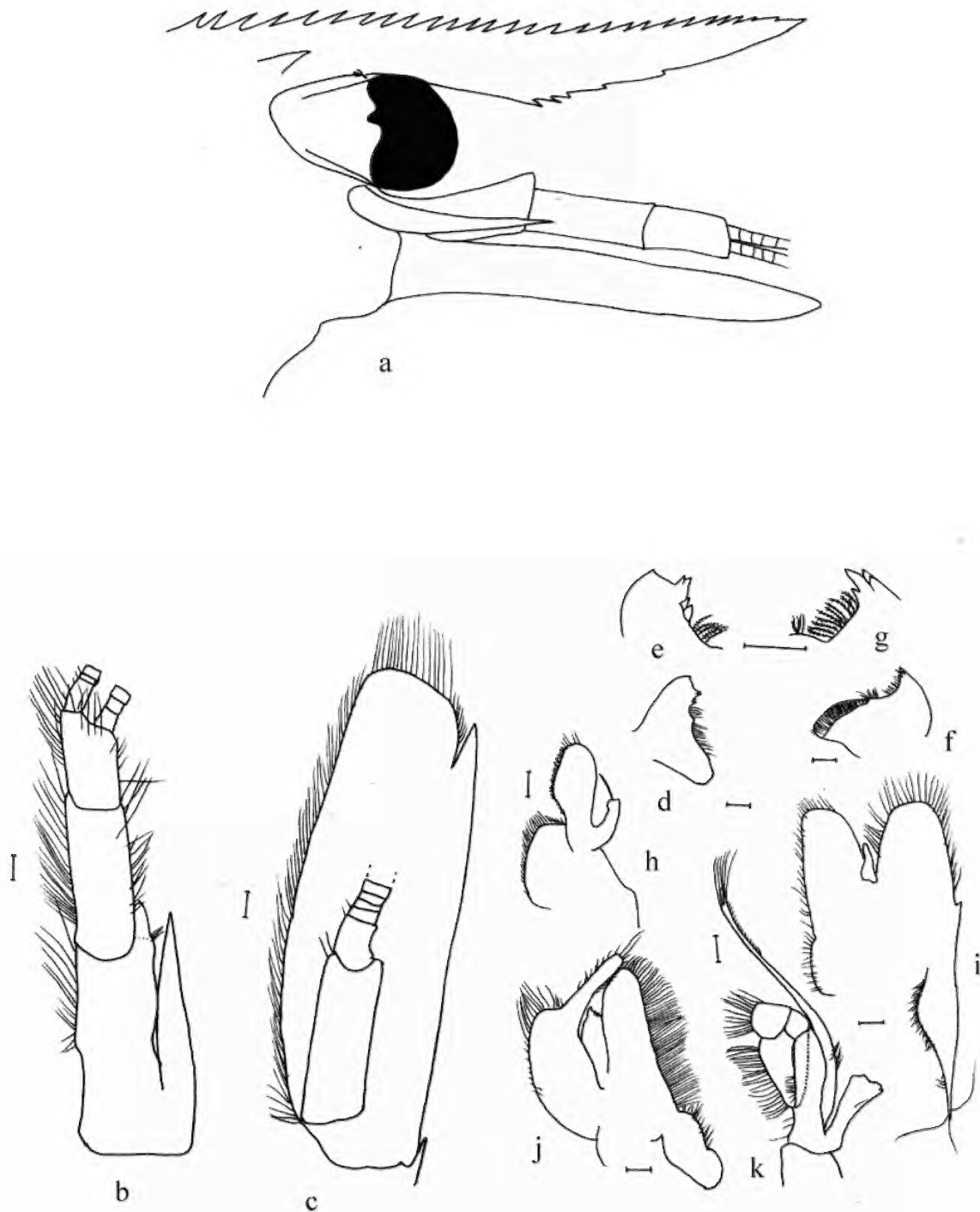
Figure 15. *Paratya williamsi* sp. nov.: a, head region and rostrum; b, antenna 1 peduncle and stylocerite; c, scaphocerite; d, left mandible; e, enlarged incisors; f, right mandible; g, enlarged incisors; h, maxilla 1; i, maxilla 2; j, maxilliped 1; k, maxilliped 2. Scale lines 0.2 mm.
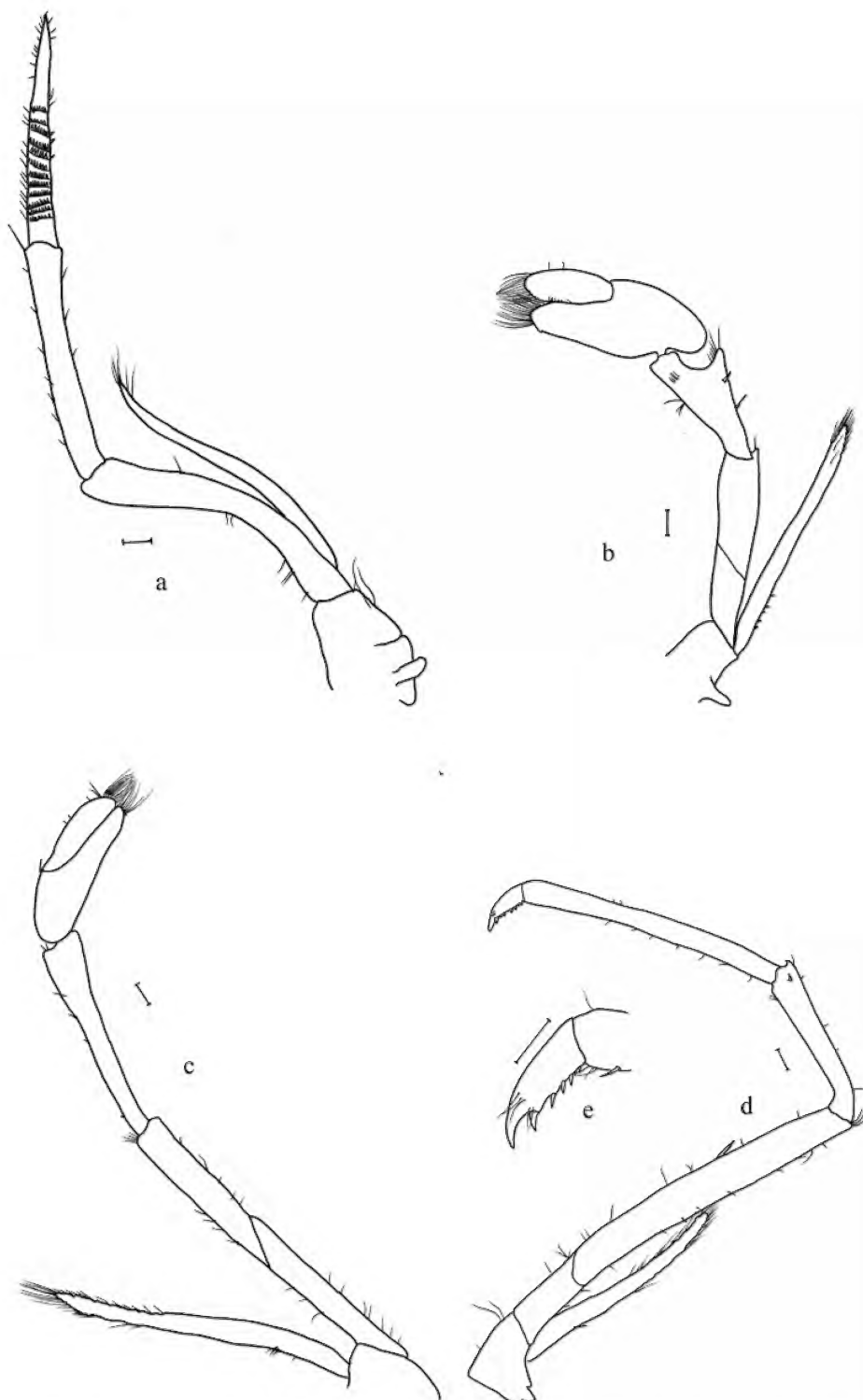
Figure 16. *Paratya williamsi* sp. nov.: a, maxilliped 3; b, pereiopod 1; c, pereiopod 2; d, pereiopod 3; e, dactylus 3. Scale lines 0.2 mm.
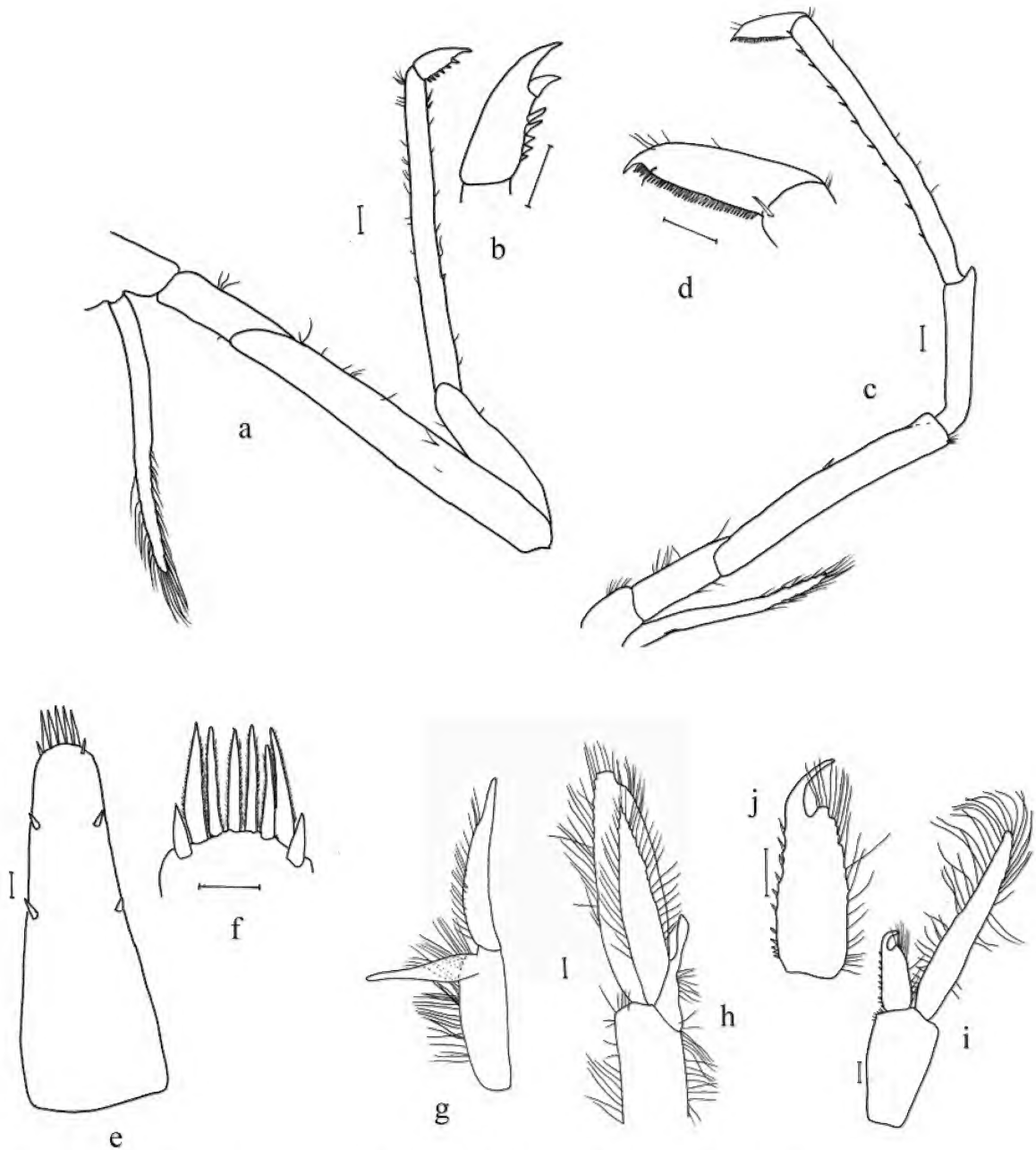
Figure 17. *Paratya williamsi* sp. nov.: a, pereiopod 4; b, dactylus 4; c, pereiopod 5; d, dactylus 5; e, telson; f, telson terminal spines; g, pleopod 1 of female; h, pleopod 2 of female; i, pleopod 1 of male; j, endopod 1 of male. Scale lines 0.2 mm.

teeth; spine row immediately below incisor process of 4–6 rugose spines (lifting spines); right mandible with 4 teeth in a single incisor process with apical and fourth teeth largest separated by 2 smaller teeth. Maxilla 2 with scaphognathite truncated distally, not extending to apex of upper endite. Chelae of pereiopod 1 short and broad, 1.40–1.51 mm long, propodus 2.28–3.02 times as long as wide, 1.87–1.97 times longer than dactylus, 1.27–1.44 times longer than carpus; palm length 1.36–1.70 times longer than wide and 1.00–1.27 times longer than dactylus length. Carpus very short 2.10–2.33 times as long as greatest width. Dactylus of pereiopod 3 with prominent terminal claw and 5–7 strong spines on medial margin. Dactylus of pereiopod 4 with prominent terminal claw and 5–6 spines on medial margin.

Carapace length 5.40 (4.85–6.00) mm.

Rostrum long, 5.40 (4.80–5.20) mm, extending beyond antennular peduncle and to end of scaphocerite (fig. 15a), rostral length 0.96 (0.84–1.03) times longer than carapace, dorsal edge curved upwards to tip, narrow and pointed, rostrum 8.00 (7.16–9.60) times longer than wide, dorsally armed with 24 (21–27) teeth, ratio of rostral spines to rostral length is 4.61 (4.38–5.38), with 2 (2–3) postorbital spines (fig. 15a); ventrally with 3 (1–5) short serrations over a length of 1.50 (0.10–2.00) mm, 1 spine at greatest depth (fig. 15a), distal half of ventral edge straight, ratio of ventral spine length to rostral length is 0.29 (0.21–1.00) and 8.00 (3.50–21.00) more dorsal spines than ventral spines; rostral length 1.27 (1.15–1.34) times length of scaphocerite.

Antenna 1 (fig. 15b) peduncle 2.75 (2.25–2.75) mm long, not reaching distal tip of scaphocerite, 0.90 (0.90–1.00) times length of scaphocerite. Stylocerite 2.25 (2.05–2.30) mm long, length 7.50 (6.83–9.20) longer than wide, 0.42 (0.38–0.45) times carapace length, reaching beyond distal border of peduncle segment but not to end of broad acute process on distal angle of first segment (fig. 15b).

Antenna 2 (fig. 15c) second segment of peduncle 1.50 (1.26–1.50) mm long, 0.37 (0.29–0.37) length of scaphocerite, 2.73 (2.29–2.73) longer than wide. Scaphocerite 4.10 (3.75–4.35) mm long, 0.76 (0.73–0.82) times length of carapace, 3.28 (3.13–3.48) longer than wide.

Mouthparts. Left mandible (fig. 15d, e) with 4–5 teeth separated by a notch from 3 less distinct apical teeth; spine row immediately below incisor process of 4–6 rugose spines (lifting spines); spine row above molar process of approximately over 20 sparsely setose spines. Right mandible (fig. 15f, g) with 4 teeth in a single incisor process with apical and third teeth largest with second and fourth teeth smaller; spine row immediately below teeth with 8–11 lifting spines; spine row above molar process. Molar process ridged.

Maxilla 1 as for *P. australiensis* (fig. 15h).

Maxilla 2 (fig. 15i) scaphognathite truncated distally, not extending to apex of upper endite; palps small, terminal parts narrow and with 1 sub–apical setose spine.

Maxilliped 1 as for *P. australiensis* (fig. 15j).

Maxilliped 2 (fig. 15k) endopod length 0.88 (0.88–1.11) mm; exopod long and narrow 2.15 (2.00–2.50) mm, exopod 2.44 (2.27–2.46) times longer than endopodite. Epipodite with podobranch.

Maxilliped 3 (fig. 16a) endopod length 6.10 (5.68–6.27) mm, 2.71 (2.32–2.71) times longer than exopod; with 3 distal segments of similar length; basal segment curved, apical segment with large terminal claw, medial distal margin with 8 (6–8) broad teeth-like spines, largest 1 in basal third, outer margin with 7 teeth-like spines. Exopod long and narrow, 2.25 (2.25–2.70) mm long, tip reaching basal third of mid segment, with several long setose spines near tip and several short setose spines near base. Epipodite with basal conical projection.

Thoracic appendages. Pereiopod 1 (fig. 16b) 4.65 (4.65–4.73) mm long, 0.86 (0.78–0.98) times carapace length. Chelae short and broad (fig. 16b), 1.40 (1.40–1.51) mm long, propodus 2.54 (2.28–3.02) times as long as wide, 1.87 (1.87–1.97) times longer than dactylus, 1.27 (1.27–1.44) times longer than carpus; palm length 1.36 (1.36–1.70) times longer than wide and equal to dactylus length (1.00–1.27). Carpus very short 2.20 (2.10–2.33) times as long as greatest width, broadening distally, distal margin excavate. Segment ratios 0.68 (0.68–0.76) : 1.27 (1.27–1.44) : 1.00 (1.10 [1.05–1.10] mm) : 1.50 (1.43–1.52) : 0.45 (0.45–0.57) : 1.27 (1.27–2.71). Exopod extending to mid merus (mid merus to mid carpus).

Pereiopod 2 (fig. 16c) 6.20 (5.80–7.50) mm long, 1.15 (1.15–1.25) times carapace length. Chelae long and slender (fig. 16c), 1.50 (1.35–1.50) mm long, nearly two-thirds length of carpus, 2.33 (2.25–3.33) times longer than wide, palm length 1.56 (1.50–1.56) times longer than width and 0.82 (0.82–1.20) times dactylus length. Propodus length 1.76 (1.76–1.80) times longer than dactylus. Carpus 5.71 (5.14–8.33) times as long as greatest width, slightly broader distally, distal margin with small excavation. Segment ratios 0.43 (0.34–0.43) : 0.75 (0.60–0.75) : 1.00 (2.00 [1.80–2.50] mm) : 0.68 (0.68–0.80) : 0.68 (0.60–0.75) : 1.50 (1.24–1.50). Exopod extending to apex of merus to base of carpus.

Pereiopod 3 (fig. 16d, e) distinctly longer than pereiopod 2 and more slender 8.45 (7.65–9.15) mm long, 1.56 (1.53–1.58) times carapace length. Dactylus with prominent terminal claw and 5 (5–7) strong spines on medial margin (fig. 16e). Propodus length 4.58 (4.46–4.58) times longer than dactylus, length 11.00 (10.00–14.50) times longer than wide with 13 (11–13) spines on inner margin. Merus with 1–3 strong spines on medial margin and 1 near ventral distal margin; segment ratios 0.40 (0.37–0.40) : 1.83 (1.67–1.83) : 1.00 (1.50 [1.50–1.65] mm) : 2.13 (2.03–2.13) : 0.67 (0.40–0.67) : 1.53 (1.53–1.88). Exopod extends to mid merus (mid merus to apex of merus).

Pereiopod 4 (fig. 17a, b) similar to pereiopod 3, 7.80 (7.45–9.63) mm long, 1.44 (1.34–1.54) times carapace length. Dactylus with prominent terminal claw and 5 (5–6) spines on medial margin (fig. 17b). Propodus length 5.40 (4.75–5.40) times longer than dactylus, length 10.80 (10.00–11.40) times longer than wide, with 11 (8–13) spines on inner margin; merus with 0–2 strong spines on medial margin and 1 near ventral distal margin. Segment ratios 0.36 (0.36–0.40) : 1.93 (1.79–1.93) : 1.00 (1.40 [1.40–1.50] mm) : 1.93 (1.80–2.04) : 0.71 (0.50–0.71) : 1.71 (1.61–1.71). Exopod extends to mid merus.

Pereiopod 5 (fig. 17c, d) slightly shorter than pereiopods 4, 7.65 (7.20–8.30) mm long, 1.42 (1.38–1.48) times longer than carapace. Dactylus with prominent terminal claw and very regular, comb-like row of 50 (49–66) spines on medial margin

(fig. 17d). Propodus length 4.07 (3.93–4.07) times longer than dactylus, length 14.25 (11.00–14.25) times longer than wide with 7 (7–10) long inner teeth and setae on external margin. Carpus with 1 large spines near distal margin. Merus with 1 strong medial spine and 1 distal spine; segment ratios 0.50 (0.47–0.56) : 2.04 (1.91–2.20) : 1.00 (1.40 [1.25–1.60] mm) : 1.71 (1.50–1.92) : 0.71 (0.64–0.78) : 1.43 (1.31–1.43). Exopod extends to base to third of merus.

Abdomen. Pleopods peduncle of first pleopod short 1.90 (1.50–2.35) mm, 0.35 (0.31–0.39) times length of carapace length, 2.92 (2.92–5.85) times width, exopod 1.08 (1.08–1.28) times peduncle length, endopod 0.60 (0.45–0.80) times peduncle length (fig. 17g); second pleopod peduncle short, 0.42 (0.36–0.45) times length of carapace, 2.50 (2.33–2.81) times width, exopod 1.16 (–) times peduncle length, endopod slightly shorter 1.04 (–) times peduncle length (fig. 17h).

Telson (fig. 17e, f) length 3.50 (3.50–4.00) mm, 0.65 (0.67–0.72) times carapace length, 3.04 (2.81–3.17) times as long as greatest width, tapering distally. Dorsal surface with 2 pairs of strong submarginal teeth-like spines. Posterior margin convex with 1 pair of teeth-like spines outermost, 6 (6–8) long, strong terminal setose spines (fig. 17f).

Uropods approximately equal to telson length.

Male smaller than female, carapace length 4.7mm; endopod of pleopod 1 strongly excavated and strongly curved (fig. 17i, j) with 11 short spines on outer margin and 12 long setae on inner margin (fig. 17j).

Etymology: The specific epithet is in honour of the late Prof. W. D. Williams who encouraged and inspired a generation of Australian limnologists and who provided one of us (PS) a unique opportunity for post-graduate study at Adelaide University.

Comments: P. williamsi has an overlap of distribution with *P. australiensis* and *P. arrostra*. Characters that distinguish these species from *P. williamsi* are listed in Table 2.

P. williamsi may also be confused with *P. whitemae* and *P. tasmaniensis*, both of which are widespread and may have distributions that overlap, but they can be distinguished by the following combination of characters: dactylus of pereiopod 3 with 5–7 teeth; dactylus of pereiopod 4 with 5–6 teeth; dactylus of pereiopod 5 with a comb of 49–74 spines; first cheliped palm length 1.00–1.27 times dactylus length; 1–5 ventral rostral spines over a length of 0.10–2.00 mm (Table 2).

P. williamsi is restricted to the upper Kangaroo Valley in the Shoalhaven R catchment south of Sydney and can be found co-existing with *P. whitemae* and *P. tasmaniensis*.

Paratya whitemae n. sp.

Figures 18– 20

http://zoobank.org/urn:lsid:zoobank.org:act:24D43065-1D31-42BC-A846-7BFB163778AB

Lineage 6 (Cook et al., 2006)
Lineage A (McClusky, 2007)

Type Material: Holotype New South Wales. The Falls at Forest Falls Retreat Johns R, −31.709 S, 152.6612 E, 31 October 2011 (MC, JM, PS); Body in ethanol and antennae, mouthparts, pereiopods and abdominal structures dissected, mounted on 2 slides. Accession Ref. MC108, AM Ref No. P.105604.

Paratypes: New South Wales. The Falls at Forest Falls Retreat Johns R, −31.709 S, 152.6612 E, 31 October 2011 (MC, JM, PS) Male, Accession Ref MC110, Genbank Registration OL420801; Bagnall's Lagoon, Albury, −36.070 S, 146.854 E, April 2011 Accession Ref. MC95, 97, 99 (PS) Genbank Registration OL420871, OL420872, OL420874; Wakool Reserve, −35.4963 S, 144.4541 E, June 2011 (JC); Nepean R at Maldon Weir, −33.7414 S, 150.6846 E, 5 April 2011 Accession Ref. MC37 (SW), Genbank Registration OL420834; Nepean R at Macquarie Grove Rd, −34.0414 S, 150.6953 E, 2 April 2011 Accession Ref. MC34 (SW), Genbank Registration OL420834; Bedford Ck −33.75 S, 150.447 E Accession Ref. MC31 (SW), Genbank Registration OL420830; Hawkesbury R at Wilberforce, −33.5702 S, 150.8382 E, 21 April 2011 Accession Ref. MC24 (SW), Genbank Registration OL420824; O'Hares Ck near George R, −34.095 S, 150.835 E, 20 April 2011 Accession Ref. MC21–23 (SW), Genbank Registration OL420821–OL420823; bodies in ethanol and other structures dissected, mounted on 2 slides each.

Material Examined: New South Wales: Bagnall's Lagoon, Albury, −36.070 S, 146.854 E, April 2011 (PS); Murray R below Lake Hume, −36.0998 S, 147.0228 E, 12 Aug 2010 (JW, MC, JM); Wakool Reserve, −35.496 S, 144.454 E, June 2011 (JC); Nepean R at Maldon Weir, −33.7414 S, 150.6846 E, 5 April 2011 (SW); Nepean R at Macquarie Grove Rd, −34.0414 S, 150.6953 E, 2 April 2011 (SW); Bedford Ck, −33.75 S, 150.447 E, 4 May 2011 (SW); Hawkesbury R at Wilberforce, −33.5702 S, 150.8382 E, 21 April 2011 (SW); O'Hares Ck near George R, −34.095 S, 150.835 E, 20 April 2011 (SW); Woolgoolga Ck, −30.1306 S, 153.1378 E, (BM), Way Way Ck, −30.7681 S, 153.1378 E, (BM); Nambucca Ck, −30.6408 S, 152.8558 E, (BM); Bellinger R, −30.4261 S, 152.7794 E, (BM); The Falls at Forest Falls Retreat Johns R, −31.709 S, 152.6612 E, 31 October 2011 (MC, JM, PS); Jerrys Ck near Forest Falls Retreat Johns R, −31.7146 S, 152.6625 E, 30 October 2011 (MC, JM, PS); The Cascades at Forest Falls Retreat Johns R, −31.70 S,152.655 E, 31 October 2011 (MC, JM, PS); Williams R at Cooreei Bridge Dungog, −32.3968 S, 151.7631 E, 29 October 2011 (MC, JM, PS); Trimble Ck in Shoalhaven catchment, −34.6847 E, 150.5252 S, 26 September 2017 (PS, JM. JH); Small Ck on Kangaroo Valley Rd, Kangaroo Valley, −34.7229 S, 150.5293 S, 27 September 2017 (PS, JM, JH); Lake Yarrunga at Bendeela Recreation Area, −34.7398 S, 150.4705 E, 27 September 2017 (PS, JM, JH); Manning R at Wingham Brush, −31.8706 S, 152.3825 E, 16 September 2016 (BM); Kangaroo R Hampden Bridge, −34.7272 S, 150.5218 E, 27 September 2017 (PS, JM. JH); Lachlan R at Glenmore, −33.4413 S, 145.5377 S, July 1999, (PS, TC); Lachlan at Cargellico −32.2033 S, 146.3589 E, June 1999, (PS, TC); Orara R at Nana Glen, −30.1328 S, 153.0077 E, no date, (BK); Hawkesbury R at Sackville Ferry, −33.5003 S, 150.8746 S, 19 September 2020 (SW); Stream on Gerrigong Ck Rd, Upper Kangaroo Valley, −34.6870 S, 150.6000 E, 27 September 2017 (PS, JM. JH); Dingo Ck, −30.3103 S, 152.9822 E, 24 May 2015 (BM); Ellenborough R at Ellenborough Falls, −31.6113 S, 152.2925 E, 31 October 2011 (PS, JM, MC); Blaxland Ck on Armidale Rd, −28.8997 S, 152.7864 E, 8 December 2011 (JW, DB).

Diagnosis: P. whitemae differs from all other species by the following combination of characters: rostrum long, extending beyond both antennular peduncle and scaphocerite, dorsal edge very slightly concave and curved upwards, dorsally armed with 20–34 teeth, 1–4 postorbital spines, ventrally with 4–11 large serrations over a length of 1.30–2.80 mm, extending from just posterior to greatest depth; distal half of ventral edge straight; left mandible with 4–5 teeth separated by finely ridged U-shaped notch from a short blunt/acute apical tooth; right mandible with

Figure 18. *Paratya whitemae* sp. nov.: a, head region and rostrum; b, antenna 1 peduncle and stylocerite; c, scaphocerite; d, left mandible; e, enlarged incisors; f, right mandible; g, enlarged incisors; h, maxilla 1; i, maxilla 2; j, maxilliped 1; k, maxilliped 2. Scale lines 0.2 mm.
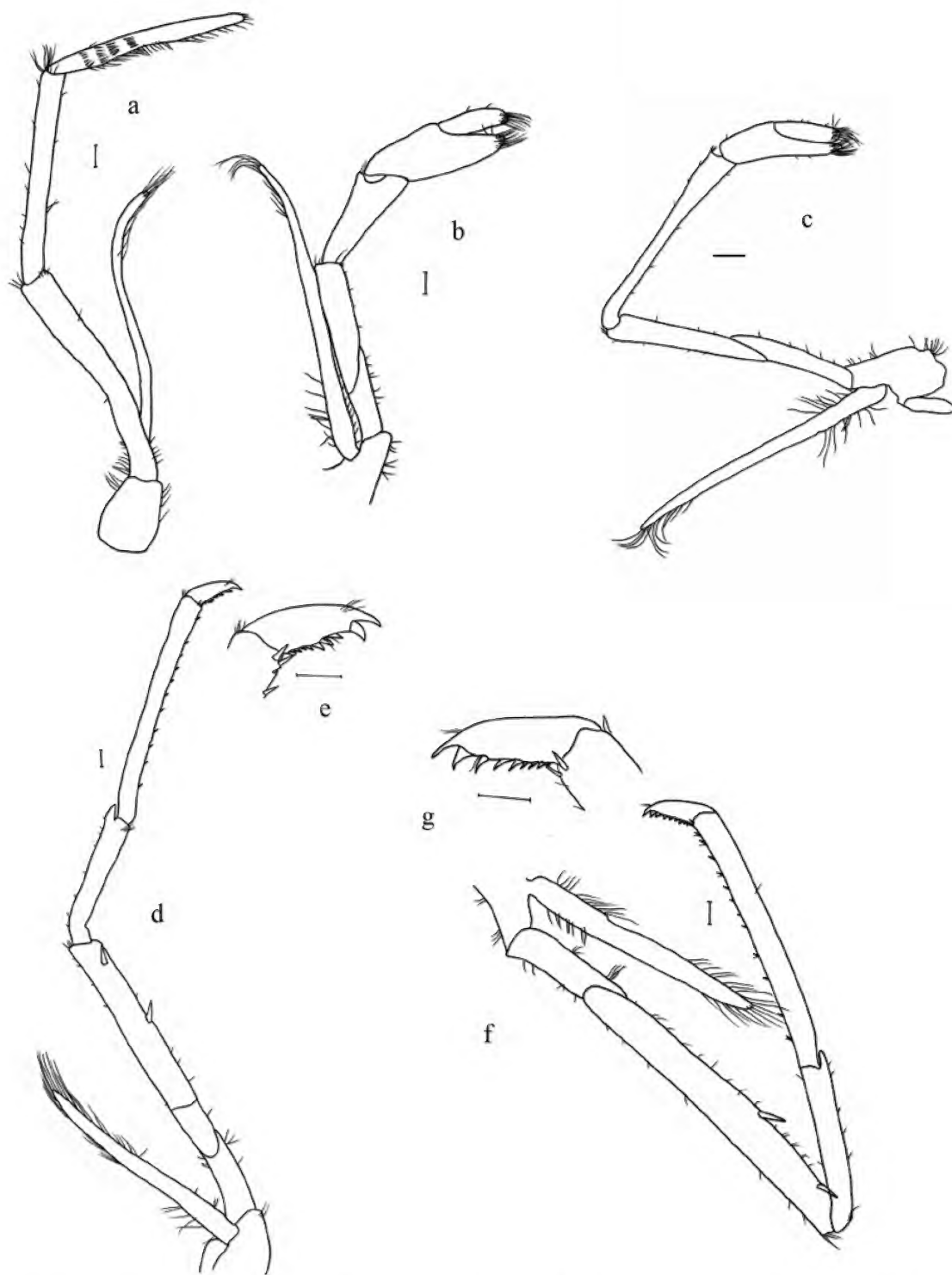
Figure 19. *Paratya whitemae* sp. nov.: a, maxilliped 3; b, pereiopod 1; c, pereiopod 2; d, pereiopod 3; e, dactylus 3; f, pereiopod 4; g, dactylus 4. Scale lines 0.2 mm.
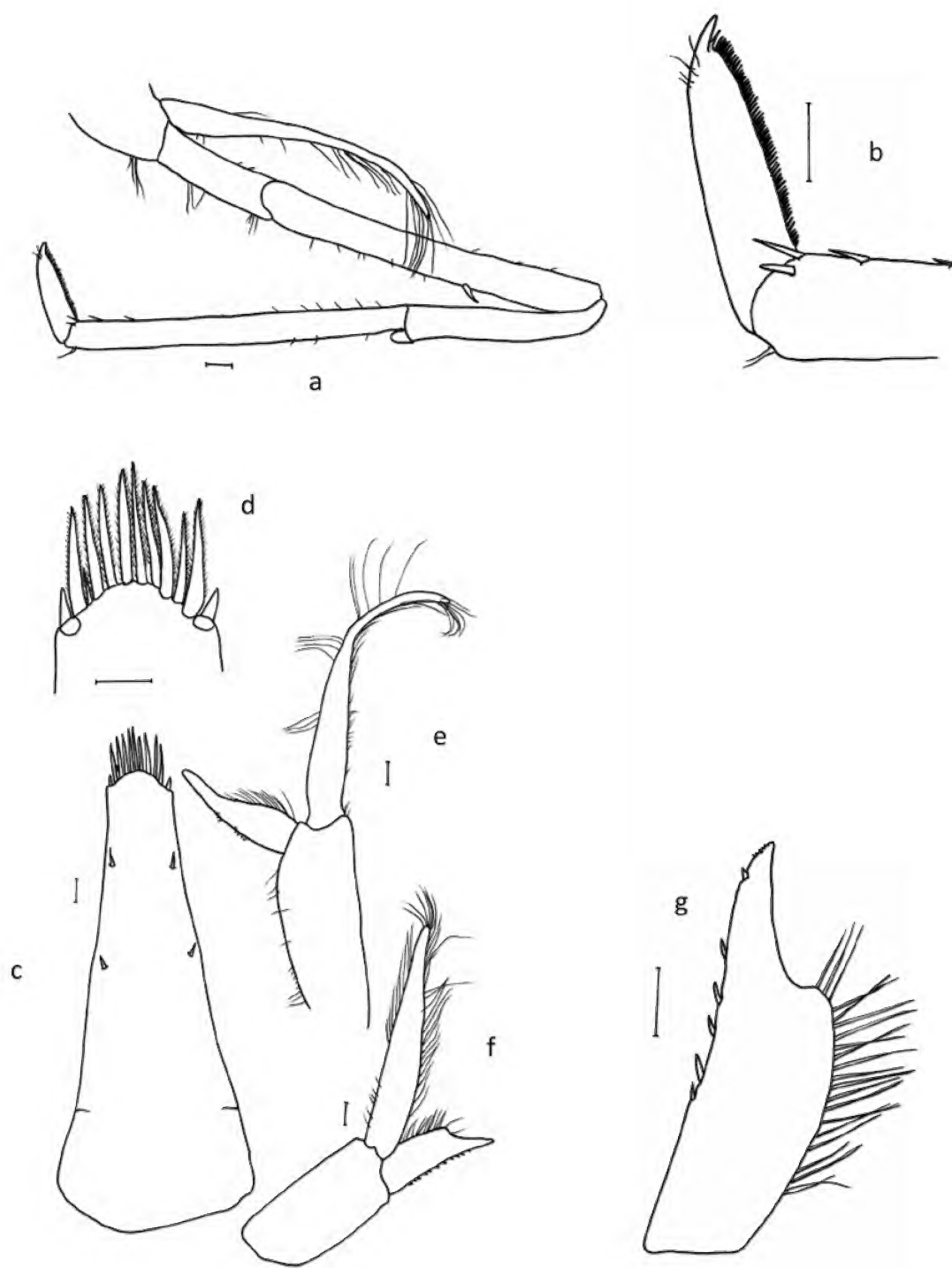
Figure 20. *Paratya whitemae* n. sp.: a, pereiopod 5; b, dactylus 5; c, telson; d, telson terminal spines; e, pleopod 1 of female; f, pleopod 1 of male; g, endopod 1 of male. Scale lines 0.2 mm.

3–4 teeth in a single incisor process; exopod of maxilliped 2 1.63–2.96 times longer than endopod; maxilliped 3 with medial distal margin of apical segment of endopod with 7–11 broad teeth-like spines, outer margin with 1–3 broad teeth-like spines, exopod long and narrow, tip over-reaching distal end of basal endopod segment; pereiopod 1 with long carpus and short and broad chelae, exopod extending to base–apex of carpus; pereiopod 2 with exopod extending to mid merus to base of carpus; dactylus of pereiopod 3 with prominent terminal claw and 7–11 strong spines on medial margin, exopod extends to mid merus; dactylus of pereiopod 4 prominent terminal claw and 8–11 spines on medial margin, exopod extends to mid merus; dactylus of pereiopod 5 with prominent terminal claw and very regular comb-like row of 81–94 small spines on medial margin, exopod extends to basal third of merus.

Carapace length 5.7 (4.5–6.6) mm.

Rostrum long 6.82 (4.55–6.82) mm, extending beyond the antennular peduncle and scaphocerite (fig. 18a), rostral length longer than carapace 1.2 (0.83–1.26) times length of carapace, shape long and slender with dorsal edge curved upwards, pointed, rostrum 8.52 (5.53–9.57) longer than rostral width; dorsally armed with 33 (20–34) teeth, ratio of number of dorsal spines to length is 4.84 (3.68–6.15), 2 (1–4) postorbital eye spines (fig. 18a); ventrally with 6 (4–14) large spines over a length of 1.88 (1.30–2.80) mm, with 1–2 spines posterior to greatest width (fig. 18a), distal half of ventral edge straight; ratio of ventral spine row length to rostral length is 0.28 (0.23–0.46) and 4.57 (2.43–5.80) times more dorsal spines than ventral spines; rostral length 1.38 (1.04–1.77) times length of scaphocerite.

Antenna 1 (fig. 18b) peduncle short 3.05 (3.05–5.28) mm, not reaching distal tip of scaphocerite, length 0.62 (0.62–1.12) times as long as scaphocerite. Stylocerite 1.97 (1.60–2.64) mm long, length 0.35 (0.32–0.51) times carapace length, reaching beyond distal border of peduncle segment and middle to just beyond process on first segment (fig. 18b).

Antenna 2 (fig. 18c) second segment of peduncle 1.03 (1.03–1.80) mm, 0.21 (0.21–0.45) times length of scaphocerite, length 2.50 (2.35–3.75) times width. Scaphocerite 4.94 (3.10–5.20) mm long, 0.87 (0.69–0.96) times carapace length, 2.93 (2.93–3.85) times as long as wide,

Mouthparts. Left mandible (fig. 18d, e) with 4–5 teeth separated by slightly ridged shallow U-shaped notch from a short blunt/acute apical tooth; spine row immediately below incisor process of 7–9 rugose spines (lifting spines); spine row above molar process of approximately over 40 sparsely setose spines. Right mandible (fig. 18f, g) with 3–4 robust teeth in incisor process with 2 central teeth larger than apical and inner teeth; spine row immediately below teeth with 8–12 spines each finely setose basally; spine row above molar process. Molar process ridged.

Maxilla 1 as for *P. australiensis* (fig. 18h).

Maxilla 2 as for *P. australiensis* (fig. 18i).

Maxilliped 1 as for *P. australiensis* (fig. 18j).

Maxilliped 2 (fig. 18k) endopod 1.40 (0.87–1.40) mm long; exopod long and narrow, length 2.56 (1.73–2.87) mm, exopod 1.82 (1.63–2.96) times longer than endopod. Epipodite with long podobranch extending to basal third of third segment of endopodite.

Maxilliped 3 (fig. 19a) endopod length 7.0 (4.85–8.3) mm, 3.38 (2.32–3.38) times longer than exopod; with 3 distal segments of similar length; basal segment curved, apical segment with large terminal claw, inner margin with 9 (7–11) broad teeth-like spines, largest 2–4 in basal half, outer margin with 1 (1–3) long teeth-like spines near terminal spine and a single spine on outer margin; several transverse spine rows near base; mid and basal segments with several short simple setae. Exopod 2.07 (1.63–2.85) mm long, narrow, tip over-reaching distal end of basal endopod segment.

Thoracic appendages. Pereiopod 1 (fig. 19b) short, 5.85 (3.56–5.85 mm), 1.03 (0.73–1.03) times carapace length. Chelae short and broad (fig. 19b), 1.6 (1.09–1.67) mm long, 2.59 (2.48–3.84) times as long as wide, 2.0 (1.82–2.48) times longer than dactylus; palm length 1.55 (1.55–2.25) longer than palm width and 1.22 (0.82–1.22) times dactylus length. Carpus short, 2.88 (2.10–2.88) times longer than greatest width. Segment ratios 0.61 (0.55–0.68) : 1.22 (1.14–1.49) : 1.00 (1.08 [0.87–1.40] mm) : 1.60 (1.11–1.60) : 0.64 (0.30–0.64) : – (2.26–2.60). Exopod extending to base–apex of carpus.

Pereiopod 2 longer than pereiopod 1, 7.23 (5.41–7.83) mm long, 1.28 (1.11–1.47) times carapace length. Chelae long and slender (fig. 19c), 1.60 (1.20–1.80) mm long, half to two-thirds length of carpus, 3.47 (3.43–4.33) times as long as wide, palm length 2.04 (1.5–2.50) times palm width and 0.87 (0.86–1.29) times dactylus length. Propodus 1.48 (1.39–1.91) times longer than dactylus. Carpus 6.54–7.48 times as long as greatest width, slightly broader distally, distal margin with small excavation. Merus shorter than carpus, parallel–sided. Ischium about half as long as merus. Segment ratios 0.39 (0.29–0.43) : 0.58 (0.56–0.70) : 1.00 (1.80–2.83) mm : 0.77 (0.66–0.82) : 0.29 (0.36–0.56) : – (1.06–1.33). Exopod extending to mid of merus to base of carpus.

Pereiopod 3 (fig. 19d, e) distinctly longer than pereiopod 2 and more slender 10.11 (7.12–10.21) mm long, 1.78 (1.38–1.78) times carapace length. Dactylus with prominent terminal claw and 10 (7–11) strong spines on medial margin (fig. 19e). Propodus length 4.28 (3.82–4.69) times longer than dactylus, length, 19.52 (12.10–19.52) times longer than wide with 11(10–18) spines on inner margin. Merus with 1 strong spine on medial margin and 1 near ventral distal margin; segment ratios 0.42 (0.37–0.49) : 1.82 (1.61–1.88) : 1.00 (1.91 [1.27–2.0] mm) : 1.91 (1.74–2.23) : 0.64 (0.45–0.64) : – (1.54–1.75). Exopod extends to mid to apex of merus.

Pereiopod 4 (fig. 19f, g) similar length to pereiopod 3, – (6.67–9.63) mm long, – (1.45–1.62) times carapace length. Dactylus with prominent terminal claw and – (8–11) spines on medial margin (fig. 19g). Propodus – (3.58–5.00) times longer than dactylus; length – (12.37–16.00) times longer than wide, with – (11–16) spines on inner margin; merus with 1–2 strong spine on medial margin and 1 near ventral distal margin. Segment ratios – (0.22–0.52) : – (1.56–2.10) : 1.00 (– [1.17–1.92] mm): – (1.77–2.23) : – (0.49–0.71) : – (1.25–1.77). Exopod extends to mid merus.

Pereiopod 5 (fig. 20a, b) similar length to pereiopod 4, 9.16 (6.57–9.73) mm long, 1.62 (1.24–1.75) times carapace length. Dactylus with prominent terminal claw and very regular, comb–like row of numerous 72 (72–94) small spines on medial margin (fig. 20b). Propodus 4.09 (2.78–4.22) times longer than

dactylus, length 14.08 (10.42–18.93) times longer than wide with 14 (10–14) long medial teeth, 2 distally and external margin without teeth. Carpus without any large spines near distal margin. Merus with 1 strong medial spine and 1 distal spine; segment ratios 0.45 (0.45–0.71) : 1.85 (1.84–2.41) : 1.00 (1.88 [1.08–1.88] mm) : 1.64 (1.56–1.79) : – (0.52–0.89) : 1.25 (1.07–1.36). Exopod extends to basal to mid third of merus.

Abdomen. Pleopods peduncle of first pleopod short, 1.64 mm, 0.28 (0.30–0.38) times length of carapace, 1.82 (1.82–3.08) times width, exopod 1.83 (1.06–1.83) times peduncle length, endopod 0.97 (0.42–0.97) times peduncle length (fig. 20e); second pleopod peduncle short, – (0.33–0.58) times length of carapace, – (2.50–3.88) times width, exopod – (0.91–1.35) times peduncle length, endopod slightly shorter – (0.83–1.20) times peduncle length. Length of first peduncle – (1.07–1.74) times length of second peduncle.

Telson (fig. 20c, d) length 3.67 (3.20–4.40) mm, 0.65 (0.58–0.83) times carapace length, 3.00 (2.83–3.66) times longer than greatest width, tapering distally. Dorsal surface with 2 pairs of strong submarginal teeth-like spines. Posterior margin convex with 1 pair of teeth-like spines outermost, 4 (4–10) long strong setose spines (fig. 20d).

Uropods approximately equal to telson length.

Male smaller than females, carapace length 4.9–6.0 mm; endopod of first pleopod strongly excavated apically with 8–12 external spines and 11–15 long setae on inner margin (fig. 20f, g).

Etymology: Named in honour of the late Dr Mary E. White (AM), an Australian paleobotanist and whose environmental publications are inspirational and whose generosity to us while staying at The Falls Forest Retreat (New South Wales; type locality) will be remembered always.

Comments: P. whitemae may be confused by other widespread species and is found in the same areas as *P. australiensis, P. arrostra* and *P. tasmaniensis.* It can be distinguished from all other long rostrum species by the carpus of pereiopod 1 which is long with a short, robust chelae; the rostrum is concave with ventral rostral spines extending from posterior to the greatest width, extending over a length of 1.30–2.80 mm (Table 2).

Paratya whitemae is a widespread species in the coastal streams of Victoria, New South Wales and in south-eastern Queensland and in the Murray R in the Murray–Darling Basin (fig. 32b) and may co-exist with *P. australiensis, P. arrostra, P. williamsi, P. rouxi* and *P. tasmaniensis* at various locations throughout its range.

Paratya strathbogiensis n. sp.

Figures 21–23

http://zoobank.org/urn:lsid:zoobank.org:act:6B825EFF-D5BB-407E-9CA9-CAA2BB6F92A0

Lineage 7 (Cook et al., 2006)

Type Material: Holotype Victoria. King Parrot Ck at Flowerdale, –37.2953 S, 145.2905 E, 28 September 2011 (PS, JM, MC). Body in ethanol and antennae, mouthparts, pereiopods and abdominal structures dissected, mounted on 2 slides. Accession Ref. MC49. Museum of Victoria Ref No NMV J75163. Genbank Registration OL420843.

Paratypes: Victoria. 1 male and 3 females, King Parrot Ck at Flowerdale, –37.2953 S, 145.2905 E, 28 September 2011 Accession Ref. MC40, 43, 46, 47 (PS, JM, MC) NMV J75164–J75167, Genbank Registration OL420836, OL420839, OL420846, OL420847; 2 males King Parrot Ck above Goulburn R confluence, –37.0075 S, 145.3212 E, 28 September 2011 Accession Ref. MC53–54 (PS, JM, MC) NMV J75168–J75169, Genbank Registration OL420845–OL420846; bodies in ethanol and other structures dissected, mounted on 2 slides each.

Material Examined: Victoria: King Parrot Ck at Flowerdale, –37.2953 S, 145.2905 E, 28 September 2011 (PS, JM, MC); King Parrot Ck above Goulburn R confluence, –37.0075 S, 145.3212 E, 28 September 2011 (PS, JM, MC).

Diagnosis: P. strathbogiensis differs from all other species by the following combination of characters: rostrum long, extending beyond both antennular peduncle and scaphocerite, dorsal edge straight, dorsally armed with 21–24 teeth, 1–2 postorbital spines, ventrally with 4–6 large serrations over a length of 1.30–1.80 mm, all forward of greatest depth; distal half of ventral edge straight; left mandible with 4 large teeth separated by a ridged straight ridged notch from a blunt apical tooth; right mandible with 4 teeth in 2 separate incisor processes with first, third and fourth teeth large; scaphognathite of maxilla 2 truncated apically and square at distal margin not extending to apex of upper endite; exopod of maxilliped 2 1.88–2.34 times longer than endopod, epipodite with long podobranchs extending to basal third of third segment of endopodite; maxilliped 3 with medial distal margin of apical segment of endopod with 8–9 broad teeth-like spines, outer margin with 2 broad teeth-like spines, exopod long and narrow, tip over-reaching distal end of basal endopod segment; pereiopod 1 with short carpus, chelae short–long and broad, exopod extending to base-mid carpus; pereiopod 2 with exopod extending to mid merus; dactylus of pereiopod 3 with prominent terminal claw and 8–13 strong spines on medial margin, exopod extends to mid merus; dactylus of pereiopod 4 prominent terminal claw and 9–12 spines on medial margin, exopod extends to apical third of merus; dactylus of pereiopod 5 with prominent terminal claw and very regular comb–like row of 64–80 small spines on medial margin, exopod extends to mid merus.

Carapace length 6.3 (5.6–6.5) mm.

Rostrum long 5.90 (5.30–6.00) mm, extending beyond the antennular peduncle and scaphocerite (fig. 21a), rostral length is 0.94 (0.82–1.00) times length of carapace, shape long and slender with straight dorsal edge, pointed (fig. 21a); rostrum 8.43 (7.50–9.33) times longer than wide; dorsally armed with 21 (21–24) spines, ratio of number of dorsal spines to length is 3.56 (3.56–4.29) with 2 (1–2) postorbital eye spines; ventrally with 6 (4–6) large serrations over a length of 1.80 (1.30–1.80) mm, all spines anterior of greatest width; distal half of ventral edge straight, ratio of ventral spine length to rostral length is 0.31 (0.23–0.31), with 3.50 (3.50–6.00) more dorsal spines than ventral spines; rostral length 1.48 (1.19–1.51) times length of scaphocerite.

Antenna 1 (fig. 21b) peduncle 4.48 (3.80–4.68) mm long, not reaching distal tip of scaphocerite, length 1.12 (0.83–1.12) times scaphocerite length. Stylocerite 2.20 (2.04–2.24) mm long, length 9.17 (6.88–9.33) times longer than width, 0.35 (0.33–0.36) times carapace length, reaching beyond distal border of peduncle segment extending to middle of process on distal angle of first segment (fig. 21b).

Figure 21. *Paratya strathbogiensis* sp. nov.: a, head region and rostrum; b, antenna 1 peduncle and stylocerite; c, scaphocerite; d, left mandible; e, enlarged incisors; f, right mandible; g, enlarged incisors; h, maxilla 1; i, maxilla 2; j, maxilliped 1; k, maxilliped 2. Scale lines 0.2 mm.
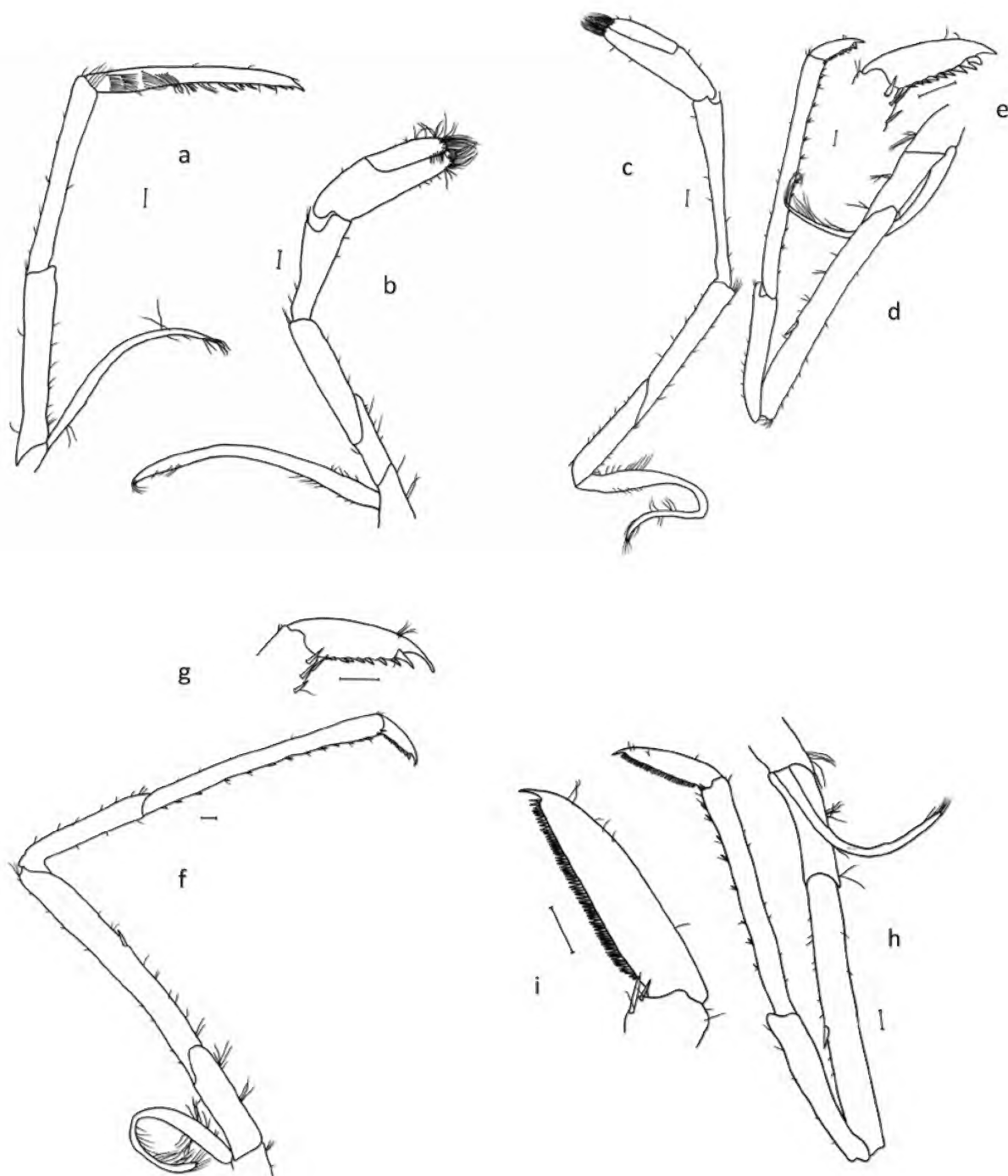
Figure 22. *Paratya strathbogiensis* sp. nov.: a, maxilliped 3; b, pereiopod 1; c, pereiopod 2; d, pereiopod 3; e, dactylus 3; f, pereiopod 4; g, dactylus 4; h, pereiopod 5; i, dactylus 5. Scale lines 0.2 mm.
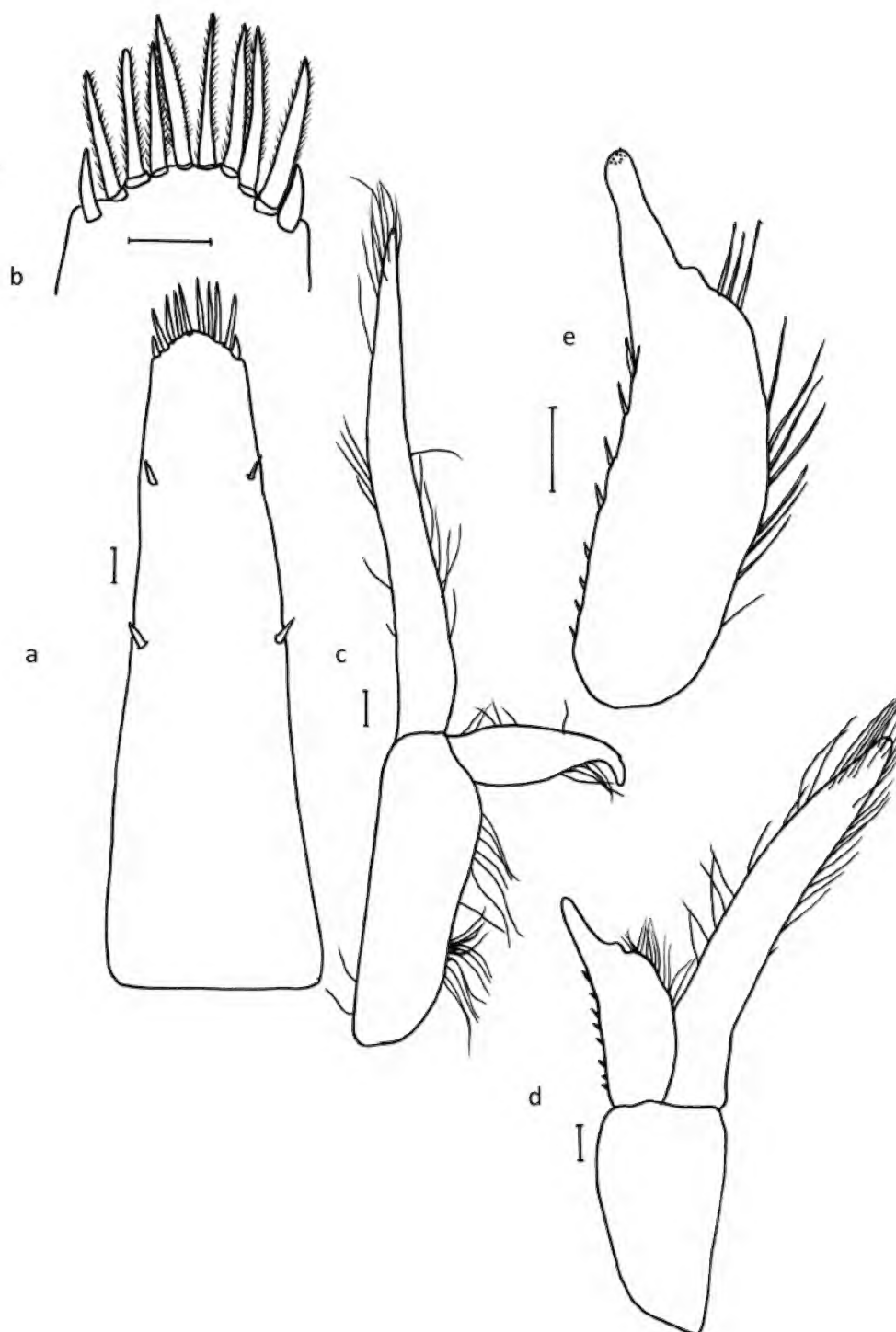
Figure 23. *Paratya strathbogiensis* sp. nov.: a, telson; b, telson terminal spines; c, pleopod 1 of female; d, pleopod 1 of male; e, endopod 1 of male. Scale lines 0.2 mm.

Antenna 2 (fig. 21c) second segment of peduncle 1.40 (1.20–1.52) mm long, 0.35 (0.25–0.38) times length of scaphocerite, 2.92 (2.53–3.18) times longer than wide. Scaphocerite 4.00 (3.70–4.80) mm long, 0.63 (0.63–0.75) times carapace length, 2.67 (2.47–2.87) times as long as wide.

Mouthpart. Left mandible (fig. 21d, e) with 4 large teeth separated from a blunt apical tooth by a ridged almost straight notch. Spine row with 7 spines, each finely setose, spine row above molar process of approximately over 40 sparsely setose spines. Right mandible (fig. 21f, g) with 4 large teeth in 2 separate incisor processes consisting of one large apical tooth and 1 small tooth and two larger separated inner teeth, Apical, third and fourth teeth large. Spine row immediately below teeth with 10 spines each finely setose, spine row above molar process. Molar process ridged.

Maxilla 1 (fig. 21h) as for *P. australiensis*.

Maxilla 2 (fig. 21i) scaphognathite truncated apically and squared off at distal margin, not extending to apex of upper endite (fig. 21i).

Maxilliped 1 (fig. 21j) as for *P. australiensis*.

Maxilliped 2 (fig. 21k) endopod length 1.09 (1.01–1.16) mm; exopod long and narrow, length 2.13 (2.00–2.40) mm, 1.95 (1.88–2.34) times longer than endopod. Epipodite with long podobranch extending to basal third of third segment of endopodite.

Maxilliped 3 (fig. 22a) endopod length 6.67 (6.35–7.36) mm, 2.77 (2.52–2.80) times longer than exopod; with 3 distal segments of similar length; basal segment curved; apical segment with large terminal claw, medial distal margin with 7 (7–9) broad teeth-like spines, largest 3 in basal half, outer margin with 1 long tooth-like spine near terminal spine and 1 long spine in proximal third. Exopod 2.40 (2.27–2.67) mm long, narrow, tip over-reaching distal end of basal endopod segment (fig. 22a).

Thoracic appendages. Pereiopod 1 (fig. 22b) short, 5.09 (3.09–5.44) mm long, 0.81 (0.48–0.84) times carapace length. Chelae short to long and broad (fig. 22b), 1.60 (1.48–1.83) mm long, propodus 3.00 (2.86–3.26) times as long as wide, 1.76 (1.76–2.36) times longer than dactylus, 1.19–1.31 times longer than carpus; palm length 2.08 (1.42–2.14) times palm width and 1.59 (1.27–1.69) times dactylus length. Carpus short, 2.88 (2.30–3.21) times longer than greatest width, broadening distally. Segment ratios 0.74 (0.54–0.74) : 1.31 (1.19–1.31) : 1.00 (1.22 [1.13–1.47] mm) : 1.41 (1.04–1.41) : 0.43 (0.42–0.52) : 2.28 (2.00–2.28). Exopod extending to base–mid carpus.

Pereiopod 2 (fig. 22c) longer than pereiopod 1, 7.17 (6.85–7.89) mm long, 1.14 (1.11–1.22) times carapace length. Chelae long and slender (fig. 22c), 1.63 (1.47–1.76) mm long, 3.59 (3.57–4.06) times as long as wide, palm length 2.09 (2.00–2.22) times longer than palm width, 1.15 (0.91–1.15) times length of dactylus. Propodus 1.74 (1.67–1.81) times longer than dactylus. Carpus 6.28 (6.28–8.00) times as long as greatest width, slightly broader distally, distal margin with small excavation. Segment ratios 0.38 (0.35–0.42) : 0.67 (0.61–0.72) : 1.00 (2.42 [2.37–2.67] mm) : 0.84 (0.80–0.85) : 0.44 (0.35–0.59) : – (1.08). Exopod extending to mid merus (fig. 22c).

Pereiopod 3 (fig. 22d, e) distinctly longer than pereiopod 2 and more slender 8.67 (8.47–9.40) mm long, 1.38 (1.35–1.51) times carapace length. Dactylus with prominent terminal claw

and 13 (8–13) strong spines on medial margin (fig. 22e). Propodus 4.60 (4.50–4.93) times longer than dactylus, length 14.38 (12.77–14.86) times longer than wide with 14 (8–14) spines on inner margin. Merus with 1 strong spine on medial margin and 1 near ventral distal margin. Segment ratios 0.38 (0.35–0.39) : 1.77 (1.63–1.89) : 1.00 (1.73 [1.57–1.88] mm) : 1.69 (1.69–2.03) : 0.54 (0.50–0.55) : 1.46 (1.43–1.46). Exopod extends to mid merus.

Pereiopod 4 (fig. 22f, g) similar to pereiopod 3, 9.12 (8.89–9.36) mm long, 1.45 (1.37–1.45) times carapace length. Dactylus with prominent terminal claw and 12 (9–12) spines on medial margin (fig. 22f, g). Propodus 3.78 (3.78–4.04) times longer than dactylus, length 11.94 (11.89–14.37) times longer than wide, with 16 spines on medial margin; merus with 1 strong spine on medial margin and 1 near ventral distal margin. Segment ratios 0.44 (0.41–0.44) : 1.68 (1.66–1.69) : 1.00 (1.80 [1.80–1.81] mm) : 1.96 (1.73–1.96) : 0.42 (0.42–0.52) : – (1.62). Exopod extends to mid-apex of merus.

Pereiopod 5 (fig. 22h, i) similar length to pereiopod 4, 9.00 (7.80–9.00) mm long, 1.43 (1.20–1.43) times carapace length. Dactylus with prominent terminal claw and very regular, comb–like row of numerous 64 (64–80) small spines on medial margin (fig. 22i). Propodus 3.11 (3.04–3.51) times longer than dactylus, length 12.00 (11.86–14.47) times longer than wide with 11 (10–11) long medial teeth and external margin without teeth. Carpus without any large spines near distal margin. Merus with 1 strong medial spine and 1 distal spine. Segment ratios 0.58 (0.49–0.63) : 1.82 (1.72–2.05) : 1.00 (1.76 [1.60–1.82] mm) : 1.69 (1.53–1.78) : 0.61 (0.54–0.61) : 1.06 (1.06–1.50). Exopod extends to mid merus.

Abdomen. Pleopods peduncle of first pleopod short, 0.29 (0.13–0.32) times length of carapace, 2.64 (1.21–3.00) times width, exopod 1.41 (1.31–3.35) times peduncle length, endopod 0.78 (0.44–0.78) times peduncle length (fig. 23c); second pleopod peduncle short, 0.37 (0.34–0.38) times length of carapace, 2.94 (2.50–2.94) times width, exopod 1.11 (1.11–1.51) times peduncle length, endopod slightly shorter 1.06 (1.06–1.33) times peduncle length. Length of first peduncle 1.27 (1.11–2.53) times length of second peduncle.

Telson (fig. 23a, b) length 3.80 (3.30–4.20) mm, 0.60 (0.57–0.66) times carapace length, 3.17 (2.80–3.17) times longer than greatest width, tapering distally. Dorsal surface with 2 pairs of strong submarginal teeth-like spines. Posterior margin convex with 1 pair of teeth-like spines outermost, 10 (8–12) long, strong setose spines (fig. 23b).

Uropods slightly longer than telson length.

Male smaller than females, carapace length 4.42 mm; endopod of first pleopod curved, not strongly excavated with 10 external spines and 16 spines on inner margin (fig. 23d, e).

Etymology: After the Strathbogie Range area in Victoria, where this species occurs and was first recognised as a distinct lineage by Cook (2006).

Comments: P. strathbogiensis shares the characteristics of a long straight rostrum extending beyond the scaphocerite with *P. spinosa*, *P. whitemae* and *P. tasmaniensis*. It differs from all other species by having a long slender palm of the chelae of pereiopod 2 (>2.00 times width); rostrum with 21–24 dorsal

spines of which 1–2 are postorbital spines and 4–6 ventral spines over a length of 1.30–1.80 mm; stylocerite extends to the middle of the process on the apex of the antenular segment 1; scaphognathite of maxilla 2 truncated (Table 2).

P. strathbogiensis is restricted to the upper Goulburn R in the Strathbogie Ranges central Victoria and overlaps with *P. tasmaniensis* (Cook, 2006) and *P. arrostra*.

Paratya tasmaniensis Riek, 1953

Figures 24–26

> *Paratya tasmaniensis* Riek, 1953 (fig. 24a); type examined by MC.
> *Paratya australiensis* Williams and Smith, 1979
> Lineage 8 (Cook et al., 2006)
> Lineage B (McClusky, 2007)
> Type Locality: Small stream at Kingston, Tasmania, just above the tidal zone, 10 January 1947 (Browns R).

Material Examined: Tasmania: Coal R near Campania, –42.6887 S, 147.4359 E, 11 July 2011 (PS); George R on Billabong Bay Rd near St Helens, –41.3137 S, 148.2656 E, 9 July 2011 (PS); Elizabeth R at Campbelltown, –41.9332 S, 147.4934 E, 13 July 2011 (PS); Browns R at Kingston, –42.9659 S, 147.3117 E, 12 July 2011 (PS); Swamp off Five Mile Rd, Flinders Island, 39.9053 S, 147.9746 E, 1 November 1973 (TW, PSL, BK).

Victoria: Wimmera R downstream of Dimboola Weir, –36.4557 S, 142.0167 E, 6 March 2012 (Vic EPA); Glenelg R at Ford Reserve, –37.2472 S, 141.8458 S, 11 July 2017 (BM); Hamilton Lake boat ramp, –37.7327 S, 142.0399 E, 2 February 2018 (PS); Glenelg R, –37.9289 S, 141.2782 E, 1 November 2017 (AC); Glenelg R near Kanagulk, –37.1497 S, 141.8637 E, 1 November 2017 (AC).

New South Wales Stream on Gerrigong Ck Rd, Upper Kangaroo Valley, –34.6870 S, 150.6000 E, 27 September 2017 (PS, JM, JH); Kangaroo R, Hampden Bridge, –34.7272 S, 150.5218 E, 27 September 2017 (PS, JM, JH); Maguire Ck, –28.0837 S, 153.3364 E 26 May 2015 (BM); Hastings R off Oxley Highway, –31.4647 S, 152.6278 E, 1 November 2011 (PS, JM, MC).

South Australia. Brenda Park wetland south of Morgan, –34.0818 S, 139.6743 E, 8 November 2011 (CM).

Diagnosis: P. tasmaniensis differs from all other species by the following combination of characters: rostrum long, extending beyond both antennular peduncle and scaphocerite, dorsal edge straight or very fine curve, dorsally armed with 22–29 spines, 2–4 postorbital spines, ventrally with 4–13 large serrations over a length of 2.10–3.40 mm, all forward of greatest depth; distal half of ventral edge straight; left mandible with 4 teeth separated by smooth notch then 4 short ridges at base of a less distinct apical tooth; right mandible with 4 teeth in a single incisor process with large third tooth; scaphognathite of maxilla 2 truncated and square apically extending to two-thirds length of upper endite; maxilliped 1 with exopod flagellum distinct, well developed and with numerous long setose spines on all margins, over half length of caridean lobe; exopod of maxilliped 2 1.57–2.50 times longer than endopod, epipodite with long podobranchs extending just to base of third segment of endopodite; maxilliped 3 with medial distal margin of apical segment of endopod with 8–11 broad teeth-like spines, outer margin with 3–9 teeth-like spines, exopod long and narrow, tip over-reaching distal end of basal endopod segment; Pereiopod 1 with short and broad to long and slender chelae, carpus short to long and exopod

extending to mid-apex of carpus; pereiopod 2 with exopod extending to mid merus; dactylus of pereiopod 3 with prominent terminal claw and 9–11 strong spines on medial margin, exopod extends to mid merus; dactylus of pereiopod 4 prominent terminal claw and 8–12 spines on medial margin, exopod extends to mid merus; dactylus of pereiopod 5 with prominent terminal claw and very regular comb-like row of 70–85 small spines on medial margin, exopod extends to basal to mid merus.

Carapace length 5.40–7.50 mm.

Rostrum long 5.65–7.10 mm, extending beyond the antennular peduncle and well beyond the scaphocerite (fig. 24a), rostral length 0.88–1.26 times carapace length, shape long and slender, usually straight, pointed; rostral length 6.90–8.50 times greater than width; dorsally armed with 22–29 teeth, ratio of dorsal spines to length is 3.33–4.60, 2–4 postorbital spines (fig. 24a); ventrally with 4–13 large spines over a length of 2.10–3.40 mm, at to anterior to point of greatest width (fig. 24a), distal half of ventral edge straight, ratio of ventral spine length to rostral length is 0.33–0.48 with 2.00–6.50 more dorsal spines than ventral spines; rostral length 1.15–1.69 times length of scaphocerite.

Antenna 1 (fig. 24b) peduncle short 4.04–5.52 mm long, not reaching distal tip of scaphocerite, 0.78–1.31 times scaphocerite length. Stylocerite 2.20–2.84 mm long, length 6.88–12.00 longer than wide, 0.33–0.41 times carapace length, reaching beyond distal border of peduncle segment extending almost to apex or just beyond distal angle process (fig. 24b).

Antenna 2 (fig. 24c) second segment 1.20–1.68 mm long, length 1.88–2.83 times width and 0.23–0.37 times length of scaphocerite. Scaphocerite 4.0–5.4 mm long, 2.86–4.33 times as long as wide and 0.56–0.85 times carapace length.

Mouthparts. Left mandible (fig. 24d, e) with a blunt apical tooth and 4 short ridges at its base, separated from incisors by part smooth and part ridged U-shaped notch. Incisors with 2 large teeth and 2 slightly smaller robust teeth at base. Spine row with 10 spines, each finely setose. Right mandible (fig. 24f, g) with incisors with 4 large teeth in a single incisor process, with third tooth larger than other 3. Spine row immediately below teeth with 9 spines each finely setose, spine row above molar process. Molar process ridged.

Maxilla 1 (fig. 24h) as for *P. australiensis*.

Maxilla 2 (fig. 24i) scaphognathite truncated and square apically extending to approximately two-thirds length of upper endite.

Maxilliped 1 (fig. 24j) as for *P. australiensis*.

Maxilliped 2 (fig. 24k) endopod 0.97–1.17 mm long, exopod long and narrow, length 1.55–2.93 mm, exopod 1.57–2.50 longer than endopod. Epipodite with long podobranch extending to basal third of third segment of endopodite.

Maxilliped 3 (fig. 25a) endopod 5.41–8.32 mm long, 2.34–3.12 times longer than exopod; with 3 distal segments of similar length; basal segment curved, apical segment with large terminal claw, medial distal margin with 8–11 broad teeth-like spines, largest 1–2 in basal half, outer margin with 1–2 long teeth-like spines; middle segment with 2–3 medial spines and 0–4 spines on outer margin. Exopod long and narrow 2.67–3.33 mm, 0.32–0.43 times length of endopod, extends to base of mid segment.

Figure 24. *Paratya tasmaniensis* Riek: a, head region and rostrum; b, antenna 1 peduncle and stylocerite; c, scaphocerite; d, left mandible; e, enlarged incisors; f, right mandible; g, enlarged incisors; h, maxilla 1; i, maxilla 2; j, maxilliped 1; k, maxilliped 2. Scale lines 0.2 mm.
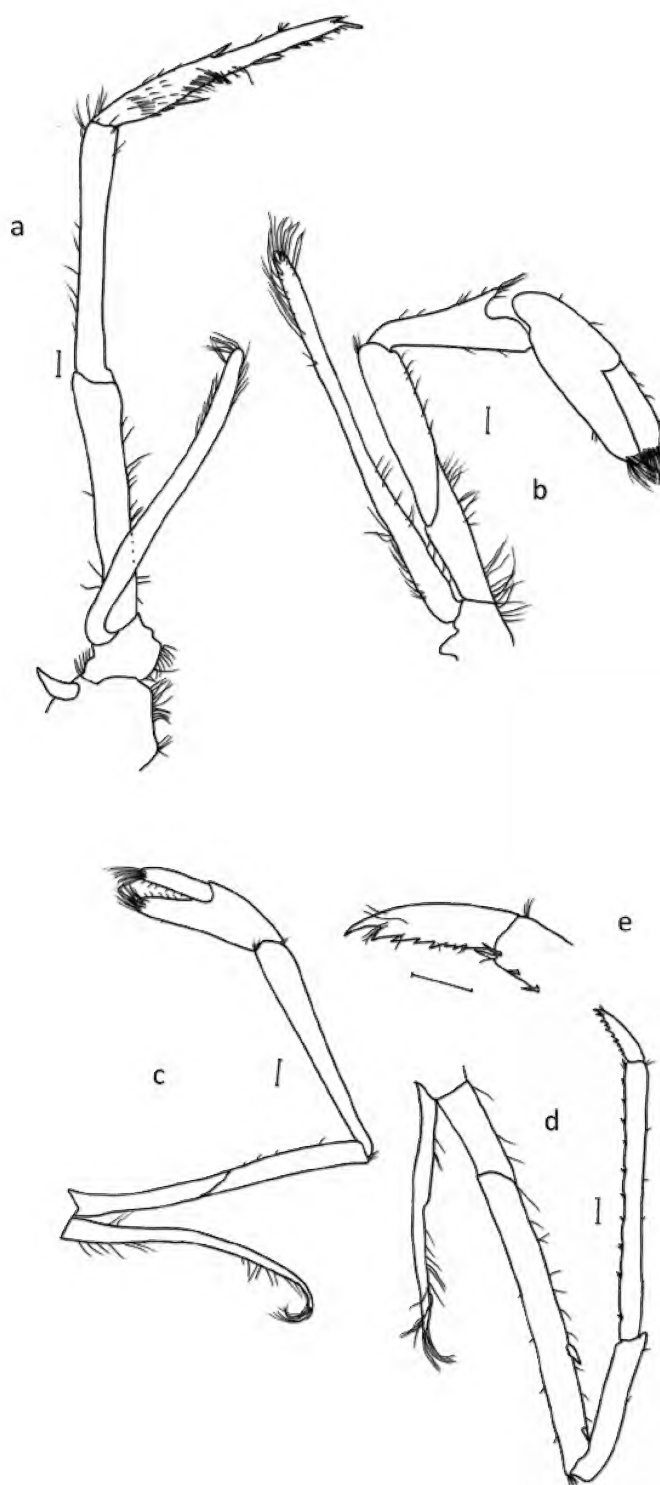
Figure 25. *Paratya tasmaniensis* Riek: a, maxilliped 3; b, pereiopod 1; c, pereiopod 2; d, pereiopod 3; e, dactylus. Scale lines 0.2 mm.
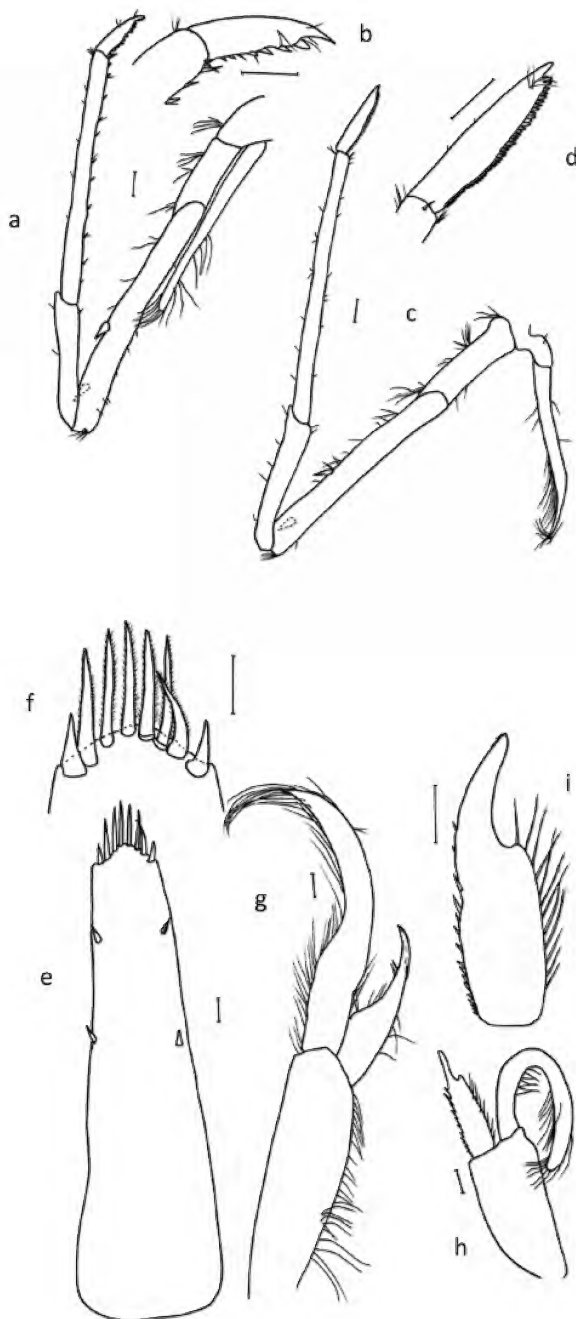
Thoracic appendages. Pereiopod 1 (fig. 25b) short, 4.87–5.68 mm long, 0.74–0.84 times carapace length. Chelae short and broad to long and slender (fig. 25b), 1.49–1.87 mm long, 2.95–3.43 times as long as wide, 1.75–2.22 times longer than dactylus, 1.25–1.41 times longer than carpus; palm length 1.60–1.83 longer than palm width, 1.33–1.67 times dactylus length. Carpus short to long, 2.00–2.87 times as long as greatest width, broadening distally, distal margin excavate. Segment ratios 0.45–0.78 : 1.25–1.41 : 1.00 (1.00–2.67) mm : 1.17–1.80 : 0.44–0.53 : 2.51–2.68. Exopod extending to mid-apex of carpus.

Pereiopod 2 (fig. 25c) longer than pereiopod 1, 6.76–8.17 mm long, 0.91–1.29 times carapace length. Chelae long and slender (fig. 25c), 1.47–1.81 mm long, 3.06–3.93 times as long as wide, half to two-thirds length of carpus; palm length 1.80–3.35 longer than palm width, 0.80–1.35 times length of dactylus. Propodus 1.57–2.06 times dactylus length. Carpus long 5.79–7.22 times as long as greatest width, slightly broader distally. Segment ratios 0.31–0.40 : 0.59–0.71 : 1.00 (2.16–2.81) mm : 0.75–1.15 : 0.34–0.50 : 0.90–1.38. Exopod extending to mid merus.

Pereiopod 3 (fig. 25d, e) distinctly longer than pereiopod 2 and more slender, length 8.43–10.05 mm, 1.32–1.71 times carapace length. Dactylus with prominent terminal claw and 9–11 strong spines on medial margin (fig. 25e). Propodus 3.87–4.81 times longer than dactylus, length 11.36–14.17 times longer than wide with 11–18 spines on inner margin and 3 transverse spines apically. Merus with 1 strong spine on medial margin and 1 near ventral distal margin. Segment ratios 0.34–0.46 : 1.48–1.77 : 1.00 (1.66–2.03) mm : 1.63–2.06 : 0.44–0.63 : 1.40–1.76. Exopod extends to mid merus.

Pereiopod 4 (fig. 26a, b) similar to pereiopod 3, 8.63–10.47 mm long, 1.29–1.76 times carapace length. Dactylus with prominent terminal claw and 8–12 spines on medial margin (fig. 26b). Propodus 3.78–4.80 times longer than dactylus, length 8.06–15.54 times longer than wide, with 14–19 spines on medial margin, none on outer margin; merus with 1–2 strong spines on medial margin and 1 near ventral distal margin. Segment ratios 0.32–0.43 : 1.52–1.77 : 1.00 (1.66–2.13) mm : 1.73–2.08 : 0.41–0.66 : 1.55. Exopod extends to mid merus.

Pereiopod 5 (fig. 26c, d) similar length to pereiopod 4, 8.31–10.03 mm long, 1.15–1.68 times carapace length. Dactylus with prominent terminal claw and very regular, comb-like row of numerous (70–85) small spines on medial margin (fig. 26d). Propodus 3.21–4.54 times longer than dactylus, length 11.80–14.71 times longer than wide with 8–14 long medial teeth and external margin without teeth. Carpus without any large spines near distal margin. Merus 1 strong spine on medial margin and 1 near ventral distal margin. Segment ratios 0.41–0.61 : 1.85–2.02 : 1.00 (1.59–1.93) mm : 1.45–1.76 : 0.53–0.70 : 0.99–1.52. Exopod extends to basal to mid third of merus.

Abdomen. Pleopods peduncle of first pleopod short, 0.27–0.37 times length of carapace, 2.00–3.93 times width, exopod 1.11–1.78 times peduncle length, endopod 0.55–0.88 times peduncle length (fig. 26g); second pleopod peduncle short, 0.34–0.42 times length of carapace, 2.25–2.94 times width, exopod 1.11–1.63 times peduncle length, endopod slightly shorter 0.91–1.50 times peduncle length. Length of first peduncle 0.96–1.34 times length of second peduncle.

Figure 26. *Paratya tasmaniensis* Riek: a, pereiopod 4; b, dactylus 4; c, pereiopod 5; d, dactylus 5; e, telson; f, telson terminal spines; g, pleopod 1 of female; h, pleopod 1 of male; i, endopod 1 of male. Scale lines 0.2 mm.

Telson (fig. 26e, f) length 3.80–4.70 mm, 0.59–0.70 times carapace length and tapering distally, 2.83–3.79 times as long as greatest width. Dorsal surface with 2 pairs of strong submarginal teeth-like spines. Posterior margin convex with 1 pair of teeth-like spines outermost, 6–12 long strong setose spines (fig. 26f).

Uropods approximately equal to telson length.

Males endopod of first pleopod excavated apically with 10–14 short spines on external margin and 16–18 long spines on inner margin (fig. 26h, i).

Comments: P. tasmaniensis was described by Riek (1953) from Browns R at Kingston, Tasmania. It is the only species in Tasmania with a wide distribution on the eastern, southern and northern streams, also on the northern west coast streams and on Flinders Island. It does not occur in lakes of the central plateau, except at Lakes Crescent and Sorrell at an altitude of 800 m (McClusky, 2007). *P. tasmaniensis* also occurs on the mainland coastal and inland streams in South Australia, Victoria and New South Wales (fig. 32c). It shares the characteristics of a long straight rostrum extending beyond the scaphocerite with *P. spinosa* and *P. strathbogiensis* and the distinguishing characters are given in Table 2.

Walker (1973), in his study of Tasmanian *Paratya*, described the morphological characteristics of *P. tasmaniensis* (not including mouthparts) and described the life history from the Coal R and a small wetland at Pawleena.

Paratya rouxi n. sp.

Figures 27–29

http://zoobank.org/urn:lsid:zoobank.org:act:8319F351-EA76-4AF9-9C63-63F0CEB5E292

P. australiensis Roux
Lineage 9 (Cook et al., 2006)

Type Material: Holotype New South Wales. Wakool Reserve, –35.496 S, 144.454 E, June 2011 (JC). Body in ethanol and antennae, mouthparts, pereiopods and abdominal structures dissected, mounted on 2 slides. AM Ref No. P.105605, Accession Ref. MC83, Genbank Registration OL420861.

Paratypes: New South Wales. Wakool Reserve, –35.4963 S, 144.4541 E, June 2011 Accession Ref. MC672 Genbank Registration OL420849, PS1–PS2 (JC), Bodies in ethanol and other structures dissected, mounted on 2 slides each.

Material Examined: As for type material.

Diagnosis: P. rouxi differs from all other species by the following combination of characters: rostrum very short, extending just beyond the first segment of the antennular peduncle, rostrum short and broad with a downward curve, dorsally armed with 11–19 spines, 0 postorbital spines, ventrally with 1–2 spines over a length of less than 0.4 mm, all forward of greatest depth; distal half of ventral edge straight, rostral length 0.57–0.73 times length of scaphocerite; left mandible with 4 teeth in two groups separated by smooth U-shaped notch from a distinct apical tooth; right mandible with 4 teeth in two separate incisor processes; scaphognathite of maxilla 2 truncated apically with an inner lobe almost extending to apex of upper endite; maxilliped 1 with exopod flagellum distinct, well developed and with numerous

long setose spines on all margins, over half length of caridean lobe; exopod of maxilliped 2 1.9–2.7 times longer than endopod, epipodite with long podobranchs extending to basal third of third segment of endopodite; maxilliped 3 with medial distal margin of apical segment of endopod with 7–10 broad teeth-like spines, outer margin with 2 long teeth-like spines near terminal spine and 1 mid outer spine, exopod long and narrow, tip over-reaching distal end of basal endopod segment; pereiopod 1 with long carpus and long slender chelae; pereiopod 2 with exopod extending to mid merus; dactylus of pereiopod 3 with prominent terminal claw and 10–12 strong spines on medial margin, exopod extends to mid merus; dactylus of pereiopod 4 prominent terminal claw and 8–12 spines on medial margin, exopod extends to apical third of merus; dactylus of pereiopod 5 with prominent terminal claw and very regular comb–like row of 70–80 small spines on medial margin, exopod extends to mid merus.

Carapace length 4.90 (4.90–5.30) mm.

Rostrum very short (fig. 27a), 2.70 (2.10–2.75) mm long, extending just beyond the first segment of the antennular peduncle, 0.55 (0.49–0.55) times length of carapace, shape convex, short and broad with downward curve, pointed; rostrum 6.75 (5.00–6.75) longer than wide; dorsally armed with 19 (11–19) spines (fig. 27a), ratio of dorsal spine number to length is 7.04 (4.61–7.04) without postorbital eye spines; ventrally with 1 (1–2) spines over a length of 0.10 (0.10–0.40) mm, all anterior to greatest width; distal half of ventral edge straight, ratio of ventral spines length to rostral length is 0.03 (0.04–0.15) and 19.00 (6.00–19.00) more dorsal spines than ventral spines; rostral length 0.73 (0.57–0.73) times length of scaphocerite.

Antenna 1 (fig. 27b) peduncle short, 3.24 (3.24–3.64) mm long, not reaching distal tip of scaphocerite, 0.88 (0.88–0.98) times scaphocerite length. Stylocerite 1.80 (1.80–2.03) mm long, length 11.25 (9.00–11.25) longer than wide, 0.37 (0.34–0.38) times carapace length, just reaching beyond distal border of peduncle segment and to base of distal angle process (fig. 24c).

Antenna 2 (fig. 27c) second segment 1.16 (1.00–1.30) mm long, 0.31 (0.27–0.34) times length of scaphocerite and 2.42 (2.42–2.50) times width. Scaphocerite 3.70 (3.65–3.80) mm long, 0.76 (0.70–0.76) times carapace length and 3.36 (2.71–3.36) times as long as wide.

Mouthparts. Left mandible (fig. 27d, e) with incisors of 4 teeth (2 large teeth and 2 robust teeth (one small and one large) at base), separated from a large acute apical tooth by a smooth U-shaped notch. Spine row with 9 spines, each finely setose, spine row above molar process of approximately over 40 sparsely setose spines. Right mandible (fig. 27f, g) with 4 teeth in 2 separate incisor processes with apical and second teeth large. Spine row immediately below teeth with 12 spines each finely setose, spine row above molar process. Molar process ridged.

Maxilla 1 (fig. 27h) as for *P. australiensis*.

Maxilla 2 (fig. 27i) scaphognathite apex truncated with an inner lobe, almost extending to apex of endite.

Maxilliped 1 (fig. 27j) as for *P. australiensis*.

Maxilliped 2 (fig. 27k) endopod 0.80 (0.76–0.84) mm long; exopod length 2.07 (1.60–2.07) mm, long and narrow, exopod 2.58 (1.90–2.71) longer than endopod. Epipodite with long podobranch extending to basal third of third segment of endopodite.
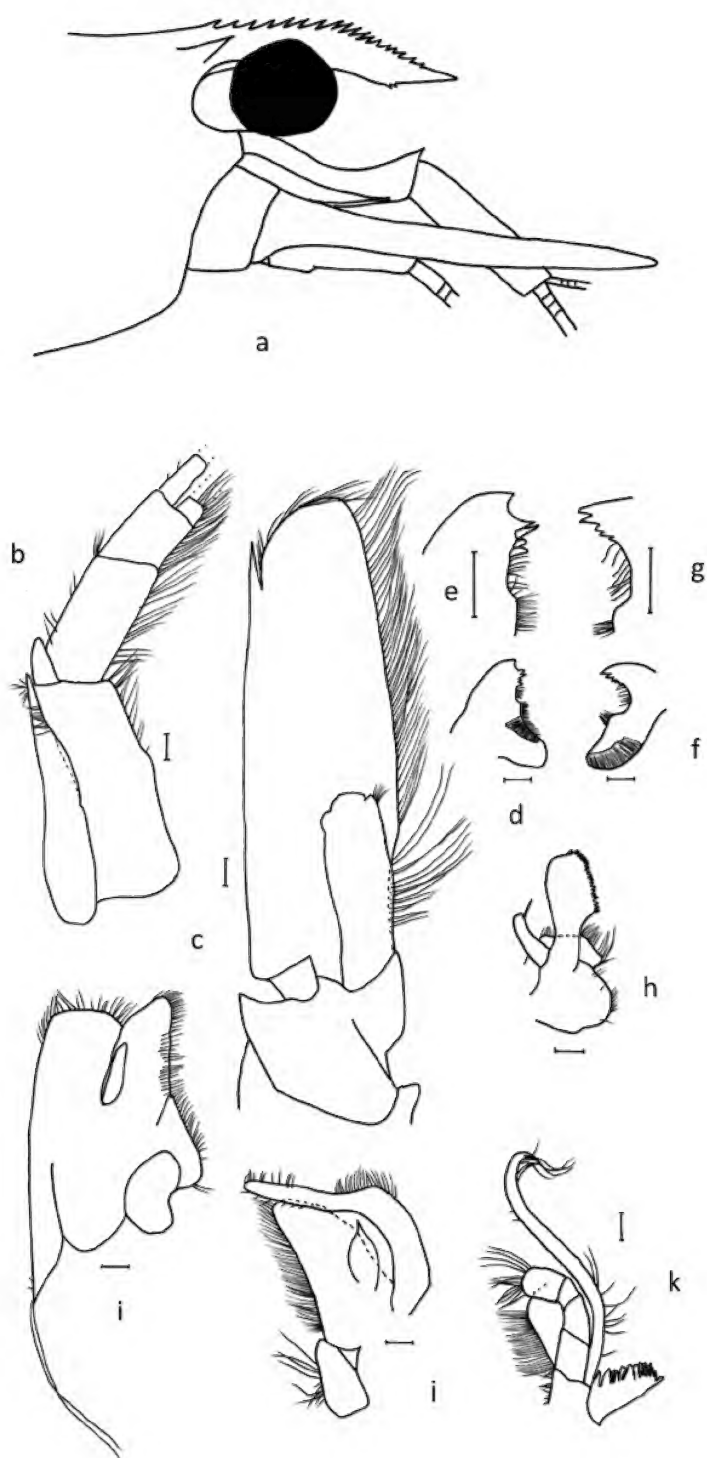
Figure 27. *Paratya rouxi* sp. nov.: a, head region and rostrum; b, antenna 1 peduncleand stylocerite; c, scaphocerite; d, left mandible; e, enlarged incisors; f, right mandible; g, enlarged incisors; h, maxilla 1; i, maxilla 2; j, maxilliped 1; k, maxilliped 2. Scale lines 0.2 mm.
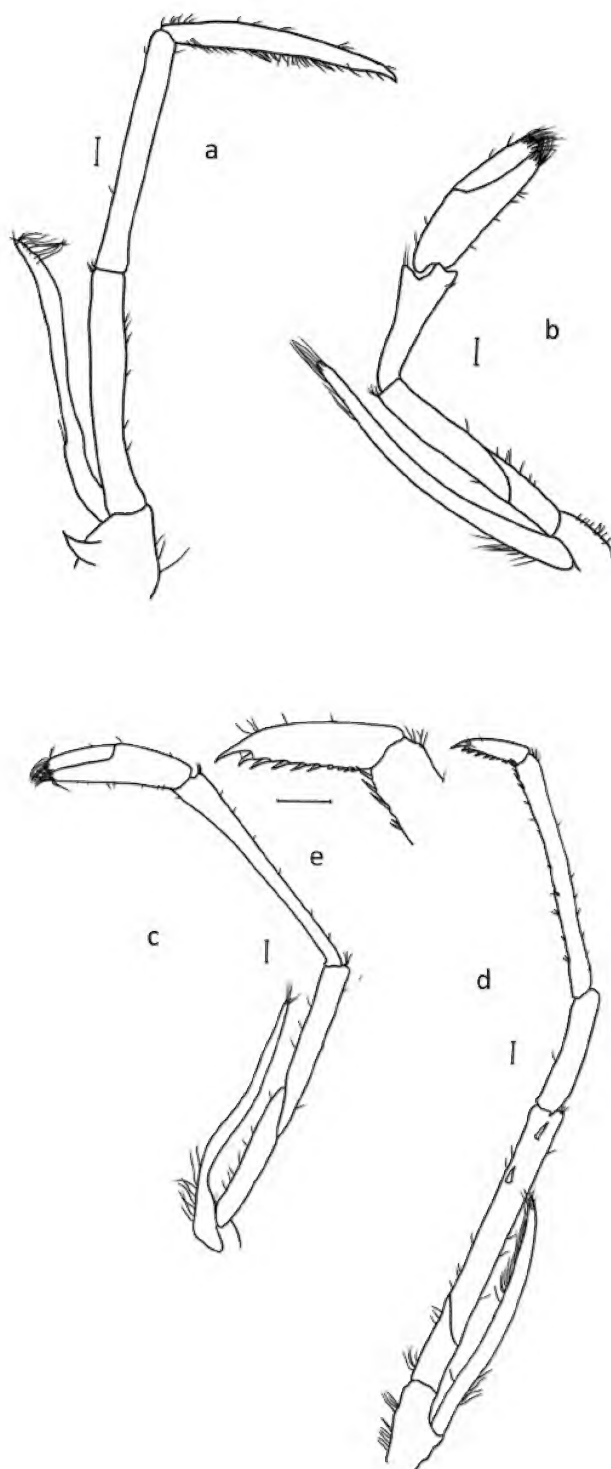
Figure 28. *Paratya rouxi* sp. nov.: a, maxilliped 3; b, pereiopod 1; c, pereiopod 2; d, pereiopod 3; e, dactylus 3. Scale lines 0.2 mm.
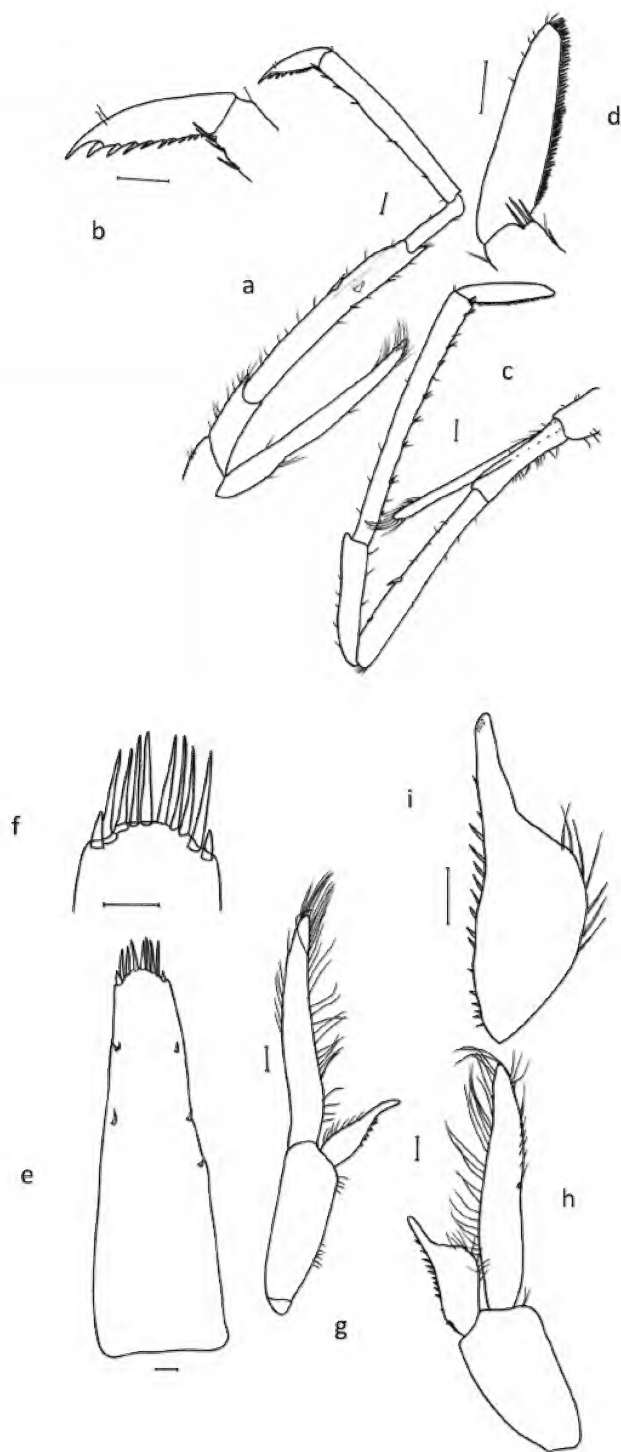
Figure 29. *Paratya rouxi* sp. nov.: a, pereiopod 4; b, dactylus 4; c, pereiopod 5; d, dactylus 5; e, telson; f, telson terminal spines; g, pleopod 1 of female; h, pleopod 1 of male; i, endopod 1 of male. Scale lines 0.2 mm.

Maxilliped 3 (fig. 28a) endopod 5.36 (5.36–5.95) mm long, 2.51 (2.07–2.51) times longer than exopod; basal segment curved, apical segment with large terminal claw, medial distal margin with 8 (8–10) broad teeth-like spines, largest 3 in mid half and 1 long spine in basal third, outer margin with 1 long tooth-like spines near terminal spine and 1 mid outer spine. Exopod 2.13 (2.13–2.88) mm long, narrow, tip over-reaching distal end of basal endopod segment.

Thoracic appendages. Pereiopod 1 (fig. 28b) short, 3.92 (3.92–4.25) mm long, 0.80 (0.74–0.85) times carapace length. Chelae short and slender (fig. 28b), 1.33 (1.25–1.35) mm long, propodus 3.85 (3.10–3.85) times as long as wide, propodus length 2.17 (1.92–2.17) times longer than dactylus; palm length 2.11 (1.90–2.11) times palm width, 1.36 (1.06–1.36) times dactylus length. Carpus long, 2.33 (2.33–3.00) times longer than greatest width. Segment ratios 0.66 (0.54–0.66) : 1.43 (1.16–1.43) : 1.00 (0.93 [0.93–1.13] mm) : 1.33 (1.15–1.33) : 0.44 (0.40–0.45) : – . Exopod extending to mid-apex of carpus.

Pereiopod 2 (fig. 28c) longer than pereiopod 1, 6.00 (6.00–6.90) mm long, 1.22 (1.19–1.38) times carapace length. Chelae long and slender (fig. 28c), 1.33 (1.28–1.33) mm long, half to two-thirds length of carpus, 4.00 (3.63–4.00) times as long as wide, palm length 2.38 (2.22–2.38) times palm width, 1.27 (1.25–1.27) times longer than dactylus. Propodus length 1.92 (1.85–2.04) times longer than dactylus. Carpus 6.96 (6.96–9.27) times as long as greatest width, slightly broader distally, distal margin with small excavation. Segment ratios 0.33 (0.27–0.33) : 0.63 (0.54–0.63) : 1.00 (2.13 [2.13–2.40] mm) : 0.79 (0.77–0.79) : 0.39 (0.38–0.39) : 0.94 (0.94–1.10). Exopod extending to mid-apical third of merus.

Pereiopod 3 (fig. 28d, e) distinctly longer than pereiopod 2 and more slender 6.96 (6.48–7.20) mm long, 1.42 (1.22–1.44) times carapace length. Dactylus with prominent terminal claw and 10 (10–12) strong spines on medial margin (fig. 28e). Propodus 3.40 (3.40–4.13) times longer than dactylus, length 12.31 (12.31–12.47) times longer than wide with 7 (7–10) spines on inner margin. Merus with 2 (1–2) strong spine on medial margin and 1 near ventral distal margin. Segment ratios 0.48 (0.47–0.54) : 1.65 (1.65–2.00) : 1.00 (1.29 [1.13–1.35] mm) : 2.19 (1.88–2.22) : 0.54 (0.54–0.78) : – (1.75–2.04). Exopod extends to mid merus.

Pereiopod 4 (fig. 29a, b) similar to pereiopod 3, 6.83 (6.05–6.83) mm long, 1.39 (1.14–1.39) times carapace length. Dactylus with prominent terminal claw and 8 (8–12) spines on medial margin (fig. 29b). Propodus 3.36 (3.03–3.58) times longer than dactylus, length 14.00 (12.57–14.00) times longer than wide, with 11 (8–11) spines on medial margin and 1 apically on outer margin; merus with 2 strong spine on medial margin and 1 near ventral distal margin. Segment ratios 0.52 (0.52–0.63) : 1.75 (1.75–2.04) : 1.00 (1.28 [1.07–1.28] mm) : 2.06 (2.00–2.06) : 0.52 (0.52–0.58) : 1.85 (1.85–2.00). Exopod extends to apical third of merus.

Pereiopod 5 (fig. 29c, d) similar length to pereiopod 4, 7.08 (6.48–7.08) mm long, 1.44 (1.22–1.44) times carapace length. Dactylus with prominent terminal claw and very regular, comb-like row of numerous 72 (70–80) small spines on medial margin (fig. 29d). Propodus 2.90 (2.59–3.00) times longer than dactylus, length 13.13 (12.94–13.13) times longer than wide, with 8 (8–9)

long medial teeth and external margin without teeth. Carpus without any large spines near distal margin. Merus with 1 strong medial spine and 1 distal spine; ischium one-third length of propodus; segment ratios 0.71 (0.67–0.78) : 2.05 (1.93–2.16) : 1.00 (1.28 [1.20–1.43] mm) : 1.67 (1.67–1.83) : 0.81 (0.67–0.81) : 1.61 (1.50–1.67). Exopod extends to mid third of merus.

Abdomen. Pleopods peduncle of first pleopod short, 0.41 (0.29–0.41) times length of carapace length, 2.67 (2.38–3.00) times width, exopod 1.25 (1.25–1.42) times peduncle length, endopod – (0.60) times peduncle length (fig. 29g); second pleopod peduncle short, 0.45 (0.38–0.55) times length of carapace, 2.93 (1.60–3.93) times width, exopod 1.14 (0.84–1.23) times peduncle length, endopod slightly shorter – (0.80–1.13) times peduncle length. Length of first peduncle 1.10 (1.10–1.83) times length of second peduncle.

Telson (fig. 29e, f) length 3.50 (3.50–3.75) mm, 0.71 (0.66–0.71) times carapace length and tapering distally, 3.24 (2.50–3.48) times as long as greatest width. Dorsal surface with 2 (2–3) pairs of strong submarginal teeth-like spines. Posterior margin convex with 1 pair of teeth-like spines outermost, 12 (8–12) long strong setose terminal spines (fig. 29f).

Uropods approximately equal to telson length.

Male smaller than females, carapace length 3.88 mm; endopod of pereiopod 1 not strongly excavated with 8 short spines on outer margin, 2 spines at apex of finger-like projection and a long spine at base of projection, inner margin with 10 long setae (fig. 29h, i).

Etymology: This species is named after Dr Jean Roux, who in 1926 clearly recorded the characteristics that are diagnostic for *P. rouxi* from North Yanco in New South Wales. Roux also recognised a second morphological form of *Paratya* at the same location, similar to specimens from the Sydney area. Roux was not prepared to describe a new species based on the rostral characters, especially as similar morphology was present in the area of the type for *P. australiensis*. The second morphological form was probably *P. arrostra*.

Comments: P. rouxi can be confused with *P. arrostra* (4C) because both have a short rostrum, but *P. rouxi* lacks post-orbital spines, has 1–2 ventral rostral spines, telson 0.66–0.70 times carapace length, rostral length 0.57–0.73 times scaphocerite length, pereiopod 1 has a long slender carpus and chelae with carpus length 2.33–3.00 times longer than wide, pereiopod 2 with dactylus 0.27–0.33 times carpus length and propodus 0.54–0.63 times carpus length and propodus 3.63–4.00 times longer than wide, whereas *P. arrostra* (4C) has 0–1 post-orbital spines, 4–5 ventral spines, telson 0.44–0.60 carapace length, rostral length 0.80–0.90 times scaphocerite length, pereiopod 1 has a short carpus and robust, broad cheliped with carpus length 1.71–1.91 times longer than wide, pereiopod 2 with dactylus 0.45–0.53 times carpus length and propodus 0.74–0.79 times carpus length and propodus 2.98–3.08 times longer than wide (see Table 3).

The distribution of *P. rouxi*, which is found in streams in the Murray Darling Basin in New South Wales, does not overlap the short rostrum *P. arrostra* (4C), which occurs in the Conondale Ranges south-eastern Queensland and in the St George district in the upper Condamine R catchment, Queensland (Calman, 1926).

Paratya gariwerdensis n. sp.

Figures 30, 31

http://zoobank.org/urn:lsid:zoobank.org:act:D691687B-83DC-4E45-81AB-26BE4F224714

Lineage D McClusky (2007)

Type Material: Holotype Victoria. Stokes R near Dartmoor −37.8745 S, 141.3014 E, 3 February 2018 (PS). Body in ethanol and antennae, mouthparts, pereiopods and abdominal structures dissected, mounted on 2 slides. Accession Ref. PS41 Genbank Registration OL420914, Museum of Victoria Ref No NMV J75170.
Paratypes: Victoria. Stokes R near Dartmoor −37.8745 S, 141.3014 E, 3 February 2018 Accession Ref PS40, Genbank Registration OL420913, PS46 Genbank Registration OL420918 (PS), NMV J75171–J75172; bodies in ethanol and other structures dissected, mounted on 2 slides each; Wannon R S of Coleraine −37.6652 S, 141.6632 E, 3 February 2018 Accession Ref. PS42–43 Genbank Registration OL420915 (PS) NMV J75173–J75174.

Material Examined: Victoria. Stokes R near Dartmoor −37.8745 S, 141.3014 E, 3 February 2018 (PS); Wannon R south of Coleraine −37.6652 S, 141.6632 E, 3 February 2018 (PS).

Diagnosis: Paratya gariwerdensis differs from all other species by the following combination of characters: rostrum long, 4.00–6.25 mm, extending beyond antennular peduncle and just to end of scaphocerite, rostral length 1.02–1.25 times longer than carapace, dorsal edge curved downwards to tip, narrow and pointed; rostral length 8.40–12.50 times greater than width; dorsally armed with 22–29 teeth, ratio of rostral spines to rostral length is 4.21–6.67; 1–2 postorbital spines; ventrally with 7–10 large serrations over a length of 1.30–2.35 mm, 2–3 spines posterior to greatest depth, distal half of ventral edge straight; ratio of ventral spine length to rostral length is 0.32–0.38 and 2.60–4.00 more dorsal spines than ventral spines; rostral length 1.27–1.35 times length of scaphocerite. Antennular peduncle 2.85–3.63 mm long, not reaching distal tip of scaphocerite, length 0.89–0.94 times length of scaphocerite. Stylocerite 1.35–2.08 mm long, length 6.60–8.30 times width, 0.38–0.43 times carapace length, reaching beyond distal border of peduncle segment but not to end of broad acute process on distal angle of first segment. Right mandible with 4 teeth in a single incisor process with all teeth approximately equal sized; spine row immediately below teeth with 5–8 lifting spines. Scaphognathite of maxilla 2 truncated distally. Pereiopod 1, 3.55–4.10 mm long, 0.82–0.99 times carapace length. Chelae short and broad, 1.10–1.30 mm long, propodus 2.44–3.07 times as long as wide, 1.91–2.19 times longer than dactylus, 1.21–1.33 times longer than carpus; palm length 1.39–1.67 times longer than wide and 1.08–1.20 times dactylus length. Carpus very short, 2.19–2.50 times as long as greatest width. Pereiopod 2 5.05–5.98 mm long, 1.20–1.40 times carapace length. Chelae long and slender 1.15–1.30 mm long, approximately two-thirds length of carpus, 2.61–3.47 times as long as wide, palm length 1.22–1.73 times longer than width and 0.84–0.96 times dactylus length. Propodus 1.68–2.04 times longer than dactylus. Carpus 6.27–7.82 times as long as greatest width. Pereiopod 3 dactylus with prominent terminal claw and 6–7 strong spines on medial margin; propodus length 3.27–3.84 times longer than dactylus, length 10.29–13.00 times longer than wide with 11–13 spines on inner margin. Pereiopod 4, 5.40–7.00 mm long, 1.32–1.54 times carapace length: dactylus with prominent terminal claw and 7–8 spines on medial margin; propodus length 3.75–3.90 times longer than dactylus, length 11.43–14.29 times longer than wide, with 10–11 spines on medial margin. Pereiopod 5, 5.65–7.80 mm long, 1.38–1.57 times longer than carapace; dactylus with prominent terminal claw and very regular, comb–like row of 44–54 small spines on medial margin; propodus length 3.00–3.11 times longer than dactylus, length 11.63–17.40 times longer than wide with 8–13 long medial teeth and no spines on external margin. Posterior margin of telson convex with 1 pair of teeth-like spines outermost, 8–9 long strong terminal setose spines.

Carapace length 4.00 (3.60–4.10) mm.

Rostrum long, 4.40 (4.00–6.25) mm, extending beyond antennular peduncle and just to end of scaphocerite (fig. 30a), rostral length 1.10 (1.02–1.25) times longer than carapace, dorsal edge curved downwards to tip, narrow and pointed; rostral length 9.78 (8.40–12.50) times greater than width; dorsally armed with 28 (22–29) teeth, ratio of rostral spines to rostral length is 6.36 (4.21–6.67); 2 (1–2) postorbital spines (fig. 30a); ventrally with 7 (7–10) large serrations over a length of 1.50 (1.30–2.35) mm, 2–3 spines posterior to greatest depth (fig. 30a), distal half of ventral edge straight; ratio of ventral spine length to rostral length is 0.33 (0.33–0.38) and 4.00 (2.60–4.00) more dorsal spines than ventral spines; rostral length 1.35 (1.27–1.35) times length of scaphocerite.

Antenna 1 (fig. 30b) peduncle 3.05 (2.85–3.63) mm long, not reaching distal tip of scaphocerite, length 0.94 (0.89–0.94) times length of scaphocerite. Stylocerite 1.70 (1.35–2.08) mm long, length 7.56 (6.60–8.30) times width, 0.43 (0.38–0.43) times carapace length, reaching beyond distal border of peduncle segment but not to end of broad acute process on distal angle of first segment (fig. 30b).

Antenna 2 (fig. 30c) second segment of peduncle 0.93 (0.88–1.13) mm long, 0.28 (0.28-0.31) length of scaphocerite and 2.31 (2.31–3.66) longer than wide. Scaphocerite 3.25 (3.15–3.90) mm long, 2.95 (2.95–3.56) longer than wide, 0.81 (0.78–0.88) times length of carapace.

Mouthparts. Left mandible (fig. 30d, e) with 4 teeth separated by a ridged notch from 1 less distinct apical tooth; spine row immediately below incisor process of 5–7 rugose spines (lifting spines); spine row above molar process of approximatelyover 20 sparsely setose spines. Right mandible (fig. 30f, g) with 4 teeth in a single incisor process with all teeth approximately equal sized; spine row immediately below teeth with 5–8 lifting spines; spine row above molar process. Molar process ridged.

Maxilla 1 (fig. 30h) as for *P. australiensis.*

Maxilla 2 scaphognathite truncated distally, not extending to apex of upper endite (fig. 30i); palps small, terminal parts narrow and with 1 sub–apical setose spine.

Maxilliped 1 (fig. 30j) as for *P. australiensis.*

Maxilliped 2 (fig. 30k) endopod 0.75 (0.73–0.93) mm long; basal segment length short, exopod long and narrow 1.75 (1.19–1.75) mm long, exopod 2.34 (1.28–2.34) times longer than endopod. Epipodite with podobranch.
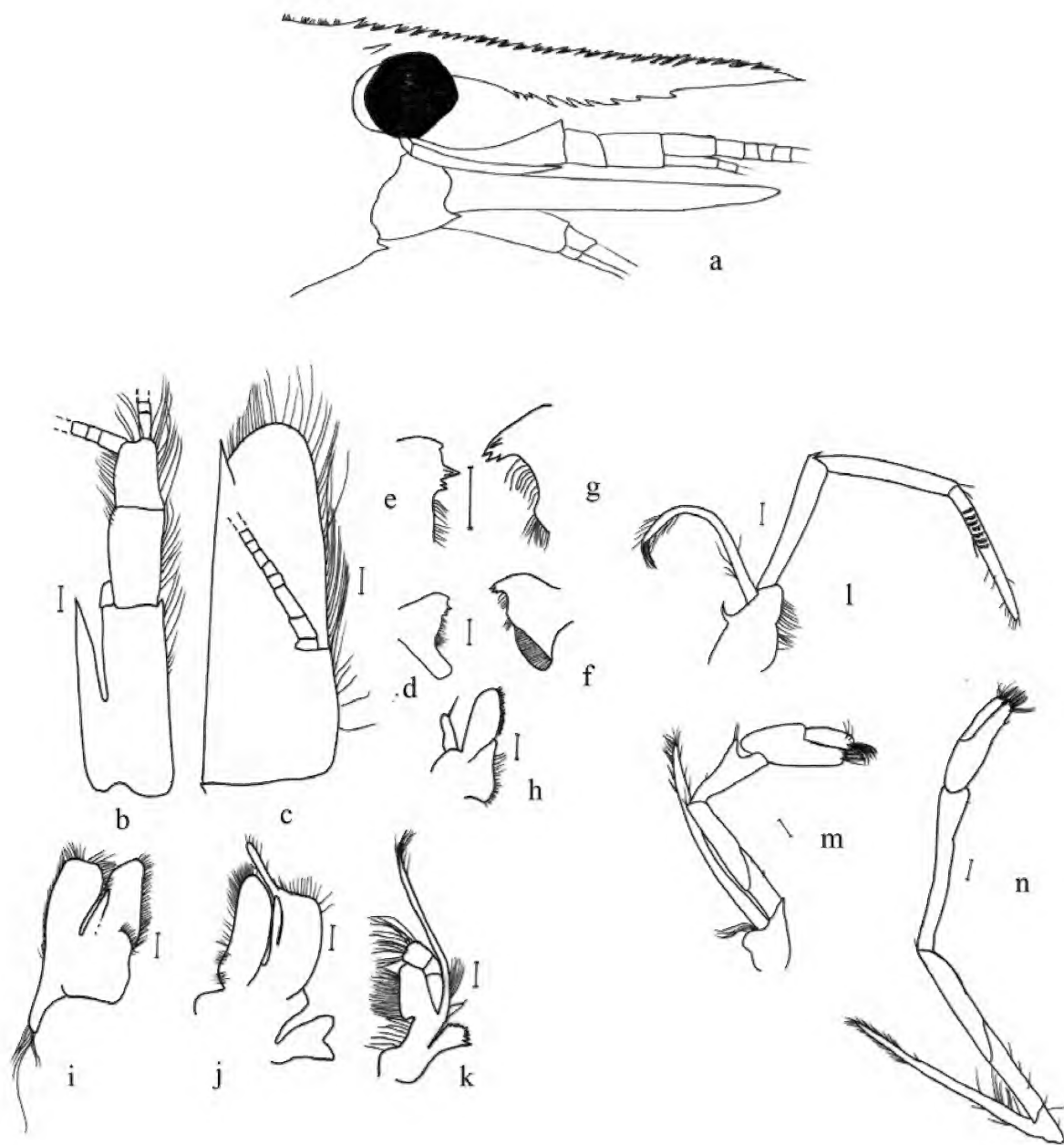
Figure 30. *Paratya gariwerdensis* n.sp.: a) head region and rostrum; b, antenna 1 peduncle and stylocerite; c, scaphocerite; d, left mandible; e, enlarged incisors; f, right mandible; g, enlarged incisors; h maxilla 1; i, maxilla 2; j, maxilliped 1; k maxilliped 2; l, maxilliped 3; m, peraeopod 1; n, peraeopod 2. Scale lines 0.2mm.

Maxilliped 3 (fig. 31i) endopod 4.63 (4.20–5.88) mm long, 2.37 (2.37–2.92) times longer than exopod; with 3 distal segments of similar length; basal segment curved, apical segment with large terminal claw, medial distal margin with 9 (6–9) broad teeth-like spines, largest 1 or 2 in basal third, outer margin with 2 (2–4) teeth-like spines plus 1 apical spine. Exopod long and narrow, 1.95 (1.55–2.25) mm long, tip reaching basal third of mid segment.

Thoracic appendages. Pereiopod 1 (fig. 30m) 3.60 (3.55–4.10) mm long, 0.90 (0.82–0.99) times carapace length. Chelae short and broad (fig. 31b), 1.10 (1.10–1.30) mm long, propodus 2.44 (2.44–3.07) times as long as wide, 1.91 (1.91–2.19) times longer than dactylus; palm length 1.39 (1.39–1.67) times longer than wide and 1.09 (1.08–1.20) times dactylus length. Carpus very short, 2.19 (2.19–2.50) times longer than greatest width, broadening distally, distal margin excavate. Segment ratios 0.66 (0.60–0.66) : 1.26 (1.21–1.33) : 1.00 (0.88 [0.88–1.08] mm) : 1.23 (1.16–1.33) : 0.63 (0.42–0.63) : 2.49 (1.58–2.49). Exopod extending to mid carpus (apex merus–mid carpus).

Pereiopod 2 (fig. 30n) 5.08 (5.05–5.98) mm long, 1.27 (1.20–1.40) times carapace length. Chelae long and slender (fig. 31c) 1.18 (1.15–1.30) mm long, 2.61 (2.61–3.47) times longer than wide, palm length 2.00 (1.22–1.73) times longer than width, 0.96 (0.84–0.96) times dactylus length. Propodus length 2.61 (2.61–3.29) times width, 2.04 (1.68–2.04) times longer than dactylus. Carpus 6.27 (6.27–7.82) times longer than greatest width, slightly broader distally, distal margin with small excavation. Segment ratios 0.33 (0.33–0.37) : 0.68 (0.60–0.68) : 1.00 (1.73 [1.73–2.15] mm) : 0.81 (0.74–0.81) : 0.45 (0.43–0.45) : 1.22 (1.11–1.22). Exopod extending to apex of merus.

Pereiopod 3 (fig. 31a, b) slightly longer than pereiopod 2 and more slender 5.83 (5.53–7.13) mm long, 1.46 (1.35–1.61) times carapace length. Dactylus with prominent terminal claw and 7 (6–7) strong spines on medial margin (fig. 31e). Propodus length 3.27 (3.27–3.84) times longer than dactylus, length 10.29 (10.29–13.00) times longer than wide with 12 (11–13) spines on inner margin. Merus with 1 strong spine on
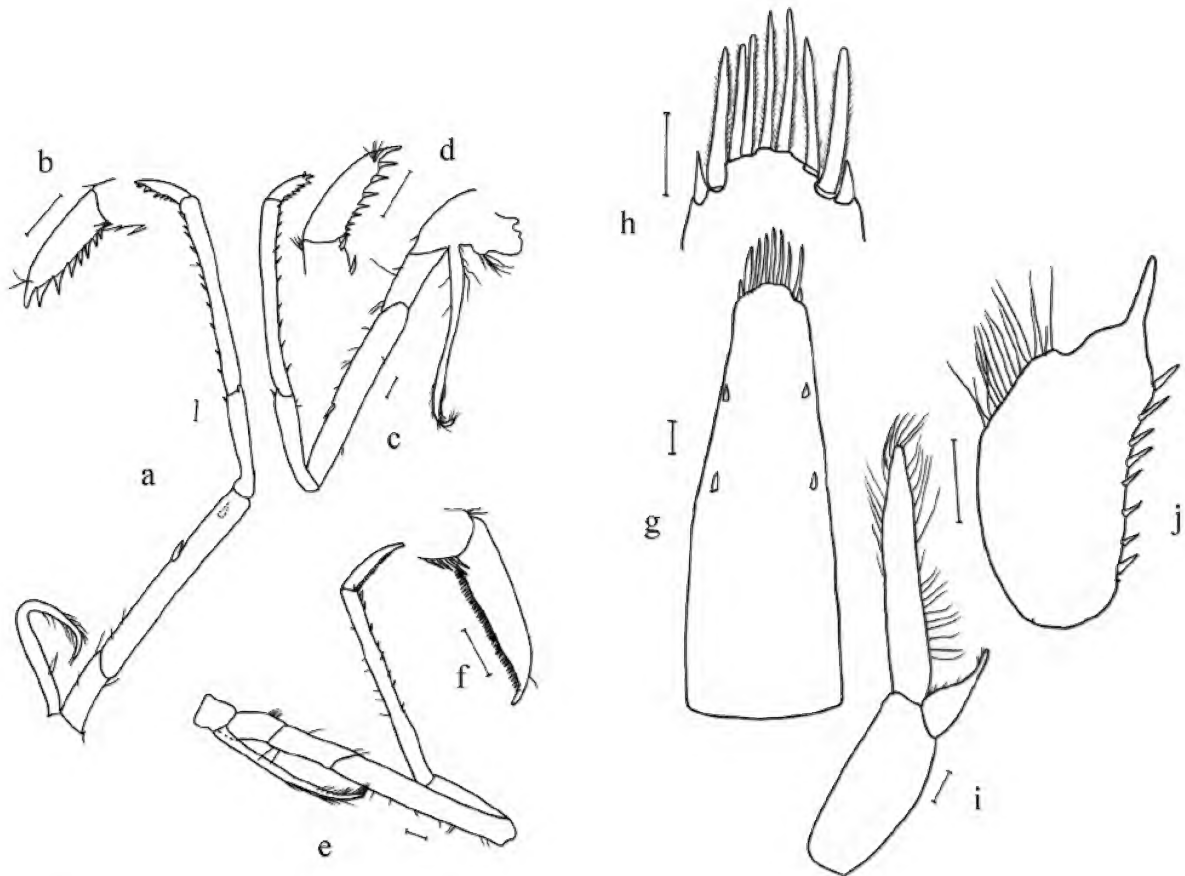
Figure 31. *Paratya gariwerdensis* sp. nov.: a, pereiopod 3; b, dactylus 3; c, pereiopod 4; d, dactylus 4; e, pereiopod 5; f, dactylus 5; g, telson; h, telson terminal spines; i, pleopod 1 of female; j, endopod of pleopod 1 of male. Scale lines 0.2 mm.

a)

b)

c)
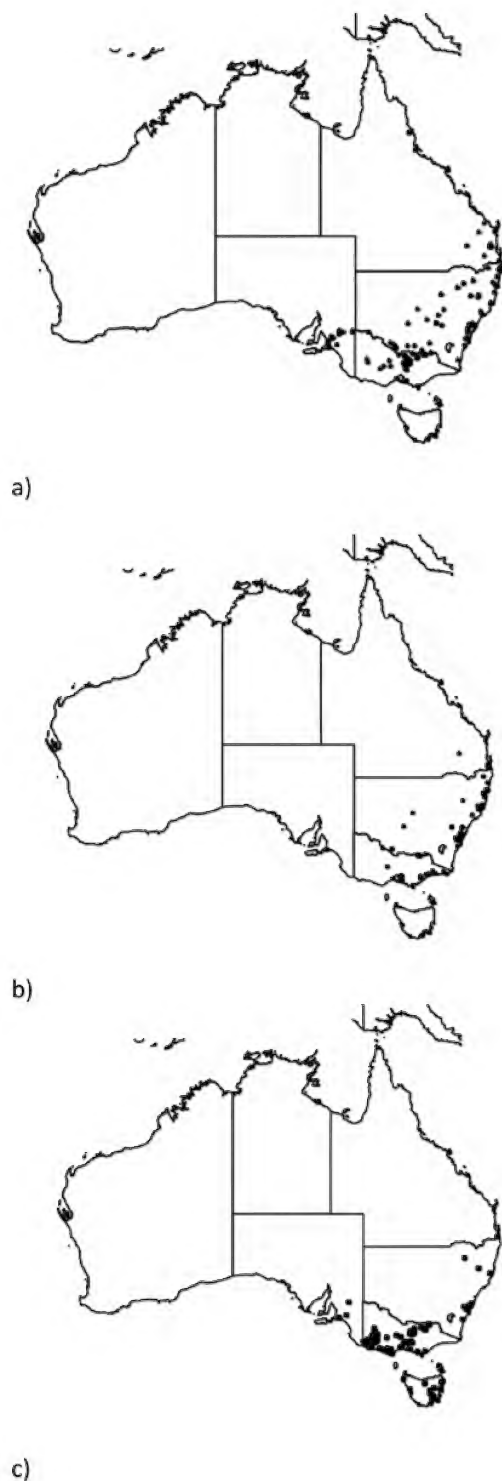
Figure 32. Distribution of material examined in this study: a, *P. arrostra*; b, *P. whitemae*; c, *P. tasmaniensis*. Maps created in Cartographica.

medial margin and 1 near ventral distal margin. Segment ratios 0.48 (0.48–0.53) : 1.57 (1.57–1.95) : 1.00 (1.15 [1.00–1.25] mm) : 1.96 (1.96–2.15) : 0.54 (0.54–0.75) : 1.52 (1.50–1.92). Exopod extends to mid merus.

Pereiopod 4 (fig. 31c d) similar to pereiopod 3, 5.68 (5.40–7.00) mm long, 1.42 (1.32–1.54) times carapace length. Dactylus with prominent terminal claw and 8 (7–8) spines on medial margin (fig. 31g). Propodus length 3.81 (3.75–3.90) times longer than dactylus, length 11.43 (11.43–14.29) times longer than wide, with 11 (10–11) spines on medial margin; merus with 1 strong spine on medial margin and 1 near ventral distal margin. Segment ratios 0.53 (0.50–0.53) : 2.00 (1.88–2.00) : 1.00 (1.00–1.25) mm : 2.05 (1.95–2.05) : 0.63 (0.58–0.63) : 1.80 (1.60–1.80). Exopod extends to mid third of merus.

Pereiopod 5 (fig. 31e f) slightly longer than pereiopods 4, 5.78 (5.65–7.80) mm long, 1.44 (1.38–1.57) times longer than carapace. Dactylus with prominent terminal claw and very regular, comb–like row of 44 (44–54) small spines on medial margin (fig. 31i). Propodus length 3.00 (3.00–3.11) times longer than dactylus, length 11.63 (11.63–17.40) times longer than wide with 11 (8–13) long medial teeth and no spines on external margin. Carpus with 1 large spine near distal margin. Merus with 1 strong medial spine and 1 distal spine Segment ratios 0.84 (0.67–0.84) : 2.51 (2.10–2.51) : 1.00 (0.93 [0.93–1.30] mm) : 2.00 (1.77–2.00) : 0.73 (0.65–0.88) : 1.68 (1.35–1.68). Exopod extends to basal third to mid third of merus.

Abdomen. Pleopods peduncle of first pleopod short 0.28 (0.28–0.35) times length of carapace length, 2.20 (2.20–3.36) times width, exopod 1.52 (1.27–1.52) times peduncle length, endopod 0.64 (0.64–0.80) times peduncle length. (fig. 31l); second pleopod peduncle short, 0.34 (0.34–0.40) times length of carapace, 2.62 (2.62–4.13) times width, exopod 1.27 (1.21–1.36) times peduncle length, endopod slightly shorter 1.16 (1.08–1.32) times peduncle length. Length of first peduncle 1.25 (1.00–1.33) times length of second peduncle.

Telson (fig. 31g h) length 2.80 (2.63–2.80) mm, 0.70 (0.53–0.70) times carapace length, 3.03 (2.76–3.06) times as long as greatest width, and tapering distally. Dorsal surface with 2 pairs of strong submarginal teeth-like spines. Posterior margin convex with 1 pair of teeth-like spines outermost, 9 (6–9) long strong terminal setose spines (fig. 31h).

Uropods slightly longer than telson.

Males smaller than females, carapace length 4.34 mm; endopod of first pleopod strongly excavated apically with 8–10 external spines and 19 long setae on inner margin (fig. 31j).

Etymology: Gariwerd is the aboriginal name for the Grampians Mountains, the Grampians (Gariwerd) National Park in south-western Victoria.

Comments: Paratya gariwerdensis is restricted to the south-western Victoria in streams that drain the Grampians Mountains where it has been recorded with *P. arrostra* and *P. tasmaniensis*.

The long concave rostrum extending beyond the antennular peduncle is a character shared with *P. walkeri*, *P. spinosa*, *P. arrostra*, *P. williamsi* and *P. tasmaniensis*. Three of these species (*P. walkeri*, *P. spinosa* and *P. williamsi*) have not been recorded in Victoria.

Paratya gariwerdensis can be distinguished from the species with a long rostrum by a combination of characters in Table 2 including: ventral spines cover length of 1.30–2.35 mm; stylocerite extending to mid process on apex of basal segment of antennule 1; carapace length of 3.60–4.10 mm; dactylus 3 with 6–7 medial spines; dactylus 4 with 7–8 medial spines; pereiopod 1 length 0.82–0.99 times carapace length; pereiopod 4 propodus length 1.88–2.00 times longer than carpus 4 length; dactylus 5 length 0.67–0.84 times longer than carpus 5 length; propodus 5 length 2.10–2.51 times longer than carpus 5 length; pereiopod 1 length 3.55–4.10 mm; pereiopod 2 length 5.05–5.98 mm; pereiopod 3–5 less than 7.80 mm; scaphognathite of maxilla 2 truncated; right mandible with a single group of incisor teeth, all 4 of similar size

Conclusion

Ten species have been recognised in this study because of the linkage between the molecular and morphological characteristics. The aims were all addressed with the genetic lineages all described with morphological characteristics. It must be added that, without the benefits of the molecular data, the conclusion by Williams and Smith (1979) of a single species is credible, but Riek's (1953) revision, although with some inadequacies as outlined by Williams (1977), was a serious attempt to address the morphological variability observed in this genus.

Key to female *Paratya* from Australia

The following key is based on mature females and caution is required if identifying immature specimens. We have found that mature males can be identified with this key. Many of the species will key out in several couplets because we have tried to incorporate the variation present in each species of *Paratya*.

1   Rostrum short, not extending beyond antennal peduncle (figs12b, c, 27a) 2

1'   Rostrum long, extending beyond antennal peduncle figs 5a, f, 6a, 9a, 12a, ... 4

2(1)   No post – orbital spines (fig. 27a), rostrum with 1–3 ventral spines over a length of less than 0.4 mm, all anterior to widest point; right mandible with paired incisors, each with two large teeth (fig. 27g); stylocerite extending to basal third of peduncle process (fig. 27b); scaphognathite of maxilla 2 truncated shorter than endite (fig. 27i) ....
        .... *P. rouxi* n.sp. [Inland Murray–Darling Basin, New South Wales]

2'   Post–orbital spines present (fig. 12b, c), rostrum with rostrum with 3–7 ventral spines over a length of 0.4–1.1 mm; right mandible with single incisor of 4–5 large teeth (fig. 12j); stylocerite extending almost to end of peduncle process (fig. 12d); scaphognathite of maxilla 2 rounded apical almost to apex of endite (fig. 12k) 3

3(2)   2–3 post orbital spines all contiguous with rostral spines, 3–7 ventral spines over a length of 0.4–1.8mm, all anterior of widest point (fig. 12b) ....
        .... *P. arrostra* (lineage 4B short rostrum)

3'   1 post–orbital spine separated posteriorly from other rostral spines (fig. 12c), 4–5 ventral spines over a length of 0.6–1.2 mm, with some spines posterior to greatest width .... *P. arrostra* (lineage 4C very short rostrum)

4(1)   Rostrum long extending to end or beyond scaphocerite (figs 5a, 6a, 9a, 12a, 18a, 21a, 24a, 30a) 8

4'   Rostrum long but not extending beyond scaphocerite (figs 5b, 12a, 15a) 5

5(4)   Post-orbital spines absent (fig. 5f); 16–17 dorsal rostral spines .... *P. australiensis* (in part) [New South Wales, Shoalhaven R catchment]

5'   Post-orbital spines present (1–3) (figs 12a, 15a); greater than 21 dorsal rostral spines 6

6(5)   Small species, carapace length less than 4.1mm; 2–3 ventral rostral spines posterior to greatest width of rostrum (fig. 30a); south-western Victoria ....
        .... *P. gariwerdensis* n.sp. [South-western Victoria in streams draining the Grampians Mts]

6'   Larger species with carapace length greater than 4.8 mm; maximum of 2 ventral rostral spines posterior to greatest width of rostrum (fig. 12a), or all spines anterior greatest width of rostrum (figs 15a, 18a) 7

7(6)   First pereiopod chelae shape short and slender (fig. 13b); telson with usually 9–10 long terminal spines (fig. 14f) but may be as few as 5 or as many as 12 spines; dactylus 3 with 8–11 teeth; dactylus 4 with 8–12 teeth ....
        .... *P. arrostra* (long rostrum)

7'   First pereiopod chelae shape short and broad (figs 16b, 19b); telson with usually 6–8 long terminal spines (fig. 17f); dactylus 3 with 5–8 teeth; dactylus 4 with 5–6 teeth .... *P. williamsi* n.sp. [New South Wales, Upper Kangaroo Valley in the Shoalhaven catchment]

8(4)   Ventral spines of rostrum all anterior to widest point 9

8'   Ventral spines of rostrum 1-2 posterior to widest point .....
        11

9(8)   Rostrum shorter than carapace; ventral rostral spines extend over a length less than 2.0 mm 10

9'   Rostrum longer than carapace; ventral rostral spines extend over a length greater than 2.0 mm ....
        . *P. tasmaniensis* [Tasmania and coastal streams in south-east Australia]

10(9)   Ventral rostral spines extend over a length of 0.6–1.5 mm (fig. 5a); telson with 6 long terminal spines (fig. 4c in Williams and Smith, 1979); carpus of pereiopod long (1.47–2.84 mm) (fig. 5d, i) ....
        .... *P. australiensis* in part [New South Wales coastal, Sydney area south of Newcastle]

10'   Ventral rostral spines extend over a length of 1.3–1.8 mm (fig. 21a); telson with 6–10 long terminal spines (fig. 23b) .... *P. strathbogiensis* n.sp. [Victoria, Strathbogie Ranges in the upper Goulburn R catchment]

11(8)   Rostrum with greater than 14 ventral spines (fig. 6a) .... *P. walkeri* n.sp. [New South Wales coastal, Bellinger and Tweed catchments]

11'   Rostrum with <14 ventral spines 12

12(11)   First pereiopod chelae shape short and slender (fig. 13b); telson with usually 9–10 long terminal spines (fig. 14f) but may be as few as 5 or as many as 12 spines .... *P. arrostra* (long rostrum)

12'   First pereiopod chelae shape short and broad (figs 16b, 19b); telson with usually 4–10 long terminal spines (figs 11f, 23d) 13

13(12)   Rostrum length longer than carapace length; Dactylus 4 with 8–11 teeth; dactylus 5 with comb of 72–94 spines; propodus 2 length 3.0–3.2 times width; 0.53–0.77 length of dactylus 2 .... *P. whitemae* n.sp. [Widespread mainland Australia, Victoria coastal and inland Murray–Darling Basin, New South Wales coastal and inland Murray–Darling Basin, Queensland coastal, South Australia inland MDB]

13'   Rostrum length shorter than carapace length; dactylus 4 with 7–8 teeth (fig. 11b); dactylus 5 with comb of less than 60 spines; propodus 2 length 3.4–4.3 times width; 0.86–1.3 times length of dactylus 2 .... *P. spinosa* n.sp.   [New South Wales, northern coastal rivers (Tweed R catchment)]

Acknowledgements

References

Baker, A.M., Hughes, J.M., Dean, J.C., Bunn, S.E. 2004. Mitochondrial DNA reveals phylogenetic structuring and cryptic diversity in Australian freshwater macroinvertebrate assemblages. *Marine and Freshwater Research* **55**(6), 629–640.

Balcombe, S.R., Closs, G.P., and Suter, P.J. 2007. Density and distribution of epiphytic invertebrates on emergent macrophytes in a floodplain billabong. *River Research and Application* **23**(8), 843–857.

Boulton, A.J. 2003. Parallels and contrasts in the effects of drought on stream macroinvertebrate assemblages. *Freshwater Biology* **48**, 1173–1185.

Bunn, S.E., and Hughes, J.M. 1997. Dispersal and recruitment in streams: evidence from genetic studies. *Journal of the North American Benthological Society* **16**(2), 338–346.

Calman, W.T. 1926. XXXII. On freshwater prawns of the family Atyidae from Queensland. *Annals and Magazine of Natural History Series 9* **17**(98), 241–246.

Chace, F.A.J. 1997. The caridean shrimps (Crustacea: Decapoda) of the *Albatross* Philippines expedition, (1907–1910), Part 7: Families Atyidae, Eugonatonotidae, Rhynchocinetidae, Bathypalaemonellidae, Processidae, and Hippolytidae. *Smithsonia Contributions to Zoology* **587**, 1–106.

Chen, Q.-H., Chen, W.-J., Zheng, X.-Z., and Guo, Z.-L. 2020. Two freshwater shrimp species of the genus *Caridina* (Decapoda, Caridea, Atyidae) from Dawanshan Island, Guangdong, China, with the description of a new species. *ZooKeys* **923**, 15–32.

Chessman, B., and Robinson, D. 1987. Some effects of the 1982–83 drought on water quality and macroinvertebrate fauna in the lower La Trobe River, Victoria. *Marine and Freshwater Research* **38**(2), 289–299.

Choy, S., Page, T.J., and Mos, B. 2019. Taxonomic revision of the Australian species of *Australatya* Chace 1983 (Crustacea, Decapoda, Atyidae), and the description of a new species. *Zootaxa* **4711**, 366–378.

Christodoulou, M., Antoniou, A., Magoulas, A., and Koukouras, A. 2012. Revision of the freshwater genus *Ataephyra* (Crustacea, Decapoda, Atyidae) based on morphological and molecular data. *ZooKeys* **229**, 53–110.

Cook, B.D. 2006. *An analysis of population connectivity in lotic fauna: constraints of subdivision for biotic responses to stream habitat restoration.* Unpublished PhD thesis, Griffith University, Brisbane, Queensland.146 pp.

Cook, B.D., Baker, A.M., Page, T.J., Grant, S.C., Fawcett, J.H., Hurwood, D.A., and Hughes, J.M. 2006. Biogeographic history of an Australian freshwater shrimp, *Paratya australiensis* (Atyidae): the role life history transition in phylogeographic diversification. *Molecular Ecology* **15**(4), 1083–1093.

Cook, B.D., Bunn, S.E., and Hughes, J.M. 2002. Genetic structure and dispersal of *Macrobrachium australiense* (Decapoda: Palaemonidae) in western Queensland, Australia. *Freshwater Biology* **47**, 2098–2112.

Cook, B.D., Bunn, S.E., and Hughes, J.M. 2007. A comparative analysis of population structuring and genetic diversity in sympatric lineages of freshwater shrimp (Atyidae: *Paratya*): concerted or independent responses to hydrographic factors? *Freshwater Biology* **52**(11), 2156–2171.

Costa, F.O., deWaard, J.R., Boutillier, J., Ratnasingham, S., Dooh, R.T., Hajibabael, M., and Hebert, P.D.N. 2007. Biological identification through DNA barcodes: the case of the Crustacea. *Canadian Journal of Fisheries & Aquatic Sciences* **64**, 272–295.

Edgar, R.C. 2004. MUSCLE: multiple sequence alignment with high accuracy and high throughput. *Nucleic Acids Research* **32**, 1792–1797.

Folmer, O., Black, M., Hoen, W., Lutz, R., and Vrijenhoek, R. 1994. DNA primers for amplification of mitochondrial cytochrome c oxidase subunit I from diverse metazoan invertebrates. *Molecular Marine Biology and Biotechnology* **3**, 294–299.

Gan, H.U., Gan, H.M., Lee, Y.P., and Austin, C.M. 2016. The complete mitogenome of the Australian freshwater shrimp *Paratya australiensis* Kemp, 1917 (Crustacea: Decapoda: Atyidae). *Mitochondrial DNA Part A* **27**, 3157–3158.

Hancock, M.A. 1998. The relationship between egg size and embryonic and larval development in the freshwater shrimp *Paratya australiensis* Kemp (Decapoda: Atyidae). *Freshwater Biology* **39**(4), 715–723.

Supplementary material

Supplementary Table 1: GenBank sequence data used as a genetic backbone for the morphological examination of lineages. GenBank accession number, source publication and new species determination for the sequences.

Sequence	Group	Species determination	Publication source
EU251947 1 McClusky haplotype D9	McClusky D	*P. gariwerdensis*	McCluskey unpublished thesis 2
EU251946 1 McClusky haplotype D8	McClusky D	*P. gariwerdensis*	McCluskey unpublished thesis 2
EU251945 1 McClusky haplotype D7	McClusky D	*P. gariwerdensis*	McCluskey unpublished thesis 2
EU251944 1 McClusky haplotype D6	McClusky D	*P. gariwerdensis*	McCluskey unpublished thesis 2
EU251943 1 McClusky haplotype D5	McClusky D	*P. gariwerdensis*	McCluskey unpublished thesis 2
EU251942 1 McClusky haplotype D4	McClusky D	*P. gariwerdensis*	McCluskey unpublished thesis 2
EU251941 1 McClusky haplotype D3	McClusky D	*P. gariwerdensis*	McCluskey unpublished thesis 2
EU251940 1 McClusky haplotype D2	McClusky D	*P. gariwerdensis*	McCluskey unpublished thesis 2
EU251939 1 McClusky haplotype D12	McClusky D	*P. gariwerdensis*	McCluskey unpublished thesis 2
EU251938 1 McClusky haplotype D11	McClusky D	*P. gariwerdensis*	McCluskey unpublished thesis 2
EU251937 1 McClusky haplotype D10	McClusky D	*P. gariwerdensis*	McCluskey unpublished thesis 2
EU251936 1 McClusky haplotype D1	McClusky D	*P. gariwerdensis*	McCluskey unpublished thesis 2
EU251935 1 McClusky haplotype C7	McClusky C/Cook 4	*P. arrostra*	McCluskey unpublished thesis 2
EU251934 1 McClusky haplotype C6	McClusky C/Cook 4	*P. arrostra*	McCluskey unpublished thesis 2
EU251933 1 McClusky haplotype C5	McClusky C/Cook 4	*P. arrostra*	McCluskey unpublished thesis 2
EU251932 1 McClusky haplotype C4	McClusky C/Cook 4	*P. arrostra*	McCluskey unpublished thesis 2
EU251931 1 McClusky haplotype C3	McClusky C/Cook 4	*P. arrostra*	McCluskey unpublished thesis 2
EU251930 1 McClusky haplotype C2	McClusky C/Cook 4	*P. arrostra*	McCluskey unpublished thesis 2
EU251929 1 McClusky haplotype C1	McClusky C/Cook 4	*P. arrostra*	McCluskey unpublished thesis 2
EU251928 1 McClusky haplotype B9	Lineage C Baker/Cook 8/McClusky B	*P. tasmaniensis*	McCluskey unpublished thesis 2
EU251927 1 McClusky haplotype B8	Lineage C Baker/Cook 8/McClusky B	*P. tasmaniensis*	McCluskey unpublished thesis 2
EU251926 1 McClusky haplotype B7	Lineage C Baker/Cook 8/McClusky B	*P. tasmaniensis*	McCluskey unpublished thesis 2
EU251925 1 McClusky haplotype B6	Lineage C Baker/Cook 8/McClusky B	*P. tasmaniensis*	McCluskey unpublished thesis 2
EU251924 1 McClusky haplotype B5	Lineage C Baker/Cook 8/McClusky B	*P. tasmaniensis*	McCluskey unpublished thesis 2
EU251923 1 McClusky haplotype B4	Lineage C Baker/Cook 8/McClusky B	*P. tasmaniensis*	McCluskey unpublished thesis 2
EU251922 1 McClusky haplotype B3	Lineage C Baker/Cook 8/McClusky B	*P. tasmaniensis*	McCluskey unpublished thesis 2
EU251921 1 McClusky haplotype B2	Lineage C Baker/Cook 8/McClusky B	*P. tasmaniensis*	McCluskey unpublished thesis 2
EU251920 1 McClusky haplotype B16	Lineage C Baker/Cook 8/McClusky B	*P. tasmaniensis*	McCluskey unpublished thesis 2
EU251919 1 McClusky haplotype B15	Lineage C Baker/Cook 8/McClusky B	*P. tasmaniensis*	McCluskey unpublished thesis 2
EU251918 1 McClusky haplotype B14	Lineage C Baker/Cook 8/McClusky B	*P. tasmaniensis*	McCluskey unpublished thesis 2
EU251917 1 McClusky haplotype B13	Lineage C Baker/Cook 8/McClusky B	*P. tasmaniensis*	McCluskey unpublished thesis 2
EU251916 1 McClusky haplotype B12	Lineage C Baker/Cook 8/McClusky B	*P. tasmaniensis*	McCluskey unpublished thesis 2
EU251915 1 McClusky haplotype B11	Lineage C Baker/Cook 8/McClusky B	*P. tasmaniensis*	McCluskey unpublished thesis 2
EU251914 1 McClusky haplotype B10	Lineage C Baker/Cook 8/McClusky B	*P. tasmaniensis*	McCluskey unpublished thesis 2
EU251913 1 McClusky haplotype B1	Lineage C Baker/Cook 8/McClusky B	*P. tasmaniensis*	McCluskey unpublished thesis 2
EU251912 1 McClusky haplotype A6	Lineage B BakerMcClusky A/Cook 6	*P. whitemae*	McCluskey unpublished thesis 2
EU251911 1 McClusky haplotype A5	Lineage B BakerMcClusky A/Cook 6	*P. whitemae*	McCluskey unpublished thesis 2
EU251910 1 McClusky haplotype A4	Lineage B BakerMcClusky A/Cook 6	*P. whitemae*	McCluskey unpublished thesis 2
EU251909 1 McClusky haplotype A3	Lineage B BakerMcClusky A/Cook 6	*P. whitemae*	McCluskey unpublished thesis 2
EU251908 1 McClusky haplotype A2	Lineage B BakerMcClusky A/Cook 6	*P. whitemae*	McCluskey unpublished thesis 2
EU251907 1 McClusky haplotype A1	Lineage B BakerMcClusky A/Cook 6	*P. whitemae*	McCluskey unpublished thesis 2
EF076817 1 Cook HAPY	McClusky C/Cook 4	*P. arrostra*	McCluskey unpublished thesis 2
EF076816 1 Cook HAPF	McClusky C/Cook 4	*P. arrostra*	McCluskey unpublished thesis 2
EF076815 1 Cook HAPQ	McClusky C/Cook 4	*P. arrostra*	McCluskey unpublished thesis 2
EF076814 1 Cook HAPS	McClusky C/Cook 4	*P. arrostra*	McCluskey unpublished thesis 2

Sequence	Group	Species determination	Publication source
EF076813 1 Cook HAPR	McClusky C/Cook 4	*P. arrostra*	McCluskey unpublished thesis 2
EF076812 1 Cook HAPG	McClusky C/Cook 4	*P. arrostra*	McCluskey unpublished thesis 2
EF076811 1 Cook HAPO	McClusky C/Cook 4	*P. arrostra*	McCluskey unpublished thesis 2
EF076810 1 Cook HAPZ	McClusky C/Cook 4	*P. arrostra*	McCluskey unpublished thesis 2
EF076809 1 Cook HAPE	McClusky C/Cook 4	*P. arrostra*	McCluskey unpublished thesis 2
EF076808 1 Cook HAPC	Lineage C Baker/Cook 8/McClusky B	*P. tasmaniensis*	McCluskey unpublished thesis 2
EF076807 1 Cook HAPOO	Lineage C Baker/Cook 8/McClusky B	*P. tasmaniensis*	McCluskey unpublished thesis 2
EF076806 1 Cook HAPI	Lineage C Baker/Cook 8/McClusky B	*P. tasmaniensis*	McCluskey unpublished thesis 2
EF076805 1 Cook HAPD	Lineage C Baker/Cook 8/McClusky B	*P. tasmaniensis*	McCluskey unpublished thesis 2
EF076804 1 Cook HAPH	Lineage C Baker/Cook 8/McClusky B	*P. tasmaniensis*	McCluskey unpublished thesis 2
EF076803 1 Cook HAPL	Lineage C Baker/Cook 8/McClusky B	*P. tasmaniensis*	McCluskey unpublished thesis 2
EF076802 1 Cook HAPMM	Lineage C Baker/Cook 8/McClusky B	*P. tasmaniensis*	McCluskey unpublished thesis 2
EF076801 1 Cook HAPM	Lineage C Baker/Cook 8/McClusky B	*P. tasmaniensis*	McCluskey unpublished thesis 2
EF076800 1 Cook HAPP	Lineage C Baker/Cook 8/McClusky B	*P. tasmaniensis*	McCluskey unpublished thesis 2
EF076799 1 Cook HAPB	Lineage C Baker/Cook 8/McClusky B	*P. tasmaniensis*	McCluskey unpublished thesis 2
EF076798 1 Cook HAPA	McClusky C/Cook 4	*P. arrostra*	McCluskey unpublished thesis 2
AY641791 1 Baker haplotype 33	Cook 7	*P. arrostra*	Cook et al. (2006)
AY641790 1 Baker haplotype 32	Cook 7	*P. arrostra*	Cook et al. (2006)
AY641789 1 Baker haplotype 63	Lineage C Baker/Cook 8/McClusky B	*P. tasmaniensis*	Cook et al. (2006)
AY641788 1 Baker haplotype 56	Lineage C Baker/Cook 8/McClusky B	*P. tasmaniensis*	Cook et al. (2006)
AY641787 1 Baker haplotype 55	Lineage C Baker/Cook 8/McClusky B	*P. tasmaniensis*	Cook et al. (2006)
AY641786 1 Baker haplotype 54	Lineage C Baker/Cook 8/McClusky B	*P. tasmaniensis*	Cook et al. (2006)
AY641785 1 Baker haplotype 62	Lineage C Baker/Cook 8/McClusky B	*P. tasmaniensis*	Cook et al. (2006)
AY641784 1 Baker haplotype 58	Lineage C Baker/Cook 8/McClusky B	*P. tasmaniensis*	Cook et al. (2006)
AY641783 1 Baker haplotype 66	Lineage C Baker/Cook 8/McClusky B	*P. tasmaniensis*	Cook et al. (2006)
AY641782 1 Baker haplotype 65	Lineage C Baker/Cook 8/McClusky B	*P. tasmaniensis*	Cook et al. (2006)
AY641781 1 Baker haplotype 81	Lineage B BakerMcClusky A/Cook 6	*P. whitemae*	Cook et al. (2006)
AY641780 1 Baker haplotype 82	Lineage B BakerMcClusky A/Cook 6	*P. whitemae*	Cook et al. (2006)
AY641779 1 Baker haplotype 118	McClusky C/Cook 4	*P. arrostra*	Cook et al. (2006)
AY641778 1 Baker haplotype 131	McClusky C/Cook 4	*P. arrostra*	Cook et al. (2006)
AY641777 1 Baker haplotype 129	McClusky C/Cook 4	*P. arrostra*	Cook et al. (2006)
AY641776 1 Baker haplotype 130	McClusky C/Cook 4	*P. arrostra*	Cook et al. (2006)
AY641775 1 Baker haplotype 128	McClusky C/Cook 4	*P. arrostra*	Cook et al. (2006)
AY641774 1 Baker haplotype 108	McClusky C/Cook 4	*P. arrostra*	Cook et al. (2006)
AY641773 1 Baker haplotype 116	McClusky C/Cook 4	*P. arrostra*	Cook et al. (2006)
AY641772 1 Baker haplotype 106	McClusky C/Cook 4	*P. arrostra*	Cook et al. (2006)
AY641771 1 Baker haplotype 104	McClusky C/Cook 4	*P. arrostra*	Cook et al. (2006)
AY641770 1 Baker haplotype 111	McClusky C/Cook 4	*P. arrostra*	Cook et al. (2006)
AY641769 1 Baker haplotype 114	McClusky C/Cook 4	*P. arrostra*	Cook et al. (2006)
AY641768 1 Baker haplotype 113	McClusky C/Cook 4	*P. arrostra*	Cook et al. (2006)
AY641767 1 Baker haplotype 110	McClusky C/Cook 4	*P. arrostra*	Cook et al. (2006)
AY308175 1 Baker isolate P1GC1	Cook 9	*P. rouxi*	Cook et al. (2006)
AY308174 1 Baker isolate SHC33	Lineage D Baker/Cook 5	*P.williamsi*	Cook et al. (2006)
AY308173 1 Baker isolate BC372	Cook 7	*P. strathbogiensis*	Cook et al. (2006)
AY308172 1 Baker isolate TR51	Lineage D Baker/Cook 5	*P.williamsi*	Cook et al. (2006)
AY308171 1 Baker isolate BC370	Cook 7	*P. strathbogiensis*	Cook et al. (2006)
AY308170 1 Baker isolate LY5	Lineage C Baker/Cook 8/McClusky B	*P. tasmaniensis*	Cook et al. (2006)
AY308169 1 Baker isolate Cro4	McClusky C/Cook 4	*P. arrostra*	Cook et al. (2006)
AY308168 1 Baker isolate NCK3	McClusky C/Cook 4	*P. arrostra*	Cook et al. (2006)

Sequence	Group	Species determination	Publication source
AY308167 1 Baker isolate SHA3	Lineage C Baker/Cook 8/McClusky B	*P. tasmaniensis*	Cook et al. (2006)
AY308166 1 Baker isolate TWR2	Lineage C Baker/Cook 8/McClusky B	*P. tasmaniensis*	Cook et al. (2006)
AY308165 1 Baker isolate RY6	Cook 2	*P.walkeri*	Cook et al. (2006)
AY308164 1 Baker isolate LY6	Lineage C Baker/Cook 8/McClusky B	*P. tasmaniensis*	Cook et al. (2006)
AY308163 1 Baker isolate 3Mo1	McClusky C/Cook 4	*P. arrostra*	Cook et al. (2006)
AY308162 1 Baker isolate SHA4	Lineage C Baker/Cook 8/McClusky B	*P. tasmaniensis*	Cook et al. (2006)
AY308161 1 Baker isolate KN3	Cook 3	*P. spinosa*	Cook et al. (2006)
AY308160 1 Baker isolate GCK5	Lineage C Baker/Cook 8/McClusky B	*P. tasmaniensis*	Cook et al. (2006)
AY308159 1 Baker isolate NCK4	McClusky C/Cook 4	*P. arrostra*	Cook et al. (2006)
AY308158 1 Baker isolate TWR1	Lineage C Baker/Cook 8/McClusky B	*P. tasmaniensis*	Cook et al. (2006)
AY308157 1 Baker isolate WR3	McClusky C/Cook 4	*P. arrostra*	Cook et al. (2006)
AY308156 1 Baker isolate JCK2	Lineage B BakerMcClusky A/Cook 6	*P. whitemae*	Cook et al. (2006)
AY308155 1 Baker isolate WR1	McClusky C/Cook 4	*P. arrostra*	Cook et al. (2006)
AY308154 1 Baker isolate GIN1	McClusky C/Cook 4	*P. arrostra*	Cook et al. (2006)
AY308153 1 Baker isolate MCK3	McClusky C/Cook 4	*P. arrostra*	Cook et al. (2006)
AY308152 1 Baker isolate PR1	McClusky C/Cook 4	*P. arrostra*	Cook et al. (2006)
AY308151 1 Baker isolate RY5	Cook 2	*P.walkeri*	Cook et al. (2006)
AY308150 1 Baker isolate RY2	Cook 2	*P.walkeri*	Cook et al. (2006)
AY308149 1 Baker isolate PR2	McClusky C/Cook 4	*P. arrostra*	Cook et al. (2006)
AY308148 1 Baker isolate BC112	Lineage C Baker/Cook 8/McClusky B	*P. tasmaniensis*	Cook et al. (2006)
AY308147 1 Baker isolate GIN2	McClusky C/Cook 4	*P. arrostra*	Cook et al. (2006)
AY308146 1 Baker isolate BC113	Lineage C Baker/Cook 8/McClusky B	*P. tasmaniensis*	Cook et al. (2006)
AY308145 1 Baker isolate BC234	Lineage C Baker/Cook 8/McClusky B	*P. tasmaniensis*	Cook et al. (2006)
AY308144 1 Baker isolate MCK1	McClusky C/Cook 4	*P. arrostra*	Cook et al. (2006)
AY308143 1 Baker isolate Vck2	McClusky C/Cook 4	*P. arrostra*	Cook et al. (2006)
AY308142 1 Baker isolate BC141	Lineage C Baker/Cook 8/McClusky B	*P. tasmaniensis*	Cook et al. (2006)
AY308141 1 Baker isolate RY1	Cook 2	*P.walkeri*	Cook et al. (2006)
AY308140 1 Baker isolate DIN2	McClusky C/Cook 4	*P. arrostra*	Cook et al. (2006)
AY308139 1 Baker isolate 85-3	Lineage A Baker/Cook 1	*P.australiensis*	Cook et al. (2006)
AY308138 1 Baker isolate BRLR1	Lineage C Baker/Cook 8/McClusky B	*P. tasmaniensis*	Cook et al. (2006)
AY308137 1 Baker isolate 85-12	Lineage A Baker/Cook 1	*P.australiensis*	Cook et al. (2006)
AY308136 1 Baker isolate TR55	Lineage C Baker/Cook 8/McClusky B	*P. tasmaniensis*	Cook et al. (2006)
AY308135 1 Baker isolate WES1	McClusky C/Cook 4	*P. arrostra*	Cook et al. (2006)
AY308134 1 Baker isolate Vck3	McClusky C/Cook 4	*P. arrostra*	Cook et al. (2006)
AY308133 1 Baker isolate 85-13	Lineage A Baker/Cook 1	*P.australiensis*	Cook et al. (2006)
AY308132 1 Baker isolate BC52	Lineage C Baker/Cook 8/McClusky B	*P. tasmaniensis*	Cook et al. (2006)
AY308131 1 Baker isolate RY3	Cook 2	*P.walkeri*	Cook et al. (2006)
AY308130 1 Baker isolate 011-5	Lineage B BakerMcClusky A/Cook 6	*P. whitemae*	Cook et al. (2006)
AY308129 1 Baker isolate BRHR1	Lineage C Baker/Cook 8/McClusky B	*P. tasmaniensis*	Cook et al. (2006)
AY308128 1 Baker isolate Yan4	McClusky C/Cook 4	*P. arrostra*	Cook et al. (2006)
AY308127 1 Baker isolate 032-2	Lineage B BakerMcClusky A/Cook 6	*P. whitemae*	Cook et al. (2006)
AY308126 1 Baker isolate 85-6	Lineage A Baker/Cook 1	*P.australiensis*	Cook et al. (2006)
AY308125 1 Baker isolate KN5	Cook 3	*P. spinosa*	Cook et al. (2006)
AY308124 1 Baker isolate KN1	Cook 3	*P. spinosa*	Cook et al. (2006)
AY308123 1 Baker isolate ECK1	Lineage B BakerMcClusky A/Cook 6	*P. whitemae*	Cook et al. (2006)
AY308122 1 Baker isolate BR4	Lineage B BakerMcClusky A/Cook 6	*P. whitemae*	Cook et al. (2006)
AY308121 1 Baker isolate LNA1	Lineage B BakerMcClusky A/Cook 6	*P. whitemae*	Cook et al. (2006)
AY308120 1 Baker isolate SHC32	Lineage B BakerMcClusky A/Cook 6	*P. whitemae*	Cook et al. (2006)
AY308119 1 Baker isolate 013-2	Lineage B BakerMcClusky A/Cook 6	*P. whitemae*	Cook et al. (2006)

Sequence	Group	Species determination	Publication source
AY308118 1 Baker isolate 034-3	Lineage B BakerMcClusky A/Cook 6	*P. whitemae*	Cook et al. (2006)
AY308117 1 Baker isolate MUR1	Lineage B BakerMcClusky A/Cook 6	*P. whitemae*	Cook et al. (2006)
AY308116 1 Baker isolate KN2	Cook 3	*P. spinosa*	Cook et al. (2006)
AY308115 1 Baker isolate 032-3	Lineage B BakerMcClusky A/Cook 6	*P. whitemae*	Cook et al. (2006)
AY308114 1 Baker isolate 013-3	Lineage B BakerMcClusky A/Cook 6	*P. whitemae*	Cook et al. (2006)
AY308113 1 Baker isolate BR3	Lineage B BakerMcClusky A/Cook 6	*P. whitemae*	Cook et al. (2006)
AY308112 1 Baker isolate CON4	Lineage B BakerMcClusky A/Cook 6	*P. whitemae*	Cook et al. (2006)
AY308111 1 Baker isolate PAR4	Lineage B BakerMcClusky A/Cook 6	*P. whitemae*	Cook et al. (2006)
AY308110 1 Baker isolate DAL2	Lineage B BakerMcClusky A/Cook 6	*P. whitemae*	Cook et al. (2006)
AY308109 1 Baker isolate S91-2	Lineage B BakerMcClusky A/Cook 6	*P. whitemae*	Cook et al. (2006)
AY308108 1 Baker isolate TR36	Lineage B BakerMcClusky A/Cook 6	*P. whitemae*	Cook et al. (2006)
AY308107 1 Baker isolate NCK1	Lineage B BakerMcClusky A/Cook 6	*P. whitemae*	Cook et al. (2006)
AY308106 1 Baker isolate BC442	Lineage B BakerMcClusky A/Cook 6	*P. whitemae*	Cook et al. (2006)
AY308105 1 Baker isolate H31	Lineage C Baker/Cook 8/McClusky B	*P. tasmaniensis*	Baker et al. (2004)
AY308104 1 Baker isolate H30	Lineage A Baker/Cook 1	*P.australiensis*	Baker et al. (2004)
AY308103 1 Baker isolate H29	Lineage B BakerMcClusky A/Cook 6	*P. whitemae*	Baker et al. (2004)
AY308102 1 Baker isolate H28	Lineage D Baker/Cook 5	*P.williamsi*	Baker et al. (2004)
AY308101 1 Baker isolate H27	Lineage C Baker/Cook 8/McClusky B	*P. tasmaniensis*	Baker et al. (2004)
AY308100 1 Baker isolate H26	Lineage A Baker/Cook 1	*P.australiensis*	Baker et al. (2004)
AY308099 1 Baker isolate H25	Lineage C Baker/Cook 8/McClusky B	*P. tasmaniensis*	Baker et al. (2004)
AY308098 1 Baker isolate H24	Lineage C Baker/Cook 8/McClusky B	*P. tasmaniensis*	Baker et al. (2004)
AY308097 1 Baker isolate H23	Lineage C Baker/Cook 8/McClusky B	*P. tasmaniensis*	Baker et al. (2004)
AY308096 1 Baker isolate H22	Lineage C Baker/Cook 8/McClusky B	*P. tasmaniensis*	Baker et al. (2004)
AY308095 1 Baker isolate H21	Lineage C Baker/Cook 8/McClusky B	*P. tasmaniensis*	Baker et al. (2004)
AY308094 1 Baker isolate H20	Lineage A Baker/Cook 1	*P.australiensis*	Baker et al. (2004)
AY308093 1 Baker isolate H19	Lineage A Baker/Cook 1	*P.australiensis*	Baker et al. (2004)
AY308092 1 Baker isolate H18	Lineage A Baker/Cook 1	*P.australiensis*	Baker et al. (2004)
AY308091 1 Baker isolate H17	Lineage B BakerMcClusky A/Cook 6	*P. whitemae*	Baker et al. (2004)
AY308090 1 Baker isolate H16	Lineage A Baker/Cook 1	*P.australiensis*	Baker et al. (2004)
AY308089 1 Baker isolate H15	Lineage B BakerMcClusky A/Cook 6	*P. whitemae*	Baker et al. (2004)
AY308088 1 Baker isolate H14	Lineage A Baker/Cook 1	*P.australiensis*	Baker et al. (2004)
AY308087 1 Baker isolate H13	Lineage A Baker/Cook 1	*P.australiensis*	Baker et al. (2004)
AY308086 1 Baker isolate H12	Lineage C Baker/Cook 8/McClusky B	*P. tasmaniensis*	Baker et al. (2004)
AY308085 1 Baker isolate H11	Lineage C Baker/Cook 8/McClusky B	*P. tasmaniensis*	Baker et al. (2004)
AY308084 1 Baker isolate H10	Lineage A Baker/Cook 1	*P.australiensis*	Baker et al. (2004)
AY308083 1 Baker isolate H9	Lineage A Baker/Cook 1	*P.australiensis*	Baker et al. (2004)
AY308082 1 Baker isolate H8	Lineage A Baker/Cook 1	*P.australiensis*	Baker et al. (2004)
AY308081 1 Baker isolate H7	Lineage A Baker/Cook 1	*P.australiensis*	Baker et al. (2004)
AY308080 1 Baker isolate H6	Lineage A Baker/Cook 1	*P.australiensis*	Baker et al. (2004)
AY308079 1 Baker isolate H5	Lineage B BakerMcClusky A/Cook 6	*P. whitemae*	Baker et al. (2004)
AY308078 1 Baker isolate H4	Lineage A Baker/Cook 1	*P.australiensis*	Baker et al. (2004)
AY308077 1 Baker isolate H3	Lineage A Baker/Cook 1	*P.australiensis*	Baker et al. (2004)
AY308076 1 Baker isolate H2	Lineage A Baker/Cook 1	*P.australiensis*	Baker et al. (2004)
AY308075 1 Baker isolate H1	Lineage A Baker/Cook 1	*P.australiensis*	Baker et al. (2004)
AF534904 1 Hurwood Pa11	Lineage B BakerMcClusky A/Cook 6	*P. whitemae*	Hurwood et al. (2003)
AF534903 1 Hurwood Pa10	Lineage B BakerMcClusky A/Cook 6	*P. whitemae*	Hurwood et al. (2003)
AF534902 1 Hurwood Pa9	Lineage B BakerMcClusky A/Cook 6	*P. whitemae*	Hurwood et al. (2003)
AF534901 1 Hurwood Pa8	McClusky C/Cook 4	*P. arrostra*	Hurwood et al. (2003)
AF534900 1 Hurwood Pa7	McClusky C/Cook 4	*P. arrostra*	Hurwood et al. (2003)

Sequence	Group	Species determination	Publication source
AF534899 1 Hurwood Pa6	McClusky C/Cook 4	*P. arrostra*	Hurwood et al. (2003)
AF534898 1 Hurwood Pa5	McClusky C/Cook 4	*P. arrostra*	Hurwood et al. (2003)
AF534897 1 Hurwood Pa4	McClusky C/Cook 4	*P. arrostra*	Hurwood et al. (2003)
AF534896 1 Hurwood Pa3	McClusky C/Cook 4	*P. arrostra*	Hurwood et al. (2003)
AF534895 1 Hurwood Pa2	McClusky C/Cook 4	*P. arrostra*	Hurwood et al. (2003)
AF534894 1 Hurwood Pa1	McClusky C/Cook 4	*P. arrostra*	Hurwood et al. (2003)
AY622605 1 Paratya howensis	Paratya outgroup		
AY661487 1 Paratya curvirostris	Paratya outgroup		
AY661488 1 Paratya compressa	Paratya outgroup		
AY661489 1 Paratya compressa	Paratya outgroup		
AY661490 1 Paratya compressa	Paratya outgroup		
AY661491 1 Paratya compressa	Paratya outgroup		
AY661492 1 Paratya norfolkensis	Paratya outgroup		
AY661493 1 Caridina indistincta	Caradina		
AY661494 1 Caridina cf imitatrix	Caradina		
AY661495 1 Paratya cf caledonica	Paratya outgroup		
AY661496 1 Paratya cf caledonica	Paratya outgroup		
AY6614981 Paratya cf caledonica	Paratya outgroup		
AY661499 1 Paratya cf intermedia	Paratya outgroup		
AY661500 1 Paratya cf intermedia	Paratya outgroup		
AY661501 1 Paratya cf intermedia	Paratya outgroup		
0L420759 JWA2019	Lineage B BakerMcClusky A/Cook 6	*P. whitemae*	This study
OL420760 JWA2020	Lineage B BakerMcClusky A/Cook 6	*P. whitemae*	This study
OL420761 JWA2023	Lineage B BakerMcClusky A/Cook 6	*P. whitemae*	This study
OL420762 JWA2026	McClusky C/Cook 4	*P. arrostra*	This study
OL420763 JWA2027	Lineage B BakerMcClusky A/Cook 6	*P. whitemae*	This study
OL420764 JWA2028	Lineage B BakerMcClusky A/Cook 6	*P. whitemae*	This study
OL420765 JWA2032	McClusky C/Cook 4	*P. arrostra*	This study
OL420766 JWA2033	Lineage B BakerMcClusky A/Cook 6	*P. whitemae*	This study
OL420767 JWA2034	Lineage B BakerMcClusky A/Cook 6	*P. whitemae*	This study
OL420768 JWA2035	Lineage B BakerMcClusky A/Cook 6	*P. whitemae*	This study
OL420769 JWA2036	Lineage B BakerMcClusky A/Cook 6	*P. whitemae*	This study
OL420770 JWA2113	McClusky C/Cook 4	*P. arrostra*	This study
OL420771 JWA2116	McClusky C/Cook 4	*P. arrostra*	This study
OL420772 JWA2118	McClusky C/Cook 4	*P. arrostra*	This study
OL420773 JWA2119	McClusky C/Cook 4	*P. arrostra*	This study
OL420774 JWA2123	McClusky C/Cook 4	*P. arrostra*	This study
OL420775 JWA2125	Lineage B BakerMcClusky A/Cook 6	*P. whitemae*	This study
OL420776 JWA2126	McClusky C/Cook 4	*P. arrostra*	This study
OL420777 JWA2127	McClusky C/Cook 4	*P. arrostra*	This study
OL420778 JWA2129	McClusky C/Cook 4	*P. arrostra*	This study
OL420779 JWA2131	Lineage B BakerMcClusky A/Cook 6	*P. whitemae*	This study
OL420780 JWA2132	Lineage B BakerMcClusky A/Cook 6	*P. whitemae*	This study
OL420781 JWA2135	Lineage B BakerMcClusky A/Cook 6	*P. whitemae*	This study
OL420782 JWA2136	McClusky C/Cook 4	*P. arrostra*	This study
OL420783 JWA2137	McClusky C/Cook 4	*P. arrostra*	This study
OL420784 JWA2138	Lineage B BakerMcClusky A/Cook 6	*P. whitemae*	This study
OL420785 JWA2141	Lineage B BakerMcClusky A/Cook 6	*P. whitemae*	This study
OL420786 JWA2143	McClusky C/Cook 4	*P. arrostra*	This study

Sequence	Group	Species determination	Publication source
OL420787 JWA2144	Lineage B BakerMcClusky A/Cook 6	*P. whitemae*	This study
OL420788 JWA2184	McClusky C/Cook 4	*P. arrostra*	This study
OL420789 JWA2435	McClusky C/Cook 4	*P. arrostra*	This study
OL420790 JWA2436	McClusky C/Cook 4	*P. arrostra*	This study
OL420791 JWA2437	McClusky C/Cook 4	*P. arrostra*	This study
OL420792 JWA2438	McClusky C/Cook 4	*P. arrostra*	This study
OL420793 JWA2439	McClusky C/Cook 4	*P. arrostra*	This study
OL420794 JWA2440	McClusky C/Cook 4	*P. arrostra*	This study
OL420795 JWA2441	McClusky C/Cook 4	*P. arrostra*	This study
OL420796 MC1	McClusky C/Cook 4	*P. arrostra*	This study
OL420797 MC10	McClusky C/Cook 4	*P. arrostra*	This study
OL420798 MC101	McClusky C/Cook 4	*P. arrostra*	This study
OL420799 MC103	Lineage C Baker/Cook 8/McClusky B	*P. tasmaniensis*	This study
OL420800 MC109	Lineage B BakerMcClusky A/Cook 6	*P. tasmaniensis*	This study
OL420801 MC110	Lineage B BakerMcClusky A/Cook 6	*P. whitemae*	This study
OL420802 MC115	Lineage B BakerMcClusky A/Cook 6	*P. tasmaniensis*	This study
OL420803 MC116	Lineage B BakerMcClusky A/Cook 6	*P. tasmaniensis*	This study
OL420804 MC117	Lineage B BakerMcClusky A/Cook 6	*P. tasmaniensis*	This study
OL420805 MC119	Lineage C Baker/Cook 8/McClusky B	*P. tasmaniensis*	This study
OL420806 MC120	Lineage C Baker/Cook 8/McClusky B	*P. tasmaniensis*	This study
OL420807 MC121	Lineage C Baker/Cook 8/McClusky B	*P. tasmaniensis*	This study
OL420808 MC125	Lineage B BakerMcClusky A/Cook 6	*P. whitemae*	This study
OL420809 MC126	Lineage B BakerMcClusky A/Cook 6	*P. whitemae*	This study
OL420810 MC130 F	Cook 7	*P. strathbogiensis*	This study
OL420811 MC133	McClusky C/Cook 4	*P. arrostra*	This study
OL420812 MC134	McClusky C/Cook 4	*P. arrostra*	This study
OL420813 MC135	Cook 9	*P. rouxi*	This study
OL420814 MC136	Cook 9	*P. rouxi*	This study
OL420815 MC137	Cook 9	*P. rouxi*	This study
OL420816 MC138	Cook 9	*P. rouxi*	This study
OL420817 MC14	Cook 3	*P. spinosa*	This study
OL420818 MC17	Cook 3	*P. spinosa*	This study
OL420819 MC2	McClusky C/Cook 4	*P. arrostra*	This study
OL420820 MC20	McClusky C/Cook 4	*P. arrostra*	This study
OL420821 MC21 F	Lineage B BakerMcClusky A/Cook 6	*P. whitemae*	This study
OL420822 MC22	Lineage B BakerMcClusky A/Cook 6	*P. whitemae*	This study
OL420823 MC23	Lineage B BakerMcClusky A/Cook 6	*P. whitemae*	This study
OL420824 MC24	Lineage B BakerMcClusky A/Cook 6	*P. whitemae*	This study
OL420825 MC26	Lineage A Baker/Cook 1	*P. australiensis*	This study
OL420826 MC28	Lineage A Baker/Cook 1	*P. australiensis*	This study
OL420827 MC29	Lineage A Baker/Cook 1	*P. australiensis*	This study
OL420828 MC3	McClusky C/Cook 4	*P. arrostra*	This study
OL420829 MC30	Lineage A Baker/Cook 1	*P. australiensis*	This study
OL420830 MC31	Lineage B BakerMcClusky A/Cook 6	*P. whitemae*	This study
OL420831 MC32	Lineage A Baker/Cook 1	*P. australiensis*	This study
OL420832 MC33	Lineage A Baker/Cook 1	*P. australiensis*	This study
OL420833 MC34	Lineage B BakerMcClusky A/Cook 6	*P. whitemae*	This study
OL420834 MC37	Lineage B BakerMcClusky A/Cook 6	*P. whitemae*	This study
OL420835 MC4	McClusky C/Cook 4	*P. arrostra*	This study

Sequence	Group	Species determination	Publication source
OL420836 MC40	Cook 7	*P. strathbogiensis*	This study
OL420837 MC41	McClusky C/Cook 4	*P. arrostra*	This study
OL420838 MC42	Cook 7	*P. strathbogiensis*	This study
OL420839 MC43	Cook 7	*P. strathbogiensis*	This study
OL420840 MC46	Cook 7	*P. strathbogiensis*	This study
OL420841 MC47	Cook 7	*P. strathbogiensis*	This study
OL420842 MC48	Cook 7	*P. strathbogiensis*	This study
OL420843 MC49	Cook 7	*P. strathbogiensis*	This study
OL420844 MC52	Cook 7	*P. strathbogiensis*	This study
OL420845 MC53	Cook 7	*P. strathbogiensis*	This study
OL420846 MC54	Cook 7	*P. strathbogiensis*	This study
OL420847 MC63	McClusky C/Cook 4	*P. arrostra*	This study
OL420848 MC66	McClusky C/Cook 4	*P. arrostra*	This study
OL420849 MC672	Cook 9	*P. rouxi*	This study
OL420850 MC70	Lineage C Baker/Cook 8/McClusky B	*P. tasmaniensis*	This study
OL420851 MC71	Lineage C Baker/Cook 8/McClusky B	*P. tasmaniensis*	This study
OL420852 MC72	Lineage C Baker/Cook 8/McClusky B	*P. tasmaniensis*	This study
OL420853 MC73	Lineage C Baker/Cook 8/McClusky B	*P. tasmaniensis*	This study
OL420854 MC74	Lineage C Baker/Cook 8/McClusky B	*P. tasmaniensis*	This study
OL420855 MC75	Lineage C Baker/Cook 8/McClusky B	*P. tasmaniensis*	This study
OL420856 MC76	Lineage C Baker/Cook 8/McClusky B	*P. tasmaniensis*	This study
OL420857 MC78	Lineage C Baker/Cook 8/McClusky B	*P. tasmaniensis*	This study
OL420858 MC79	Lineage C Baker/Cook 8/McClusky B	*P. tasmaniensis*	This study
OL420859 MC80	Lineage C Baker/Cook 8/McClusky B	*P. tasmaniensis*	This study
OL420860 MC82	McClusky C/Cook 4	*P. arrostra*	This study
OL420861 MC83	Cook 9	*P. rouxi*	This study
OL420862 MC84	Cook 9	*P. rouxi*	This study
OL420863 MC86	McClusky C/Cook 4	*P. arrostra*	This study
OL420864 MC87	McClusky C/Cook 4	*P. arrostra*	This study
OL420865 MC88	McClusky C/Cook 4	*P. arrostra*	This study
OL420866 MC89	McClusky C/Cook 4	*P. arrostra*	This study
OL420867 MC9	McClusky C/Cook 4	*P. arrostra*	This study
OL420868 MC90	Lineage B BakerMcClusky A/Cook 6	*P. whitemae*	This study
OL420869 MC90 F8	McClusky C/Cook 4	*P. arrostra*	This study
OL420870 MC91	McClusky C/Cook 4	*P. arrostra*	This study
OL420871 MC95	Lineage B BakerMcClusky A/Cook 6	*P. whitemae*	This study
OL420872 MC97	Lineage B BakerMcClusky A/Cook 6	*P. whitemae*	This study
OL420873 MC98	Lineage B BakerMcClusky A/Cook 6	*P. whitemae*	This study
OL420874 MC99	Lineage B BakerMcClusky A/Cook 6	*P. whitemae*	This study
OL420875 PJ1	Lineage A Baker/Cook 1	*P. australiensis*	This study
OL420876 PJ2	Lineage A Baker/Cook 1	*P. australiensis*	This study
OL420877 PJ3	Lineage A Baker/Cook 1	*P. australiensis*	This study
OL420878 PJ4	Lineage A Baker/Cook 1	*P. australiensis*	This study
OL420879 PJ5	McClusky C/Cook 4	*P. arrostra*	This study
OL420880 PJ6	McClusky C/Cook 4	*P. arrostra*	This study
OL420881 PS100	Lineage C Baker/Cook 8/McClusky B	*P. tasmaniensis*	This study
OL420882 PS101	McClusky C/Cook 4	*P. arrostra*	This study
OL420883 PS102	Lineage D Baker/Cook 5	*P. williamsi*	This study
OL420884 PS103	Lineage D Baker/Cook 5	*P. williamsi*	This study

Sequence	Group	Species determination	Publication source
OL420885 PS104	Lineage B BakerMcClusky A/Cook 6	*P. whitemae*	This study
OL420886 PS105	Lineage D Baker/Cook 5	*P. williamsi*	This study
OL420887 PS106	Lineage C Baker/Cook 8/McClusky B	*P. tasmaniensis*	This study
OL420888 PS107	Lineage C Baker/Cook 8/McClusky B	*P. tasmaniensis*	This study
OL420889 PS108	Lineage C Baker/Cook 8/McClusky B	*P. tasmaniensis*	This study
OL420890 PS109	Lineage C Baker/Cook 8/McClusky B	*P. tasmaniensis*	This study
OL420891 PS110	Lineage C Baker/Cook 8/McClusky B	*P. tasmaniensis*	This study
OL420892 PS111	Lineage C Baker/Cook 8/McClusky B	*P. tasmaniensis*	This study
OL420893 PS112	Lineage C Baker/Cook 8/McClusky B	*P. tasmaniensis*	This study
OL420894 PS113	Lineage B BakerMcClusky A/Cook 6	*P. whitemae*	This study
OL420895 PS114	Lineage C Baker/Cook 8/McClusky B	*P. tasmaniensis*	This study
OL420896 PS115	Lineage C Baker/Cook 8/McClusky B	*P. tasmaniensis*	This study
OL420897 PS116	Lineage B BakerMcClusky A/Cook 6	*P. whitemae*	This study
OL420898 PS117	Lineage B BakerMcClusky A/Cook 6	*P. whitemae*	This study
OL420899 PS12	Cook 2	*P. walkeri*	This study
OL420900 PS14	Lineage B BakerMcClusky A/Cook 6	*P. whitemae*	This study
OL420901 PS15	Lineage B BakerMcClusky A/Cook 6	*P. whitemae*	This study
OL420902 PS16	Lineage B BakerMcClusky A/Cook 6	*P. whitemae*	This study
OL420903 PS18	Lineage B BakerMcClusky A/Cook 6	*P. whitemae*	This study
OL420904 PS20	Lineage B BakerMcClusky A/Cook 6	*P. whitemae*	This study
OL420905 PS22	McClusky C/Cook 4	*P. arrostra*	This study
OL420906 PS24	Lineage B BakerMcClusky A/Cook 6	*P. whitemae*	This study
OL420907 PS25	Lineage A Baker/Cook 1	*P. australiensis*	This study
OL420908 PS26	Lineage B BakerMcClusky A/Cook 6	*P. whitemae*	This study
OL420909 PS27	Lineage A Baker/Cook 1	*P. australiensis*	This study
OL420910 PS28	Lineage A Baker/Cook 1	*P. australiensis*	This study
OL420911 PS29	Lineage A Baker/Cook 1	*P. australiensis*	This study
OL420912 PS4	McClusky C/Cook 4	*P. arrostra*	This study
OL420913 PS40	McClusky D	*P. gariwerdensis*	This study
OL420914 PS41	McClusky D	*P. gariwerdensis*	This study
OL420915 PS43	McClusky D	*P. gariwerdensis*	This study
OL420916 PS44	McClusky D	*P. gariwerdensis*	This study
OL420917 PS45	Lineage C Baker/Cook 8/McClusky B	*P. tasmaniensis*	This study
OL420918 PS46	McClusky D	*P. gariwerdensis*	This study
OL420919 PS47	Lineage C Baker/Cook 8/McClusky B	*P. tasmaniensis*	This study
OL420920 PS48	Lineage C Baker/Cook 8/McClusky B	*P. tasmaniensis*	This study
OL420921 PS49	Lineage C Baker/Cook 8/McClusky B	*P. tasmaniensis*	This study
OL420922 PS50	Lineage C Baker/Cook 8/McClusky B	*P. tasmaniensis*	This study
OL420923 PS51	McClusky D	*P. gariwerdensis*	This study
OL420924 PS53	McClusky D	*P. gariwerdensis*	This study
OL420925 PS54	McClusky D	*P. gariwerdensis*	This study
OL420926 PS55	McClusky D	*P. gariwerdensis*	This study
OL420927 PS6	Lineage B BakerMcClusky A/Cook 6	*P. whitemae*	This study
OL420928 PS7	Lineage B BakerMcClusky A/Cook 6	*P. whitemae*	This study
OL420929 PS8	Cook 2	*P. walkeri*	This study
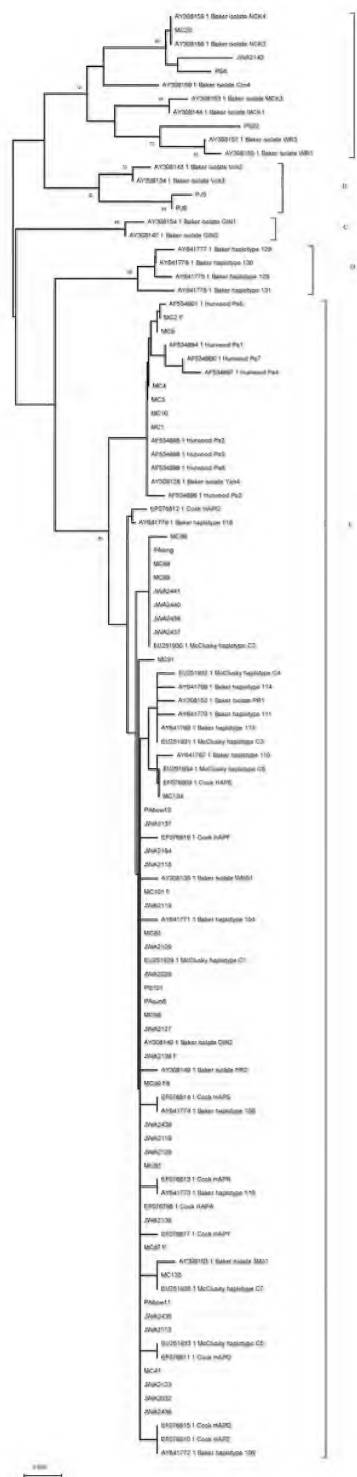
Supplementary Figure 1: Expanded sub-tree for *Paratya arrostra* Riek from fig. 3 in text.
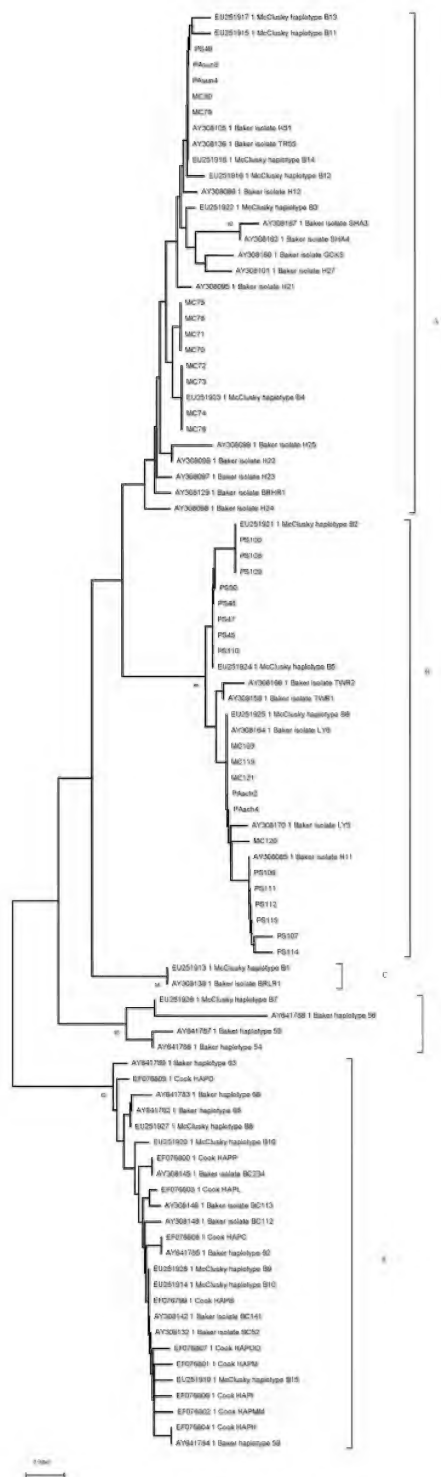
Supplementary Figure 2: Expanded sub-tree for *Paratya tasmaniensis* Riek from fig. 4 in text.
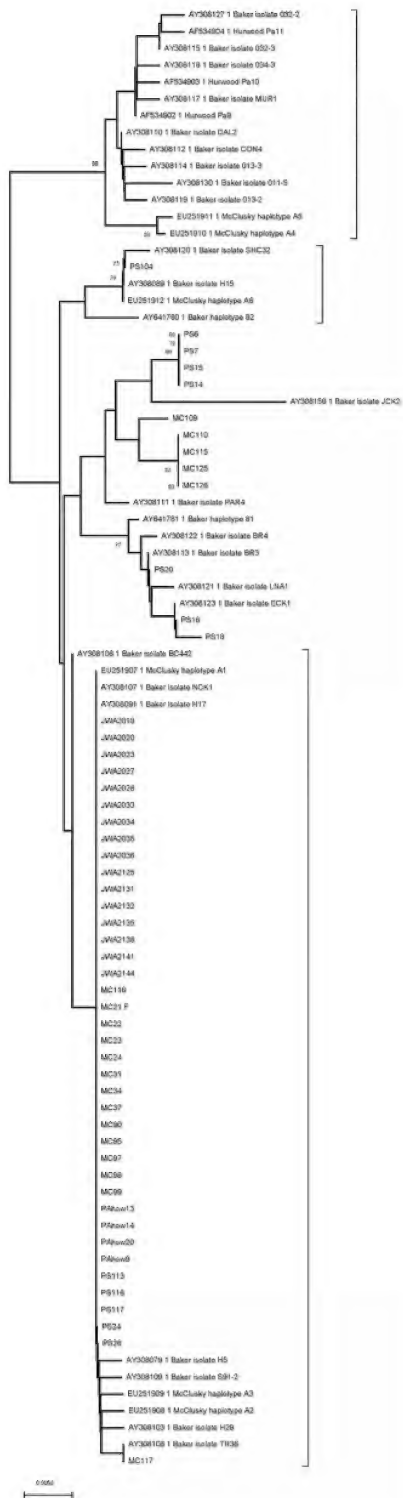
Supplementary Figure 3: Expanded sub-tree for *Paratya whitemae* n.sp.

Articullichirus, a new genus of ghost shrimp (Crustacea: Axiidea: Callichiridae) with one new species

(http://zoobank.org/urn:lsid:zoobank.org:pub:449E07EF-3824-4B86-87CA-D8433AF0D166)

GARY C.B. POORE[1], PETER C. DWORSCHAK[2] AND KAREEN E. SCHNABEL[3]

[1] Museums Victoria, GPO Box 666, Melbourne, Vic. 3001, Australia [gpoore@museum.vic.gov.au] (http://zoobank.org/urn:lsid:zoobank.org:author:c004d784-e842-42b3-bfd3-317d359f8975; https://orcid.org/0000-0002-7414-183X)
[2] Dritte Zoologische Abteilung, Naturhistorisches Museum, Burgring 7, A-1010 Vienna, Austria [peter.dworschak@nhm-wien.ac.at] (http://zoobank.org/urn:lsid:zoobank.org:author:4BCD9429-46AF-4BDA-BE4B-439EE6ADC657; https://orcid.org/0000-0003-4705-6426)
[3] Coasts and Oceans Centre, National Institute of Water & Atmospheric Research, Private Bag 14901 Kilbirnie, Wellington 6241, New Zealand [kareen.schnabel@niwa.co.nz] (http://zoobank.org/urn:lsid:zoobank.org:author:90CD9E5D-8E26-4E08-8A5F-3263CBE9D6BD; https://orcid.org/0000-0002-9965-9010)

Abstract　　　Poore, G.C.B., Dworschak, P.C., and Schnabel, K.E. 2022. *Articullichirus*, a new genus of ghost shrimp (Crustacea: Axiidea: Callichiridae) with one new species. *Memoirs of Museum Victoria* 81: 123–133.

Articullichirus gen. nov., close to *Corallianassa* Manning, 1987 and *Calliapagurops* de Saint Laurent, 1973, is diagnosed to include *Callianassa articulata* Rathbun, 1906 from Hawaii and French Polynesia, *Callianassa collaroy* Poore and Griffin, 1979 from southern Australia and *Articullichirus chiltoni* sp. nov. from northern New Zealand. Previous records of the two described species from the Indo-West Pacific are reassigned.

Introduction

Callichiridae Manning and Felder, 1991 is one of seven families of callianassid-like Axiidea de Saint Laurent, 1979, most recently reviewed by Poore et al. (2019), whose classification was based on their molecular phylogeny (Robles et al., 2020). *Corallianassa* Manning, 1987, one of its 17 genera, has proved problematic. The question of differences between *Corallianassa*, *Corallichirus* Manning, 1992 and *Glypturus* Stimpson, 1866 was settled by Komai et al. (2015). Manning (1987) was uncertain whether to include *Callianassa articulata* Rathbun, 1906 in *Corallianassa*; this question is investigated here by re-examining this species and two similar others. During this study, it was realised that *Calliapagurops* de Saint Laurent, 1973, a small genus with exceptionally long eyestalks, shares several features with *Corallianassa*. Here, we erect a new genus for *Callianassa articulata* and two others, one new.

Material is lodged in Museums Victoria, Melbourne, Australia (NMV), Canterbury Museum, Christchurch, New Zealand (CMNZ), Muséum national d'Histoire naturelle, Paris, France (MNHN) and Naturhistorisches Museum, Vienna, Austria (NHMW), Bernice P. Bishop Museum, Honolulu, USA (BPBM), and National Museum of Natural History, Washington, D.C., USA (USNM). Size is expressed as carapace length (cl.), including rostrum, in mm. The

diagnosis of the new genus is derived from the same DELTA database (Dallwitz, 2018) used by Poore et al. (2019).

Family Callichiridae Manning and Felder, 1991

Articullichirus gen. nov.

http://zoobank.org/urn:lsid:zoobank.org:act:EB81E6A6-9CF1-4B8B-BF06-3E2440B2A6BA

Type species. *Callianassa articulata* Rathbun, 1906 by present designation.

Diagnosis. Anterior branchiostegal lobe sclerotised, well-produced anteriorly beyond junction with oblique branchiostegal ridge with which it articulates by means of a virtual condyle; rostrum spine-like; anterolateral spines prominent. Pleomere 1 tergite undivided or with weak transverse step. Antennal scaphocerite acute. Maxilliped 3 ischium and merus together ovoid, axial length slightly greater than width at their articulation; crista dentata of few separate spines proximally and toothed ridge distally overlapping proximal margin of merus; propodus about as wide as long, propodus free distal margin nearly transverse. Male major cheliped merus with 3 proximal sharp oblique spines, 1 or more distally along length of lower margin; without spines on upper margin of merus and propodus or lower

margin of carpus. Minor cheliped of male slightly more than half wide as major, carpus slightly shorter than palm, fingers as long as palm; merus lower margin with row of spines. Pereopod 3 propodus subpentagonal, with strong broad proximal lobe on lower margin, lower margin straight. Pereopod 4 subchelate, fixed finger shorter than dactylus. Male pleopod 1 of 2 articles. Male pleopod 2 appendix interna absent. Pleopods 3–5 appendices internae longer than broad, clearly emerging from margin of endopod. Uropodal endopod with convex anterior margin, acute-rounded apex, slightly curved posterior margin, longer than wide; exopod with elevated dorsal plate with row of setae diverging from row of setae on distal margin. Telson wider than long, convex-sided, widest near midpoint, posterior margin concave between rounded posterolateral corners, with transverse row of spiniform setae at midpoint.

Etymology. Alliteration of *articulata*, specific name of the type species, and *Callichirus*, type genus of the family.

Included species. *Callianassa articulata* Rathbun, 1906; *Callianassa collaroy* Poore and Griffin, 1979; *Articullichirus chiltoni* sp. nov.

Remarks. *Callianassa articulata* Rathbun, 1906 was provisionally included in *Corallianassa* by Manning (1987) and Dworschak (1992) and without qualification by Poore et al. (2019). Poupin (1998) argued for its inclusion in *Cheramus* Bate, 1888, a genus now belonging in another family, Callianassidae Dana, 1852. Sakai (1999, 2005, 2011) included the species in *Glypturus* Stimpson, 1866. Dworschak (1992) noted how the telson, without a median posterior prominence, and the more operculiform maxilliped differed from other species of *Corallianassa* (see figures here and in Rathbun, 1906; Edmondson, 1944). *Callianassa collaroy* Poore and Griffin, 1979 has been variously included in *Glypturus* (Sakai, 1988, 2011), *Corallianassa* (Tudge et al., 2000; Davie, 2002; Komai et al., 2015; Poore et al., 2019) and *Neocallichirus* Sakai, 1988 (Sakai, 1999). It was included in Komai et al.'s (2015) thorough review of differences between *Glypturus* and *Corallianassa*, but differences between *C. articulata* and both these genera were not commented on. The discovery of new material of *C. articulata* from French Polynesia, of *C. collaroy* in Australia, and of a similar species from New Zealand, stimulated a reappraisal of specimens from throughout the Pacific identified as one or the other of these two species. Several are misidentified and a new genus is warranted.

Articullichirus resembles *Corallianassa* and *Glypturus* (but not *Neocallichirus*) in the possession of a pair of sharp anterolateral carapace spines. *Articullichirus* differs from both genera in the much broader oval maxilliped 3 (narrow with an oblique meral margin in *Glypturus* and *Corallianassa*); shape of the telson (evenly convex-sided, with concave posterior margin in *Articullichirus*, with semicircular posterior half in *Glypturus*, tapering from greatest width anteriorly in *Corallianassa*); and an acute scaphocerite (small in *Glypturus*, sometimes absent in *Corallianassa*). In addition, *Articullichirus*, like *Corallianassa*, differs from *Glypturus* in the absence of spines along the upper margin of the chelipeds and in having a horizontal rostrum. Komai et al. (2015) noted that the combined length of pleomeres 1 and 2 of at least four

species of *Corallianassa* is greater than or equal to the carapace length, whereas in *G. armatus*, *Corallianassa intesi* (de Saint Laurent and Le Loeuff, 1979) and *Articullichirus collaroy* comb. nov. pleomeres 1 and 2 are shorter than the carapace.

Calliapagurops differs from all callichirids in having exceptionally stout antennae, much more prominent than the antennules; the antennae may be used for suspension feeding (Dworschak and Wirtz, 2010). *Calliapagurops* was placed in its own subfamily Calliapaguropinae by Sakai (1999) but its relationship to Callichiridae was realised by Ngoc-Ho (2002). *Calliapagurops* is notable for exceptionally long eyestalks with terminal cornea, differing from most callichirids that have more or less flattened eyestalks with subterminal cornea and a mesiodistal lobe (Ngoc-Ho, 2002; Dworschak and Wirtz, 2010). While the eyestalks of species of *Corallianassa*, *Glypturus* and *Articullichirus* are much shorter, the cornea is terminal with only a small mesiodistal lobe. *Calliapagurops* and these three genera all have sharp prominent anterolateral carapace spines that, with the sharp rostrum, have more or less weakly calcified bases. Species of *Articullichirus* resemble the two recognised species of *Calliapagurops*. The oval telson with a transverse row of robust setae is similar to that of *Articullichirus*, quite different from those of *Corallianassa* and *Glypturus*. The chelipeds of *Calliapagurops* are generally similar to those of *Articullichirus*; the coxae carry a pair of mesial hooks as in *A. collaroy* and *A. chiltoni*, but these are absent in *A. articulatus*. The uropodal endopod of *Calliapagurops* bears two proximal teeth on the dorsal surface similar to those seen in most species of *Articullichirus*, but not seen in the other two genera. The maxilliped of *Calliapagurops* is operculate as in *Articullichirus*, more so than in the other two genera. Its merus bears four distal teeth, whereas some individuals of *A. articulatus* and all those of *A. collaroy* have a single tooth or tubercle; *A. chiltoni* has a tubercle.

Articullichirus articulatus (Rathbun, 1906) comb. nov.

Figures 1, 2

Callianassa articulata Rathbun, 1906: 892, fig. 47.—Manning, 1987: 396.
Callianassa (*Callichirus*) *articulata*.—De Man, 1928: 28, 94, 108.—Edmondson, 1944: 54, fig. 9.
Corallianassa articulata.—Dworschak, 1992: 210, fig. 14.—Tudge et al., 2000: 144.—Komai et al., 2015: 54.—Poore et al., 2019: 136, 144.
Corallianassa collaroy.—Sakai, 1992: 212, fig. 1.
Glypturus articulatus.—Sakai, 2011: 433 (part).
Cheramus articulatus.—Poupin, 1998: 31.
Not *Callianassa articulata*.—Chilton, 1911: 551–552 = *Articullichirus chiltoni* sp. nov.

Material examined. **Hawaii**, Oahu, Honolulu, Harbour Entrance, coll. V. Pietschmann, 1927, NHMW 6621 (ovigerous female, 7.5 mm). **French Polynesia**, Tuamotu, Mataiva, Hoa Papino platier, coll. Mario Monteforte, 1982, MNHN IU-2013-19994 (=Th1232) (female, 7.3 mm).

Material not examined. **Hawaii**, Oahu, Kahala, coll. C.H. Edmondson, 1930–1933, BPBM S4669, S4670, S4671, S4672, S4673, S4674 (6 specimens); Kawailoa, coll. C.H. Edmondson, 1921, BPBM S4668; Hanauma, coll. C.H. Edmondson, 1933, BPBM S4675, S4676 (2); coll. Banner, 1938, S4677 (1); Waikiki, coll. Simon, 1941, BPBM S4678 (1).

Nihoa Island, RV *Albatross*, 48–60 m, USNM 30532 (female, holotype); Nihoa Island, RV *Albatross*, 42–48 m, USNM 30995 (female). Oahu Island, Waikiki, coll. C.H. Edmondson, 1921 USNM 78119 (1).

Size. Cl. to 7.5 mm.

Type locality. USA, Hawaii, 42–60 m.

Diagnosis. Maxilliped 3 basis without mesial tooth or with 2 small mesial teeth; merus with or without small tooth on distal margin. Pereopod 1 coxa with small mesiodistal process with terminal setae. Uropodal endopod midlength about 1.3–1.4 times as long as wide, with tapering apex, with 2 dorsal clusters of setae, with 2 proximal dorsal teeth. Telson 1.4–1.7 times as wide as long, with sinuous posterior margin; with transverse dorsal row of 2 pairs of spiniform setae.

Description of female from Tuamotu (MNHN IU-2013-19994). Carapace length 0.28 of total length; cervical groove at 0.8 length of carapace; dorsal oval well defined; hepatic region with weakly sclerified line between dorsal oval and linea thalassinica. Rostrum and anterolateral carapace spines with unsclerified basal region; rostrum an anteriorly directed, acute spine as long as eyestalk; anterolateral spines set well back from rostrum, acute, one third

as long as rostrum. Anterolateral branchiostegal margin extending dorsal to linea thalassinica, with small separate sclerified plate near beginning of linea thalassinica. Pleomere 1 with weak transverse groove, with dorsolateral longitudinal setal row; pleomere 2 about 1.4 times as long as pleomere 1 tergite; pleomeres 3–5 scarcely expanded laterally, with dense setose areas; pleomere 6 1.2 times as long as pleomere 5, pleomere 6 with posterolateral notch, with pair of lobes on posterior margin.

Eyestalks shorter than first article of antenna 1; with rounded mesiodistal lobe not visible in dorsal view; cornea globular, distally placed. Antennular peduncle reaching two thirds along antennal peduncle article 5. Antennal peduncle with acute scaphocerite. Right maxilliped 3 (left missing) basis with 2 small mesial teeth; ischium with crista dentata of 13 teeth, larger distally; merus width about 0.7 as long as ischium and merus together; merus shorter than ischium, with tooth on free distal margin; carpus articulating distolaterally on merus; propodus as wide as long, expanded as asymmetrical lobe; dactylus one third as wide as propodus, 0.7 times as long.

Pereopods 1 unequal, dissimilar; coxae with small mesiodistal process with terminal setae. Major pereopod 1 (right cheliped) carpus-propodus upper margin 0.8 times carapace length; ischium lower margin with row of 6 spines,
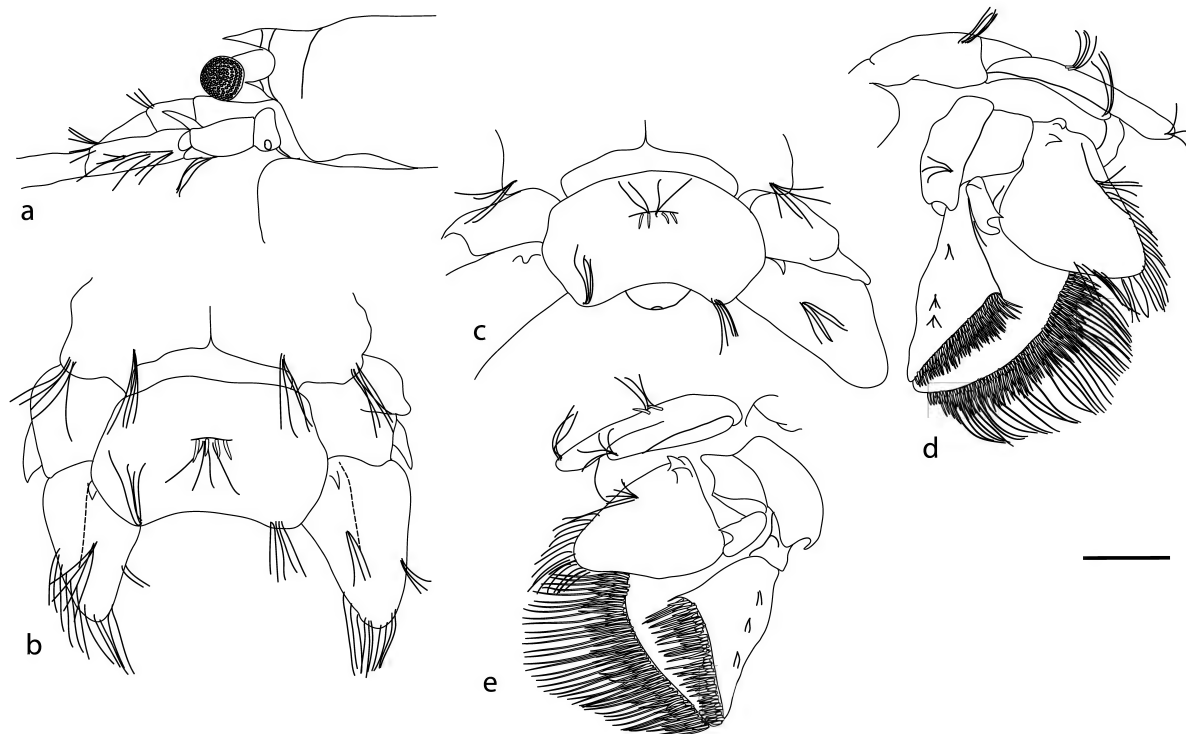

Figure 1. *Articullichirus articulatus* (Rathbun, 1906). Hawaii, NHMW 6621 (ovigerous female, 7.5 mm). a, anterior carapace, eyestalks, antennular peduncle, antennal peduncle; b, c, telson, uropods (depressed); d, left uropod, telson; e, right uropod, telson. Scale bar = 1 mm.
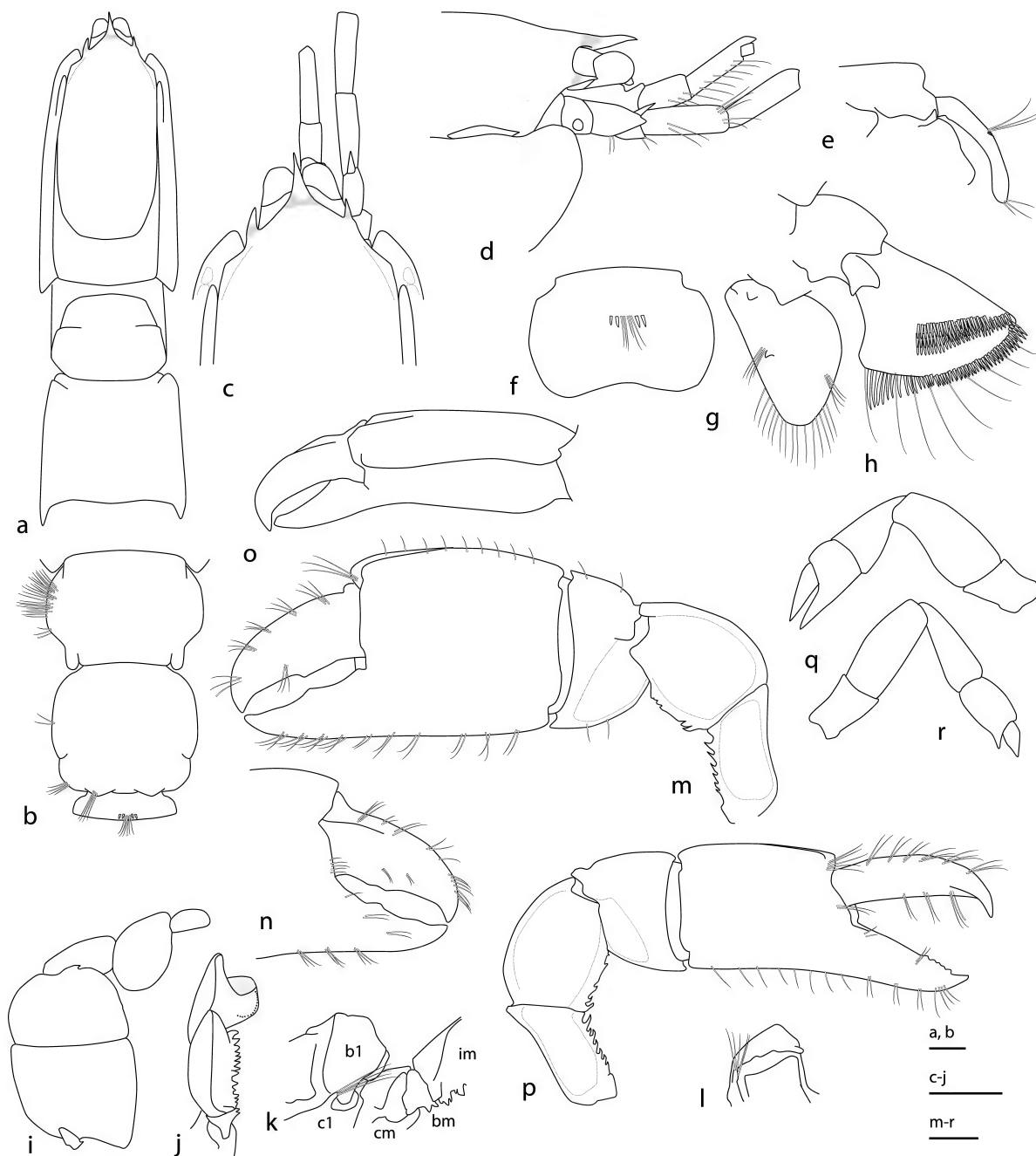
Figure 2. *Articullichirus articulatus* (Rathbun, 1906). French Polynesia, MNHN IU-2013-19994 (female, 7.3 mm). a, carapace, eyestalks, pleomeres 1, 2; b, pleomeres 5, 6, telson (depressed); c, d, anterior carapace, eyestalks, antennular peduncle, antennal peduncle; e, pleomere 6, telson, lateral view; f, telson, dorsal view; g, uropodal endopod, dorsal view; h, uropodal exopod, dorsal view; i, maxilliped 3, outer view; j, right maxilliped 3, coxa to merus, mesial view (palp removed); k, proximal articles of left maxilliped 3 and cheliped in situ, ventral oblique view; l, left cheliped coxa, ventral view; m, right cheliped, mesial view; n, right cheliped fingers, lateral view; o, right cheliped propodus, dactylus, upper view; p, left cheliped; q, pereopod 2; r, pereopod 4. Scale bars = 1 mm. c1, b1, coxa, basis of right cheliped; cm, bm, im, coxa, basis, ischium of maxilliped 3. Scale bars = 1 mm.

larger distally; merus lower margin with 2 proximal teeth followed by irregularly toothed blade, upper margin evenly convex; carpus twice as wide as long, with blunt tooth at end of upper and lower margins; propodus upper margin smooth, with submarginal carina on mesial face, most visible distally, palm 1.1 times as long as wide, distomesial edge straight; fixed finger 0.45 times upper margin, cutting edge with broad tooth at midlength; dactylus stout, slightly longer than fixed finger, with terminal tooth, cutting edge with blunt tooth at midlength; ratio of dorsal lengths, merus: carpus: propodus – 1 : 0.5 : 1.45.

Minor pereopod 1 (left cheliped) about as long as major; ischium lower margin with 7 similar spines; merus lower margin with 3 proximal spines followed by irregularly toothed blade; carpus 1.1 times as wide as long, with tooth at end of upper and lower margins; propodus upper margin 1.2 times as long as greatest width; fixed finger 0.8 times upper margin, cutting edge lateral, crenellate over distal third; dactylus overreaching fixed finger, cutting edge smooth; ratio of dorsal lengths, merus: carpus: propodus – 1 : 0.7 : 1.0.

Uropod endopod 1.5 times as long as wide, anterior margin convex, without setae; posterior margin slightly concave, tapering to a narrowly rounded apex; marginal setae confined to distal and posterodistal margins; upper face with cluster of setae close to posterior margin, few scattered setae near anterior margin, with 2 proximal teeth and another at midlength. Exopod subtriangular, anterior margin straight, posterior margin concave, width 0.7 times anterior margin, upper face with proximal tooth; dorsal plate oblique, well separate from distal margin, armed with imbricating robust setae, posterodistal angle rounded, armed with imbricating robust setae, diminishing along posterior margin.

Telson 1.4 times as wide as long, lateral margins strongly evenly convex, posterior margin concave; with dorsal transverse row of 2 pairs of spiniform setae separated medially by cluster of fine setae; posterolateral margin with row of setae.

Distribution. Eastern Indo-Pacific (Hawaii, French Polynesia); upper shelf.

Remarks. We were unable to examine the holotype at the USNM but have illustrated others. *Articullichirus articulatus* is distinguished from the other two species by its tapering uropodal endopod, narrower in published figures (Rathbun, 1906; Edmondson, 1944) than in our figures. Rathbun (1906) and Edmondson (1944: fig. 9d) noted a meral tooth on maxilliped 3 of specimens from Hawaii, also present on the female from French Polynesia examined by GCBP, but the tooth is absent on NHMW 6621 from Hawaii examined by PCD. Both specimens examined have a submarginal mesial crest on the major cheliped propodus, two pairs of short spiniform setae on the telson and a sharp scaphocerite. The mesial hook on the pereopod 1 coxa (present in *A. collaroy* and *A. chiltoni*) is absent or replaced in the French Polynesian female by a short fingerlike process.

The description above is based on the specimen reported by Poupin (1998). We have not examined the individual from Moorea now in the Senckenburg Museum, Frankfurt, illustrated by Sakai (1992), which we assume to belong to this species.

Articullichirus chiltoni sp. nov.

Figures 3, 4

http://zoobank.org/urn:lsid:zoobank.org:act:5205A319-D237-4CEE-9ABE-6A037685A386

Callianassa articulata.—Chilton, 1911: 551–552.
? *Glypturus articulatus.*—Sakai, 1999: 76–78, fig. 15 (Gilbert Is, Kiribati).
Glypturus collaroy.—Sakai, 2005: 139–141, fig. 29 (New Zealand).

Material examined. Holotype. **New Zealand**, Kermadec Is, Sunday I. [now Raoul I.], rockpool, Captain Bollons, 1907, CMNZ AQ3372 (male, 14.7 mm).

Diagnosis. Maxilliped 3 basis with mesial spine; merus with tubercle on distal margin. Pereopod 1 coxa with mesiodistal hook. Uropodal endopod midlength about 1.5 times as long as wide, with broadly rounded apex, with submarginal dorsal cluster of setae midway along posterior margin, with 1 proximal tooth. Telson 1.4 times as wide as long, with excavate posterior margin; with transverse dorsal row of 12 or 13 pairs of contiguous spiniform setae plus 1 or 2 more lateral.

Description of holotype. Carapace length 0.28 of total length; cervical groove at 0.8 length of carapace; dorsal oval well defined; hepatic region with weakly sclerified line between dorsal oval and linea thalassinica. Rostrum and anterolateral carapace spines with unsclerified basal region; rostrum an anteriorly directed, acute spine nearly as long as eyestalk; anterolateral spines acute, set slightly back from rostrum, half as long as rostrum. Anterolateral branchiostegal lobe margin extending dorsal to linea thalassinica, with sclerified plate below linea thalassinica. Pleomere 1 (damaged) with weak transverse groove, with dorsolateral longitudinal setal row; pleomere 2 about 1.5 times as long as pleomere 1 tergite; pleomeres 3–5 scarcely expanded laterally, with dense setose areas; pleomeres 5 and 6 subequal in length, with posterolateral notch.

Eyestalks shorter than first article of antennular peduncle, without produced mesiodistal apex; cornea globular, distally placed. Antennular peduncle little shorter than antennal peduncle. Antennal peduncle with acute scaphocerite. Right maxilliped 3 (left missing) basis with recurved mesial hook; ischium with distinct crista dentata, teeth diminishing distally; merus width about 0.8 as long as ischium and merus together; merus slightly shorter than ischium, with blunt tooth on free distal margin; carpus articulating distolaterally on merus; propodus slightly wider than long, expanded as round lobe on lower margin; dactylus one third as wide as propodus, 0.7 times as long.

Pereopods 1 unequal, dissimilar; coxae with strong mesial hook. Major pereopod 1 (left cheliped) carpus-propodus upper margin 0.9 times carapace length; ischium lower margin with row of 6 spines, larger distally; merus lower margin with 3 proximal spines, upper margin strongly convex proximally; carpus 1.6 times as wide as long, with blunt tooth at end of upper and lower margins; propodus upper margin smooth, with submarginal carina on mesial face, palm slightly longer than wide, distomesial edge convex; fixed finger 0.5 times upper margin, cutting edge with broad tooth at midlength, proximally serrated; dactylus stout, slightly longer than fixed finger, with terminal tooth, cutting edge slightly concave, with
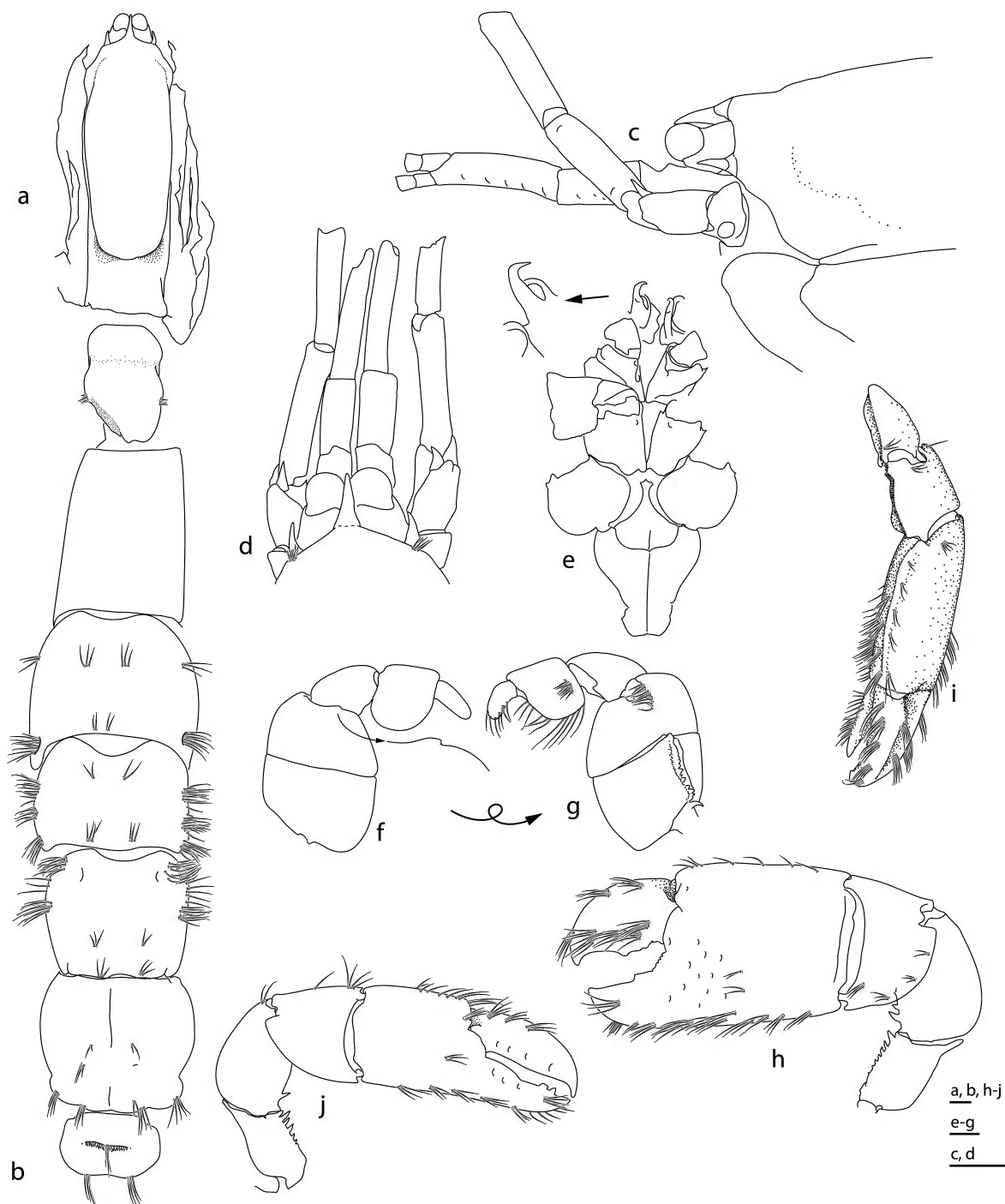
Figure 3. *Articullichirus chiltoni* sp. nov. New Zealand, CMNZ AQ3372 (holotype male, 14.7 mm). a, carapace, eyestalks, dorsal view; b, pleon, telson, dorsal view; c, anterior carapace, pterygostomium, eyestalk, antennular peduncle, antennal peduncle, lateral view; d, anterior carapace, eyestalk, antennular peduncle, antennal peduncle, dorsal view; e, thoracic sternite 7, pereopodal coxae 1–4, detail of right pereopodal coxa 1; f, maxilliped 3, outer view, detail of tooth on upper meral margin; g, maxilliped 3, inner view; h, major cheliped, left, lateral view; i, major cheliped, left, upper view; j, minor cheliped, right, lateral view. Scale bars = 1 mm.

blunt tooth at midlength; ratio of dorsal lengths, merus: carpus: propodus – 1 : 0.76 : 1.38.

Minor pereopod 1 (right cheliped) about 0.8 times length of major; ischium lower margin with 5 spines, larger distally; merus lower margin with 1 proximal spine; carpus subtriangular, 1.2 times as wide as long, with tooth at end of upper and lower margins; propodus upper margin about as long as greatest width; fixed finger 1.1 times upper margin, cutting edge with 2 teeth in distal quarter; dactylus as long as fixed finger, cutting edge smooth; ratio of dorsal lengths, merus: carpus: propodus – 1 : 0.85 : 0.92.

Pereopod 2 chelate. Pereopod 3 ischium slightly longer than wide, about half length of merus; carpus slightly shorter than merus; propodus 0.7 times length of carpus, lower margin broadly expanded proximally, densely setose; dactylus simple, about half length of propodus. Pereopod 4 propodus semichelate, with spiniform seta at base of finger; dactylus simple.

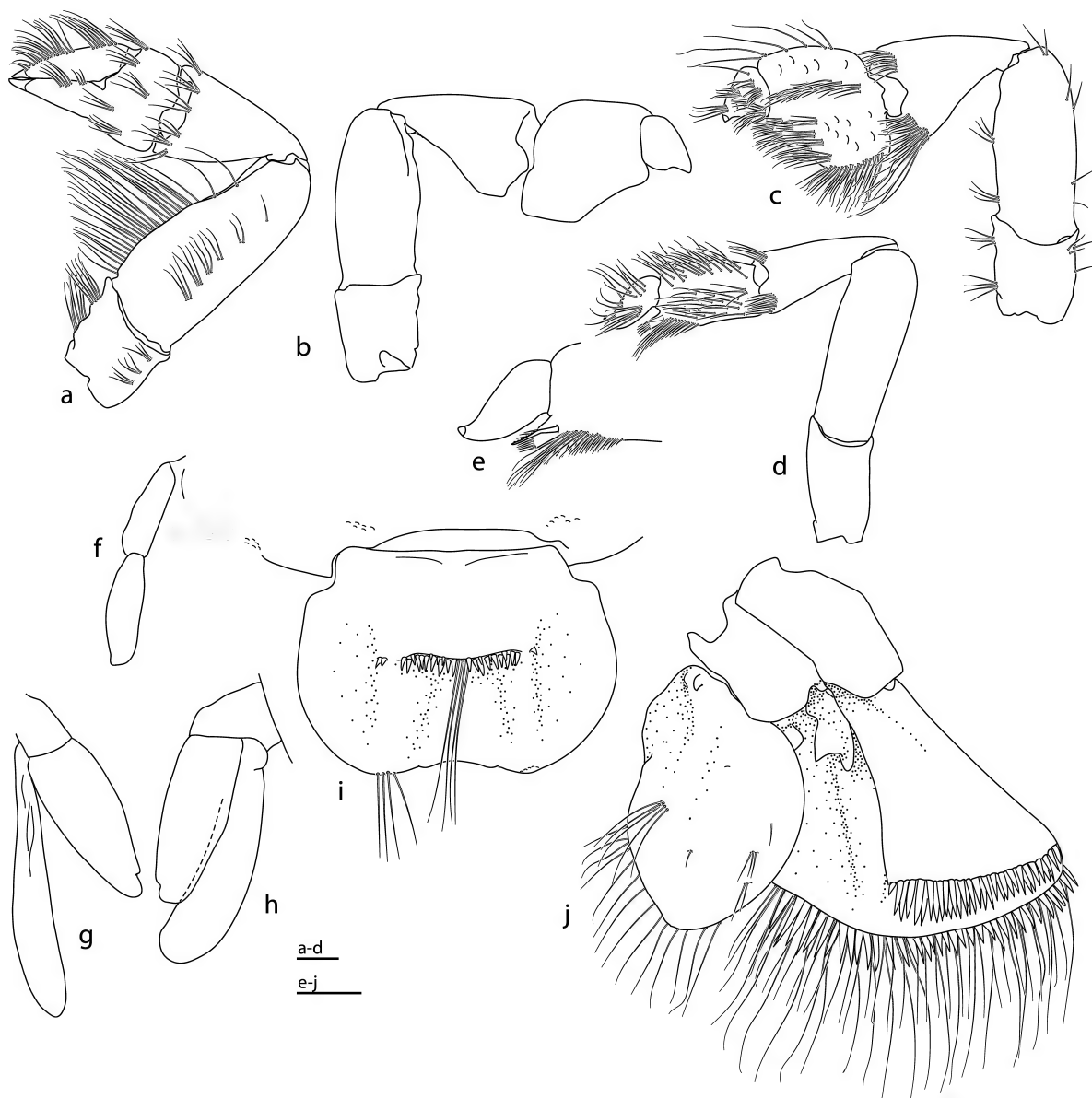Figure 4. *Articullichirus chiltoni* sp. nov. New Zealand, CMNZ AQ3372 (holotype male, 14.7 mm). a, left pereopod 2, outer view; b, left pereopod 3, inner view (setae not shown); c, left pereopod 3, outer view; d, left pereopod 4; e, left pereopod 4, detail of distal propodus and dactylus; f, pleopod 1; g, h, right and left pleopods 2; i, telson; j, uropodal endopod and exopod. Scale bars = 1 mm.

Male pleopod 1 uniramous, biarticulate; article 2 with small distolateral triangular lobe. Male pleopod 2 biramous; endopod with obsolete distomesial appendix masculina; exopod longer than endopod.

Uropod endopod 1.5 times as long as wide, anterior margin convex, without setae; posterior margin slightly concave, tapering to a narrowly rounded apex; marginal setae confined to distal and posterodistal margins; upper face with cluster of setae close to posterior margin, few scattered setae near anterior margin, with 1 proximal tooth. Exopod longer than endopod, subtriangular, as wide as anterior margin, upper face with proximal tooth; dorsal plate oblique, well separate from distal margin, armed with imbricating robust setae, posterodistal angle rounded, armed with imbricating robust setae.

Telson 1.4 times as wide as long, lateral margins evenly convex, posterior margin concave; with dorsal transverse row of spiniform setae, 1 or 2 robust setae placed laterally, remote from row of 12 (right) and 13 (left), separated medially by cluster of fine setae; posterolateral margin with row of setae.

Etymology. Named after New Zealand carcinologist Charles Chilton (1860–1929) who first reported this specimen from the Kermadec Islands.

Distribution. Kermadec Islands, New Zealand and possibly Kiribati; intertidal.

Remarks. The single specimen collected from the Kermadec Islands is more similar to *Articullichirus collaroy* than to *A. articulatus*. The new species differs from *A collaroy* and *A. articulatus* as follows: the transverse row of 28 spiniform setae on the telson exceeds those of the other species (< 9), and the single or two spiniform setae placed laterally on the outside of the submedian ridges are absent in both *A. collaroy* and *A. articulatus*. The uropodal endopod has one distinct proximal spine on the dorsal surface, rather than two distinct spines as in both other species. *Articullichirus chiltoni* shares the distinct curved spine on the maxilliped 3 basis and the hook on the pereopod 1 coxa with *A. collaroy*; these are absent or reduced in *A. articulatus*.

Sakai (2005) identified and partly illustrated two ovigerous females of "*Glypturus collaroy*" from Flax Bush Bay, New Zealand – these specimens cannot now be found (R. Webber, pers. comm., 14 Dec 2021). Sakai (2005) specifically mentioned a spine on the merus of maxilliped 3 and a telson with a concave posterior margin. These features are consistent with *Articullichirus* but the upturned rostrum is enigmatic, more like that of *Glypturus*. Sakai (1999) recorded a very small male (cl. 4.5 mm) from Gilbert Is (Kiribati) as "*Glypturus articulatus*"; this specimen (Swedish Museum of Natural History, SMNH 16226) cannot now be found (S. Stöhr, pers. comm., 7 Mar 2022). Sakai's illustrations of the short excavate telson, uropodal endopod and maxilliped 3 resemble those of *A. chiltoni*. Minor differences, such as more teeth on the merus of the major cheliped, could be due to this specimen being only one third of the size of the holotype from New Zealand.

Articullichirus collaroy (Poore and Griffin, 1979) comb. nov.

Figure 5

> *Callianassa collaroy* Poore and Griffin, 1979: 260–263, figs 24, 25.
> *Glypturus collaroy.*—Sakai, 1988: 61.—Sakai, 2011: 434 (part).
> *Corallianassa collaroy.*—Tudge et al., 2000: 144.—Davie, 2002: 460.
> *Neocallichirus collaroy.*—Sakai, 1999: 98.
> *Corallianassa* sp. MoV 4965.—Poore et al., 2008: 95, colour figure.
> Not *Glypturus collaroy.*—Sakai, 2005: 139–141, fig. 29 ? = *Articullichirus chiltoni* sp. nov.
> Not *Corallianassa collaroy.*—Sakai, 1992: 212, fig. 1 = *Articullichirus articulatus*.

Material examined. **Australia**, Western Australia, Great Australian Bight, 110 nm (204 km) SW of Eucla, 33° 20'S, 127° 45'E, 260 m, SAM C17888 (female, 9.3 mm). Off Bald Island, 35.19°S, 118.649°E, 161–169 m (stn SS10/2005/038), NMV J55438 (female, 13.2 mm). Off Two Rocks, 31.7244°S, 115.244°E, 102 m, NMV J53458 (male, 10.5 mm)

Diagnosis. Maxilliped 3 basis with mesial spine; merus with tooth on distal margin. Pereopod 1 coxa with mesiodistal hook. Uropodal endopod midlength about 1.2 times as long as wide, with semicircular apex, with 5 dorsal clusters of setae in distal half, with 2 proximal dorsal teeth. Telson 1.3 times as wide as long, with excavate posterior margin; with transverse dorsal row of 5 pairs of spiniform setae.

Supplementary description. Carapace length 0.27 of total length; cervical groove at 0.9 length of carapace; dorsal oval well defined; hepatic region with weakly sclerified line between dorsal oval and linea thalassinica. Rostrum and anterolateral carapace spines with unsclerified basal region; rostrum an anteriorly directed, acute spine longer than eyestalk; anterolateral spines set slightly back from rostrum, acute, half as long as rostrum. Anterolateral branchiostegal lobe well defined, margin extending dorsal to linea thalassinica, with sclerified plate below linea thalassinica. Pleomere 1 without transverse groove, with dorsolateral longitudinal setal row followed by cluster of simple setae; pleomere 2 1.8 times as long as pleomere 1 tergite; pleomeres 3–5 scarcely expanded laterally with dense setose areas; pleomere 6 1.3 times as long as pleomere 5, with posterolateral notch.

Eyestalk without produced mesiodistal apex; cornea swollen, distal. Antenna with acute scaphocerite. Antennular peduncle reaching almost to end of antennal peduncle article 5. Antennal peduncle with acute scaphocerite. Maxilliped 3 basis with recurved mesial hook; merus with prominent tooth on free distal margin.

Pereopods 1 coxae each with strong mesial hook. Major pereopod 1 (cheliped) ischium lower margin spinose; merus lower margin with 3 proximal spines, upper margin strongly convex; carpus with tooth at end on upper and lower margins; propodus upper margin rounded, with submarginal carina on mesial face, about as long as greatest width, distomesial edge straight; fixed finger 0.8 times upper margin, cutting edge with small tooth; dactylus as long as fixed finger, cutting edge with triangular tooth.

Minor pereopod 1 (cheliped) 0.8 times length of major; ischium lower margin spinose; merus lower margin with 2 proximal spines; carpus as long as wide; propodus upper margin as long as greatest width; fixed finger 1.3 times upper margin,
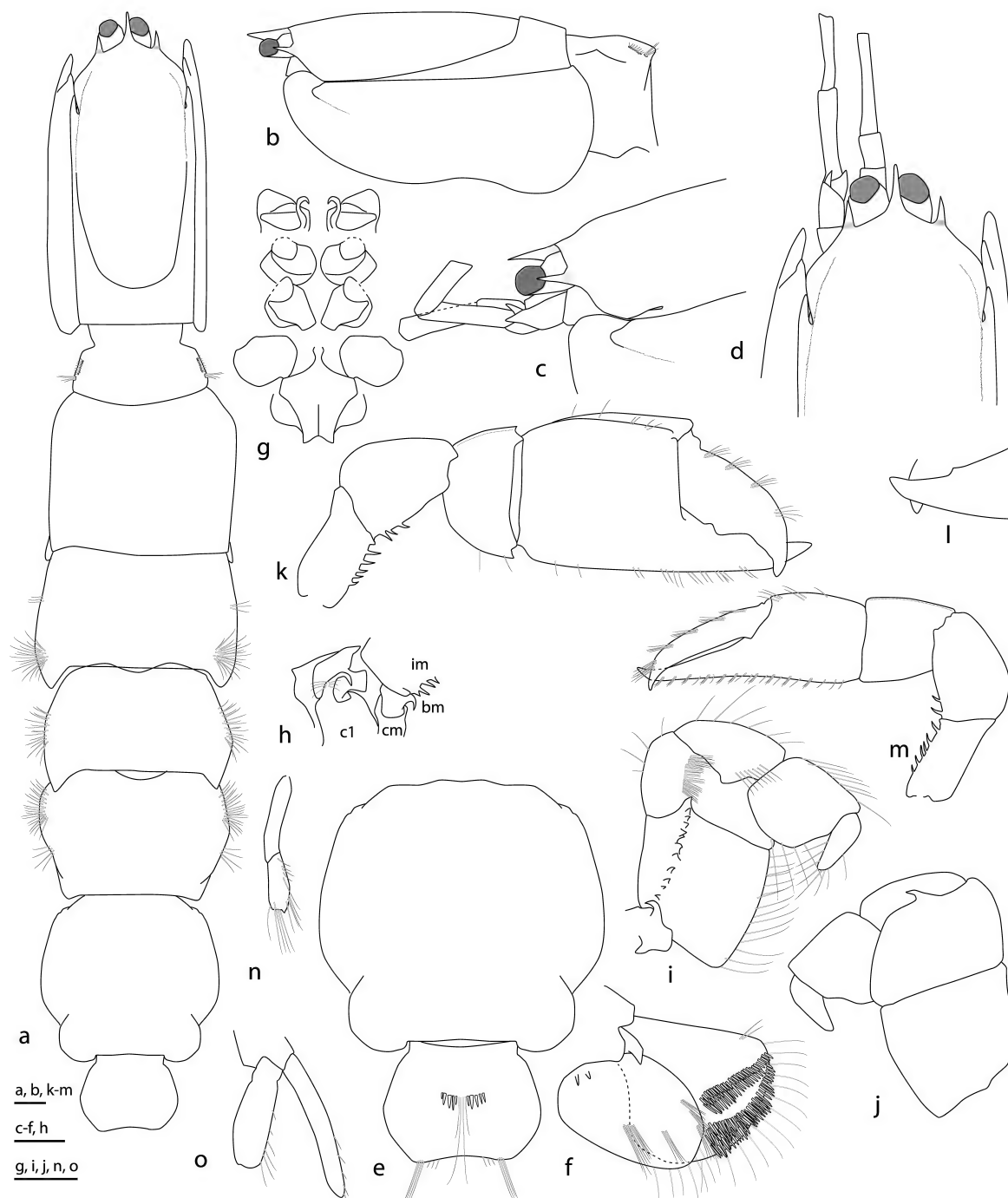
Figure 5. *Articullichirus collaroy* (Poore and Griffin, 1979). Western Australia, NMV J53438 (male, 10.5 mm). a, carapace, eyestalks, pleon, telson, dorsal view; b, carapace, eyestalk, pleomere 1, lateral view; c, d, anterior carapace, eyestalk, antennular peduncle, antennal peduncle, lateral and dorsal views; e, pleomere 6, telson, dorsal view; f, right uropod, dorsal view; g, pereopodal coxae 1–4, thoracic sternite 7, ventral view; h, proximal articles of right cheliped and maxilliped 3 in situ, ventral oblique view; i, j, maxilliped 3, inner and outer views; k, major cheliped (left), mesial view; l, major cheliped fingers, lateral view; m, minor cheliped (right), mesial view; n, o, right pleopods 1, 2, posterior views. Scale bars = 1 mm. c1, coxa of right cheliped; cm, bm, im, coxa, basis, ischium of maxilliped 3. Scale bar = 1 mm.

cutting edge smooth; dactylus as long as fixed finger, cutting edge smooth.

Male pleopod 1 biarticulate; article 2 with small distolateral triangular lobe. Male pleopod 2 biramous; endopod with obsolete distomesial appendix; exopod longer than endopod. Uropod endopod 1.6 times as long as wide, with distal marginal setae, upper face with 5 clusters of setae over distal half, with 2 proximal teeth. Exopod about as wide as anterior margin, with proximal tooth on dorsal face, dorsal plate oblique, well separate from distal margin, setose, posterodistal angle rounded, densely setose.

Telson 1.3 times as wide as long, lateral margins strongly convex, posterior margin concave; with 5 pairs of dorsal spiniform setae in transverse row, finer setae mesially.

Size. Cl. to 13 mm.

Type locality. Australia, New South Wales, Long Reef, Collaroy.

Distribution. Temperate Australia (from off Sydney to off Perth); intertidal–260 m.

Remarks. Poore and Griffin's (1979) figures did not show the acute scaphocerite or spiniform setae on the telson that characterise this new genus. This is remedied here.

Sakai's uses of the species name are in error. His "*Glypturus collaroy*" from New Zealand (Sakai, 2005) has an upturned rostrum, not typical of the genus, but could otherwise be synonymous with *A. chiltoni* (see comments under that species above). His "*Corallianassa collaroy*" from French Polynesia (Sakai, 1992) is *A. articulatus*.

The present identifications extend the distribution of this species from the intertidal of central NSW to deep water off southeastern WA, Australia.

Acknowledgements

References

Bate, C.S. 1888. Report on the Crustacea Macrura collected by H. M. S. *Challenger* during the years 1873–76. *Report on the Scientific Results of the Voyage of H. M. S. Challenger during the years 1873–76. Zoology* 24: 1–942. https://www.biodiversitylibrary.org/page/2020399

Chilton, C. 1911. The Crustacea of the Kermadec Islands. *Transactions of the New Zealand Institute* 43: 544–573. https://www.biodiversitylibrary.org/item/37657

Dallwitz, M.J. 2018. Overview of the DELTA system. https://www.delta-intkey.com/www/overview.htm

Davie, P.J.F. 2002. *Crustacea: Malacostraca: Phyllocarida, Hoplocarida, Eucarida (Part 1)*. Vol. 19.3A. CSIRO Publishing: Melbourne. xii, 551 pp.

Dworschak, P.C. 1992. The Thalassinidea in the Museum of Natural History, Vienna; with some remarks on the biology of the species. *Annalen des Naturhistorischen Museums in Wien, B* 93: 189–238.

Dworschak, P.C., and Wirtz, P. 2010. Discovery of the rare burrowing shrimp *Calliapagurops charcoti* de Saint Laurent, 1973 (Decapoda: Axiidea: Callianassidae) in shallow water: first record of the infraorder for Madeira Island. *Zootaxa* 2691: 53–56. https://doi.org/10.11646/zootaxa.2691.1.3

Edmondson, C.H. 1944. Callianassidae of the Central Pacific. *Bernice P. Bishop Museum Occasional Paper* 18: 35–61.

Komai, T., Maenosono, T., and Osawa, M. 2015. Records of three species of callianassid ghost shrimp from the genera *Glypturus* Stimpson, 1866 and *Corallianassa* Manning, 1987 (Crustacea: Decapoda: Axiidea) from the Ryukyu Islands, Japan, with remarks on the taxonomic status of the two genera. *Fauna Ryukyuana* 27: 13–59.

Man, J.G. de 1928. The Decapoda of the Siboga-Expedition. Part 7. The Thalassinidea and Callianassidae collected by the Siboga-Expedition with some remarks on the Laomediidae. *Siboga-Expéditie* 39a6: 1–187.

Manning, R.B. 1987. Notes on western Atlantic Callianassidae (Crustacea: Decapoda: Thalassinidea). *Proceedings of the Biological Society of Washington* 100: 386–401. http://biodiversitylibrary.org/page/34570790

Manning, R.B. 1992. A new genus for *Corallianassa xutha* Manning (Crustacea: Decapoda: Callianassidae). *Proceedings of the Biological Society of Washington* 105: 571–574. https://www.biodiversitylibrary.org/page/35607750

Manning, R.B., and Felder, D.L. 1991. Revision of the American Callianassidae (Crustacea: Decapoda: Thalassinidea). *Proceedings of the Biological Society of Washington* 104: 764–792. https://www.biodiversitylibrary.org/page/34809466

Ngoc-Ho, N. 2002. A new species of *Calliapagurops* de Saint Laurent from the Philippines with a discussion of the taxonomic position of the genus (Thalassinidea, Callianassidae). *Crustaceana* 75: 539–549. https://doi.org/10.1163/156854002760095589

Poore, G.C.B., and Griffin, D.J.G. 1979. The Thalassinidea (Crustacea: Decapoda) of Australia. *Records of the Australian Museum* 32: 217–321. https://doi.org/10.3853/j.0067-1975.32.1979.457

Poore, G.C.B., McCallum, A.W., and Taylor, J. 2008. Decapod Crustacea of the continental margin of southwestern and central Western Australia: preliminary identifications of 524 species from FRV *Southern Surveyor* voyage SS10-2005. *Museum Victoria Science Reports* 11: 1–106. https://doi.org/10.24199/j.mvsr.2008.11

Poore, G.C.B., Dworschak, P.C., Robles, R., Mantelatto, F.L., and Felder, D.L. 2019. A new classification of Callianassidae and related families (Crustacea: Decapoda: Axiidea) derived from a molecular phylogeny with morphological support. *Memoirs of Museum Victoria* 78: 73–146. https://doi.org/10.24199/j.mmv.2019.78.05

Poupin, J. 1998. Crustacea Decapoda and Stomatopoda of French Polynesia (Dendrobranchiata, Stenopodidea, Caridea, Thalassinidea, and Stomatopoda, with additions to Astacidea, Palinuridea, Anomura, and Brachyura). *Atoll Research Bulletin* 451: 1–62. https://doi.org/10.5479/si.00775630.451.1

Rathbun, M.J. 1906. The Brachyura and Macrura of the Hawaiian Islands. *Bulletin of the United States Fish Commission* 23: 827–930, pls 1–24.

Robles, R., Dworschak, P.C., Felder, D.L., Poore, G.C.B., and Mantelatto, F.L. 2020. A molecular phylogeny of Callianassidae and related families (Crustacea: Decapoda: Axiidea) with morphological support. *Invertebrate Systematics* 34: 113–132. https://doi.org/10.1071/IS19021

Saint Laurent, M de. 1973. Sur la systématique et la phylogénie des Thalassinidea: définition des familles des Callianassidae et des Upogebiidae et diagnose de cinq genres nouveaux. *Comptes Rendus Hebdomadaires de Séances de l'Académie des Sciences (Sér. D)* 277: 513–516.

Saint Laurent, M. de, and Le Loeuff, P. 1979. Campagnes de la *Calypso* au large des côtes Atlantiques Africaines (1956 et 1959) (suite). 22. Crustacés Décapodes Thalassinidea. I. Upogebiidae et Callianassidae. In: Forest, J. (ed.), Résultats Scientifiques des Campagnes de la *Calypso*. Fasc. 11. *Annales de l'Institut Océanographique, Monaco et Paris* 55 suppl.: 29–101.

Sakai, K. 1988. A new genus and five new species of Callianassidae (Crustacea: Decapoda: Thalassinidea) from northern Australia. *The Beagle, Occasional Papers of the Northern Territory Museum of Arts and Sciences* 5: 51–69. https://doi.org/10.5962/p.260916

Sakai, K. 1992. Notes on some species of Thalassinidea from French Polynesia (Crustacea: Decapoda). *Senckenbergiana Maritima* 22: 211–216. https://research.nhm.org/pdfs/21962/21962.pdf

Sakai, K. 1999. Synopsis of the family Callianassidae, with keys to subfamilies, genera and species, and the description of new taxa (Crustacea: Decapoda: Thalassinidea). *Zoologische Verhandelingen* 326: 1–152. https://repository.naturalis.nl/pub/219414

Sakai, K. 2005. Callianassoidea of the world (Decapoda: Thalassinidea). *Crustaceana Monographs* 4: 1–285. https://doi.org/10.1163/9789047416890

Sakai, K. 2011. Axioidea of the world and a reconsideration of the Callianassoidea (Decapoda, Thalassinidea, Callianassida). *Crustaceana Monographs* 13: 1–616. https://doi.org/10.1163/9789047424185

Stimpson, W. 1866. Descriptions of new genera and species of macrurous Crustacea from the coasts of North America. *Proceedings of the Chicago Academy of Science* 1: 46–48.

Tudge, C.C., Poore, G.C.B., and Lemaitre, R. 2000. Preliminary phylogenetic analysis of generic relationships within the Callianassidae and Ctenochelidae (Decapoda: Thalassinidea: Callianassoidea). *Journal of Crustacean Biology* 20 (Special Issue 2): 129–149. https://doi.org/10.1163/1937240X-90000015

Taxonomic revision of the Australian native bee subgenus *Australictus* (Hymenoptera: Halictidae: Halictini: genus *Lasioglossum*) – "Wood-Splitting Axe Bees"

http://zoobank.org/urn:lsid:zoobank.org:pub:D5DBDF43-838A-4C99-8F73-38ED597A6CF4

KENNETH L WALKER

(ORCID ID https://orcid.org/0000-0001-8750-2035). Museums Victoria, GPO Box 666, Melbourne, Vic. 3001, Australia. [kwalker@museum.vic.gov.au]

Abstract   Walker, K.L. 2022. Taxonomic revision of the Australian native bee subgenus *Australictus* (Hymenoptera: Halictidae: Halictini: genus *Lasioglossum*) – "Wood-Splitting Axe Bees". *Memoirs of Museum Victoria* 81: 135–162.

The Australian *Lasioglossum* Curtis 1833 subgenus *Australictus* Michener 1965 is revised.

Of the 11 available names listed by Michener (1965) for the subgenus *Australictus*, six are placed in synonymy. A species placed by Michener (1965) in the *Lasioglossum* subgenus *Parasphecodes* Smith 1853 is recombined to the subgenus *Australictus*, and four other species, placed in *Parasphecodes* by Michener (1965), are synonymised with this valid, recombined taxon, and the species name of the taxon is reverted to its original spelling. In addition, a species placed in *Australictus* by Michener (1965) is synonymised with a valid species in the *Lasioglossum* subgenus *Chilalictus* Michener 1965. These changes provide five valid names for the subgenus *Australictus*.

New synonymies, recombined names and valid species proposed for *Lasioglossum (Australictus)* are as follows: New synonymies – *Lasioglossum (Australictus) kurandense* (Cockerell 1914) **syn. nov.**, *Lasioglossum (Australictus) nigroscopaceum* (Friese 1917) **syn.** by Cockerell 1929 but listed by Michener (1965: 165) as valid = *Lasioglossum (Australictus) davide* (Cockerell 1910a); *Lasioglossum (Australictus) insculptum* (Cockerell 1918) **syn. nov.**, *Lasioglossum (Australictus) rufitarsum* (Rayment 1929) **syn. nov.** and *Lasioglossum (Australictus) fulvofasciae* Michener 1965 **syn. nov.** = *Lasioglossum (Australictus) tertium* (Dalla Torre 1896); *Lasioglossum (Australictus) franki* (Friese 1924) **syn. nov.** = *Lasioglossum (Chilalictus) orbatum* (Smith 1853). New combination and new synonymies – *Lasioglossum (Parasphecodes) lithuscum* (Smith 1853) **comb. nov.** moved to *Lasioglossum (Australictus) lithusca*; *Lasioglossum (Parasphecodes) adelaidae* (Cockerell 1905) **syn. nov.**, *Lasioglossum (Parasphecodes) griseipenne* (Cockerell 1929) **syn. nov.**, *Lasioglossum (Parasphecodes) stuchilum* (Smith 1853) **syn. nov.**, *Lasioglossum (Parasphecodes) wellingstoni* (Cockerell 1914) **syn. nov.** = *Lasioglossum (Australictus) lithusca*. Valid is *Lasioglossum (Australictus) plorator* (Cockerell 1910b).

New female subgeneric mandibular characters are added to Michener's (1965) diagnostics for *Australictus* – mandible with elongated and enlarged preapical tooth, reduction in width of basal tooth at apical end and in dorsal view, broadening of width at base of mandible. The mandibular modifications, widening of the head basally and enlarged gena are associated with *Australictus* behaviour to nest in wood rather than ground nesting in soil as is usual for Halictidae bees. The shape of the female mandible, especially in dorsal view, resembles a wood-splitting axe – hence the common name coined here, "Wood-Splitting Axe Bees". *Australictus* is the first record of wood-nesting bees for Australian Halictidae.

All valid species are redescribed; keys to both sexes, montage diagnostic images and distribution maps are provided to assist with species identification.

Keywords   Hymenoptera, Halictidae, Halictini, *Lasioglossum*, *Parasphecodes*, *Chilalictus*, *Australictus*, nesting behaviour.

Introduction

The world's bee fauna consists of seven families, Apidae, Colletidae, Halictidae, Megachilidae, Stenotritidae, Andrenidae and Melittidae, with the latter two families absent from Australia. Halictidae is the second largest bee family in the world, with 4,510 species (Ascher and Pickering, 2022), and is found on all continents except Antarctica (Michener, 2007). Most of this species richness is concentrated in the tribe Halictini, with 2,882 species (Ascher and Pickering, 2022).

Lasioglossum Curtis 1833 is one of the most species-rich and taxonomically challenging groups of all world bee genera, with 2,645 named species to date (Ascher and Pickering, 2022). *Lasioglossum* bees are distinguished from other Halictini genera by having the third submarginal (2rs-m) ("strong-veined *Lasioglossum* series") and sometimes the second submarginal

cross veins (1rs-m) ("weak-veined Hemihalictus series") weaker than the first submarginal cross vein (Michener 2007, see especially figs. 66–6a and c).

The Australian component of this most diverse genus within the Halictidae has 308 available names (ABRS, 2022a; note: update to ABRS, 2022a includes changes for *Callalictus* Michener 1965 – see Walker (2022); and here, *Homalictus* Cockerell 1919 is treated as a subgenus of *Lasioglossum* – see Danforth, 1999, Danforth et al., 2001, 2003, 2008; Gibbs et al., 2012, 2013; Zhang et al., 2022). In Australia, *Lasioglossum* is divided into nine subgenera as follows: *Australictus* Michener 1965 (11 species); *Austrevylaeus* Michener 1965 (six species); *Callalictus* (three species); *Chilalictus* Michener 1965 (139 species); *Ctenonomia* Cameron 1903 (nine species); *Glossalictus* Michener 1965 (one species); *Homalictus* (46 species); *Parasphecodes* Smith 1853 (92 species); and *Pseudochilalictus* Michener 1965 (one species).

The subgenus *Australictus*, with 11 available names, is a striking *Lasioglossum* subgenus of the Australian bee fauna. The subgenus occurs from north Queensland (two species), down coastal New South Wales, across Victoria, widely in Tasmania (two species), and there are three specimen records from south-east South Australia (figs. 12A–E). Bees of this subgenus nest in wood, either excavating their own nests or modifying the vacated burrows of beetles. This is the first record of wood-nesting Halictidae in Australia. To accommodate this wood-nesting behaviour, the mandibles of females have been modified as described below.

A full morphological diagnosis for the subgenus *Australictus* is provided. Species can be generally distinguished from other Australian *Lasioglossum* subgenera by the following characters: body length moderately large (females: 8.32 mm to 10.23 mm; males: 8.01 mm to 10.21 mm); female head widened basally in frontal view, with lower inner eye width almost equal to or wider than upper inner eye width (fig. 1A); bidentate mandible of females with elongated and enlarged preapical tooth (fig. 1C) and broadened at base (fig. 1E); female labrum medium process truncate apically with lateral margins pectinate (fig. 2A); dorsolateral angles of pronotum rounded (figs. 5A, 6A, 7A, 8A, 9A); body colour black, one species with metasoma red-brown (figs. 6A, 6B); several species with no body tomentum (figs. 5A–D, 6A–D, 8A–D), several species with various combinations of yellow/white tomentum on dorsolateral angles of pronotum, mesoscutum, metanotum and basal band across metasomal T2-T3 (figs. 7A–D, 9A–D); female anterior metatibial spur finely serrate (fig. 2B); and male genitalia with gonobase either basally widened (figs. 10A, 10B, 11C, 11D) or narrowed (figs. 10C–F, 12A, 12B), retrorse lobe either short (figs. 11A, 11C) or elongate (figs. 10A, 10C, 10E) and gonostylus either short (figs. 10A, 10C, 11A) or absent (figs. 10E, 11C).

The shape of the female mandible, especially in dorsal view, is broad basally and apically pointed (fig. 1E), resembling a wood-splitting axe – hence the common name suggested here, "Wood-Splitting Axe Bees".

The Australian *Lasioglossum* subgenus *Australictus* is revised. Of the 11 available names listed by Michener (1965) for the subgenus, six are placed in synonymy. A species placed by

Michener (1965) in the *Lasioglossum* subgenus *Parasphecodes* is recombined to the subgenus *Australictus* and four other species, placed in *Parasphecodes* by Michener (1965), are synonymised with this valid, recombined taxon, and the species name of the taxon is reverted to its original spelling. In addition, a species placed in *Australictus* by Michener (1965) is synonymised with a valid species in the *Lasioglossum* subgenus *Chilalictus* Michener 1965. These changes provide five valid names for the subgenus *Australictus*.

All valid species are redescribed, keys to both sexes, montage images and distribution maps are provided to assist with species identifications.

Material and methods

Terminology follows Michener (2007), except the propodeum is called the metapostnotum (Brothers, 1976; Gibbs et al., 2013; Gibbs et al., 2022; Engel and Gonzalez, 2022) and the inner hind tibial spur is called the anterior metatibial spur (Aguiar and Gibson, 2010). To assist with the descriptions, the following notes are provided: relative head measurements were standardised to a head width of 100 units; absolute measurements are expressed as minimum–mean–maximum if multiple specimens were available; body length was measured from antennal sockets to end of metasoma; forewing length was measured from the base of the arcuate basal vein (vein M) to the distal margin of the third submarginal cell (vein 2rs-m); and, intertegular distance was measured as the greatest width between the tegulae. Sculpture nomenclature follows Harris (1979). Mesoscutum punctation nomenclature is as follows: dense, interspaces between punctures less than diameter of a puncture; close, interspaces between punctures equal to diameter of puncture; open, interspaces between punctures greater than 1 × but less than 2 × diameter of puncture; sparse, interspaces between punctures equal to or greater than 2 × diameter of puncture. To standardise the description of the mesoscutum punctation, the mesoscutum was subdivided into areas as follows: anteromesial, area along the leading edge of the mesoscutum and on each side of the midline; anterolateral, area on the anterior lateral corners of the mesoscutum; mesial, area between parapsidal lines; parapsidal, areas between parapsidal line and nearest lateral margin; laterad of parapsidal lines, area adjacent to outer margin of the parapsidal lines; mesiad of parapsidal lines, area adjacent to the inner margin of the parapsidal lines; posterior, area along the posterior margin of the mesoscutum (see diagram in Walker, 1995: 258, fig. 3).

Due to the importance of vestiture as diagnostic characters on the male *Lasioglossum* genital capsule, in particular on the gonocoxa, retrorse lobe and gonostylus, a decision was made to photograph dry mounted capsules rather than the usual method of photography in glycerol. Treatment of the genital capsule was as usual: specimen placed in humid chamber for 24 hours, removal of genital capsule from the bee using a hooked no. 3 entomological pin (38 mm x 0.53 mm), 24 hours in 10% KOH cold, several water washes, then placed on tissue paper and allowed to dry for several hours. A micro-headless pin B3 (0.193 mm x 15 mm) was pinned to a piece of foam

attached to a no. 3 entomological pin so that the blunt end of the micropin was pointing out. A droplet of water-soluble glue was placed on the end of the micropin, one side of the micropin was scraped to reduce the amount of glue, and the blunt end was brought in contact with the left side basal corner of the gonobase and the genitalia allowed to dry. While drying, it is important to keep the glued genital capsule at the tip of the micropin. To achieve this dried position, the micropin must be held in a horizontal position with the genital capsule underneath its tip. If not placed in this drying position, the genital capsule can move down or around the micropin, obscuring the gonobase for photography. Ventral and dorsal montage images were taken against a black background to highlight diagnostic vestiture and structures. Following photography, each pinned capsule was attached to the specimen's pin pith. A decision was made to exclude images of the seventh and eighth metasomal sternal segments. These two sterna were similar in shape across all species and offered no unique diagnostic characters.

Photographs were taken using a Leica M205C microscope with a Leica DFC500 c-mount camera using LAS Version 3.8 to create image montage stacks and montaged images. Images were then post-processed and image plates formed in Adobe Photoshop 6.

Abbreviations used in the text are as follows: AOD, antennocular distance; AF, antennal flagellomeres; CL, clypeal length; EW, eye width, in side view; FL, flagellum length; GW, gena width, in side view; HL, head length; HW, head width; IAD, interantennal distance; IOD, interocellar distance; LID, lower interorbital distance; OAD, ocellantennal distance; OOD, ocellocular distance; SE – South East; SW – scutum width; S1–S5, metasomal sterna 1–5; SL, scape length; SW, scutum width; T1–T6, metasomal terga 1–6; UID, upper interorbital distance.

This study was based on examination of just over 1,000 specimens (and several citizen science images posted on Facebook – links within species descriptions) from the following collections.

AM – Australian Museum, Sydney, New South Wales; ANIC – Australian National Insect Collection, CSIRO, Canberra, Australian Capital Territory; BDBSA – Department for Environment and Water, SA Fauna, Adelaide, South Australia; BMNH – Natural History Museum, London, United Kingdom; Cornell – Cornell University, Ithaca, New York; NMV Museums Victoria (formerly the National Museum of Victoria), Melbourne, Victoria; QDPI – Queensland Department of Primary Industries, Brisbane, Queensland; OAI – Orange Agricultural Institute, Orange, New South Wales; QM – Queensland Museum, Brisbane, Queensland; SEM – Snow Entomological Museum, Kansas University Biodiversity Institute, University of Kansas, Kansas, United States of America; TMAG – Tasmanian Museum and Art Gallery Invertebrate Collection, Hobart, Tasmania; TDA – Tasmanian Department of Agriculture, Hobart, Tasmania; WAM – Western Australian Museum, Perth, Western Australia.

Keys to both sexes of Lasioglossum (Australictus) *species*

1 Metasoma with yellow/white basal tomentum bands on T2-T3 (figs. female: 7A, 9A; male: 7C, 9C) 2

\- Metasoma without tomentum bands on terga (figs. female: 5A, 6A, 8A; male: 5C, 6C, 8C) 3

2 Female with yellow/white tomentum on posterolateral corners of mesoscutum and on metanotum (fig. 7A); male with an apical V-patch of tomentum on posterior vertical posterior surface of metapostnotum (figs. 2C, 7C) .... *L. peraustrale* (Cockerell, 1904)

\- Female without yellow/white tomentum on mesoscutum or metanotum (fig. 9A); male without apical V-patch of tomentum on posterior vertical posterior surface of metapostnotum (fig. 9C) .... *L. tertium* (Dalla Torre, 1896)

3 Metasoma red-brown (figs. female: 6A; male: 6C) .... *L. lithusca* (Smith, 1853)

\- Metasoma black (figs. female: 5A, 8A; male: 5C, 8C) 4

4 Dorsal surface of metapostnotum posterior rim defined by raised carina, dorsal sculpture ruguloso-striolate (figs. female: 2E, 5A; male: 5C) .... *L. davide* (Cockerell, 1910a)

\- Dorsal surface of metapostnotum posterior rim not defined by carina, rim smooth and elevated, dorsal sculpture microalveolate (figs. female: 2F, 8A; male: 8C) .... *L. plorator* (Cockerell, 1910b)

Taxonomy

Subgeneric diagnosis: body length moderately large (female: 8.32 mm to 10.83 mm; male: 8.01 mm to 10.21 mm), robust, non-metallic species; in both sexes, body colour black (figs. 5A–D, 7A–D, 8A–D, 9A–D) except *L. lithusca* metasoma red-brown (figs. 6A–D); *L. tertium* male metasoma either black (figs. 9C–D) or banded with alternating dark to light red-brown tergal colours (fig. 2D); mesoscutum and metasomal terga of *L. davide* and *L. plorator* with tinge of deep blue colour (figs. 5A, 8A); female inner eye widths vary from narrowed to almost parallel to diverging basally from upper to lower inner eye widths (e.g. in *L. tertium* lower inner eye width 1.2 x upper inner eye width), meaning head widened ventrally (fig. 1A), and gena width enlarged (fig. 9B), (Australian *Lasioglossum* subgenera typically with eyes widths converging basally – e.g. *L. (Parasphecodes) hiltacum* (Smith, 1853) lower inner eye width 0.94 x upper inner eye width (fig. 1B)); female bidentate mandible modified by elongation and enlargement of preapical tooth, reduction in width of basal tooth, enlargement of height and width at base of mandible, reduced width of condylar groove (figs. 1C, 1E) (see Table 1 for comparison of *Australictus* (figs. 1C, 1E) with *Parasphecodes* (figs. 1D, 1F)); labrum medium process apically truncate, laterally pectinate (fig. 2A); pronotum with rounded dorsolateral angles (figs. 5A, 6A, 7A, 8A, 9A); wing veins with second transverse cubital vein (1rs-m) strong, 1st recurrent vein (1m-cu) entering second submarginal cell or in line with 1rs-m except in *L. tertium*, where 1st recurrent vein enters third submarginal cell; female hind basitibial plate rounded to weakly pointed apically; female anterior metatibial spur finely serrate (fig. 2B) to smooth; dorsal surface of metapostnotum either carinate, as defined by raised carina forming raised lip or ridge (fig. 2E), or acarinate, as defined by crescent-shaped, elevated

Table 1. Female mandibular morphological differences between *Lasioglossum* subgenera *Australictus* and *Parasphecodes*. (Note: *L. (Australictus) lithusca* and *L. (Parasphecodes) hiltacum* were used for measurements)

Character	*Australictus* (figs. 1C, 1E)	*Parasphecodes* (figs. 1D, 1F)
Preapical tooth length	Preapical tooth elongated to almost same length (0.93 x length) as basal tooth	Preapical tooth shorter than length (0.79 x length) of basal tooth
Preapical tooth width	Preapical tooth enlarged and broader (1.14 x width) than width of basal tooth	Preapical tooth not enlarged and narrower (0.42 x width) than width of basal tooth
Basal tooth width	Width of basal tooth 0.13 x width of base of mandible	Width of basal tooth 0.21 x width of base of mandible
Condylar groove	Width of condylar groove 0.14 x width of base of mandible between the acetabulum and condyle	Width of condylar groove 0.18 x width of base of mandible between the acetabulum and condyle
Base of mandible width in side view	Base of mandible length between acetabulum and condyle at 0.53 x length of mandible	Base of mandible length between acetabulum and condyle at 0.44 x length of mandible
Base of mandible width in dorsal view	Dorsal width at base of mandible 0.47 x length of mandible	Dorsal width at base of mandible 0.21 x length of mandible

medium area distinctly raised above vertical and lateral surfaces (fig. 2F); in both sexes, metasomal terga of *L. peraustrale* and *L. tertium* with conspicuous basal bands of tomentum on metasomal T2–T3 (figs. 7A–D, 9A–D), *L. davide*, *L. lithusca* and *L. plorator* without such metasomal tergal tomentum bands (figs. 5A–D, 6A–D, 8A–D). Male: some species with lateral hair tufts on metasomal S3–S5 (figs. 6F, 7F, 8F, 9F); genitalia with gonobase widened basally (figs. 10A, 11C) or narrowed (figs. 10C, 10E, 11A), gonostylus small (figs. 10A, 10B, 11A) to absent (figs. 10E, 11C), retrorse lobes small (figs. 11A, 11C) to enlarged (figs. 10A, 10C, 10E), either not meeting at midline (figs. 10A, 10E) or overlapping at midline (fig. 10C), either glabrous (figs. 10A, 11A, 11C) or setose (figs. 10C, 10E).

Notes. The elongated and enlarged preapical mandibular tooth, the narrowing of basal tooth and condylar groove, enlargement at the base of the mandible, the widening of the head basally and the enlargement of the gena are all adaptations to provide effective wood-splitting and wood-excavating mandibles for female *Australictus* to nest in wood rather than in soil as is usual for Halictidae bees.

Several specimen labels (at least five labels) refer to collected specimens found nesting in "rotten wood", and one specimen had a label observation "from Sirex emergence hole".

A series of Facebook images by Christopher Robbins for *L. (Australictus) plorator* documented the wood excavation nesting of this species (figs. 3A–F). The same species was also found using a vacated beetle exit hole as a nesting site in wood (fig. 4) (https://www.facebook.com/groups/1041684025880609/search?q=christopher%20robbins).

Christopher Robbins posted these bee observations with his Facebook images:

Chapple Vale, Victoria 19/04/2020. Found today while splitting wood. There was no bark on the log though, the crack in the log they make their tunnels into where the brood cells were filled with old termite bed from an extinct termite colony.

There were four adults all up and two pupae. They do not seem to worry about their access point to the log, they used cracks on the top, sides and underneath, in some cases they had excavated the chambers into decayed wood, a reddish wood rot, I believe commonly known as red cube rot, we used to find the larvae of a small reddish stag beetle in the same substrate.

These images and observations demonstrate that *Australictus* bees nest in wood.

Danforth et al. (2019) summarised the nest architecture of bees. The most common nesting strategy used by solitary bees is ground nesting in soil. An estimated 64% of non-parasitic bee species nest in underground soil excavations (Cane and Neff, 2011). However, a few bee species excavate nests in wood (both solid and rotten). Of the 27 known subfamilies of bees worldwide, wood-nesting occurs primarily in only the subfamilies Xylocopinae, Lithurginae and Callomelittinae (Danforth et al., 2019). The tunnels and cells of wood-nesting bees are entirely constructed using their mandibles, and wood-nesting bees have modified mandibles that differ from the mandibles of ground soil-nesting bees.

Most Halictidae are ground soil-nesting bees, and halictid bees show limited diversity in their mandibular structures (Danforth et al., 2019). However, wood-nesting halictids have been recorded in several Halictini genera. Of the 37 genera of halictine Augochorini that occur in North and South America, four are known to nest in wood (*Augochlora* Smith 1853, *Megalopta* Smith 1853, *Neocorynura* Schrottky 1910 and *Xenochlora* Engel, Brooks and Yanega 1997 (Tierney et al., 2008). Wood-nesting halictids have specialised bidentate mandibles (Michener and Fraser, 1978). The mandible of wood-excavating halictids is characterised as more stout and more robust than the mandible shape of ground soil-nesting Halictidae, with modified apical teeth, in particular an elongated and enlarged preapical tooth; the mandible is widened at its base and has groove variations on the outer and inner surfaces (Michener and Fraser, 1978).

Australictus is the first record of wood nesting for any Australian Halictidae. The bidentate mandible of *Australictus* looks similar in shape and structure to the mandible of the wood-nesting *Lasioglossum* subgenus *Eickwortia* McGinley 1999, especially the elongated and enlarged preapical tooth found in both subgenera (for an *Eickwortia* mandible image, see Gibbs and Dumesh, 2013, fig. 3). However, *Australictus* belongs to the informal "strong-veined" Lasioglossum series, whereas *Eickwortia* belongs to the informal "weak-veined" Hemihalictus series of *Lasioglossum*, which can be recognised by the weaken 1rs-m and 2rs-m veins in the forewing (Michener, 2007; Gibbs and Dumesh, 2013).

Species descriptions

Lasioglossum (Australictus) davide (Cockerell)

(Figs. 2E, 5A-F, 10A-B, 12A)

> *Halictus davidis* Cockerell 1910a: 234.
> *Halictus kurandensis* Cockerell 1910a: 234. **syn. nov.**
> *Halictus nigroscopaceus* Friese H. 1917 **syn.** by Cockerell 1929: 211.
> *Lasioglossum (Australictus) davide* – Michener 1965: 165.
> *Lasioglossum (Australictus) kurandense* – Michener 1965: 165.
> *Lasioglossum (Australictus) nigroscopaceum* – Michener 1965: 165.

Material examined: Holotype of *davidis* ♀, Queensland, Kuranda (has Cairns typed on label and Kuranda hand written), 4. 02. Turner BMNH Hym.17.a.914 (BMNH) (view type data and image at https://data.nhm. ac.uk/object/f00271eb-7e4e-41fb-9e8d-2736fa9ff79f accessed 16 August 2022).

Holotype of *kurandensis* ♂, Queensland, Kuranda (Cairns typed on label and Kuranda handwritten), 4. 02. Turner BMNH Hym.17.a.956 (BMNH) (view type data and image at https://data.nhm.ac.uk/object/e1eec50b-a2b4-4b89-84ca-6bea23587e8e accessed 16 August 2022).

Syntypes ("TYPUS") of *nigroscopaceus* – Queensland: Malanda, Mjöberg. All three specimens have same label and type number: Am. Mus. Nat. Hist. Dept. Invert. Zool. No. 26926 (2♀, 1♂). The male specimen has Cockerell's handwritten label saying "Halictus davidis Ckll" (AMNH).

Other specimens examined: (13♀, 6♂): QUEENSLAND: (1♀) Upper Mulgrave 19 June 1991, J.H. Barrett, nesting in rotten log (QDPI); (1♀) Tully Falls, S.F. 730m, 18 km SSW Ravenshoe, 7 Dec 1987 – 7 Jan 1988, R. Storey & B. Dickinson (QDPI); (1♀) Mt Halifax summit, 45 km WNW Townsville, 4 Dec 1990 – 8 Jan 1991, A. Graham, pitfall and intercept traps (QDPI); (1♀) Mt Halifax summit, 45 km WNW Townsville, 2 Dec 1990, A. Graham, hand collecting (QDPI); (1♀) Mt Lewis nr Mossman, 22 Oct 1984, N.W. Rodd (AM); (1♀, 1♂) Cairns District, F.P. Dodd (SAM); (2♀) Kuranda, 2 Jan 1953 & 25 Sept 1954, GB (NMV); (5♀, 3♂) Kuranda Black Mountain Forest Road, Jan 2001, K. Walker, on *Lophostemon grandifloris* subsp. *riparius* (NMV); (1♂) Kuranda, Jan 1952, J.G. Brooks (AM); (1♂) Mt Spec Nat. Pk, 10 km E Paluma, 22 Nov 1988, K. Walker, on *Eucalyptus* (NMV).

Floral record: Family visited: 1 (Myrtaceae (2)). Genera visited: 2 (*Eucalyptus,* (1), *Lophostemon* (1)).

Flight phenology capture records: Jan (3) Feb (0) Mar (0) Apr (0) May (0) June (1) July (0) Aug (0) Sept (1) Oct (1) Nov (1) Dec (3).

Diagnosis. *Lasioglossum (Australictus) davide* is most like *L. (Australictus) plorator* in body colours. This species can be distinguished, in both sexes, from other *Australictus* species by black body colour with bluish tinge on mesoscutum; the lack of tomentum on the mesosoma or metasoma; dorsal surface of metapostnotum posterior margin carinate, defined by raised posterior and lateral carinae; metapostnotum dorsal surface sculpture ruguloso-striolate (figs. 2E, 5A–D); male genitalia with gonobase widened basally (a characteristic shared only with *L. tertium*), large retrorse lobes with small, apically rounded gonostylus (figs. 10A, 10B); and males lacking any distinctive metasomal sternal vestiture (fig. 5F). This species is restricted to North Queensland (fig. 12A).

Description of female: (figs. 5A–B, 5E) body length: 9.58–9.68–10.21 mm (n=10); forewing length: 2.45–2.47–2.49 mm (n=10); head width: 2.78–2.88–2.93 mm (n=10); intertegular width: 2.06–2.38–2.40 mm (n=10). Relative head measurements: HW: 100, HL: 84–85, UID: 54–55, LID: 50–52, IAD: 08–09, OAD: 21–22, IOD: 08–09, OOD: 14–15, CL: 19–21, GW: 18–20, EW: 20–22, SL: 37–40, FL: 63–65.

Head: (fig. 5E) inner eyes margins weakly narrowed basally; median frontal carina reaching less than one third way to median ocellus; clypeus entirely polished and smooth, anterior half weakly concave medially, sparsely deeply punctate, punctures rounded to elongate; supraclypeal area distinctly raised above paraocular area, polished, smooth, punctures small, round and open with small rounded punctures; frons sculpture above antennal bases smooth but dull, microtessellate with small punctures for setae insertion points, paraocular area smooth and closely punctate.

Mesosoma: (fig. 5A) mesoscutum anterior mesial margin weakly produced mesoanteriorly, surface smooth with dull, "oily" sheen, medially openly punctate, laterad of parapsidal areas closely punctate, parapsidal areas and posterior margin densely punctate; scutellum 2 x as long as dorsal surface of metapostnotum, scutellum smooth, with dull sheen, weakly, openly punctate; dorsal surface of metapostnotum carinate (fig. 2E), posterior margin with well-defined, raised, semicircular carina and posterolateral carinae, dorsal surface transversely ruguloso-striolate medially, striate laterally, sculpture reaches posterior carina, lateral margins smooth microalveolate, vertical posterior surface of metapostnotum defined by lateral carinae meeting dorsal surface posterolateral carinae; mesepisternum and metepisternum plicate; first recurrent vein (1m-cu) meeting 1rs-m vein or entering second submarginal cell.

Metasoma and legs: (figs. 5A, 5B) metasomal T1–T5 dull, smooth, closely to densely punctate with minute punctures; anterior metatibial spur finely serrate to simple, with no distinct teeth.

Colour: (figs. 5A, 5B) body and legs black except mesoscutum and scutellum dark "oily" grey with bluish tinge.

Vestiture: (figs. 5A, 5B, 5E) sparse, clypeus and supraclypeal area glabrous, frons with sparse small, black, erect hair; mesoscutum and scutellum almost glabrous but with sparse small, black, erect hair; long hair on lateral, vertical posterior surface of metapostnotum; apical one third of T1 with long, erect, white hair, remainder of T1 and T2 glabrous, T3 and T4 with some black, adpressed hair apically.
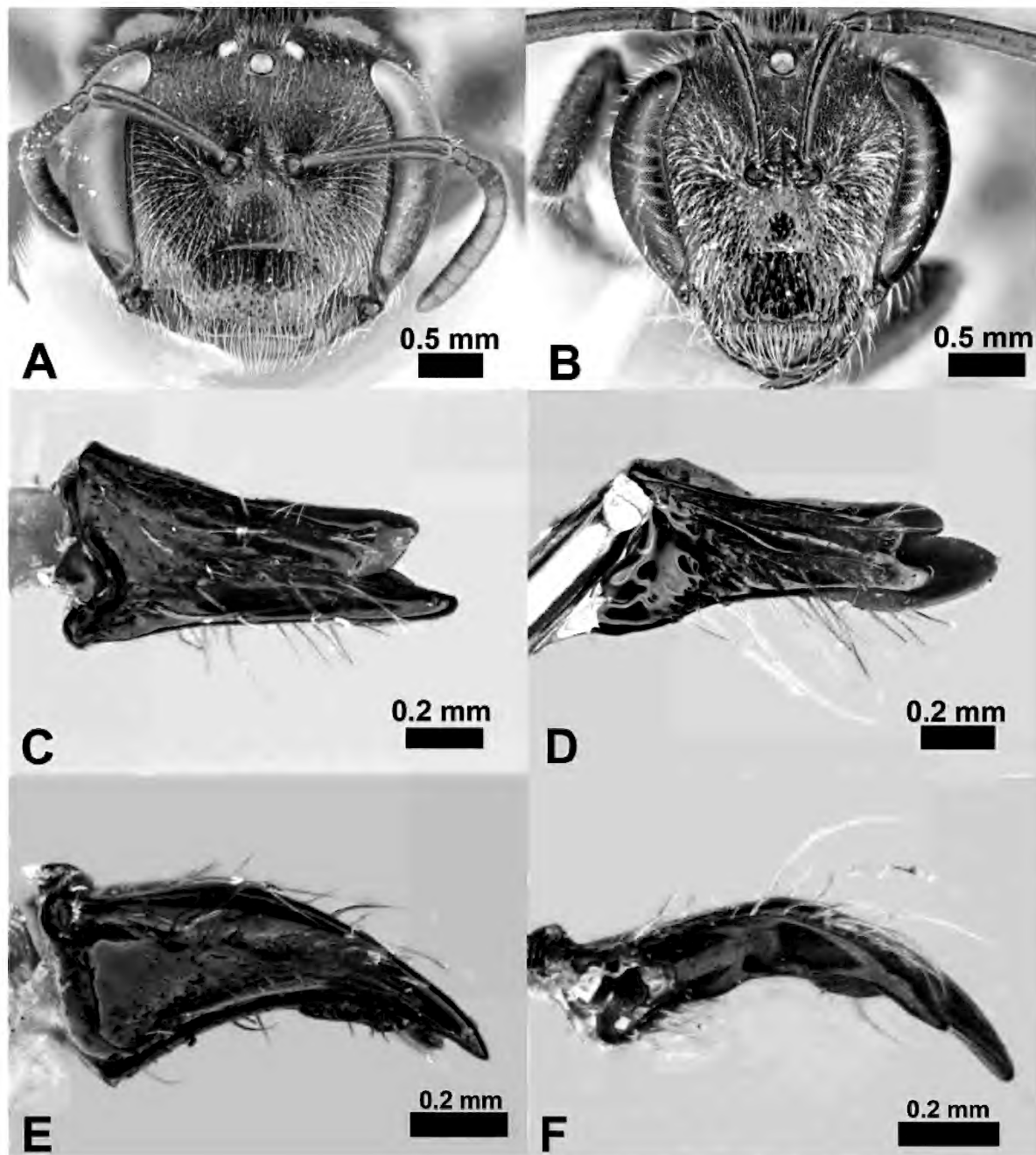
Figure 1. *Lasioglossum (Australictus) tertium* A; *Lasioglossum (Australictus) lithusca* C, E; *Lasioglossum (Parasphecodes) hiltacum* B, D, F. Head front: A & B; Mandible outer view: C & D; mandible dorsal view: E & F. All female images.
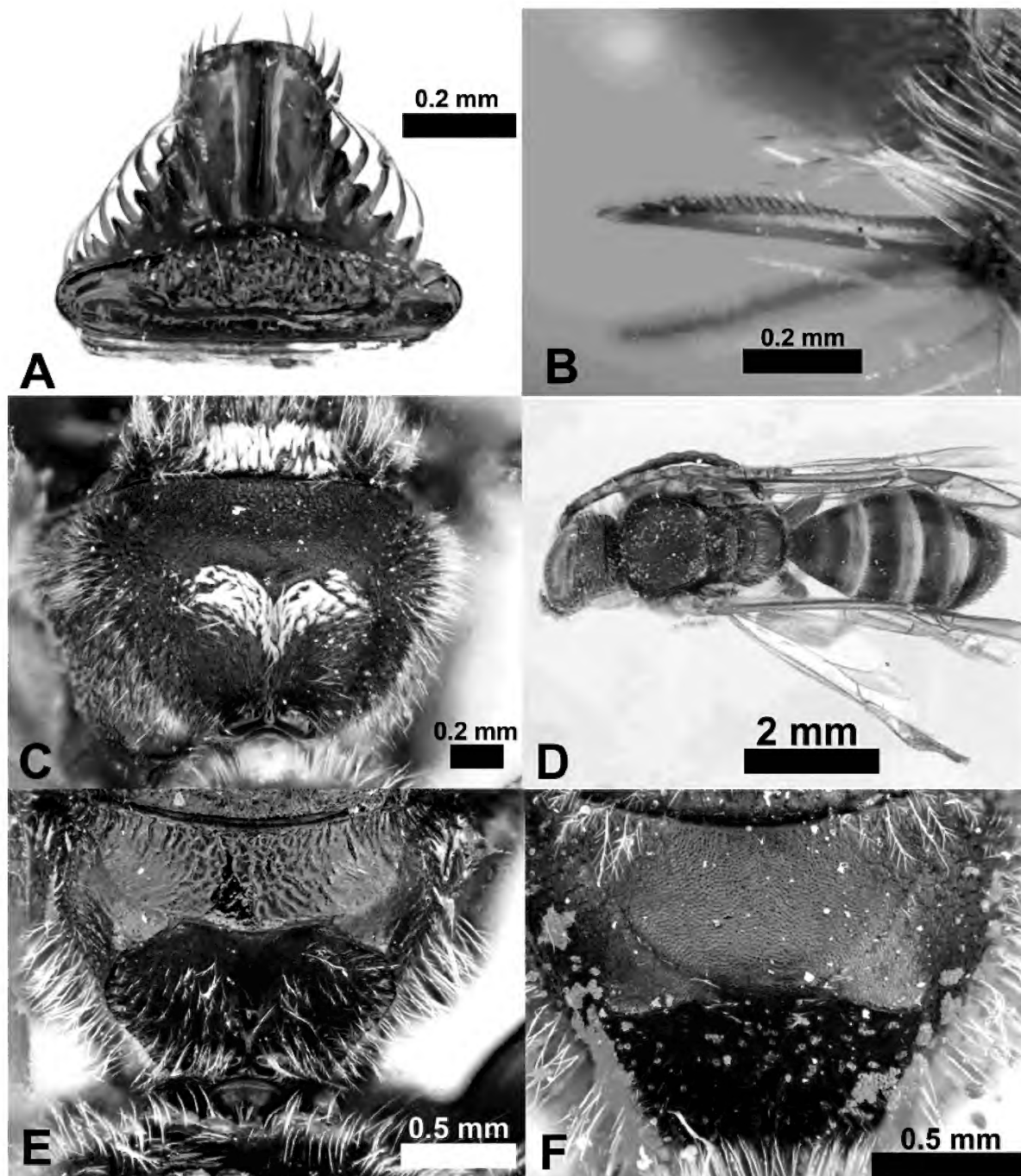
Figure 2. A, *Lasioglossum (Australictus) lithusca* female labrum; B, *Lasioglossum (Australictus) tertium* female anterior metatibial spur; C, *Lasioglossum (Australictus) peraustrale* male vertical metapostnotum tomentum; D, *Lasioglossum (Australictus) tertium*, banded male metasoma form; E, *Lasioglossum (Australictus) davide* female dorsal surface of metapostnotum; F, *Lasioglossum (Australictus) plorator* female dorsal surface of metapostnotum.
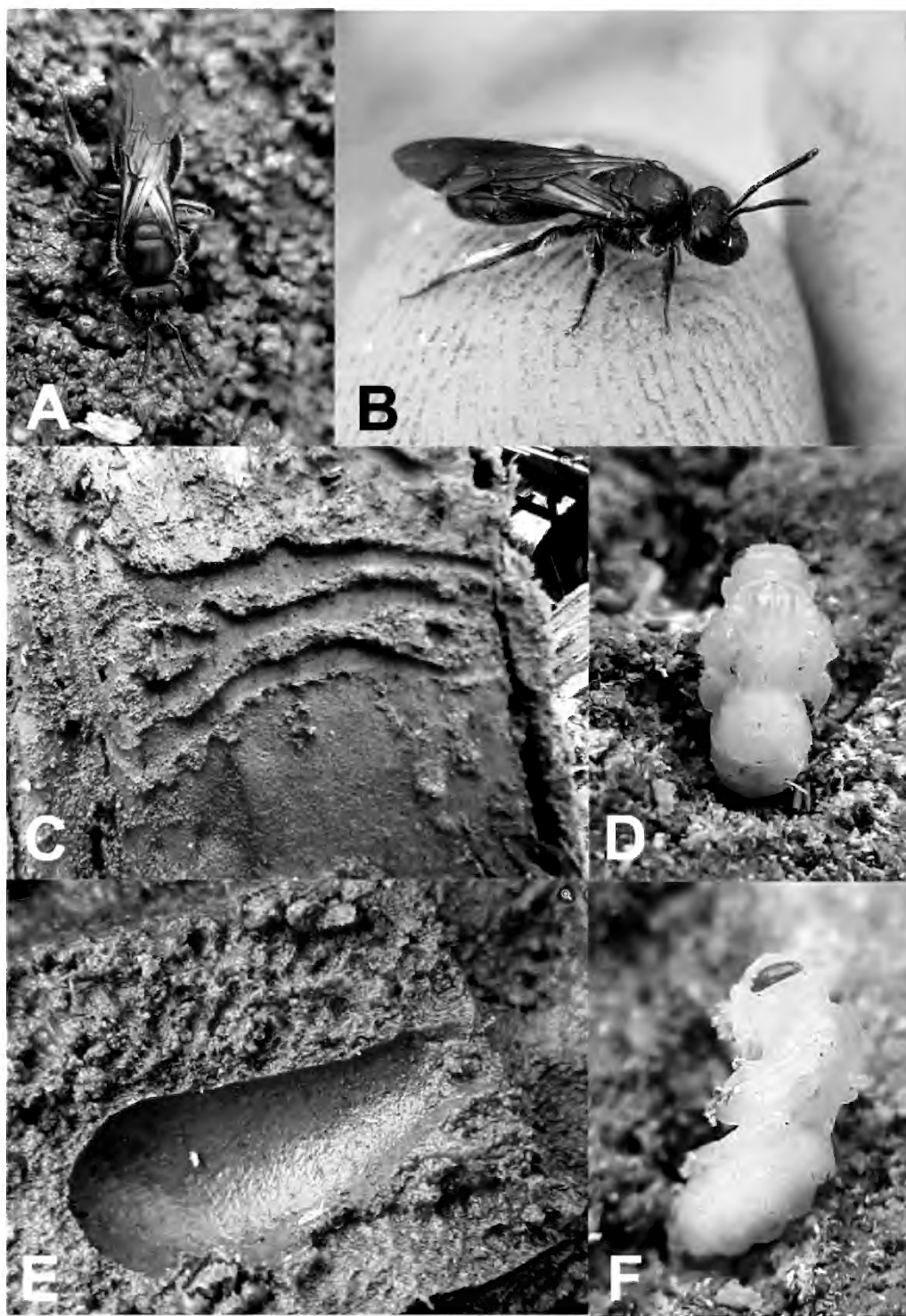
Figure 3. A–F *Lasioglossum (Australictus) plorator*: A, B, live female; C, wood nesting gallery construction; D, dorsal view of pupa; E, brood cell; F, lateral view of pupa. All images copyright Christopher Robbins.

Figure 4. *Lasioglossum (Australictus) plorator* female using a beetle exit hole in wood. Image copyright Christopher Robbins.

Description of male: (figs. 5C, 5D, 5F) body length: 7.07–8.45–8.79 mm (n=6); forewing length: 1.94–2.48–2.54 mm (n=6); head width: 1.82–2.42–2.50 mm (n=6); intertegular width: 1.44–2.15–2.21 mm (n=6). Relative head measurements: HW: 100, HL: 88–89, UID: 56–57, LID: 42–43, IAD: 12–13, OAD: 23–24, IOD: 15–16, OOD: 14–15, CL: 26–29, GW: 16–18, EW: 28–29, SL: 20–23, AF4/AF2+3 (18/14, 20/14) 1.29–1.43, FL: 178–180.

Differs from female as follows: inner eyes converging more basally; median frontal carina reaching about one quarter to median ocellus; frons sculpture reticulate across surface to inner margins of eyes; scape reaches basally level of median ocellus; clypeus surface shiny weakly microtessellate basally, medium area rounded not concave, openly punctate, supraclypeal area protruding above paraocular area, supraclypeal area bulbous, shining, openly to closely punctate; mesoscutum surface similar to female in colour but densely punctate medially, openly punctate laterad of parapsidial areas, densely punctate in parapsidal areas and anterolaterally; scutellum shiny as in female but closely punctate; dorsal surface of metapostnotum same as in female, posteriorly carinate, dorsal surface ruguloso-striolate; apical two thirds of clypeus pale yellow and metasoma in some specimen with distinct blue tinge.

Vestiture: frons hair dense, erect, black; paraocular area hair sparse, white, adpressed; mesoscutum appearing glabrous but with sparse, short, erect, black hair; metapostnotum lateral sides with short, white, adpressed hair; apical posterior vertical posterior surface of metapostnotum glabrous; metasomal sterna with moderately dense, short erect and adpressed black setae, no distinct patterns observed (fig. 5F).

Genitalia: (figs. 10A, 10B) gonobase widened basally, complete ventroapically, gonocoxa wider and longer than gonobase, with sparse, erect setae dorsoapically, glabrous ventrally, dorsal inner margins of gonocoxa basally rounded, apical inner margin not produced continuing contour of gonostylus, glabrous; retrorse lobes large, overlapping at midline, membranous, basal inner margins with short setae, apical inner margins of retrorse lobes glabrous; gonostylus small (about one third length of gonocoxa) erect, small, apically rounded, with sparse short setae; penis valves curved apically, with short dense hair dorsolaterally.

Distribution: (fig. 12A) the species is restricted to north Queensland between approximately Townsville to Cairns.

Remarks: Cockerell (1929: 211) synonymised *Halictus nigroscopaceus* with *Halictus davidis*; however, Michener (1965: 165) listed *Lasioglossum (Australictus) nigroscopaceum* as a valid species. Cockerell's (1929) synonymy was checked and accepted here. Due to the restricted distribution of this species, fewer than 20 specimens were located for this study. The only significant variation observed was in the body length of males (7.07 mm to 8.79 mm). *Lasioglossum davide* and *L. tertium* are the only two *Australictus* species in which the gonobase is widened basally (figs. 10A, 11C); in the other three *Australictus* species, the gonobase narrows basally (figs. 10A, 10E, 11A).
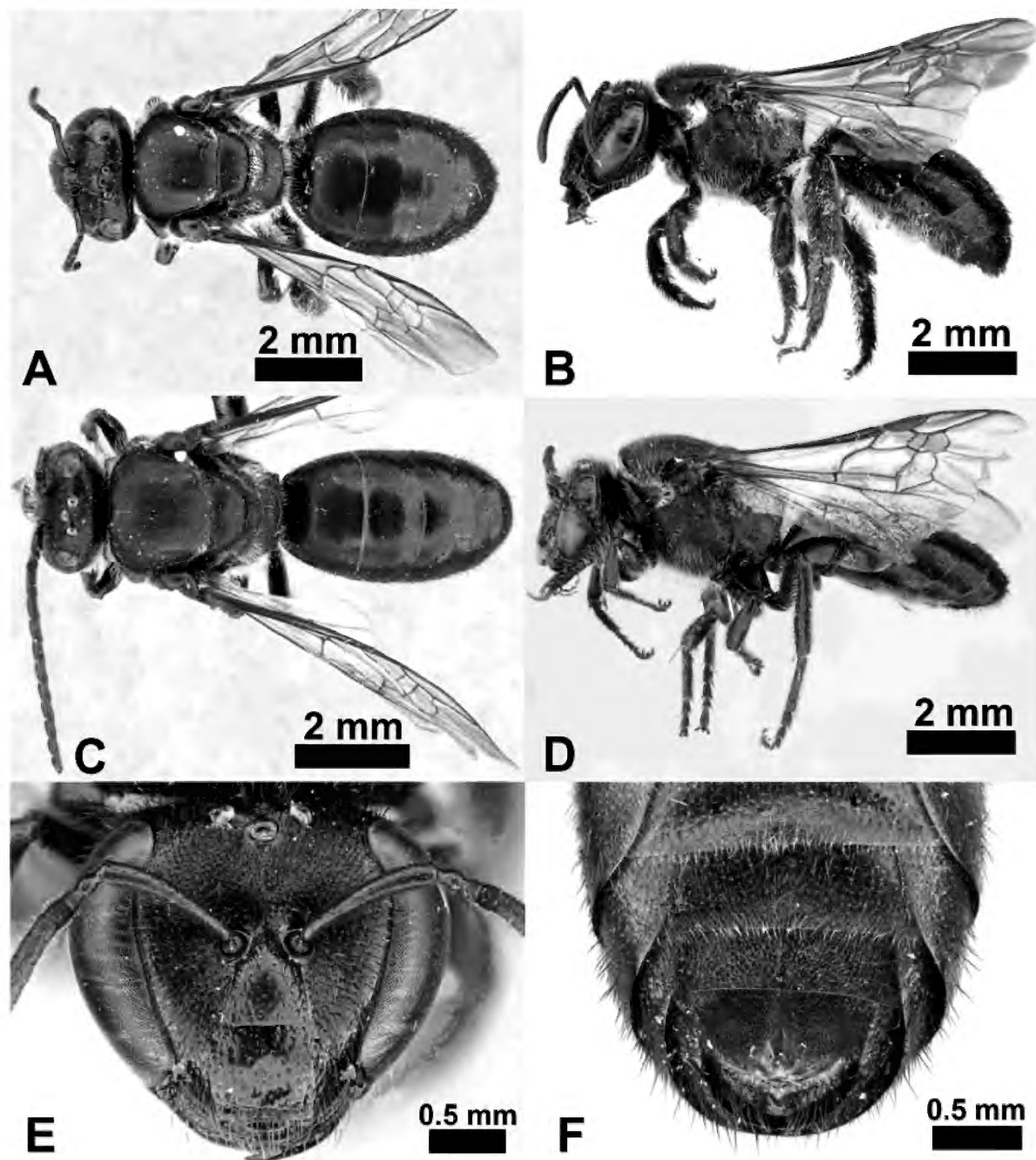
Figure 5. A–F *Lasioglossum (Australictus) davide*: A, dorsal female; B, lateral female; C, dorsal male; D, lateral male; E, female head front; F, male vestiture on metasomal sterna.

Figure 6. A–F *Lasioglossum (Australictus) lithusca*: A, dorsal female; B, lateral female; C, dorsal male; D, lateral male; E, female head front; F, male vestiture on metasomal sterna.

Figure 7. A–F *Lasioglossum (Australictus) peraustrale*: A, dorsal female; B, lateral female; C, dorsal male; D, lateral male; E, female head front; F, male vestiture on metasomal sterna.

Figure 8. A–F *Lasioglossum (Australictus) plorator*: A, dorsal female; B, lateral female; C, dorsal male; D, lateral male; E, female head front; F, male vestiture on metasomal sterna.

Figure 9. A–F *Lasioglossum (Australictus) tertium*: A, dorsal female; B, lateral female; C, dorsal male; D, lateral male; E, female head front; F, male vestiture on metasomal sterna.
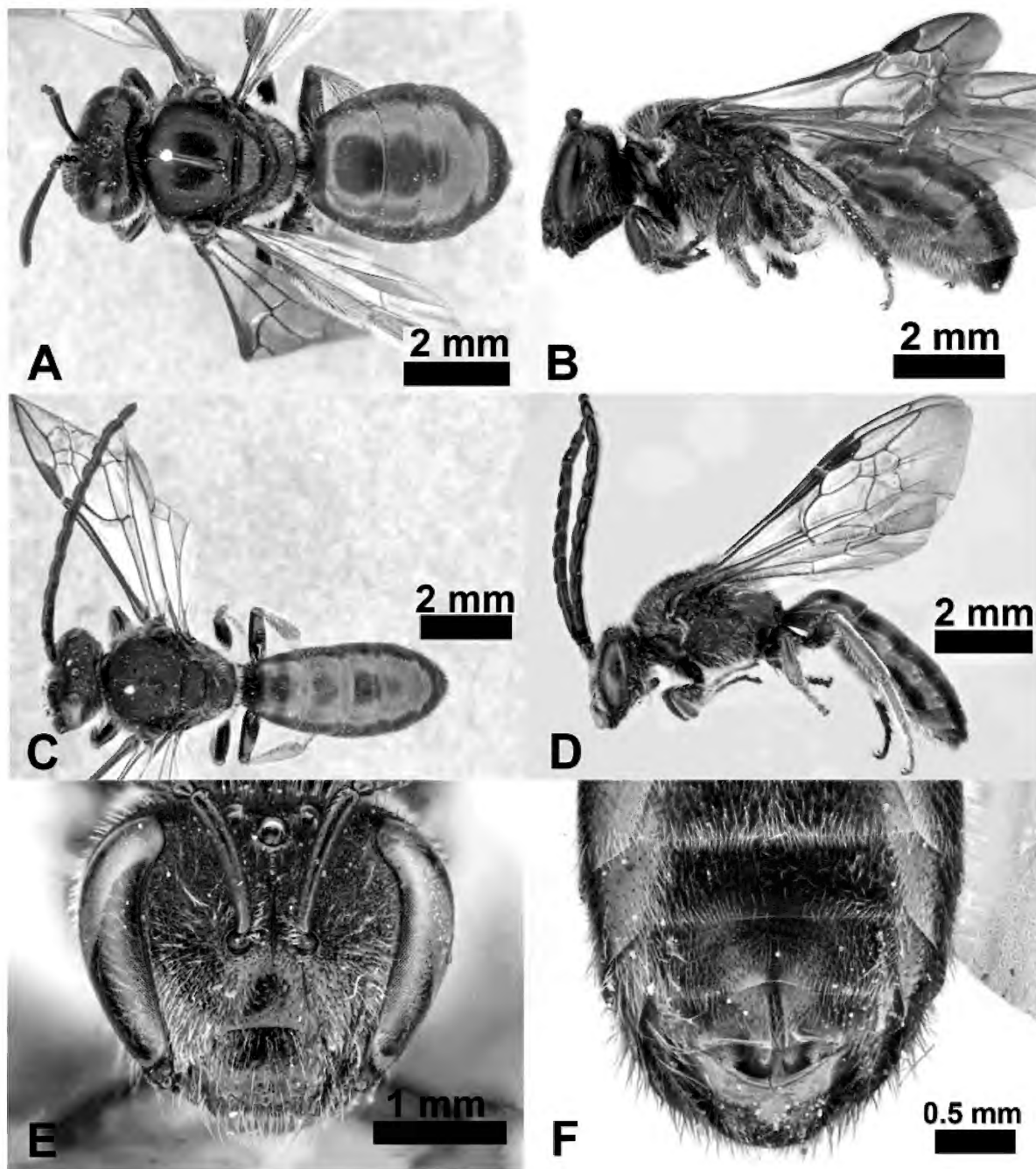
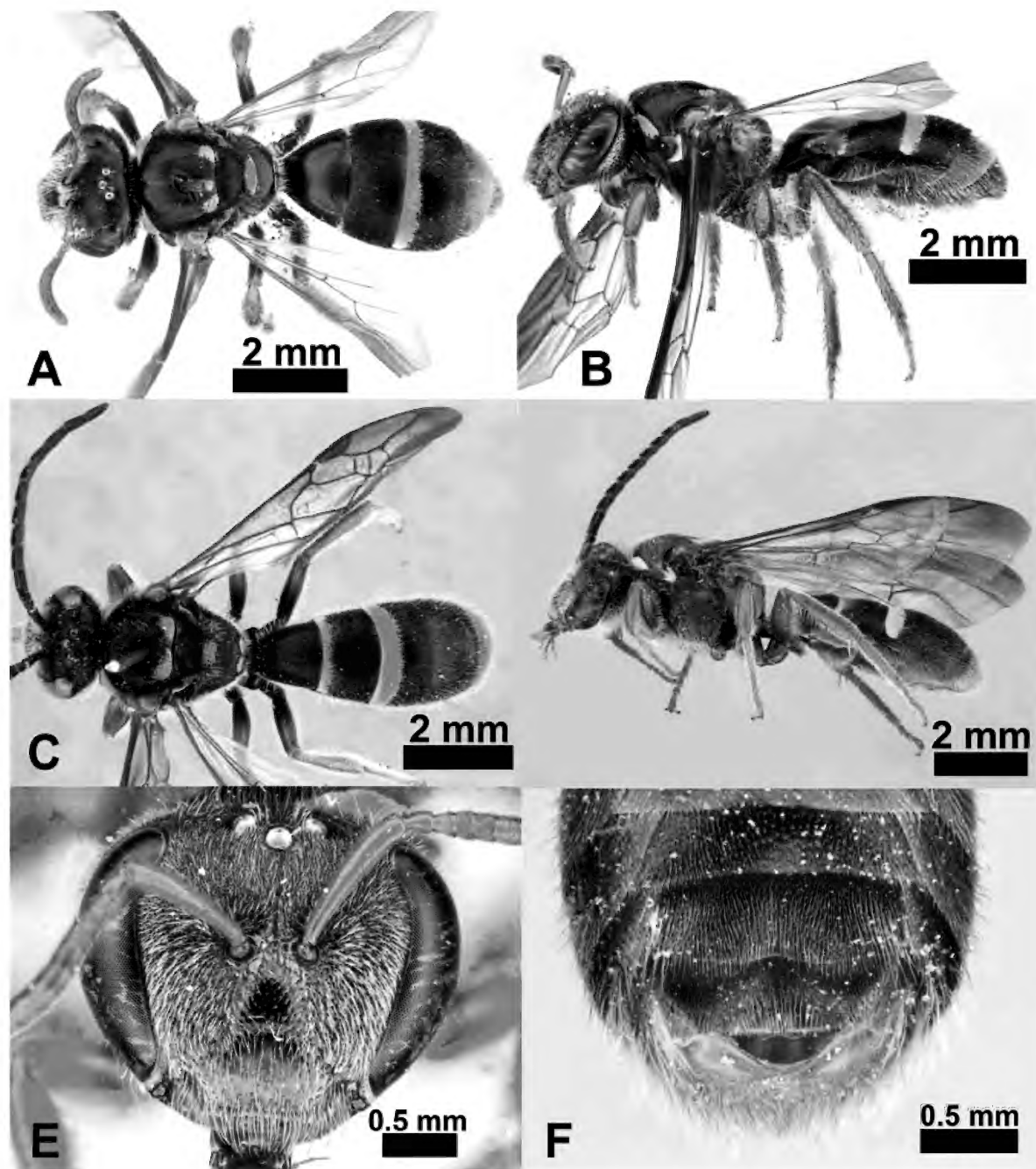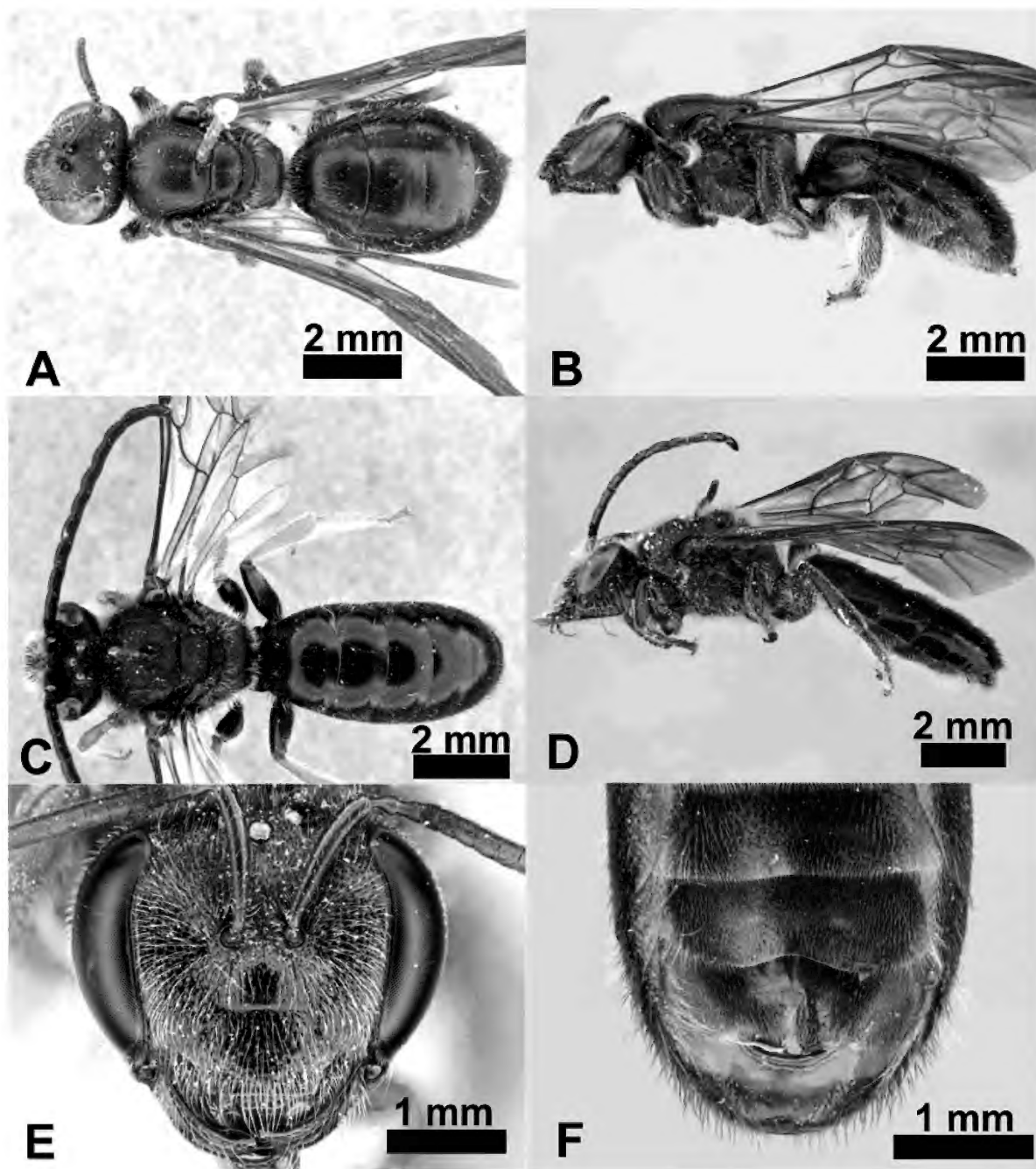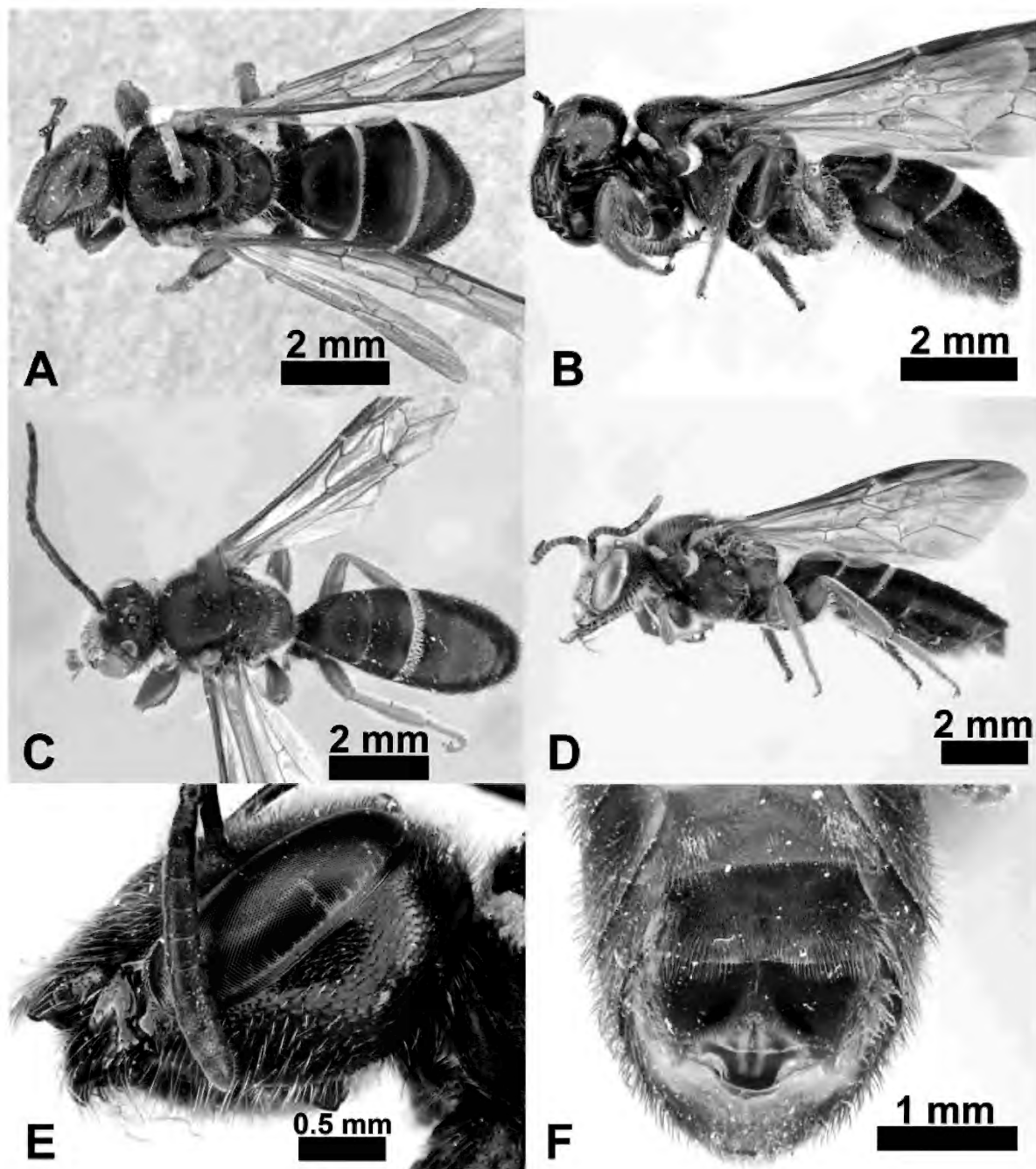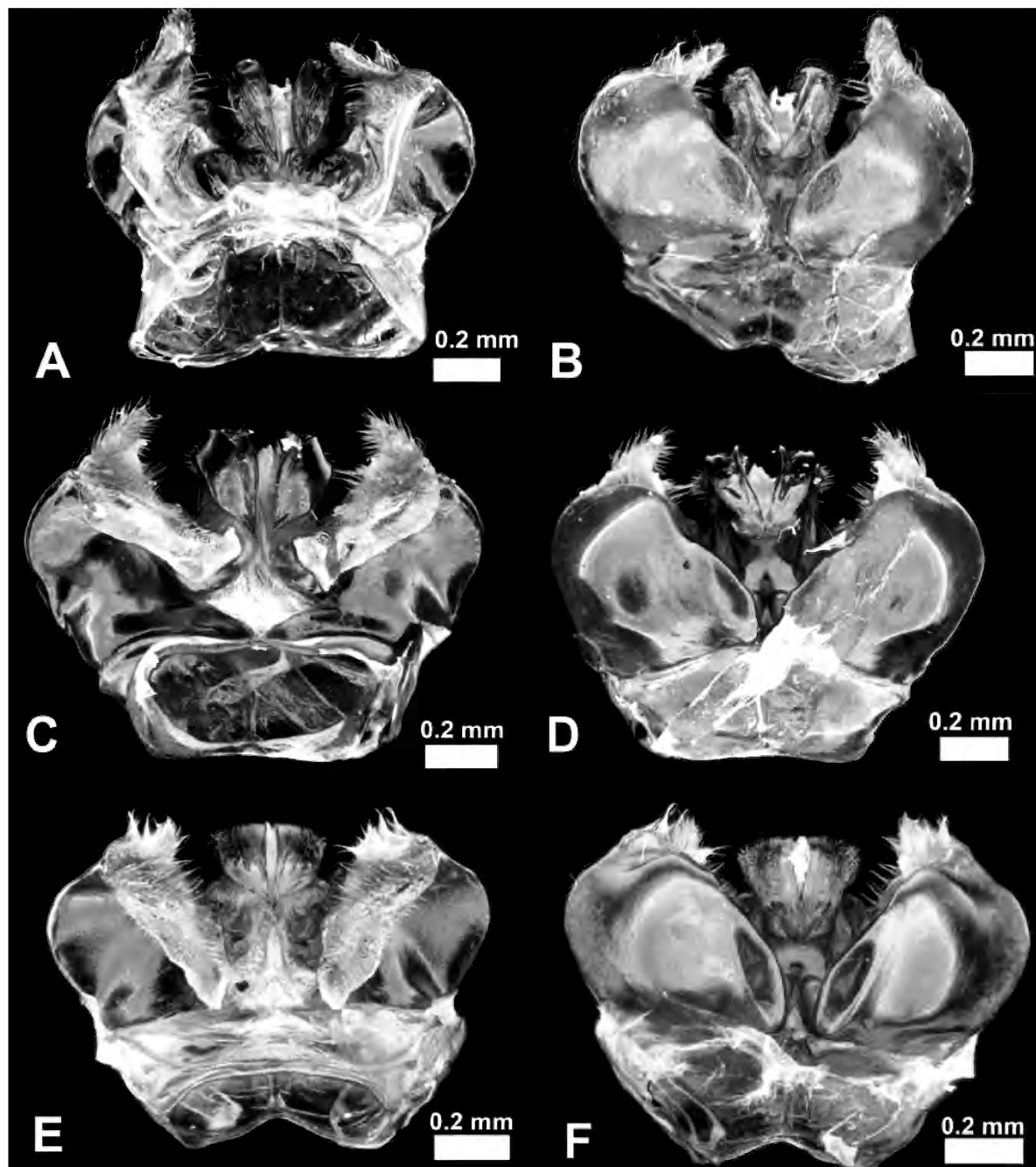Figure 10. *Lasioglossum (Australictus)* male genital capsules: Lasioglossum davide, A, ventral view, B, dorsal view; Lasioglossum lithusca, C, ventral view, D, dorsal view; Lasioglossum peraustrale, E, ventral view, F, dorsal view.
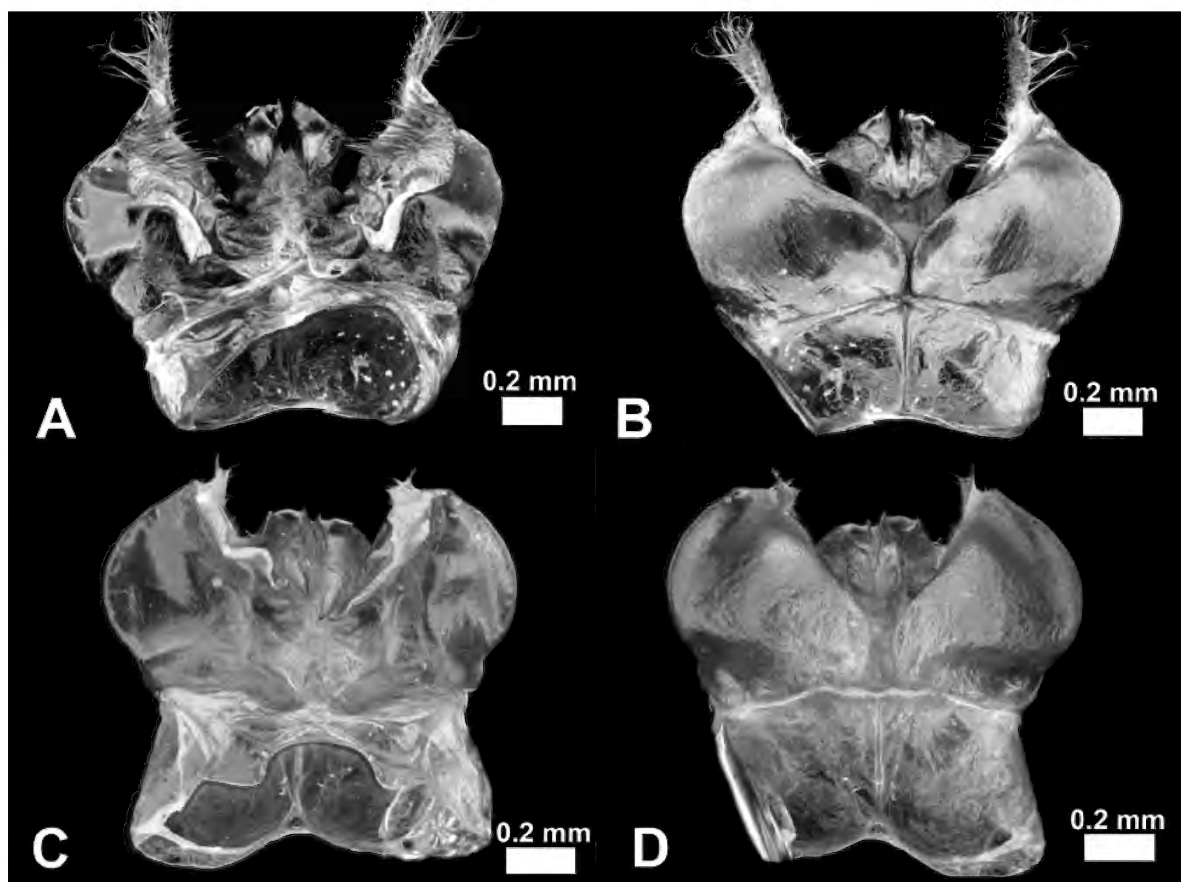
Figure 11. *Lasioglossum (Australictus)* male genital capsules: *Lasioglossum plorator*, A, ventral view, B, dorsal view; *Lasioglossum tertium*, C, ventral view, D, dorsal view.

Lasioglossum (Australictus) lithusca (Smith)

(Figs. 1C, 1E, 2A, 6A–F, 10C–D, 12B)

> *Parasphecodes lithusca* Smith 1853: 41.
> *Parasphecodes adelaidae* Cockerell 1905: 297. **syn. nov.**
> *Parasphecodes wellingstoni griseipennis* Cockerell 1929: 11. **syn. nov.**
> *Parasphecodes stuchila* Smith 1853: 43. **syn. nov.**
> *Parasphecodes wellingstoni* Cockerell 1914: 45. **syn. nov.**
> *Lasioglossum (Parasphecodes) lithuscum* – Michener 1965: 168.
> *Lasioglossum (Australictus) lithusca* **comb. nov.**
> *Lasioglossum (Parasphecodes) adelaidae* – Michener 1965: 167.
> *Lasioglossum (Parasphecodes) griseipenne* – Michener 1965: 168.
> *Lasioglossum (Parasphecodes) stuchilum* – Michener 1965: 168.
> *Lasioglossum (Parasphecodes) wellingtoni* – Michener 1965: 169.

Material examined: Holotype of *lithusca* ♀, Van Diemen's Land (ie. Tasmania) F. Sm Coll. 79.22 BMNH Hym.17.a.618 (BMNH) (view type data and image at https://data.nhm.ac.uk/object/9179e027-f637-4d01-aff4-8cb0bc82d480 accessed 16 August 2022).

Holotype of *adelaidae* ♀, South Australia: Adelaide BMNH Hym.17.a.628 (BMNH) (view type data and image at https://data.nhm. ac.uk/object/646ab614-8703-419a-9f3b-0805dbecac2e accessed 16 August 2022).

Holotype of *griseipennis* ♀, New South Wales: Jenolan, 20 April W.P. Cockerell (ANIC).

Holotype of *stuchila* ♀, Van Diemen's Land (ie. Tasmania) F. Sm Coll. 79.22 BMNH Hym.17.a.613 (BMNH) (view type data and image at https://data.nhm.ac.uk/object/2fe14c22-bac0-44f2-8f09-1250906cfbaf accessed 16 August 2022).

Holotype of *wellingtoni* ♀, Tasmania, Mt Wellington Jan 15 – Feb 6 1913, 1,300–2,000 ft R.E. Turner. Four females are mentioned in the description but one specimen is labelled "type". BMNH Hym.17.a.636 (BMNH) (view type data and image at https://data. nhm.ac.uk/object/3b470052-986f-43f2-a975-7dab4b48a12e accessed 16 August 2022).

Other specimens examined (239♀, 41♂): QUEENSLAND: (1♀) Mt Norman area, via Wallangarra, 7–8 Oct 1972, S.R. Monteith (ANIC); (1♀) Mt Norman area, via Wallangarra, 2–3 Oct 1971, G.B. Monteith (QM).

NEW SOUTH WALES & AUSTRALIAN CAPITAL TERRITORY: (2♀) 3.19 km SW Condor Ck Bridge, Brindabella Rd, 06 Nov 1992, G.J. Davis (NMV); (2♀) 1.9 km S Condor Ck, Bridge,

Brindabella Rd, 17 Oct 1993, G.V. Maynard & G.J. Davis, on *Davesia* sp. (NMV); (1♀) Lees Camp, Warks Rd, 10 Dec 1993, G.J. Davis on *Leptospermum* (NMV); (3♀) Bull's Head Repeater Station, 26 Nov 1994, G.V. Maynard & G.J. Davis, on *Pultenea* and *Davesia* (NMV); (1♀) Hill W side Condor Ck Bridge, 06 Nov 1993, G.V. Maynard & G.J. Davis on *Davesia mimosoides* (NMV); (1♀) Jink Ck, Blue Mtns, 21 Jan 1982, N.W. Rodd (AM); (1♀) Mt Boboyan 6 March 1993, G.J. Davis on *Kunzea ericoides* (NMV); (4♀) New England Nat. Pk, 5 Nov 1981, N.W. Rodd (AM); (1♀) 8 km S Mt Wilson, Blue Mtns, 10 Oct 1978, N.W. Rodd (AM); (4♀) Mt Tomah Blue Mtns, 26–29 Aug 1977 – 2 Oct 1977, N.W. Rodd (AM); (3♀) Clyde Mt, 27 Oct 1968, (ANIC); (2♀) Picadilly Circus, Brindabella Ra., 24 Nov 1981, J.C. Cardale (ANIC); (1♀) Blundell's 15 Oct 1952, Paramonov (ANIC); (1♀) Blundell's, 14 Oct 1947, E.F. Riek (ANIC); (1♀) Blundell's, 13 Feb 1950, E.F. Riek (ANIC); (1♀) Blundell's, 10 Oct 1930, L.F. Graham (ANIC); (1♀, 1♂) Mt Gingera, 6 Feb 1951, E.F. Riek (ANIC); (3♀) Winburndale, 12 mi E Bathurst, 6 Dec 1974 (ANIC); (2♂) Bendora, 6 Feb 1952, E.F. Riek (ANIC); (1♀) Brindabella, 24 Nov 1931, L.F. Graham (ANIC); (1♀) Bull's Head, 26 Feb 1952, L.J. Nick (ANIC); (1♀) Mt Tomah, Blue Mtns, 5 Nov 1980, N.W. Rodd (AM); (30♀) Picadilly Circus, Brindabella Ra.,1 Nov 1988, R.R. Snelling & J. Grey #88 (LACM); (2♀) Mt Victoria, 20 Oct 1930, A.N. Burns (NMV); (10♀) NE Nat. Pk, near Entrance, 04-20 Nov 1960, C.W. Frazier (ANIC); (1♂) New England Nat. Pk, via Ebor, 22–23 Jan 1966, B. Cantrell (QM); (1♀) 15 km SW Ebor, 12 Dec 1984, D. Yeates, on *Leptospermum mrytifolium* (ANIC); (1♀, 1♂) Nadgee Reserve, 4 km N Newton's Beach, 29 Dec 1985, E.A. Sugden (AM); (1♂) Guthega Pondage, Kosciusko Nat. Pk, 16 Mar 1983, G.R. Brown & A.E. Westcott by sweeping (OAI).

VICTORIA: (11♀) Warburton, 19 Dec 1968, E.M. Exley, on *Leptospermum ericoides* (QM); (1♀) Halls Gap, 1 Nov 1928, GB (SAM); (1♀) Black Sands, 16 Oct 1936 (ANIC); (1♀) Brisbane Ranges, Oct 1982, P. Bernhardt, on *Acacia* (NMV); (1♀) Mason's Ck, Kinglake, 20 Oct 1976, A.A. Calder (NMV); (3♀) Gorae West, 7 Oct 1957, A.N. Burns (NMV); (18♀) Gorae West, 10 Jan 1950, T. Rayment (ANIC); (1♀) Cockatoo, 24 Dec 1950, RD (NMV); (1♀) Arthur Plain, 4 Feb 1965, Neboiss (NMV); (1♀) Ferntree Gully, 1909, F.P. Spry (ANIC); (4♀) Grampians, Oct 1928, F.E. Wilson (NMV); (1♀) Reefton, 9 Feb 1955, Neboiss (NMV); (1♀) Brighton (NMV); (23♀, 31♂) Mt Hotham, 18 March & 6 April 2021, K. Walker, on *Achillea millefolium* (NMV); (2♀) Portland, Dec 1979, G. Knerer (NMV); (1♀) Asgard Swamp, 4 km NE Victoria, 10 Oct 1981, G.R. Brown (OAI); (1♀) Mt Drummer, 4 Dec 1956, E.F. Riek (ANIC); (2♀) Mt Difficult, Grampians, 2600 ft, 2 Jan 1966, B. Cantrell (QM); (1♀) Mt St Bernard, 4000 ft, 9 Jan 1932, A.N. Burns (NMV); (3♀) Flowerdale, 8 Dec 1954, Neboiss (NMV); (1♀) Mt Donna Buang, 5 Feb 1955, Neboiss (NMV); (1♀) Ferntree Gully, 1 Nov 1911, A.D.D (NMV); (1♂) Crystal Brook, Mt Buffalo, 24 Feb 1955, A.N. Burns (NMV); (1♀) 5 km W Toolangi, 7 Nov 2000, Thomas Walker, on *Ranunculus lappaceus* (NMV).

TASMANIA: (1♀) Huon Camping Area, 25 Jan 1983, I.D. Naumann & J.C. Cardale (ANIC); (3♀) Mt Wellington, 2,500 ft, Feb 1936, A.J. Turner (QM); (1♀) Mt Field Nat Pk, 13 Jan 1997, A. Hingston (NMV); (1♀) 5 km WNW Mt Alma, 27 Jan 1981, I.D. Naumann & J.C. Cardale (ANIC); (2♀) SW Nat. Pk, (Tyenna) 11 Jan 1997, A. Hingston (NMV); (2♀) Tasmania, A. Simson (SAM); (5♀) 6 mi SW Queenstown, 1 Jan 1969, E.M. Exley on *Melaleuca* (QM); (4♀) 11 mi E Strahan, 1 Jan 1968, E.M. Exley, on *Melaleuca* (QM); (6♀) 9 mi E Strahan, 1 Jan 1969, E.M. Exley, on *Bursaria* (QM); (2♀) just N of junction of Waratah & Murchison Hwys, 31 Dec 1968, E.M. Exley (QM); (1♀) nr Nunamarra, 9 Jan 1969, E.M. Exley, on *Melaleuca* (QM); (4♀) Marrawah, 30 Jan 1949, E.F. Riek (ANIC); (1♀) Southport, 18 Jan 1948, E.F. Riek (ANIC); (1♀) Meredith R, 12 mi from Corinna, 6 Jan 1954, T.G. Campbell (ANIC); (1♀) Derwent R, 740 m Lake St Clair, 24–28 Jan 1980, Lawrence & Weir (ANIC); (1♀) 7 km SWW Derwent Bridge, 16 Jan – 2 Feb 1983, I.D. Naumann & J.C. Cardale, ex pantrap (ANIC); (1♀) 7 km S Frodshams Pass, 25 Jan 1983, I.D. Naumann & J.C. Cardale (ANIC);

(1♀) Lake St Clair, 15 Apr 1955, T. Rayment (ANIC); (1♀) Lake St Clair, alt. 2,500 ft, 08 Apr 1956, T. Rayment (ANIC); (1♀) Collinsvale Road, 6 Jan 1972, W.F. Calvert (TDA); (1♀) Scarlet Ck, 3 km W Collingwood R, 8 Jan 1992, G. & A. Daniels (QM); (1♀, 1♂) 3.5 km SE Murdunna, 10 Feb 1988, G. & A. Daniels (QM); (1♀) 22 km N Dunkeld, 6 Nov 1988, R.R. Snelling & J. Grey (LACM); (8♀) Hasting, 15 Jan 1949, E.F. Riek (ANIC); (1♀) Hobart, 4 March 1989, K. Walker, on *Eucalyptus* (NMV); (1♀) Melaleuca nr Bathurst Harbour, 9 Nov 1991, I. Naumann & G. Clarke, heathy sedge land & closed forest margin (ANIC); (1♀) Melaleuca nr Bathurst Harbour, 3–7 Dec 1990, I. Naumann, margin *Melaleuca / Leptospermum* (ANIC); (2♀) Celery Top Is., Bathurst Harbour, 4 Dec 1990, I.D. Naumann (ANIC); (1♀) Claytons, Bathurst Harbour, 6 Dec 1990, I.D. Naumann (ANIC); (1♀) Railton, 8 Jan 1991, B.B. Lowery, in rotten log (ANIC); (1♀) Liffey Valley, May 1980, S. Fearn, ex alcohol storage (ANIC); (2♀) 9 km WSW Derwent Bridge, 21 Jan 1983, I.D. Naumann & J.C. Cardale (ANIC); (2♀) Mt Wellington, 6 Jan 1918, G.H. Hardy (QM); (4♀) Hobart, 10 Dec & 20 Dec 1913, G.H. Hardy (QM); (1♀) Lake St Clair, 13 Jan 1937, C. & C. Davis (AM); (1♀) Pieman Bridge, 8 Jan 1937, C. & C. Davis (AM); (1♀) Dover, 1963, from Sirex emergence hole (QM).

SOUTH AUSTRALIA: (1♀) Adelaide (BMNH).

Floral record: Families visited: 6 (Asteraceae (2), Fabaceae (4), Orchidaceae (1), Myrtaceae (11), Pittosporaceae (2), Ranunculaceae (1)). Genera visited: 10 (*Acacia* (1), *Achillea* (2), *Brenesia* (1), *Bursaria* (2), *Davesia* (2), *Kunzea* (1), *Eucalyptus* (3), *Leptospermum* (3), *Pultenaea* (1), *Ranunculus* (1)).

Flight phenology capture records: Jan (27) Feb (14) Mar (7) Apr (3) May (1) June (0) July (0) Aug (1) Sept (0) Oct (17) Nov (14) Dec (14).

Diagnosis. *Lasioglossum (Australictus) lithusca* is unlike any other *Australictus* species in body colour. This species can be distinguished, in both sexes, from other *Australictus* species by red-brown-coloured metasoma contrasting with black mesosoma; lack of tomentum on mesosoma or metasoma; dorsal surface of metapostnotum posterior margin acarinate but dorsal surface elevated above surrounding lateral and vertical surfaces; metapostnotum dorsal surface sculpture ruguloso-striolate (figs. 6A–D); male genitalia with gonobase narrowed basally, large retrorse lobes and small, erect gonostylus (figs. 10C–D); and metasomal sternal S5 lateral margins with distinct white, semi-erect hair tufts (fig. 6F). This species occurs in SE Australia, including Tasmania (fig. 12B).

Description of female: (figs. 6A, 6B, 6E) body length: 9.11–10.49–10.83 mm (n=10); forewing length: 2.73–2.76–2.78 mm (n=10); head width: 2.64–2.72–2.78 mm (n=10); intertegular width: 1.92–2.04–2.06 mm (n=10). Relative head measurements: HW: 100, HL: 88–90, UID: 56–57, LID: 53–54, IAD: 10–11, OAD: 22–23, IOD: 14–15, OOD: 14–15, CL: 23–25, GW: 21–23, EW: 21–23, SL: 39–40, FL: 71–73.

Head: (fig. 6E) inner eyes weakly narrowed basally; median frontal carina reaching about than one third way to median ocellus; clypeus smooth, polished with microtellesate sculpture on basal one third, medially flattened to weakly concave, closely punctate with large, deep, rounded punctures, medially with vertical grooves, supraclypeal area distinctly raised above paraocular area, surface dull, dense microtessellate pattern, open to sparsely punctate with shallow punctures; frons dull, close, vertical striae and punctate, paraocular area smooth, shining closely punctate.
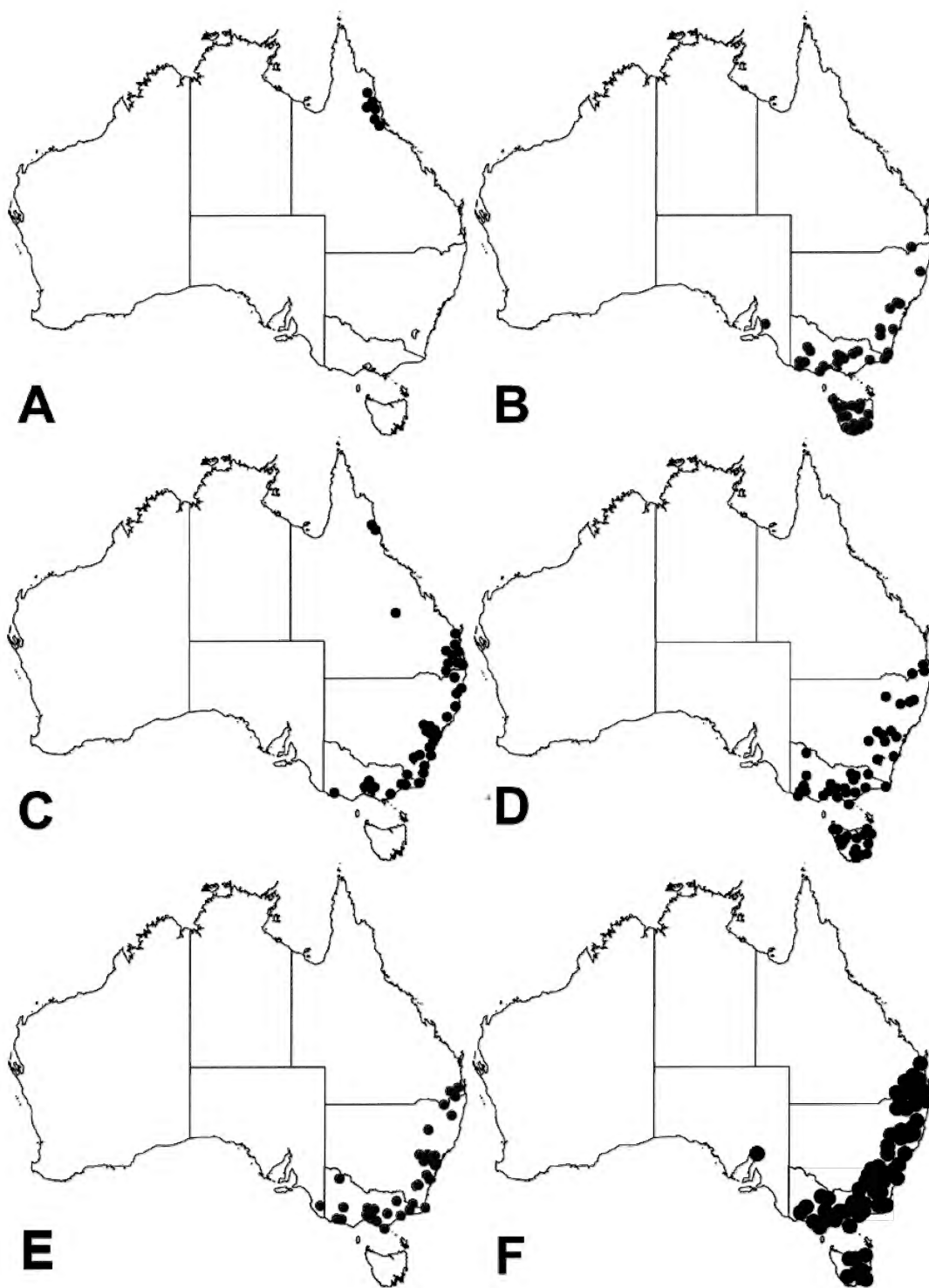
Figure 12. Species distribution maps: A, *Lasioglossum (Australictus) davide*; B, *Lasioglossum (Australictus) lithusca*; C, *Lasioglossum (Australictus) peraustrale*: D, *Lasioglossum (Australictus) plorator*; E, *Lasioglossum (Australictus) tertium*; F, *Lasioglossum (Chilalictus) orbatum*.

Mesosoma: (fig. 6A) mesoscutum anterior mesial margin weakly produced mesoanteriorly, surface dull, with minute microtessellate pattern, medially openly to closely punctate, laterad of parapsidal areas open to sparsely punctate, in parapsidal areas densely punctate, densely punctate along posterior margin; scutellum 2 x longer than dorsal surface of metapostnotum, scutellum smooth, shining, openly to sparsely punctate; dorsal surface of metapostnotum acarinate across posterior margin defined by crescent shaped ridge distinctly raised above vertical and lateral surfaces, dorsal surface ruguloso-striolate, sculpture reaches posterior margins, lateral margins smooth, dull with microalveolate pattern, vertical posterior surface of metapostnotum defined by lateral carinae; mesepisternum and metepisternum plicate; first recurrent vein (1m-cu) entering second submarginal cell.

Metasoma and legs: (figs. 6A-B) metasomal T1- T5 with dull sheen, appears impunctate, sparsely punctate with minute punctures; anterior metatibial spur finely serrate with distinct, small, backwardly pointing teeth.

Colour: (figs. 6A-B) head and mesosoma black, some specimens apical half of clypeus red-brown, T1-T3 red-brown, T4-T5 red-brown suffused with black; legs with fore, mid coxae, trochanters, femora black, remainder red-brown.

Vestiture: (figs. 6A-B, 6E) body sparse, clypeus and supraclypeal area glabrous, frons with sparse small, black, erect hair, paraocular area with downwardly pointing white hair, mesoscutum and scutellum appear glabrous with sparse small, black, erect hair, long, white hair on lateral, vertical posterior surface of metapostnotum, metasoma sparse, laterally with short, erect white hair.

Description of male: (figs. 6C-D) Body length: 8.95–10.08–10.21 mm (n=10); forewing length: 2.69–2.81–2.98 mm (n=10); head width: 2.35–2.61–2.69 mm (n=10); intertegular width: 1.92–2.07–2.16 mm (n=10). Relative head measurements: HW: 100, HL: 88–89, UID: 56–57, LID: 42–43, IAD: 12–13, OAD: 22–23, IOD: 16–18, OOD: 13–14, CL: 25–26, GW: 16–18, EW: 28–29, SL: 22–23, AF4/AF2+3 (24/15, 22/14) 1.57–1.60, FL: 248–252.

Differs from female as follows: upper and lower inner eye margins converging basally; median frontal carina extending just beyond antennal bases; frons sculpture densely reticulate across surface to inner margins of eyes; scape reaches basally level of median ocellus; clypeus surface shiny with weak microtessellate pattern basally, medium area weakly concave, openly punctate with shallow punctures, supraclypeal area protruding above paraocular area, bulbous, dull, with dense microtessellate sculpture, closely punctate with minute, shallow punctures; mesoscutum dull, with dense microtessellate sculpture, closely to densely punctate, scutellum and metanotum similar to mesoscutum; dorsal surface of metapostnotum same as in female, acarinate, dorsal surface defined by raised ridge, dorsal surface coarsely ruguloso-striolate; colour similar to female except apical two thirds of clypeus pale yellow, metasoma colour ranges from T1–T3 red-brown, T4–T6 red-brown suffused with black, or T1 almost black, T2–T3 red-brown with median black band, T4–T6 almost black.

Vestiture: lower half of frons, between antennal bases and paraocular area with dense, erect, white hair, gena with dense

beard of long, plumose, white hair, mesoscutum with sparse, short, erect, brown hair, metapostnotum lateral sides with short, white, adpressed hair, apical posterior vertical posterior surface of metapostnotum glabrous, metasomal sterna S1–S4 with sparse white, adpressed hair, S5 lateral margins with distinct white, semi-erect hair tufts (fig. 6F).

Genitalia: (figs. 10C, 10D) gonobase sides narrowed basally, complete ventroapically, gonobase width almost half of gonocoxa width, gonocoxa glabrous ventrally and dorsally, dorsal inner margins of gonocoxa basally rounded, gonocoxa apical inner margin not produced, continues contours of gonostylus, glabrous; retrorse lobes large, meeting at midline, membranous, inwardly pointing, outer margins of retrorse lobes glabrous, inner margins basally with erect, large setae, apically with short adpressed, erect setae; gonostylus small (about one third length of gonocoxa), erect, apically rounded, with simple, erect hair; penis valves curved apically, with short dense hair dorsolaterally.

Distribution: (fig. 12B) this species occurs from SE Queensland, down New South Wales coast, across Victoria, throughout Tasmania and one South Australian record. It has been recorded from sea level (Portland 7.23 m) up to high elevations in Victoria (Mt Hotham 1,861 m) and Tasmania (Mt Wellington 1,271 m).

Remarks: Australian Halictidae species now in the genus *Lasioglossum* were originally placed in either *Halictus* Latreille 1804 or *Parasphecodes*, and most original species names ended with "us" or "a". Michener's (1965) revision of the Australian bee fauna recombined these species into the genus *Lasioglossum*. In accordance with ICZN rules (Articles 31 and 34), Michener changed species name endings to agree with the gender of *Lasioglossum* and endings with "us" or "a" were changed to "um". Therefore, Michener 1965 changed *Parasphecodes lithusca* to *Lasioglossum (Parasphecodes) lithuscum*.

John Ascher (pers. comm.) argued that some of these names should not have been changed. John reasoned that 12 of Smith's (1853) new species names were partial anagrams of the word "Halictus", meaning these species names should be treated as nouns in apposition rather than adjectival and therefore should not have been changed in Michener's (1965) revision. Accordingly, Michener's (1965) *L. (Parasphecodes) lithuscum* name has been reverted to Smith's (1853) original species name of *L. (Australictus) lithusca*.

Cockerel (1914: 46) commented that *Parasphecodes wellingtoni* was close to *Parasphecodes lithusca* but differed in leg colour; that colour difference is within the known colour range. Cockerell (1929: 11) commented that *Parasphecodes wellingtoni griseipennis* was "typical" of *Paraspheodes wellingtoni* but that species occurred in Tasmania, whereas the new subspecies "*griseipennis*" occurred in New South Wales. *Lasioglossum (Australictus) lithusca* is now recorded from SE Queensland across to South Australia, including Tasmania. Several female specimens carried deutonymphal *Anoetus* Dujardin 1842 (Sarcoptiformes: Astigmatina: Histiostomatidae) hypopial mites apically across T1, though one specimen had several mites on the right forewing. No acarinarium was present on T1, but this area has a moderate cover of erect setae. See Walter et al. (2002) for full discussion of mites on bees.

Rayment identified a specimen as this species, his handwritten label reading "Bolgart WA, 12 Jan 1950". This is the only specimen of this species and the entire subgenus recorded from Western Australia. I consider it to be an incorrect labelling, because Rayment also collected and labelled, in his handwriting, specimens of *L. lithusca* at Gorae West, Victoria on 10 Jan 1950. I have not included Rayment's WA specimens in the "Other Material Examined" or on the species distribution map.

Although this species was originally described in *Parasphecodes* by Smith (1853) and placed in *Lasioglossum (Parasphecodes)* by Michener (1965), it is better placed in *Lasioglossum (Australictus)* due to the presence of all the *Australictus* subgeneric diagnostic characters, especially the elongated and enlarged preapical tooth on the mandible, finely serrate anterior metatibial spur, shape of labrum and male genitalia characters.

Lasioglossum (Australictus) peraustrale (Cockerell)

(Figs. 2C, 7A–F, 10E, 10F, 12C)

> *Halictus peraustralis* Cockerell 1904: 211.
> *Halictus odyneroides* Rayment 1939: 279. **syn. nov.**
> *Lasioglossum (Australictus) peraustrale* – Michener 1965: 165.
> *Lasioglossum (Australictus) odyneroides* – Michener 1965: 165.

Material examined: Holotype of *peraustralis* ♀, South Australia. "bicingulatus var. Smith" F. Sm. Coll. 79.22 BMNH Hym.17.a.693 (BMNH) (view type data and image at https://data.nhm.ac.uk/object/c23639db-a1d1-40e5-886a-ef654e4d3c8f accessed 16 August 2022).

Holotype of *odyneroides* ♀, New South Wales, White Swamp, Macpherson Range, May 1939, J. Hardcastle. (ANIC).

Other specimens examined (219♀, 47♂): QUEENSLAND: (11♀) Kuranda, Black Mountain Road, 3 Oct 2005, K. Walker, on *Lophostemon grandifloris* (NMV); (1♀) Cairns dist. F.P. Dodd (QM); (34♀) Brisbane, 4 Jul 1914, 1 Sept 1914, 24 Sept 1914, 29 Sept 1914, 2 Feb 1918, 13 Mar 1918, 12 Feb 1918, 6 Mar 1918, H. Hacker (QM); (1♀) Mt Moffat Nat Pk, Kenniff Cave, 840 m, 22 Nov 1995, C. Burwell (QM); (5♀) Stradbroke Is., 3 Dec 1912, 7 Sept 1914, 17 Sept 1915, H. Hacker (QM); (1♀) Birkdale, 13 Mar 1918, H. Hacker (QM); (2♂) Cairns district, F.P. Dodd (SAM); (2♂) Upper Cedar Creek via Samford, 21 Nov 1965, B. Cantrell (QM); (3♂) Cedar Ck, 21 Nov 1965, T. Weir (QM); (1♂) Brisbane, 17 Apr 1955, J. Kerr (NMV); (2♂) 5 km N Karara, 6 Jan 1984, K. Walker on *Eucalyptus* (NMV); (1♂) Murphy's Creek, 30 Nov 1988, K. Walker, on *Eucalyptus* (NMV); (2♀, 1♂) Leslie Dam, 13 km W Warwick, 13 Nov 1978, K. Walker, on *Eucalyptus* (QM); (1♂) Broken R, Eungella, 16–17 Nov 1992, 750 m, Monteith, Thompson, Cook & Janetzki (QM); (1♀, 3♂) 3 mi Cunningham's Gap, 25 Feb 1959, C.D. Michener on *Bursaria spinosa* (SEM); (1♂) Tambourine, 18 Dec 1958, C.D. Michener (SEM); (1♀) Tambourine, 1923, W.H. Davidson (QM); (2♀) Amiens, 4 Nov 1965, J.C. Cardale (QM); (1♀) Severnlea via Stanthorpe, 10 Dec 1980, E.M. Exley & J. King on *Leptospermum* (QM); (2♀) 11 km S Cunningham's Gap, 12 Nov 1980, J. & C. King, on *Bursaria spinosa* (QM); (1♀) Lucas Heights, 5 Nov 1995, A. Sundholm, on *Leptospermum polygalifolium* (QM); (2♀) Springbrook, 12 Feb 1943, A.J. Turner (QM); (2♀) 8 mi N of Landsborough, 28 Oct 1965, J.C. Cardale (QM); (1♀) Capalaba, 23 Sept 1961, R. Shepard (QM); (2♀) Burleigh, 28 Sept 1958, A.N. Burns (NMV); (1♀) 13 mi N Stanthorpe, 29 Dec 1958, C.D. Michener (SEM).

NEW SOUTH WALES & AUSTRALIAN CAPITAL TERRITORY: (23♀) In rotten log, Bankstown nr Sydney, 30 June 1984, B.J. Day (AM); (33♀, 1♂) Bilpin Blue Mtns, 11 Mar 1981, 28 Feb 1986, 10 Sept 1979, 14 Nov 1977, 22 Sept 1977, 19 Apr 1978, 21 Nov 1978, 2 Oct 1978, N.W. Rodd (AM); (1♀) Kurrajong Heights, 27 Feb 1978 (AM); (1♀) Woronara, 12 Jan 1982, M.L. Mason (AM); (4♂) Castle Flat, Clyde R, 4.5 km W Pigeon House, 8 Jan 1984, L. Hill, ex cluster c. 150 on twigs (AM); (1♂) Liston, 23 Dec 1969, J.C. Cardale, on *Eucalyptus* (ANIC); (1♀) National Park, 23 Dec 1906, C. Gibbons (AM); (1♀) Patonga, 25 Nov 1945 (AM); (33♀, 2♂) Cheltenham, 22 Oct 1949, 1 Apr 1950 (AM); (1♀) Approx. 1 km S Kew, 23 Dec 1981, G. & T. Williams, on *Leptospermum* blossoms (AM); (1♂) Brunswick Heads, 12 Jan 1938, E.F. Riek (ANIC); (1♂) Hornsby, C. Gibbons (AM); (9♀, 1♂) Nadgee Reserve, 7 km S of Newton's Beach, 21 Dec 1985, E.A. Sugden (AM); (1♂) Gosford, 13 Mar 1932, A.J. Turner (QM); (1♀) Mountain Lagoon, Blue Mtns, 23 Nov 1977, N.W. Rodd (AM); (4♀) Sydney, W.W, Froggatt (ANIC); (1♀) Pearl Beach, near Woy Woy, 9-11 Dec 1988, M.J. Fletcher & J.A. MacDonald (OIA); (1♀) nr Glenbrook Ck, Blue Mtns, 23 Dec 1998, G.R. Brown (OIA); (1♀) Lane Cove, 26 Sept 1987, S.G. Hunter (OIA); (1♀) Georges River, nr Lugarno, 16 Apr 1941, A. Holmes (AM); (1♀) Barrington House via Salisbury, 25–28 May 1963, A. Macqueen (QM); (3♀) State Forest Gibraltar Range, 29 Dec 1969, C.W. Frazier (ANIC); (1♀) Nelligen, 3 Nov 1949, Cane & Gemmell (ANIC); (1♀) Jervis Bay, 7 Nov 1956, E.F. Riek (ANIC); (1♀) 2.7 km NE Queanbeyan, 670 m, 16 Dec 1979, I.F.B. Common (ANIC); (1♀) 3 km N Lansdowne, nr Taree, 3 Jan 1992, G. Williams on *Tristaniopsis laurina* blossoms (NMV); (2♀) Royal National Park, 28 Dec 1970, D.K. McApline (AM); (1♀) Black Mountain, 15 Jan 1934, F.J. Gray (ANIC); (2♀) Wisemans Ferry, 18 Dec 1927, A.N. Burns (NMV); (1♀) Buchan, 26 Jan 1937, A.N. Burns (NMV); (1♀) Mt Wilson, 4 Jan 1931, A.N. Burns (NMV); (1♀) Wattle Flat, W.W. Froggatt (ANIC).

VICTORIA: (2♀, 1♂) N of Lakes Entrance, Colquhoun State Forest, 21 Feb 1985, 6 Feb 1987, K. Walker, on *Eucalyptus* (NMV); (6♂) 9 km N Bruthen, 8 Feb 1992, G. Daniels & C. Burwell (QM); (3♀) Coranderrk, 16 Nov 1984, P. Bernhardt on *Acacia mearnsii* (NMV); (2♀) Woori Yallock, 23 Nov 1930, A.N. Burns (NMV); (4♀) Tambo Crossing, Jan 1935, F.E. Wilson (NMV).

Floral record: Families visited: 3 (Fabacaea (1), Myrtaceae (10), Pittosporaceae (2)). Genera visited: 6 (*Acacia* (1), *Bursaria* (2), *Eucalyptus* (4), *Lophostemon* (1), *Leptospermum* (2), *Tristaniopsis* (1)).

Flight phenology capture records: Jan (27) Feb (14) Mar (7) Apr (3) May (1) June (0) July (0) Aug (1) Sept (0) Oct (17) Nov (13) Dec (14).

Diagnosis. *Lasioglossum (Australictus) peraustrale* is most like *L. (Australictus) tertium* with pronotum and metasomal tomentous yellow hair bands. This species can be distinguished in both sexes from other *Australictus* species by black body colour; tomentum on pronotum, posterolateral corners of mesoscutum, metanotum and metasomal bands on T2–T3; dorsal surface of metapostnotum posterior margin acarinate but elevated above surrounding lateral and vertical surfaces; metapostnotum dorsal surface sculpture microalveolate; metapostnotum vertical surface with V-shaped patch of white tomentum (weak in female and dense in male) (figs. 2C, 7A–D); male genitalia with gonobase narrowed basally, large retrorse lobes and gonostylus absent (absent gonostylus is shared with *L. tertium* only; figs. 10E, 10F, 11C, 11D); and metasomal sternal S5 lateral margins with weak, white, semi-erect hair tufts (fig. 7F). This species occurs in North Queensland but is primarily found in SE Australia, and is absent from Tasmania (fig. 12C).

Description of female: (figs. 7A, 7B, 7E) body length: 8.32–9.59–10.05 mm (n=10); forewing length: 2.35–2.89–3.07 mm

(n=10); head width: 2.54–2.76–2.83 mm (n=10); intertegular width: 1.68–1.83–1.92 mm (n=10). Relative head measurements: HW: 100, HL: 80–81, UID: 58–59, LID: 56–57, IAD: 09–10, OAD: 21–22, IOD: 12–13, OOD: 16–17, CL: 21–22, GW: 20–21, EW: 23–25, SL: 41–42, FL: 62–65.

Head: (fig. 7E) distance between inner upper and lower inner eye margins almost parallel; median frontal carina reaching about half way to median ocellus; clypeus smooth, polished with minute microtesellate sculpture, medially flattened, closely to sparsely punctate with shallow, rounded punctures, medially several punctures; supraclypeal area slightly raised above paraocular area, surface with dull sheen, with weak microtessellate pattern, open to closely punctate with shallow punctures; frons dull, with dense reticulate punctures which extend to inner margins of eye, paraocular area shining, close to densely punctate.

Mesosoma: (fig. 7A) mesoscutum anterior mesial margin rounded, continuing lateral contour, surface with dull sheen, with dense punctures, many punctures fused; scutellum 1.35 x longer than dorsal surface of metapostnotum, scutellum dull, with densely punctate sculpture; dorsal surface of metapostnotum acarinate across posterior margin but defined by V-shaped ridge, distinctly raised above vertical and lateral surfaces, dorsal surface microalveolate but with several weak rugulose striae basally, striae not reaching mid-point of dorsal surface, dorsal surface pattern forming V-shape onto vertical posterior surface, lateral margins smooth, dull with microalveolate pattern, with some large, shallow punctures, vertical posterior surface of metapostnotum microalveolate with carinae extending basal one third of length; mesepisternum and metepisternum plicate; first recurrent vein (1m-cu) interstitial with or entering second submarginal cell.

Metasoma and legs: (figs. 7A-B) metasomal T1–T5 with dull sheen, densely punctate across entire surfaces; anterior metatibial spur finely serrate to smooth.

Colour: (figs. 7A, 7B, 7E) body black except: apical two thirds of clypeus, lower paraocular area, antennae red-brown, T4–T5 red-brown, coxa, trochanter dark brown to black, remainder of legs red-brown; coloured dense patches of vestiture as follows: dense white vestiture around spiracle, yellow to orange on pronotum corners, lateral corners of mesoscutum, mesial of metanotum, dense tomentum basally across T2–T3, T3 tomentum thicker than tomentum on T2, T4–T5 brown; forewing with brown tinge from submarginal cells to tip of wing.

Vestiture: (figs. 7A, 7B, 7E) body vestiture sparse, clypeus with sparse simple hair, supraclypeal area almost glabrous, frons with sparse, small, black, erect hair, paraocular area with downwardly pointing adpressed, white branched hair, mesoscutum, scutellum almost glabrous but with tomentum on posterolateral corners of mesoscutum, metanotum, basally on T2–T3, sparse small, black, erect hair, long, white hair on lateral, vertical posterior surface of metapostnotum, except for tomentum bands, metasomal terga appears glabrous but with sparse, short, adpressed hair.

Description of male: (figs. 2C, 7C, 7D) body length: 8.01–9.25–9.42 mm (n=10); forewing length: 2.50–2.54–2.59 mm (n=10); head width: 2.06–2.33–2.40 mm (n=10); intertegular width: 1.82–

1.85–1.87 mm (n=10). Relative head measurements: HW: 100, HL: 90–92, UID: 57–58, LID: 42–43, IAD: 16–17, OAD: 23–24, IOD: 15–16, OOD: 16–17, CL: 26–27, GW: 15–16, EW: 29–30, SL: 22–23, AF4/AF2+3 (23/15, 22/14) 1.53–1.57, FL: 215–220.

Differs from female as follows: upper and lower inner eye margins converging basally; median frontal carina extending about one third to two thirds to medium ocellus; frons sculpture densely reticulate-punctate across surface to inner margins of eyes; scape reaches level of median ocellus; clypeus surface polished, shiny, weakly convex, openly punctate with shallow punctures; supraclypeal area weakly protruding above paraocular area, rounded, polished, closely punctate with minute, shallow punctures with microalveoate sculpture; mesoscutum as in female, dull, densely punctate appearing as coarse reticulate sculpture, scutellum, metanotum similar to mesoscutum; dorsal surface of metapostnotum same as in female though reticulation more extensive, acarinate, dorsal surface defined by raised, rounded ridge, dorsal surface with microtessellate sculpture but without weak striae basally; colour similar to female except apical two thirds of clypeus pale yellow, with similar yellow-orange vestiture except V-shaped tomentum on upper vertical posterior surface of metapostnotum (fig. 2C), T3 basal tomentum much broader than basal tomentum on T2.

Vestiture: lower half of frons, between antennal bases, paraocular area with dense erect, white hair, gena with moderate beard of long, plumose, white hair, mesoscutum appears glabrous but with sparse, short, erect, brown hair, metapostnotum lateral sides with short, white, adpressed hair, apical vertical posterior surface of metapostnotum with V-shaped tomentum of white hair (fig. 2C), metasomal sterna S1–S4 with sparse white, adpressed hair, S5 lateral margins with weak white, semi-erect hair tufts (fig. 7F).

Genitalia: (figs. 10E-F) gonobase sides narrowed basally, complete ventroapically, gonobase width almost half of gonocoxa width, gonocoxa with single seta dorsolaterally, remainder glabrous, dorsal inner margins of gonocoxa basally rounded, gonocoxa apical inner margin not produced, continues contours of gonostylus, glabrous; retrorse lobes large, meeting at midline, membranous inwardly pointing, outer margins of retrorse lobes with small, erect setae, inner margins of retrorse lobes basally with area of erect, large setae, apically with fine, short adpressed, some larger erect setae; gonostylus absent but area with simple, erect hair; penis valves curved apically, with short dense cover of hair dorsolaterally.

Distribution: (fig. 12C) this species extends from north Queensland (Cairns), down eastern New South Wales and across Victoria, but is absent from Tasmania. The type locality of *Halictus peraustralis* is South Australia, but no location was named so the South Australian record has not been mapped.

Remarks: Cockerell's (1904) description of "*Halictus peraustralis*" was unusual as the species description was part of a dichotomous key to "Halictus specimens in the British Museum", with the species description of "*Halictus peraustralis*" as part of couplet one. Cockerell noted (1904: 211) that the specimen used for the species description (Type) was originally labelled by F. Smith as a variety of "*Halictus bicingulatus* var Smith". Note that

Michener (1965) placed "*bicingulatus*" in the *Lasioglossum* subgenus *Chilalictus*, but Cockerell recognised the variety as a valid species. Rayment (1939) commented that his new species "*odyneroides*" belonged to the "*bicingulatus*" group and that it was closest to "*H. peraustralis*", but he distinguished it as a new species due to a minor colour variation. This colouration is recognised within *L. peraustrale*. The colour patterns of *L. peraustrale* are best described as mimetic, because they are replicated in a range of species in *Lasioglossum* subgenera.

Lasioglossum (Australictus) plorator (Cockerell)

(Figs. 2F, 3A–F, 4, 8A–F, 11A, 11B, 12D)

> *Halictus plorator* Cockerell 1910b: 274; Rayment 1953: 29.
> *Lasioglossum (Australictus) plorator* – Michener 1965: 165.

Material examined: Holotype of *plorator* ♀, Victoria Melbourne Aug 1900, C.F. Turner Collection 1900-7 C.7. 8.00 BMNH Hym.17.a.633 (BMNH) (view type data and image at https://data.nhm.ac.uk/object/9154124c-377b-4ea6-8421-90965bbc6284 accessed 16 August 2022).

Other specimens examined (248♀, 159♂): QUEENSLAND: (1♀) Beechmont, 3 Oct 1984, N.W. Rodd (AM); (2♀) Wyberba National Park, 8 Jan 1967 Houston, T.F. on *Eucalyptus* (WAM).

NEW SOUTH WALES & AUSTRALIAN CAPITAL TERRITORY: (5♀) Blue Mtns, 26 Sept 1978, N.W. Rodd (AM); (2♀, 1♂) Tianjara Falls, 60 km SW Tomerong, 5 Feb 1988, N.W. Rodd (AM); (1♀) Orange, Jan 1934 (ANIC); (2♀, 1♂) 3 km S Mt Wilson, Blue Mtns, 12 Sept 1978, N.W. Rodd (AM); (1♂) Narrow Neck, Blue Mtns, 27 March 1979, N.W. Rodd (AM); (1♀) Mt Victoria, Blue Mtns, 29 Dec 1981, N.W. Rodd (AM); (2♂) 6 km NE Bilpin, Blue Mtns, 4 March 1986, N.W. Rodd (AM); (3♀,1♂) Mt Tomah, Blue Mtns, 9 Feb 1986, N.W. Rodd (AM); (1♀, 1♂) Mt York, Blue Mtns, 29 Jan 1982, N.W. Rodd (AM); (1♀, 1♂) Haystack Ridge, 26 Feb 1979, N.W. Rodd (AM); (1♀, 1♂) 3 km S Mt Wilson, Blue Mtns, 13 Jan 1986, N.W. Rodd (AM); (1♀,1♂) Mt Tomah, 25 Jan 1979, N.M. Rodd (AM); (1♀, 1♂) Nadgee Reserve, 7 km S Newton Beach, 29 Dec 1985, E.A. Sugden, sweeping *Kunzea ercoides* (AM); (2♀) 8 km W Tyalgum, 24 Sept 1983, N.W. Rodd (AM); (2♀) Mt Kaputar Nat. Park, 1362 m, 5 Dec 1974, I.F.B. Common & G.E.D. Edwards (ANIC); (4♀) Dawson's Spring, Mt Kaputar Nat. Pk, 30 Nov – 10 Dec 1978, G.R. Brown (OIA); (1♀) Armidale, 18 Nov 1959, C.W. Frazier (ANIC); (5♀) NE Nat. Pk, 4 Nov 1960, C.W. Frazier (ANIC); (9♀) Blundell's, 18 Feb 1931, L.F. Graham (ANIC); (1♀) Blundell's, 18 Feb 1950, E.F. Riek (ANIC); (1♂) Mt Wilson, 4 Jan 1931, A.N. Burns (NMV); (2♀) Winburndale, 12 mi E Bathurst, 6 Dec 1974 (ANIC); (2♀) Picadilly Circus, Brindabella Ra.,1 Nov 1988, R.R. Snelling & J. Grey #88 (LACM); (3♀) NE Nat Pk, near Entrance, 04–20 Nov 1960, C.W. Frazier (ANIC).

VICTORIA: (3♀) Gorae West, 1951, 22 Aug 1956 (ANIC); (1♀) Packenham, 20 Nov 1936 (ANIC); (2♀) Grampians, Oct 1928, F.E. Wilson (ANIC); (1♀) Grampians, 20 Oct 1945, A.N. Burns (NMV); (3♀) Flowerdale, 15 Dec 1954, A.N. Burns (NMV); (3♀) Flowerdale, 8 Dec 1954, Neboiss (NMV); (1♀) Melbourne, F.P. Spry 1909 (ANIC); (1♀) Erica, 20 April 1983, P. Bernhardt (NMV); (7♀) Warburton, 19 Dec 1968, E.M. Exley on *Leptospermum ericoides* (QM); (1♀) Warburton, 19 Dec 1968, E.M. Exley on *Prostanthera lasianthoe* (QM); (2♀) Portland, 6 Dec 1974, G. Knerer (NMV); (1♀) Macedon, 29 Feb 1967 (ANIC); (1♀, 5♂) Emerald, 26 July 1936, Rayment (ANIC); (1♀) 11 km Halls Gap, 21 Oct 1983, I.D. Naumann & J.C. Cardale (ANIC); (1♀) Mt Difficult, Grampians, 2 Jan 1966, B. Cantrell (QM); (2♂) Anglers Rest, 5 March 1992, K. Walker, on *Eucalyptus* (NMV); (2♀,1♂) Reefton, 9 Feb 1955, Neboiss (NMV); (17♀) Croydon (NMV); (2♀)

Lake Hattah, 11 Apr 1920, J.E. Dixon (NMV); (1♀) San Remo, 17 Oct 1927, A.D.D. (NMV); (3♀) Hamilton, 14 Sept 1914, G.S. (NMV); (3♀) Wombargo Ck, 9 May 1947, G.B. (NMV); (1♀) Grampians, 19 Oct 1945, G.B. (NMV); (1♀) High Tap, 7 Aug 1951 (NMV); (1♀) Lorne, 3 March 1954, F.E. Wilson, burrowing in punk of rotten log (NMV); (2♀) Mt Dandenong, 2,000 ft, 21 Dec 1930, A.N. Burns (NMV); (1♀) Dromana, 3 Nov 1931, G.B. (NMV); (2♀) Warburton, 8 Sept 1959, A.N. Burns (NMV); (2♀) Ferntree Gully, 5 Dec 1915, F.P. Spry (NMV); (1♀) Nariel, 12 Feb 1963, A.N. Burns (NMV); (34♀) Cobboboonee State Forest, 1.3 km E Wright's Swarm Road, 3 March 1990, W.T. Wcislo ex *Brenesia* (SEM); (37♀) Cobboboonee State Forest, 12–13 March 1990, W.T. Wcislo, ex Eucalyptus (SEM); (3♀, 9♂) 22 km N Portland farm, at NW Border of Cobboboonee State Forest and Glenelg National Forest, 15 Feb 1990, W.T. Wcislo ex red *Eucalyptus* (SEM); (11♀, 14♂) Cobboboonee State Forest, 4 Feb 1997, K. Sparks and C. Mcphee on *Bursaria* (NMV); (1♀) Victoria Valley, 11 Feb 1947, B. Given (NMV); (1♀) 715 Lt Hampton Rd Glenlyon, Gayle Osborne, on *Achillea millefolium* (iNaturalist https://www.inaturalist.org/observations/68516396); (1♀) Wilsons Promontory, 5 Mile Beach Road, 26 Feb 1996, K. Walker, on *Eucalyptus* (NMV); (3♀) Mt Hickey, Tallarook, 14 Nov 1987, P. Carwardine (NMV).

TASMANIA: (1♀) 3 km SEE Black River, 18 Jan 1983, I.D. Naumann & J.C. Cardale (ANIC); (2♀) 11 mi E Strahan, 1 Jan 1969, E.M. Exley on *Melaleuca* (QM); (1♀) 10 mi W Upper Blessington, 29 Dec 1968, E.M. Exley, on *Leptospermum* (QM); (1♀) Tullah, 31 Dec 1968, E.M. Exley on *Leptospermum* (QM); (3♀) 1 km SSE Gladstone, 29 Jan 1983, I.D. Naumann & J.C. Cardale (ANIC); (1♀) The Lea, 6 km S Hobart, 27 Dec 1979, J.C. Cardale (ANIC); (1♀) Hobart, Lea (SAM); (2♀) Sandy Bay, 20 May 1947, A.N. Burns (NMV); (1♂) 7 km SW Buckland, 27 Jan 1983, I.D. Naumann & J.C. Cardale (ANIC); (2♀) Huon–Picton R Junction, 14 Nov 1972, A. Neboiss (NMV); (21♀) Marrawah, 30 Jan 1949, E.F. Riek (ANIC); (1♀) Mt Claude, 680m, 21 March 1990, L. Hill, on *Leptospermum* (TDA); (2♀) Lake Leake, 2000 ft, 27 Feb 1963, I.F.B. Common & M.S. Upton (ANIC); (1♀) 10 km NNW St. Helens, 14 Jan 1983, I.D. Naumann & J.C. Cardale (ANIC); (1♀) 2 km NNE Pioneer, 29 Jan 1983, I.D. Naumann & J.C. Cardale (ANIC); (2♀) Bruny I Lea (SAM); (14♀) Hastings, 15 Jan 1949, E.F. Riek (ANIC); (2♀) SW Nat. Park, Tyenna, 11 Jan 1997, A. Hingston, on *Leptospermum lanigerum* (TDA); (1♀) 4 km WSW Maydena, 11 Dec 1981, I.D. Naumann (ANIC); (2♀) Tyenna, 16 Dec 1917, C.E. Cole, (SAM); (1♀) National Park, 21 Jan 1949, E.F. Riek (ANIC); (1♀, 110♂) Florentine Valley, 20 km W Maydena, 9 Feb 1986, K. Walker, on *Leptospermum* (NMV); (1♀) Ellendale, 30 Jan 1973, R.J. Hardy (TDA); (1♀) Mount Wellington, Icehouse Track, 27 Jan 2001, K. Hergstrom (TDA); (1♀) Mt Wellington, Hobart, 8 Nov 1996, A. Hingston, on *Hakea lissosperma* (TDA); (2♀) Mt Nelson, 31 Jan 1997, A. Hingston, on *Leptospermum scoparium* (NMV); (1♀) Liffey: Fernery, 4 Dec 1993, C.P. Spencer & L. Richards (TMAG); (1♀) 6 mi SW Queenstown, 1 Jan 1969, E.M. Exley, on *Melaleuca* (QM); (1♀, 2♂) 6 km N Zeehan, 6 March 1989, K. Walker, on *Eucalyptus* (NMV); (1♀, 1♂) Cradle Mountain, 7 March 1989, K. Walker, on *Leptospermum rupestre* (NMV).

Floral record: Families visited: 4 (Asteraceae (1), Lamiaceae (1), Myrtaceae (5), Proteaceae (1)). Genera visited: 5 (*Achillea* (1), *Eucalyptus* (6), *Hakea* (1), *Kunzea* (1), *Leptospermum* (7), *Prostanthera* (1)).

Flight phenology capture records: Jan (18) Feb (14) Mar (7) Apr (3) May (2) June (0) July (1) Aug (2) Sept (4) Oct (6) Nov (8) Dec (15).

Diagnosis. *Lasioglossum (Australictus) plorator* is most like *L. (Australictus) davide* in body colour. This species can be distinguished, in both sexes, from other *Australictus* species by black body colour with bluish tinge on metasoma; lack of tomentum on mesosoma or metasoma; dorsal surface of metapostnotum posterior margin acarinate but surface elevated

above surrounding lateral, vertical surfaces; metapostnotum dorsal surface sculpture microalveolate (figs. 2F, 8A–D); male genitalia with gonobase narrowed basally, moderate sized retrorse lobes, small, erect gonostylus (figs. 11A, 11B); and metasomal sterna with erect lateral hair tufts on S4-S5 (fig. 8F). This species occurs in SE Australia, including Tasmania (fig. 12D).

Description of female: (figs. 2F, 8A, 8B) body length: 9.89–10.12–10.21 mm (n=10); forewing length: 2.97–3.05–3.12 mm (n=10); head width: 2.64–2.71–2.78 mm (n=10); intertegular width: 1.87–1.98–2.06 mm (n=10). Relative head measurements: HW: 100, HL: 82–83, UID: 60–62, LID: 59–60, IAD: 09–10, OAD: 22–23, IOD: 08–09, OOD: 17–18, CL: 20–21, GW: 20–21, EW: 20–21, SL: 43–45, FL: 70–72.

Head: (fig. 8E) upper and lower inner eye margins almost parallel; median frontal carina barely reaching above upper antennal bases; clypeus polished, smooth on apical half, remainder with microtessellate sculpture pattern giving dull sheen, surface weakly convex, openly punctate with shallow punctures, few irregular, elongate punctures apically, supraclypeal area distinctly raised above paraocular area, surface dull with microtessellate sculpture pattern, sparsely punctate with shallow punctures; frons sculpture above antennal bases densely reticulate, laterally almost smooth but plicate with weak, wavy, raised, vertical carinae extending laterally to inner margins of eyes, apically to just basally level of median ocellus, paraocular area smooth, shining, weakly plicate.

Mesosoma: (figs. 2F, 8A-B) mesoscutum anterior mesial margin weakly produced mesoanteriorly, surface smooth, with dull sheen due to weak microtessellate sculpture pattern across surface, medially open to closely punctate, laterad of parapsidal areas closely punctate, in parapsidal areas densely punctate, densely punctate along posterior margin; scutellum 1.6 x length of dorsal surface of metapostnotum, scutellum with dull sheen, with microtessellate sculpture pattern, open to closely punctate; dorsal surface of metapostnotum acarinate across posterior margin with weak carinae in posterolateral corners, dorsal surface defined by rounded, raised ridge above vertical, lateral surfaces, dorsal surface with microalveolate sculpture but with several weak striae basally, striae not reaching mid-point of dorsal surface, lateral margins smooth with microalveolate pattern, vertical posterior surface of metapostnotum defined by lateral carinae (fig. 2F); mesepisternum and metepisternum plicate; first recurrent vein (1m-cu) meeting 1rs-m vein or entering second submarginal cell.

Metasoma and legs: metasomal T1–T5 shining, smooth, sparsely punctate with minute punctures; anterior metatibial spur finely serrate, teeth barely discernible.

Colour: (figs. 8A, 8B) body black except scapes dark brown, flagella segments light brown, metasomal tergal segments black with bluish tinge, legs dark brown.

Vestiture: (figs. 8A, 8B, 8E) body vestiture sparse, clypeus, supraclypeal area almost glabrous, frons with sparse, small, black, erect hair, mesoscutum, scutellum almost glabrous but with sparse, small, black, erect hair; long hair on lateral, vertical posterior surface of metapostnotum, apical one third of T1 with some long, erect, hair, remainder of T1, T2 glabrous, T3–T4 with some black, adpressed hair apically.

Description of male: (figs. 8C, 8D) body length: 8.48–9.98–10.99 mm (n=10); forewing length: 2.64–3.08–3.12 mm (n=10); head width: 2.26–2.57–2.64 mm (n=10); intertegular width: 1.58–2.07–2.16 mm (n=10). Relative head measurements: HW: 100, HL: 83–85, UID: 60–62, LID: 47–48, IAD: 09–10, OAD: 20–21, IOD: 15–16, OOD: 16–17, CL: 27–28, GW: 19–20, EW: 28–29, SL: 19–20, AF4/AF2+3 (21/14, 22/15) 1.46–1.50, FL: 210–214.

Differs from female as follows: upper and lower inner eye margins converging basally; median frontal carina reaching about one quarter to median; frons sculpture reticulate across surface to inside inner margins of eyes; scape almost reaches level of median ocellus; clypeus smooth, shiny, with weak microtessellate pattern basally, medium area rounded, open to closely punctate; supraclypeal area protruding above paraocular area, surface dull with microtessellate sculpture covering entire surface, openly punctate; mesoscutum surface dull with reticulate, densely punctate sculpture, except anterolaterally with microtessellate sculpture, openly punctate; scutellum surface dull with reticulate, densely punctate sculpture except medially openly punctate but dull; dorsal surface of metapostnotum same as in female except V-shaped, weak striae reaching dorsolateral margin, posterolaterally weakly plicate; colour similar to female except apical two thirds of clypeus pale yellow, fore tibiae light brown and metasoma with distinct blue tinge; apical margin of T6 yellow.

Vestiture: frons with erect, black hair; between antennal bases, paraocular area with dense white semi-erect hair, gena with erect, long beard-like, white hair; mesoscutum with short, erect, brown hair, metapostnotum lateral sides with sparse, long, white, erect hair, apical posterior vertical posterior surface of metapostnotum glabrous; metasomal sterna with short erect, adpressed black setae, S4–S5 with elongate, erect lateral hair tufts (fig. 8F).

Genitalia: (figs. 11A-B) gonobase sides narrowed basally, complete ventroapically, gonobase width almost half of gonocoxa width, gonocoxa glabrous dorsally and ventrally, dorsal inner margins of gonocoxa basally broadly truncate to broadly rounded, gonocoxa apical inner margin not produced, continues contours of gonostylus, glabrous; retrorse lobes moderate in length, not meeting at midline, membranous, inwardly pointing, outer margins of retrorse lobes glabrous, inner margins of retrorse lobes with area of erect, large, inwardly pointed setae, apically retrorse lobes glabrous; gonostylus moderate sized (about one third length of gonocoxa), erect, apically rounded, sparse short setae on inner margin, dense elongate simple, erect hair on outer margin; penis valves curved apically, glabrous dorsolaterally.

Distribution: (fig. 12D) this species occurs from SE Queensland, down eastern New South Wales, across Victoria, and is widespread in Tasmania.

Remarks: Rayment (1953) described the male of *L. plorator*, from Victoria (Gorae West) and labelled the specimen an Allotype; however, this specimen has no type status. *Lasioglossum plorator* is the species found nesting in rotting wood in the Facebook posts mentioned above (figs. 3A–F, 4).

Lasioglossum (Australictus) tertium (**Dalla Torre**)

(Figs. 1A, 2B, 9A–F, 11C, 11D, 12E)

Halictus rufipes Smith 1853: 56. [junior primary homonym of *Halictus rufipes* Fabricius, 1793]

Halictus tertius Dalla Torre 1896: 86. [**nom. nov.** for *Halictus rufipes* Smith, 1853]

Parasphecodes insculptus Cockerell 1918: 118. **syn nov.**

Parasphecodes rufitarsus Rayment 1929: 127. **syn nov.**

Lasioglossum (Australictus) fulvofasciae Michener 1965: 310. **syn nov.**

Lasioglossum (Australictus) tertium – Michener 1965: 165.

Lasioglossum (Australictus) insculptum – Michener 1965: 165.

Lasioglossum (Australictus) rufitarsum – Michener 1965: 165.

Lasioglossum (Australictus) fulvofasciae –Michener 1965: 165.

Material examined: Holotype of *rufipes* ♀, label reads "Melb N.H. F. Sm. Coll. 79.22" = Australia, Victoria, Melbourne (has additional label as: Halictus rufipes Sm Type = tertius D.T. Det. Michener 1960) BMNH Hym.17.a. 2837 (BMNH) (view type data and image at https://data.nhm.ac.uk/object/68143dfc-d0b8-474d-af44-71aacdecb776 accessed 16 August 2022).

Holotype of *insculptus* ♀, Queensland, Tamborine Mountain, 28 Dec 1911, H. Hacker (190) Hy/4142 (QM). Note the holotype of *insculptus* has a Cockerell handwritten label designating this specimen as the type. Associated with the Holotype are two specimens with the same locality data, one female and one male. Neither specimen carries Cockerell's handwritten label; they are not mentioned in the original description and have no type status.

Holotype of *rufitarsus* ♀, Victoria, Cann River, Nov 1928, J. Clark. T-11864 (NMV) (view type data at https://collections.museumsvictoria.com.au/specimens/1018349 accessed 16 August 2022).

Holotype of *fulvofasciae* ♂, Queensland, 3 mi W Cunningham's Gap, 25 Feb 1959, C.D. Michener, on *Bursaria spinosa* T-6910 (QM). Allotype ♀, same data as Holotype except has an additional label of "375". T-6911 (QM). The Holotype locality label is printed, while the allotype locality label is handwritten by Michener.

Other specimens examined (23♀, 51♂): QUEENSLAND: (1♀) Mt Lindesay, 25 Sept 1967, T.F. Houston, 87/450 (WAM); (20♂) 3 mi W Cunningham's Gap, 25 Feb 1959, C.D. Michener, on *Bursaria spinosa* (SEM); (1♀) Bald Mt area, 3–4000 ft via Emu Vale, 17–22 May 1980, G.B. Monteith (QM); (1♂) 13 mi N Stanthorpe, 29 Dec 1958, C.D. Michener (SEM); (3♂) Barney Ck, 7 Mar 1965, S.R. Curtis (QM).

NEW SOUTH WALES: (1♂) Nadgee State Forest, 7 km S of Newton's Beach, 7 Dec 1985, E.A. Sugden (AM); (2♂) Cheltenham, 12 Feb 1950 (AM); (2♀, 9♂) 6 km NE Bilpin, Blue Mtns, 13 Dec 1984, 28 Feb, 4 Mar 1986, N.W. Rodd (one pair labelled "in cop") (AM); (1♂) Haystack Ridge, nr Mt Tomah, 29 Mar 1978, N.W. Rodd (AM); (1♀) Dunns Swamp, nr Kandos, 13 Nov 1982, N.W. Rodd (AM); (2♂) 7 km NE Bilpin nr Kurrajong, 17 Mar 1981, N.W. Rodd (NMV); (1♂) Murray Beach, Jervis Bay, 18 Feb 1987, N.W. Rodd (AM); (1♂) Narrow Neck, Blue Mtns, 21 Mar 1979, N.W. Rodd (AM); (1♂) Tianjara Falls, 60 km SW Tomerong, 5 Feb 1988, N.W. Rodd (AM); (1♂) 3 km S Mt Wilson, Blue Mtns, 9 Mar 1978, N.W. Rodd (AM); (1♀) Mt White, 23 Sept 1995, A. Sundholm, on *Leptospermum* (QM); (1♀) Mt Wilson, 4 Jan 1931, A.N. Burns (NMV); (2♀) Wisemans Ferry, 18 Dec 1927, G.B. (NMV); (1♀) Gibraltar Range, 29 Dec 1969, C.W. Frazier (ANIC); (1♀) Dawson's Spring, 1420m, Mt Kaputar Nat. Park, 1–10 Dec 1987, G.R. Brown (OIA).

VICTORIA: (3♀, 4♂) N of Lakes Entrance, Colquhoun State Forest, 21 Feb 1985, K. Walker, on *Eucalyptus* (NMV); (1♂) LaTrobe Survey, Tanjil Junction (NMV); (1♂) Wilson's Promontory, 5 Mile Beach Road, 26 Feb 1996, K. Walker, on *Eucalyptus* (NMV); (1♂)

Anglers Rest, 5 March 1992, K. Walker, on *Eucalyptus* (NMV); (1♂) Cobboboonee State Forest, 3 Feb 1997, K. Sparks & C. McPhee, on *Bursaria* (NMV); (1♂) 22 km N Portland, Cobboboonee State Forest, 15 Feb 1990, W.C. Wcislo (SEM); (4♀) Warburton, 2 Dec 1918, Mar 1920, F.P. Spry (NMV); (2♀) Lake Hattah, Jan 1920, J. Dixon (NMV); (1♀) Mittagong, 17 Dec 1947, G.M. Goldfinch (NMV); (1♀) 35 km N Cann River, 3 Nov 1988, R.R. Snelling & J. Grey (LACM); (1♀) 8 km S Cann River, 5 Feb 1987, K. Walker & C. McPhee, on *Eucalyptus* (NMV); (1♀) Freestone Creek Rd, Moornapa, M. Smith (iNaturalist – https://www.inaturalist.org/observations/26301693); (1♀) 115 Cranbourne–Frankston Rd, Langwarrin (iNaturalist – https://www.inaturalist.org/observations/25985414); (1♀) Yan Yean, 19 Nov 1999, Walker & Danforth (Cornell); (1♀) 42 Reserve Rd, Wonga Park (iNaturalist – https://www.inaturalist.org/observations/25749227); (1♀) Edgar Track, Montrose, R. Richter (iNaturalist – https://www.inaturalist.org/observations/25719040); (1♀) Rocklands–Cherrypool Rd, Rocklands, R. Richter (iNaturalist – https://www.inaturalist.org/observations/25735753).

SOUTH AUSTRALIA: (1♀) Nangwarry, 09 Nov 2014, R. Leijs, on *Leptospermum* (BDBSA).

Floral record: Families visited: 2 (Myrtaceae (5), Pittosporaceae (2)). Genera Visited: 3 (*Bursaria* (2), *Eucalyptus* (3), *Leptospermum* (2)).

Flight phenology capture records: Jan (1) Feb (9) Mar (7) Apr (0) May (1) June (0) July (0) Aug (0) Sept (2) Oct (0) Nov (4) Dec (8).

Diagnosis. Lasioglossum (Australictus) tertium is most like *L. (Australictus) peraustrale* with yellow tomentum on pronotum and metasomal hair bands. This species can be distinguished, in both sexes, from other *Australictus* species by: black body colour (except some males in the SE Queensland area with light coloured banded metasomal tergal segments (fig. 2D)); dense, yellow tomentum on pronotum lateral corners, vestiges of yellow tomentum on posterolateral corners of mesoscutum, none on metanotum but with metasomal bands on T2–T3; dorsal surface of metapostnotum posterior margin carinate; metapostnotum dorsal surface sculpture microalveolate (figs. 9A–D); male genitalia with gonobase widened basally (a character shared with *L. davide*), small retrorse lobes, gonostylus absent (figs. 10E, 10F); and metasomal sternal S3–S5 with erect, lateral hair tufts, more so on S4 and even more so on S5 (fig. 9F). This species occurs in SE Australia but is absent from Tasmania (fig. 12E).

Description of female: (figs. 1A, 9A, 9B) body length: 8.79–10.37–10.83 mm (n=10); forewing length: 2.50–2.79–2.83 mm (n=10); head width: 2.64–3.06–3.17 mm (n=10); intertegular width: 1.78–1.85–1.87 mm (n=10). Relative head measurements: HW: 100, HL: 74–75, UID: 55–56, LID: 64–65, IAD: 10–11, OAD: 20–21, IOD: 11–12, OOD: 16–17, CL: 16–17, GW: 24–25, EW: 23–24, SL: 41–42, FL: 65–66.

Head: (fig. 1A) upper and lower inner eye margins diverging basally (head widened basally); median frontal carina reaching about one third way to median ocellus; clypeus smooth, polished, medially flattened, open to closely punctate with small, shallow, rounded punctures except densely punctate along apical margin; supraclypeal area not distinctly raised above paraocular area, surface flat, smooth, polished, open to closely punctate with shallow punctures; frons smooth, polished, above antennal bases half way to inner margins of eyes closely to densely punctate, along inner

eye margins closely to densely punctate with minute punctures with smaller diameters than punctures above antennal bases, paraocular area smooth, shining, close to densely punctate; gena enlarged (fig. 9B).

Mesosoma: (figs. 9A, 9B) mesoscutum anterior mesial margin produced forward over pronotum, surface smooth, polished with dull sheen, medially open to closely punctate, laterad of paraspidal lines closely punctate, anterolaterally, in parapsidal areas densely punctate; scutellum 0.81 x shorter than length of dorsal surface of metapostnotum, scutellum smooth, polished, long midline densely punctate, laterally sparse to openly punctate; dorsal surface of metapostnotum carinate posterolaterally only, dorsal margin not defined by raised ridge, dorsal surface covered with microalveolate sculpture but with several weak striae, striae just reaching mid-point of dorsal surface, dorsal surface pattern forming rounded V-shape pattern onto vertical posterior surface, lateral margins smooth, dull with microalveolate pattern, vertical posterior surface of metapostnotum with carinae extending to dorsal posterolateral carinae; mesepisternum and metepisternum plicate; first recurrent vein (1m-cu) entering third submarginal cell.

Metasoma and legs: (figs. 9A, 9B). metasomal T1–T5 with dull sheen, densely punctate across entire surfaces; anterior metatibial spur finely serrate to smooth (fig. 2B).

Colour: (figs. 1A, 9A, 9B) frons, supraclypeal area, apical one third of clypeus, mesoscutum, scutellum black suffused with dark blue tinge, in some specimens basal two thirds of clypeus red-brown, in other specimens entire clypeus dark brown, metanotum, dorsal surface of metapostnotum black suffused with blue tinge, metasomal T1–T5 black, in some specimens terga suffused with brown tinge, in some specimens T4–T4 light red-brown coxa, trochanter, basal two thirds of femur dark brown, remainder of legs light red-brown; tegula light red-brown, forewing with brown tinge from submarginal cells to tip of wing; pronotum dorsolateral corners, basal margin of T2–T3 with dense yellow tomentum.

Vestiture: (figs. 1A, 9A, 9B) body vestiture sparse, frons, clypeus, supraclypeal area, paraocular area with sparse, erect hair, pronotum dorsolateral margins with dense tomentum, mesoscutum scutellum almost glabrous with sparse cover of small, black, erect hair, in some specimens posterolateral corners of mesoscutum with weak, yellow tomentum or hair tufts, in other specimens, perhaps worn, with no tomentum or hair tufts, lateral surfaces of metapostnotum with long, black hair; metasoma terga appears glabrous but with dense cover of short, adpressed hair.

Description of male: (figs. 2D, 9C, 9D) body length: 8.63–9.87–10.21 mm (n=10); forewing length: 2.31–2.62–2.68 mm (n=10); head width: 2.11–2.35–2.40 mm (n=10); intertegular width: 1.73–1.87–1.92 mm (n=10). Relative head measurements: HW: 100, HL: 90–92, UID: 57–59, LID: 48–49, IAD: 15–16, OAD: 23–24, IOD: 15–16, OOD: 17–18, CL: 30–31, GW: 20–22, EW: 27–28, SL: 25–26, AF4/AF2+3 (20/15, 18/14) 1.28–1.33, FL: 187–190.

Differs from female as follows: upper and lower inner eye margins converging basally; median frontal carina extending about one third to medium ocellus; frons sculpture densely

reticulate-punctate across surface to inner margins of eyes; scape reaches level of median ocellus; clypeus surface polished, shiny, surface weakly convex, close to openly punctate with shallow punctures; supraclypeal area weakly protruding above paraocular area, supraclypeal area rounded, dull, with microtessellate sculpture pattern, closely punctate with minute, shallow punctures; mesoscutum as in female, anterior margin produced forward, mesoscutum smooth with dull sheen, medially closely punctate, anterolaterally, laterad or paraspidal lines, in parapsidal areas densely punctate, scutellum, metanotum similar to mesoscutum; dorsal surface of metapostnotum acarinate, not defined by raised ridge, with microtessellate sculpture, with weak striae, striae just reaching mid-point of dorsal surface; colour similar to female except apical two thirds of clypeus pale yellow, with similar yellow-orange vestiture on pronotum dorsolateral corners, metasomal T2–T3 with basal, yellow tomentum on T3 broader than basal tomentum on T2, in some specimens metasoma with light brown colour banding across metasomal terga T1–T3 (fig. 2D).

Vestiture: lower half of frons, between antennal bases, paraocular area with dense, erect, white hair, gena with moderate beard of long, plumose, white hair, mesoscutum appear glabrous but with sparse cover of short, erect, brown hair, metapostnotum lateral sides with basal, short, white, adpressed hair, metasomal sterna S1–S4 with sparse, white, adpressed hair, S3–S5 with erect, lateral hair tufts, more so on S4 and even more so on S5 (fig. 9F).

Genitalia: (figs. 11C, 11D) gonobase sides widened basally, complete ventroapically, gonocoxae 1.1 x than width of gonobase, 1.2 x longer than length of gonobase, gonocoxa glabrous, dorsal inner margins of gonocoxa basally broadly truncate to broadly rounded. Gonocoxa apical inner margin not produced, continue contours of gonostylus, glabrous; retrorse lobes small, narrow, not meeting at midline, membranous, retrorse lobes glabrous except for one or two setae; gonostylus small to almost absent, apically rounded, with cover of short erect setae; penis valves curved apically, glabrous dorsolaterally.

Distribution: (fig. 12E) this species extends from SE Queensland down eastern New South Wales, across Victoria, one record from SE South Australia, and is absent from Tasmania.

Remarks: Cockerell (1918: 118) commented that *Parasphecodes insculptus* was close to *P. plorator* but noted a colour and sculpture difference. The metasomal T2–T3 yellow tomentum is weak on this type specimen; however, the head measurements are typical for this species. Rayment (1929: 128) commented that *P. rufitarsus* was also close to *P. plorator* but noted colour differences. Michener (1965: 311) commented that *Lasioglossum fulvofasciae* was close to *L. peraustrale* but differed in metasomal colour banding on his new species. Michener (1965: 311) primarily used the metasomal colour banding in the male only to distinguish his new species from *L. insculptum*. Note that Michener's male Holotype of *L. fulvofasciae* has the metasomal colour banding, but his allotype female is typical colouration for *L. tertium*. Apart from Michener's type series for *L. fulvofasciae* collected at Cunngingham's Gap, I have located only a few other specimens with similar banded metasomal colour markings. It

appears the distinctive metasomal banding seen on male specimens of *L. fulvofasciae* are all from SE Queensland (e.g. Cunningham's Gap, Emu Vale, Mt Lindesay and Bald Mountains), suggesting some kind of colour morph variant in that area. I have examined a series of male specimens without the metasomal colour banding also collected by Michener at Cunningham's Gap when he collected the type specimens of *L. fulvofasciae*. Male genitalia examinations of the Cunningham's Gap banded type series specimens and the non-banded males collected by Michener at Cunningham's Gap at the same time showed no differences between these specimens and between other male *L. tertium* genitalia examinations. This is the basis for the *L. fulvofasciae* synonymy. Of note, the banded metasomal morph specimens occur about the northernmost known distribution for this species. The male genitalia of *L. tertium* have shared characters with two other *Australictus* species: the gonobase widened basally is shared with *L. davide* (figs. 10A, 10B, 11C, 11D), and the absence of gonostylus is shared with *L. peraustrale* (figs. 10E, 10F, 11C, 11D). Note that *L. davide*, *L. peraustrale* and *L. tertium* are all absent from Tasmania, while both *L. lithusca* and *L. plorator* do occur in Tasmania.

Lasioglossum (Chilalictus) orbatum (Smith)

(Figs. 12F; Walker 1995, pp. 193–194, figs. 132 A–H)

Halictus orbatus Smith 1853: 58-59.
Halictus viridarii Cockerell 1930: 42. **syn.** by Walker 1995: 193.
Halictus franki Friese H. 1924 **syn. nov.**; Cockerell 1929: 13.
Lasioglossum (Chilalictus) orbatum – Michener 1965: 177.
Lasioglossum (Chilalictus) viridarii – Michener 1965: 177.
Lasioglossum (Australictus) franki – Michener 1965: 165.

Remarks: in the present study, the TYPUS of *Halictus franki* could not be located. ABRS (2022b) lists the type of *Halictus franki* as in AMNH. A search of the AMNH Invertebrate Zoology database for "Halictus franki" returned "Objects 0" result (AMNH, 2022a) and a search for just "franki" returned one result for *Paracolletes franki* Cockerell 1929 (AMNH 2022b).

The description of *Halictus franki* lists the TYPUS sex and location as "♀ Freemantle (sic Fremantle), 20 July 1906 Frank leg". This study has determined that for valid *Lasioglossum (Australictus)* species, the subgenus occurs only along the east coast of Australia and a few records in SE South Australia (figs. 12A–E). If this species does belong to the subgenus *Australictus*, it would suggest the TYPUS location label for *Halictus franki* in Western Australia (Fremantle) is doubtful.

While searching for the *Halictus franki* TYPUS specimen in AMNH, a Friese specimen, missing the metasoma, labelled as TYPUS was located (this specimen was borrowed and examined) with Friese's handwritten label as "Halictus" and with an unpublished Australian place-based species name. This specimen has the following labels in descending order: the location label of "Australia: Sydney, 14.9.06 Frank"; a Friese handwritten species name label with "1909 Friese det"; a printed orange TYPUS label; a printed AMNH registration number of "Am. Mus. Nat. Hist. Dept. Invert. Zool. No. 26905"; a handwritten Cockerell determination label; and an undated, typed and handwritten label stating "Lasioglossum [typed] Australictus [handwritten] det. G.C. Eickwort".

Below the orange Friese TYPUS label is a Cockerell handwritten label with "Halictus franki". Cockerell (1929: 13) examined this specimen and under the species name "*Halictus franki*", wrote these remarks:

A second specimen, which has lost the abdomen, but is evidently the same species, is labeled (sic) Sydney, 14.9.06 (Frank). It carries a manuscript name by Friese referring to it as Australian. I assume that Friese withdrew the latter from publication, finding it to be identical with *H. franki*. The hind spur has short noduliform teeth. The mesothorax is excessively densely punctured all over.

Cockerell's (1929) remarks and his handwritten specimen label of *Halictus franki* on the unpublished Friese named specimen provide an insight into the actual species *Halictus franki*. Examination of this unpublished Friese TYPUS specimen confirmed that it is *Lasioglossum (Chilalictus) orbatum*. The identification was confirmed by the specimen having the following subgeneric and species characters. Subgeneric characters: mandibular preapical tooth is not enlarged or elongated but of typical *Chilalictus* length and shape; anterior metatibial spur is typical of *Lasioglossum (Chilalictus)* species (i.e. one large basal tooth followed by a wavy margin to the apex). Species characters: mesoscutum punctation is typical of *L. (Chilalictus) orbatum*; shape of dorsal surface of the metapostnotum is diagnostic for *L. (Chilalictus) orbatum* (i.e. lateral margins of metapostnotum expanded at level of dorsal surface). Only five species of *Chilalictus* have this type of metapostnotum sculpture (Walker, 1995: 193), and the Sydney location is within the known distribution for *L. (Chilalictus) orbatum* (fig. 12F). From the identification of this specimen, I conclude that *Halictus franki* is a synonym of *Lasioglossum (Chilalictus) orbatum*, a species which is restricted to the east coast of Australia (Walker, 1995, fig. 12F).

Acknowledgments

References

ABRS. 2022a. ABRS 2022. *Australian Faunal Directory*. Lasioglossum statistics. Australian Biological Resources Study, Canberra. https://biodiversity.org.au/afd/taxa/Lasioglossum/statistics (accessed 31 May 2022)
ABRS. 2022b. ABRS 2022. *Australian Faunal Directory*. Lasioglossum (Australictus) franki. Australian Biological Resources Study, Canberra. https://biodiversity.org.au/afd/taxa/36aed2d6-3905-4e00-aff1-6c5cccdc2819 (accessed 31 May 2022)

Aguiar, A.P., and Gibson, G.A.P. 2010. The spatial complexity in describing leg surfaces of Hymenoptera (Insecta), the problem and a proposed solution. *Zootaxa* 2415: 54–62. https://doi.org/10.11646/zootaxa.2415.1.5

AMNH. 2022a. Search on Invertebrate Zoology database at AMNH for Halictus franki returned no results: https://emu-prod.amnh.org/imulive/iz.html#view=list&id=8685&modules=ecatalogue&IdeCurrentGenusLocal=Halictus&IdeCurrentSpeciesLocal=franki&SecDepartment_tab=Invertebrate%20Zoology&SecLookupRoot=Invertebrate%20Zoology&CatDepartment=Invertebrate%20Zoology&CatObjectType=Specimen%2FLot&AdmPublishWebNoPassword=Yes (accessed 31 May 2022)

AMNH. 2022b. Search on Invertebrate Zoology database at AMNH for just franki returned one result for Paracolletes franki: https://emu-prod.amnh.org/imulive/iz.html#view=list&id=d2ba&modules=ecatalogue&IdeCurrentSpeciesLocal=franki&SecDepartment_tab=Invertebrate%20Zoology&SecLookupRoot=Invertebrate%20Zoology&CatDepartment=Invertebrate%20Zoology&CatObjectType=Specimen%2FLot&AdmPublishWebNoPassword=Yes (accessed 31 May 2022)

Ascher, J.S., and Pickering, J. 2022. *Discover Life bee species guide and world checklist (Hymenoptera: Apoidea: Anthophila)*. https://www.discoverlife.org/mp/20q?guide=Apoidea_species [accessed on 04 October 2022]

Brothers, D.J. 1976. Modifications of the metapostnotum and origin of the 'propodeal triangle' in Hymenoptera Aculeata. *Systematic Entomology* 1: 177–182. https://doi.org/10.1111/j.1365-3113.1976.tb00036.x

Cane, J.H., and Neff, J.L. 2011. Predicated fates of ground-nesting bees in soil heated by wildfire: thermal tolerance of life stages and a survey of nesting depths. *Biological Conservation* 144(11): 2631–2636. https://doi.org/10.1016/j.biocon.2011.07.019

Cockerell, T.D.A. 1904. The halictine bees of the Australian region. *Annals and Magazine of Natural History* 14(81): 208–213. https://doi.org/10.1080/03745480409442995

Cockerell, T.D.A. 1905. Descriptions and records of bees. II. *Annals and Magazine of Natural History* 16(93): 292–301. https://doi.org/10.1080/03745480509442865

Cockerell, T.D.A. 1910a. New and little-known bees. *Transactions of the American Entomological Society* 36(3/4): 19–-249.

Cockerell, T.D.A. 1910b. Descriptions and records of bees. XXXII. *Annals and Magazine of Natural History* 6(3): 272–284. https://doi.org/10.1080/00222931008692850

Cockerell, T.D.A. 1914. Descriptions and records of bees. LXI. *Annals and Magazine of Natural History* 14: 39–49. https://doi.org/10.1080/00222931408693540

Cockerell, T.D.A. 1918. Some bees collected in Queensland. *Memoirs of the Queensland Museum* 6: 112–120.

Cockerell, T.D.A. 1919. The metallic-coloured Halictine bees of the Philippine Islands. *Philippine Journal of Science* 15: 9–13. https://doi.org/10.5962/bhl.part.11763

Cockerell, T.D.A. 1929. Bees, chiefly Australian species, described or determined by Dr. H. Friese. *American Museum Novitates* 343: 1–20.

Dalla Torre, C.G. 1896. *Catalogus Hymenopterorum*, Vol. 10 Apidae (Anthophila), viii + 643 pp. Leipig: Engelmann.

Danforth, B.N. 1999. Phylogeny of the bee genus Lasioglossum (Hymenoptera: Halictidae) based on mitochondrial COI sequence data. *Systematic Entomology* 24: 377–393. https://doi.org/10.1046/j.1365-3113.1999.00087.x

Danforth, B.N., and Ji, S. 2001. Australian Lasioglossum + Homalictus form a monophyletic group: resolving the "Australian enigma". *Systematic Biology* 50: 268–283. https://doi.org/10.1080/713849618

Danforth, B.N., Conway, L., and Ji, S. 2003. Phylogeny of eusocial Lasioglossum reveals multiple losses of eusociality within a primitively eusocial clade of bees (Hymenoptera: Halictidae). *Systematic Biology* 52: 23–36. https://doi.org/10.1080/10635150390132687

Danforth, B.N., and Almeida, E.A.B. 2008. Insights into bee evolution: a tribute to Charles D. Michener. *Apidologie* 39: 1–2. https://doi.org/10.1051/apido:2008011

Danforth, B.N., Minckley, R.L., Neff, J.L., and Fawcett, F. 2019. *The solitary bees: biology, evolution, conservation*. Princeton University Press: Princeton, NJ. 488 pp. https://doi.org/10.1515/9780691189321

Dujardin, F. 1842. Sous la nom d'Anoete (Anoetus), un petit animal articulé, roisin des Acariens. L'Institut, Section [1], *Sciences Mathématiques, Physiques et Naturelles (Paris)* 454: 316.

Engel, M.S., Brooks, R.W., and Yanega, D., 1997. New genera and subgenera of augochlorine bees (Hymenoptera: Halictidae). *Scientific Papers of the Natural History Museum of the University of Kansas* 5: 1–21. https://doi.org/10.5962/bhl.title.4042

Engel, M.S., and Gonzalez, V.H. 2022. A new bee genus from the pampas of eastern Argentina, with appended notes on the classifcation of "paracolletines" (Hymenoptera: Colletidae). *Journal of Melitology* 109: 1–39. https://doi.org/10.17161/jom.i109.16424

Fabricius, J.C. 1793. *Entomologica systemica emendata et acuta, Secundum classes, ordines, genera, species, adjectis synonymis, locis, observationibus, descriptionibus*. C.G. Proft: Hafniae. 519 pp. https://doi.org/10.5962/bhl.title.125869

Friese, H. 1917. Results of Dr. E. Mjöberg's Swedish scientific expeditions to Australia, 1910–1913. *Apidae. Arkiv* för *Zoologi* 11(2): 1–9. https://doi.org/10.5962/bhl.part.1499

Friese, H. 1924. Ueber die Bienen Australiens. *Konowia* 3: 216-249.

Gibbs, J., Brady, S.G., Kanda, K., and Danforth, B.N. 2012. Phylogeny of halictine bees supports a shared origin of eusociality for Halictus and Lasioglossum (Apoidea: Anthophila: Halictidae). *Molecular Phylogenetics and Evolution* 65: 926–939. https://doi.org/10.1016/j.ympev.2012.08.013

Gibbs, J., and Dumesh, S. 2013. A new species, *Lasioglossum (Eickwortia) hienae*, from Mexico (Apoidea: Halictidae). *Journal of Melittology* 13: 1–11. https://doi.org/10.17161/jom.v0i13.4518

Gibbs, J., Packer, L., Dumesh, S., and Danforth, B.N. 2013. Revision and reclassification of Lasioglossum (Evylaeus), L. (Hemihalictus) and L. (Sphecodogastra) in eastern North America (Hymenoptera: Apoidea: Halictidae). *Zootaxa* 3672: 1–117. https://doi.org/10.11646/zootaxa.3672.1.1

Gibbs, J., Bass, A., and Morgan, K. 2022. Habralictus and Lasioglossum of Saint Lucia and Saint Vincent and the Grenadine, Lesser Antilles (Hymenoptera, Apoidea, Halictidae). *Zookeys* 1089: 125–167. https://doi.org/10.3897/zookeys.1089.72645

Harris, R.A. 1979. A glossary of surface sculpturing. *Occasional Papers in Entomology, State of California Department of Food and Agriculture* 28: 1-31.

Latreille, P.A. 1804. Tableau méthodique des insects. Pp. 129-200 in: *Nouveau Dictionnaire d'Histoire Naturelle* (vol. 24). Paris: Détereville

McGinley, R.J. 1999. *Eickwortia* (Apoidea, Halictidae), a new genus of bees from Mesoamerica. *University of Kansas Natural History Museum Special Publication* 24: 111–120.

Michener, C.D. 1965. A classification of the bees of the Australian and South Pacific regions. *Bulletin of the American Museum of Natural History* 130: 1–362.

Michener, C.D., and Fraser, A. 1978. A comparative anatomical study of mandibular structure in bees (Hymenoptera: Apoidea). *University of Kansas Science Bulletin* 51(14): 463–482. https://doi.org/10.5962/bhl.part.17245

Michener, C.D. 2007. *The Bees of the World*. Second edition. The John Hopkins University Press, Baltimore. 953pp.

Rayment, T. 1929. Bees from East Gippsland. *Victorian Naturalist* 46: 124–129.

Rayment, T. 1939. Bees from the high lands of New South Wales and Victoria. *The Australian Zoologist* 9: 263–294.

Rayment, T. 1953. *Bees of the Portland district*. Portland Field Naturalist Club. 39pp.

Schrottky, C. 1910. Berichtigung (Hym.). *Deutsche Entomologische Zeitschrift* 1910: 540. https://doi.org/10.1002/mmnd.4801910505

Smith, F. 1853. *Catalogue of Hymenopterous insects in the collection of the British Museum. Part I. Andrenidae and Apidae*. London: British Museum. 197 pp.

Tierney, S.M., Gonzales-Ojeda, T., and Wcislo, W.T. 2008. Nesting Biology and Social Behavior of Xenochlora Bees (Hymenoptera: Halictidae: Augochlorini) from Perú. *Journal of the Kansas Entomological Society* 81(1): 61–72. https://doi.org/10.2317/JKES-704.24.1

Walker, K.L. 1995. Revision of the Australian native bee subgenus *Lasioglossum (Chilalictus)* (Hymenoptera: Halictidae). *Memoirs of the Museum of Victoria* 55(1-2): 1–423. https://doi.org/10.24199/j.mmv.1995.55.02

Walker, K.L. 2022. Taxonomic revision of the Australian native bee subgenus *Callalictus* (Hymenoptera: Halictidae: Halictini: genus *Lasioglossum*). *Australian Journal of Taxonomy* 7: 1–19. https://doi.org/10.54102/ajt

Walter, D.E, Beard, J.J., Walker, K.L., and Sparks, K. 2002. Of mites and bees: A review of mite-bee associations in Australia and a revision of *Raymentia* (Acari: Mesostigmata: Laelapidae), with description of two new species of mites from *Lasioglossum (Parasphecodes)* spp. (Hymenoptera: Halictidae). *Australian Journal of Entomology* 41: 128–148. https://doi.org/10.1046/j.1440-6055.2002.00280.x

Zhang, D., Niu Z-Q., Luo, A., Orr, M., Ferrari, R, Jin. J., Wu, Q., Zhang, F., and Zhu, C. 2022. Testing the systematic status of Homalictus and Rostrohalictus with weakened cross-vein groups within Halictini (Hymenoptera: Halictidae) using low-coverage whole-genome sequencing. *Insect Science*. https://doi.org/10.1111/1744-7917.13034